Vol. 64 June, 1960 No. 6

THE JOURNAL OF PHYSICAL CHEMISTRY

(Registered in U. S. Patent Office)

CONTENTS

NOTES

COMMUNICATIONS TO THE EDITOR

THE JOURNAL OF PHYSICAL CHEMISTRY

(Registered in U. S. Patent Office)

Published monthly by the American Chemical Society at 20th and Northampton Sts., Easton, Pa.

Second-class mail privileges authorized at Easton, Pa. This publication is authorized to be mailed at the special rates of postage prescribed by Section 131.122.

The *Journal of Physical Chemistry* is devoted to the publication of selected symposia in the broad field of physical chemistry and to other contributed papers.

Manuscripts originating in the British Isles, Europe and Africa should be sent to F. C. Tompkins, The Faraday Society, 6 Gray's Inn Square, London W. C. 1, England.

Manuscripts originating elsewhere should be sent to W. Albert Noyes, Jr., Department of Chemistry, University of Rochester, Rochester 20, N. Y.

Correspondence regarding accepted papers, proofs and reprints should be directed to Assistant Editor, Allen D. Bliss, Department of Chemistry, Simmons College, 300 The Fenway, Boston 15, Mass.

Business Office: Alden H. Emery, Executive Secretary, American Chemical Society, 1155 Sixteenth St., N. W., Washington 6, D. C.

Advertising Office: Reinhold Publishing Corporation, 430 P[illegible]venue, New York 22. N. Y.

A[illegible]s must be submitted in duplicate, typed and double spa[illegible] They should have at the beginning a brief Abstract, in n[illegible]ase exceeding 300 words. Original drawings should accompany the manuscript. Lettering at the sides of graphs (black on white or blue) may be pencilled in and will be typeset. Figures and tables should be held to a minimum consistent with adequate presentation of information. Photographs will not be printed on glossy paper except by special arrangement. All footnotes and references to the literature should be numbered consecutively and placed in the manuscript at the proper places. Initials of authors referred to in citations should be given. Nomenclature should conform to that used in *Chemical Abstracts*, mathematical characters be marked for italic, Greek letters carefully made or annotated, and subscripts and superscripts clearly shown. Articles should be written as briefly as possible consistent with clarity and should avoid historical background unnecessary for specialists.

Notes describe fragmentary or incomplete studies but do not otherwise differ fundamentally from articles and are subjected to the same editorial appraisal as are articles. In their preparation particular attention should be paid to brevity and conciseness. Material included in Notes must be definitive and may not be republished subsequently.

Communications to the Editor are designed to afford prompt preliminary publication of observations or discoveries whose value to science is so great that immediate publication is imperative. The appearance of related work from other laboratories is in itself not considered sufficient justification for the publication of a Communication, which must in addition meet special requirements of timeliness and significance. Their total length may in no case exceed 500 words or their equivalent. They differ from Articles and Notes in that their subject matter may be republished.

Symposium papers should be sent in all cases to Secretaries of Divisions sponsoring the symposium, who will be responsible for their transmittal to the Editor. The Secretary of the Division by agreement with the Editor will specify a time after which symposium papers cannot be accepted. The Editor reserves the right to refuse to publish symposium articles, for valid scientific reasons. Each symposium paper may not exceed four printed pages (about sixteen double spaced typewritten pages) in length except by prior arrangement with the Editor.

Remittances and orders for subscriptions and for single copies, notices of changes of address and new professional connections, and claims for missing numbers should be sent to the American Chemical Society, 1155 Sixteenth St., N. W., Washington 6, D. C. Changes of address for the *Journal of Physical Chemistry* must be received on or before the 30th of the preceding month.

Claims for missing numbers will not be allowed (1) if received more than sixty days from date of issue (because of delivery hazards, no claims can be honored from subscribers in Central Europe, Asia, or Pacific Islands other than Hawaii), (2) if loss was due to failure of notice of change of address to be received before the date specified in the preceding paragraph, or (3) if the reason for the claim is "missing from files."

Subscription Rates (1960): members of American Chemical Society, $12.00 for 1 year; to non-members, $24.00 for 1 year. Postage to countries in the Pan-American Union $0.80; Canada, $0.40; all other countries, $1.20. Single copies, current volume, $2.50; foreign postage, $0.15; Canadian postage, $0.05; Pan-American Union, $0.05. Back volumes (Vol. 56–59) $25.00 per volume; (starting with Vol. 60) $30.00 per volume; foreign postage per volume $1.20, Canadian, $0.15; Pan-American Union, $0.25. Single copies: back issues, $3.00; for current year, $2.50; postage, single copies: foreign, $0.15; Canadian, $0.05; Pan American Union, $0.05.

The American Chemical Society also publishes *Journal of the American Chemical Society, Chemical Abstracts, Industrial and Engineering Chemistry*, International Edition of *Industrial and Engineering Chemistry, Chemcial and Engineering News, Analytical Chemistry, Journal of Agricultural and Food Chemistry, Journal of Organic Chemistry, Journal of Chemical and Engineering Data* and *Chemical Reviews.* Rates on request.

THE JOURNAL OF PHYSICAL CHEMISTRY

(Registered in U. S. Patent Office) (© Copyright, 1960, by the American Chemical Society)

VOLUME 64 JUNE 21, 1960 NUMBER 6

CALORIMETRIC STUDIES OF THE KINETICS OF DISORDERING IN $MgCd_3$ AND Mg_3Cd[1,2,3]

BY K. F. STERRETT, W. V. JOHNSTON, R. S. CRAIG AND W. E. WALLACE

Contribution No. 1062 from the Department of Chemistry, University of Pittsburgh, Pittsburgh 13, Pennsylvania

Received May 21, 1958

Measurements of the net disordering rates of samples slightly displaced from equilibrium have been carried out using conventional adiabatic specific heat calorimetry. First order rate constants were measured between 217 and 312°K. for $MgCd_3$ and between 316 and 334°K. for Mg_3Cd. The investigation showed regions in which the rate constants diminished with increasing temperature. The interpretation of this behavior is discussed in terms of the Bragg–Williams theory.

Introduction

There are three compositions in the magnesium–cadmium system, represented by the chemical formulas $MgCd_3$, MgCd, and Mg_3Cd, which are characterized at room temperature by ordered structures. X-Ray studies have shown the existence of superlattices which disappear at higher temperatures as the order–disorder Curie temperatures are reached, and specific heat measurements have shown the lambda shaped curves usually associated with order–disorder transitions. The kinetics of the order–disorder tranformation for these alloys has been studied previously by several investigators,[4-7] the parameter measured as a function of time generally having been the volume or the electrical resistance. Previously $MgCd_3$ has been studied in this Laboratory using the dilatometric technique and measuring the rate of approach to equilibrium at successively higher temperatures approaching the Curie point.[8] It was found that the disordering process could be described as taking place in two stages, both of which are, within the limit of error, first order processes. Further, there was evidence that the rate of disordering decreased when the temperature increased toward the Curie point.

The energy evolved or absorbed on ordering or disordering is in some respects the parameter which is most unambiguously related to the change of order in a system. This paper describes studies of the rate of disordering of Mg_3Cd and $MgCd_3$ in which the heat absorbed by the sample is taken as the measure of the extent of the reaction. The sensitivity of the method is such that measurements were made, in the case of $MgCd_3$, at temperatures as low as 217°K. The experiments were carried out under conditions very close to equilibrium, so that the rate measured was actually the net rate, *i.e.*, the difference between the disordering and ordering rates. The measurements were made in conventional adiabatic specific heat calorimeters which have been described previously.[9-11]

The samples were those which had been used in previous specific heat studies.[12] They were in the form of cylinders approximately 3 inches in length, 1.5 inches in diameter, with tapered holes about 9/16 inch in diameter at the large end bored along

---

(1) From portions of the doctoral theses of W. V. Johnston (Ph.D., University of Pittsburgh, 1955) and of K. F. Sterrett (Ph.D., University of Pittsburgh, 1957).

(2) This work was supported by the Atomic Energy Commission.

(3) The editors have decided to publish this article even though there remain certain points of disagreement between authors and referees.

(4) N. I. Stepanov and S. A. Bulakh, *Compt. rend. Acad. Sci. U.S.S.R.* [*N.S.*], **4**, 147 (1935).

(5) N. I. Stepanov and I. I. Kornilov, *Ann. secteur. anal. phys.-chim., Inst. chim. gen. (U.S.S.R.)*, **10**, 78 (1938).

(6) N. I. Stepanov and I. I. Kornilov, *ibid.*, **10**, 97 (1938).

(7) I. I. Kornilov, *Compt. rend. Acad. Sci. (U.S.S.R.)*, **19**, 157 (1938).

(8) R. A. Flinn W. E. Wallace and R. S. Craig, THIS JOURNAL, **61**, 236 (1957).

(9) C. B. Satterthwaite, R. S. Craig and W. E. Wallace, *J. Am. Chem. Soc.*, **76**, 232 (1954).

(10) R. S. Craig, C. A. Krier, L. W. Coffer, E. A. Bates and W. E. Wallace, *ibid.*, **76**, 238 (1954).

(11) W. V. Johnston, K. F. Sterrett, R. S. Craig and W. E. Wallace, *ibid.*, **79**, 3633 (1957).

(12) L. W. Coffer, R. S. Craig, C. A. Krier and W. E. Wallace, *ibid.*, **76**, 241 (1954).

the axes. When a sample was in place in the calorimeter, a tapered metal plug containing a platinum resistance thermometer and a heater fitted into the axial hole of the sample. The $MgCd_3$ sample weighed 597.991 grams, and the Mg_3Cd sample weighed 262.179 grams.

Thermal Equilibration in Mg–Cd Alloys

During the course of specific heat studies on these substances some rather unusual thermal effects were observed.[9,11,12] In the normal operation of the calorimeter a sample, initially at equilibrium and maintained under adiabatic conditions, is heated electrically through a temperature interval of about 5 degrees. After the heating period the temperature is measured as a function of time until an essentially constant value is obtained. This process is repeated stepwise up the temperature scale to determine C_p as a function of T. Ordinarily, temperature equilibrium is attained within about 20 minutes after the cessation of heating. For the Mg–Cd superlattices it was observed that in certain temperature ranges the temperature of the sample continued to fall after the heating period for abnormally long periods of time. In some cases the downward drifts were followed for as long as 24 hours. The temperature *versus* time curve in general seemed to approach a limiting value in an exponential manner. The total drop in temperature following the 20 minute equilibration period after the cessation of heating was not great, being in most cases less than 0.1 degree for $MgCd_3$ and less than 0.3 degree for Mg_3Cd. For comparison, it may be noted that for "normal operation," that is, for a sample not displaying kinetic effects, the sample during this period would be at essentially constant temperature, or, at worst, would be drifting in temperature at a constant rate which was generally less than 0.002 degree/hour.

For the compound $MgCd_3$ the thermal sluggishness first made its appearance at about 190°K. At successively higher temperatures the rate of the downward drift increased until at about 240°K. the process had become so fast as to be virtually completed during the 20 minute period normally required for thermal equilibration of the calorimeter. At about the ice point, however, the thermal sluggishness again set in and the rate of the process now decreased with increasing temperature as the Curie point, 357.0°K., was approached.

With the compound Mg_3Cd the thermal sluggishness set in at about 308°K., and the rate of the process increased with temperature until at about 343°K. equilibrium was reached within the normal 20 minute period. At about 408°K. the downward drift again made its appearance and the rate at which equilibrium was attained decreased as the Curie temperature, 423.8°K., was approached.

The compound MgCd behaved in a manner similar to the other two in the low temperature region. Thermal sluggishness set in at about 230°K. and the rate of attainment of thermal equilibrium increased with temperature until the behavior became normal at about room temperature. Equilibration times then remained normal up to the Curie point, 524 5°K.

Determination of Rate Constants

In discussing the thermal behavior described in the preceding section it is convenient to introduce the long range order parameter, S, for the system. To do this the lattice is divided into sublattices α and β, which contain exclusively atoms of species A and B, respectively, in the perfectly ordered state. When disorder is introduced, an A atom on an α site changes places with a B atom on a β site. The order parameter S is defined by the relationship $S = (r_\alpha - F_A)/F_B$, where r_α is the fraction of α sites which are correctly occupied, and F_A and F_B are the mole fractions of A and B, respectively.[13] The order parameter defined in this way acquires a value of unity for the perfectly ordered lattice and a value of zero for the case in which the two species are randomly distributed over the lattice sites. In many instances mobility in the lattice permits ready attainment of configurational equilibrium. Under these circumstances there is an equilibrium value of the order parameter. In the remainder of this paper the equilibrium order parameter will be denoted by S_e and the general, or non-equilibrium, value simply as S.

Theory and experiment both indicate a monotonic fall of S_e with increasing temperature from a value of unity at 0°K. to zero at the critical temperature, T_c, the temperature above which long range order does not exist. Because alteration of the order in the specimen requires a movement of atoms the order parameter does not readjust instantaneously when the temperature of the specimen is altered. The thermal behavior described in the preceding section can be interpreted as resulting from the slowness with which the order parameter alters when the temperature of the system is changed. If a sample, initially at a temperature T_1 and possessing order $(S_e)_1$, is heated through a 5 degree interval, it will then possess a higher degree of order than that characteristic of the equilibrium system at the new temperature. The order parameter decreases toward the new equilibrium value, and since the disordering process absorbs heat, the specific heat calorimeter can be employed to follow the kinetics of the disordering process. The total energy absorbed in the process is the sum of the energies absorbed in the individual AB interchanges. If the total change in order is relatively small the energy absorbed per AB interchange will be essentially constant, and the total energy absorbed will be proportional to the number of AB interchanges, and hence to the change in S. The change in temperature of the sample relaxing toward its equilibrium degree of order is thus proportional to the change in S.

In this method of studying kinetics there are some limitations which are imposed by the nature of the calorimetric apparatus. First, the net rate of the order–disorder process must be slow compared to the rate at which thermal equilibrium with respect to vibrational energy is achieved in the calorimeter. Obviously one cannot ascribe temperature drifts to changes in configurational energy until the temperature distribution in the sample has become uniform. On the other hand, if the absorption of heat by configurational changes takes place over a period of many hours or perhaps days, the rate becomes too small to be measured with precision. In addition, as the precision of the temperature measurements is increased it becomes clear that the adiabatic conditions in the calorimeter are never perfectly realized. There is in general a slight temperature drift caused by parasitic potentials in the difference thermocouple circuits. Usually this "normal" drift is less than about 0.002° per hour, and the exponential drop in temperature caused by the disordering process is superimposed upon this "normal" drift. Corrections for the latter can be made if the observations are continued until the process has essentially run its course. This was feasible when the experiment was of two to six hours duration. However, as mentioned above, in some cases the temperature was followed for as long as 24 hours. In such cases correction for the normal drift could not be made with complete confidence.

Prior to beginning a series of measurements considerable care was taken to assure initial equilibrium conditions in the sample. Before the low temperature measurements on $MgCd_3$ were taken, for example, the process of cooling from room temperature to Dry Ice temperature consumed about six days.[14]

As indicated above when the system is displaced from equilibrium (by heating), its order parameter relaxes toward the equilibrium value producing a drop in temperature. The rate at which the temperature fell appeared to be proportional to the difference between the value at any instant and the final equilibrium value T_∞, suggesting that the following simple first order rate expression might be applicable

$$\ln(T - T_\infty) = kt + \text{constant}$$

Linearity of a plot of ln $(T - T_\infty)$ *versus* t would indicate first order behavior, and the rate constant k could be determined from the slope of such a plot. The resistance of the platinum thermometer used to measure the sample tempera-

---

(13) This is the order parameter which was introduced by W. L. Bragg and E. J. Williams, *Proc. Roy. Soc. (London)*, **A145**, 699 (1934).

(14) It was found that if the $MgCd_3$ was cooled relatively fast (say from room temperature to liquid nitrogen temperature in a few hours) the order parameter was frozen in at about 230°K. When such a "quenched" sample was warmed back up to about 190 or 200°K., a slow upward drift was observed. This was interpreted as resulting from the ordering of the sample as S relaxed from the value at which it was frozen in at about 230°K. to the equilibrium value at about 200°K. The upward drifts persisted up to about 230°K. At higher temperatures they changed sign and became downward drifts.

ture is very nearly proportional to temperature and in the range of these experiments the sensitivity is such that 0.1 ohm is approximately equivalent to 1 degree. The quantity ln $(R - R_\infty)$ was therefore plotted directly without first converting resistance to temperature.[15] Figures 1 and 2 show these plots for the measurements on $MgCd_3$. Clearly the decay of the excess temperature in $MgCd_3$ follows first order kinetics and similar plots indicate the same kinetic behavior for Mg_3Cd. The constants determined from these plots apply to the over-all rates of the order–disorder process near equilibrium.

The over-all rate constants determined for $MgCd_3$ and Mg_3Cd are listed in Table I. When the data are plotted as log *k versus* $1/T$, straight lines can be drawn through the points within the limit of accuracy of the measurements. This formal procedure gave an activation energy of 15.5 ± 1.0 kcal. for $MgCd_3$ between 217 and 234°K. In the range 282 to 312°K., $MgCd_3$ showed an apparent activation energy of −7.2 ± 0.5 kcal. The activation energy for Mg_3Cd was found to be 26.2 ± 2 kcal. in the temperature range between 316 and 334°K. The justification for the use of the Arrhenius plots and the interpretation of the activation energies will be discussed in a later section.

TABLE I

FIRST ORDER RATE CONSTANTS FOR THE DISORDERING PROCESS

Low Temperature Series

$MgCd_3$		Mg_3Cd	
T, °K.	k (min.$^{-1}$)	T, °K.	k (min.$^{-1}$)
217.1	0.0045	316.4	0.0038
222.8	.0109	321.4	.0106
228.4	.0223	325.9	.0112
233.9	.0627	330.3	.022
		334.6	.036

$MgCd_3$
High Temperature Series

T, °K.	k (min.$^{-1}$)
282.2	0.0325
287.2	.0273
292.4	.0217
297.5	.0182
302.4	.0147
307.3	.0115
312.3	.0097

It will be noted that the first value reported for $MgCd_3$ is at 217°K. Below this temperature the rates were too slow to be measured with precision, although the occurrence of the process could be detected at somewhat lower temperatures. Between 234 and 282°K., the rates were too fast for measurement with the existing calorimetric apparatus, and above 312°K. the rate had become too slow for measurement with reasonable precision. The rate constants for Mg_3Cd were only measured between 316 and 334°K. where the rates were observed to increase with temperature. Experimental difficulties prevented reliable rate measurements above 408°K. where abnormally long thermal equilibration times were again observed.

Discussion of Results

The results in Table I are of considerable interest in that they reveal a region in which the rate constant diminishes with increasing temperature. It should be clear that this is not due to the need for nucleation such as is required for phase transitions and which leads to a negative temperature coefficient of the rate of transformation at temperatures just below the transition point. A qualitative explanation for the anomalous temperature coefficient in the present case apparently is provided by the original Bragg–Williams theory of order–disorder processes.

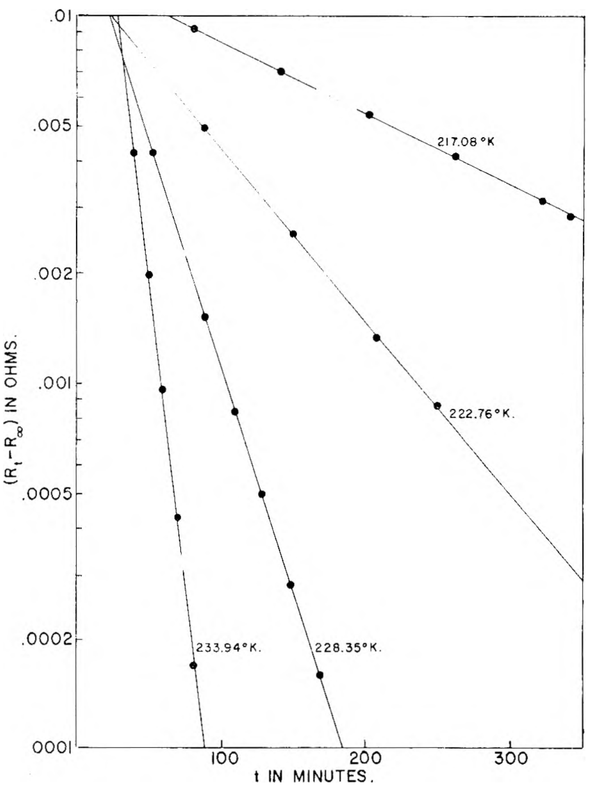

Fig. 1.—Low temperature kinetic experiments on $MgCd_3$.

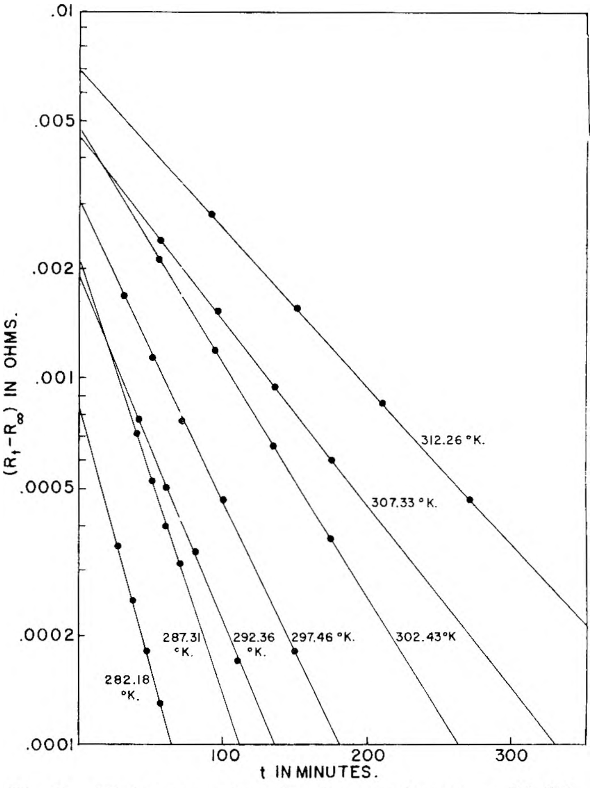

Fig. 2.—High temperature kinetic experiments on $MgCd_3$.

The treatment put forth by Bragg and Williams dealt with both principal aspects of order–disorder phenomena—(1) The dependence of S_e on temperature and (2) the kinetics of relaxation of S for systems displaced from equilibrium. Later Takagi

---

(15) In some of the experiments for which excessively long times were required for the sample to reach equilibrium, the limiting value of the resistance, R_∞, had to be found by applying the method of Guggenheim.

provided[16] a very elegant treatment of the order–disorder process and showed among other things that it was possible to obtain the Bragg–Williams expression for the temperature dependence of S_e by formally treating the process as if it were a chemical reaction. More recently Dienes[17] has shown that the kinetics of relaxation can also be treated formally by regarding the process as if it were a chemical reaction. The formulation by Dienes provides a convenient means for treating the present problem.[18] The following expression is, with slightly altered nomenclature, his equation 10

$$-\frac{dS}{dt} = k_1[S + F_AF_B(1 - S)^2] - k_2F_AF_B(1 - S)^2 \tag{1}$$

In this equation k_1 and k_2 are the rate constants for the disordering and ordering, respectively, and F_A and F_B are the mole fractions of the two species present, as defined earlier.

We may now evaluate k_1 and k_2 in terms of conventional rate theory. Consider the interchange of an AB pair of atoms, each being correctly situated before and incorrectly situated after the interchange. Designate the increase in energy of the system by V/N_0 and the energy of activation for this disordering process by W/N_0. Then the energy of activation for the reverse process is $(W - V)/N_0$, where N_0 is the Avogadro number.

The rate constants k_1 and k_2 are given by the expressions

$$\begin{aligned} k_1 &= \nu_1 e^{-W/RT} \\ k_2 &= \nu_2 e^{-(W-V)/RT} \end{aligned} \tag{2}$$

where ν_1 and ν_2 are constants involving frequency and orientation factors. Introducing the assumption of Bragg and Williams that $V = V_0S$ and, further, assuming that $\nu_1 = \nu_2 = \nu$, we obtain the expression for the net rate of disordering

$$-\frac{dS}{dt} = \nu e^{-W/RT}\,[S + F_AF_B(1 - S)^2 - e^{SV_0/RT}\,F_AF_B(1 - S)^2] \tag{3}$$

For the system at equilibrium S becomes S_e and, of course, $(dS/dt)_{S = S_e} = 0$. We thus obtain for the special case of equilibrium an equation analogous to equation 3

$$-\left(\frac{dS}{dt}\right)_{S=S_e} = 0 = \nu e^{-W/RT}\,[S_e + F_AF_B(1 - S_e)^2 - e^{S_eV_0/RT}\,F_AF_B(1 - S_e)^2] \tag{3'}$$

From equation 3′ one obtains the Bragg–Williams expression for the dependence of S_e on T

$$\frac{S_e + F_AF_B(1 - S_e)^2}{F_AF_B(1 - S_e)^2} = e^{S_eV_0/RT} \tag{4}$$

To obtain an expression for the first order rate constant for the net process near equilibrium we first note from equation 3 that at constant temperature the rate is a function only of S, that is

$$-\frac{dS}{dt} = f(S) \tag{5}$$

Expanding $f(S)$ in a Taylor series about the equilibrium value of the order parameter S_e

$$-\frac{dS}{dt} = f(S_e) + \left[\frac{df(S)}{dS}\right]_{S_e}(S - S_e) + \ldots \tag{6}$$

Higher terms may be neglected since we are interested in values very close to equilibrium. At equilibrium $dS/dt = 0$. Hence $f(S_e)$ is zero, and equation 6 becomes

$$-\frac{dS}{dt} = \left[\frac{df(S)}{dS}\right]_{S_e}(S - S_e) \tag{7}$$

This is a standard expression for first order kinetics, and the rate constant is identified with the term $[df(S)/dS]_{S_e}$. It will be apparent that the mathematical procedure used here will yield a first order expression for the net rate of any reaction if the displacement from equilibrium is sufficiently small, and that the rate constant will be independent of the variable in terms of which the rate is expressed. This principle has been discussed in detail by Manes and others.[19,20]

The rate constant for the over-all reaction near equilibrium may now be obtained directly from equation 3 by differentiation and evaluating the derivative at $S = S_e$. The result is

$$k = \nu e^{-W/RT}\,[1 - 2F_AF_B(1 - S_e) - e^{S_eV_0/RT}\,\{(V_0/RT)\,F_AF_B(1 - S_e)^2 - 2F_AF_B(1 - S_e)\}] \tag{8}$$

By making use of equation 4 (the equilibrium relationship between S_e and T), equation 8 may be re-written in the form

$$k = \nu\left[\frac{(1 + S_e)\sqrt{F_AF_B}}{\sqrt{S_e + F_AF_B(1 - S_e)^2}} - \sqrt{F_AF_B}\,(1 - S_e)\,\sqrt{S_e + F_AF_B(1 - S_e)^2}\,\frac{V_0}{RT}\right] e^{-(W - V/2)/RT} \tag{9}$$

It may be shown that at sufficiently low temperatures the expression in brackets has the value $2\sqrt{F_AF_B}$. Even at somewhat higher temperatures, say when S is approximately 0.8 or 0.9, the expression in brackets is a very weak function of T, and hence an Arrhenius plot in this temperature range should yield an energy of activation which is approximately equal to $(W - V_0)/2$. At still higher temperatures, however, the pre-exponential term becomes a very strong negative function of T. There is no justification, then, for applying an Arrhenius plot to the data in this region, and the apparent negative activation energy is of course meaningless.

To investigate the properties of equation 9 at higher temperatures numerical calculations have been employed, the results of which are shown in Fig. 3. The constant V_0 was evaluated from the Bragg–Williams theory, taking the Curie temperature to be 355°K. The constant W was evaluated from the low temperature Arrhenius plot, using the values of V_0 and assuming the pre-exponential term in equation 9 to be constant. Corresponding values of S_e and T were found by substituting chosen values of S_e in equation 4 and solving the resulting expression for T. Curve A was com-

---

(16) Y. Takagi, *Proc. Phys.-Math. Soc. Japan*, **23**, 44 (1941).

(17) G. J. Dienes, *Acta Met.*, **3**, 549 (1955).

(18) The original method of Bragg and Williams has also been used and identical results emerge. The "chemical" approach is presented here for the sake of brevity.

(19) M. Manes, L. J. E. Hofer and Sol Weller, *J. Chem. Phys.*, **18**, 1355 (1950).

(20) M. Manes, *ibid.*, **21**, 1791 (1953).

puted for the case in which $F_A = F_B = 1/2$, whereas $F_A = 1/4$ and $F_B = 3/4$ for curve B. The S_e values at various temperatures used to compute curve B were 0.9, 0.8, 0.7, 0.6, 0.55, 0.5, and 0.467 at 252, 296, 323, 341, 348, 352 and 355°K. (T_c), respectively. Arbitrary values of the constant ν were used for the three curves and the scales used for the ordinates were chosen so that the curves would be of comparable height on the graph. Curve B is the one which might be expected to be applicable to the present experiments.

It is clear that although the curves are in qualitative agreement with the experimental data, the computed maxima are considerably closer to the Curie point than are the experimental maxima. This sort of agreement is about all that could be expected considering the over-simplifications of the theory.

There is another respect in which the Bragg-Williams model is not in conformity with the experimental situation, at least for $MgCd_3$. Elsewhere[21,22] it has been pointed out that alteration in S affects its axial ratio appreciably so that a complete theory must include possible effects due to relaxation of the axial ratio.

It is of some interest to indicate qualitatively why the inverse relationship between rate constant and temperature exists immediately below the Curie point. The expression for k (equation 9) includes both the effect of the forward (disordering) and reverse (ordering) processes. The forward reaction depends upon two factors: (1) the number of ways (n_w) atoms can "go wrong" and (2) the probability per unit of time (P_w) of an interchange of a pair of correctly situated atoms.[23] n_w is proportional to the product of (1) the number of correctly situated A atoms and (2) the number of correctly situated B atoms which are in the immediate vicinity of these A atoms. The percentage variation of n_w is slight over the entire temperature range. P_w, however, varies exponentially with temperature, introducing the term $e^{-W/RT}$ in equation 9.

Similarly the reverse reaction depends on n_r, the number of ways atoms can "go right" and P_r, the probability of interchange per sec. of a pair of incorrectly situated atoms. Both of these increase with increasing temperature. At very low temperatures the effect of the reverse reaction is to introduce the term $e^{V/2RT}$ into equation 9. Now if V were independent of T, this would be the effect of the reverse reaction at all temperatures. The normal exponential rise in k would be merely retarded by the factor $e^{V/2RT}$. However, the reduction in V as temperature approaches the Curie temperature results in an enormous increase in the number of incorrectly situated atoms and produces a corresponding increase in n_r. This greatly enhances the importance of the back reaction and as can easily be shown leads to the negative temperature coefficient of k.

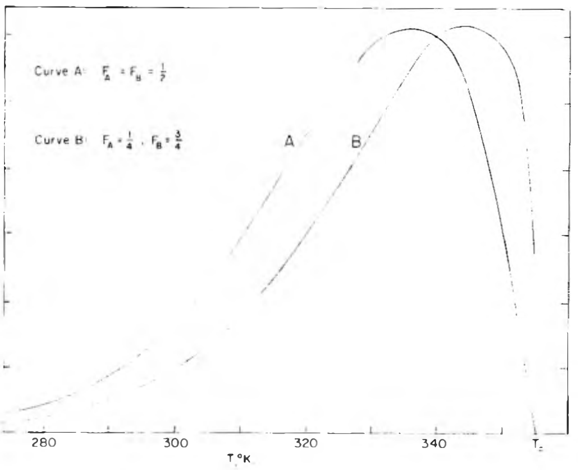

Fig. 3.—First order rate constants calculated from Bragg-Williams theory.

The variation of V with temperature produces the second term in brackets in equation 9. The first term in brackets of that equation is a slowly varying function of temperature. The second term is a slightly stronger function of temperature. However, near the Curie temperature the difference between these two terms is an exceedingly strong inverse function of temperature, more so in fact than the exponential. Hence k diminishes with temperature in this range.

Some interesting inter-relationships exist between the present study and an investigation of this system by Lulay and Wert.[24] They have studied the stress-induced disordering of $MgCd_3$ using internal friction techniques. Their activation energy for the disordering process is 18 kcal. which compares favorably with the value for W of 17.4 kcal. computed[25] from equation 9. Using their relaxation time (measured near the ice point) Wert and Lulay estimate relaxation times of 1 min. and 6×10^4 min. at 240 and 180°K., respectively. The corresponding times estimated from the present data are 6.5 and 33×10^4 min.

---

(21) D. A. Edwards, W. E. Wallace and R. S. Craig, *J. Am. Chem. Soc.*, **74**, 5256 (1952).

(22) T. D. Brotherton, W. E. Wallace and R. S. Craig, *J. Chem. Phys.*, **25**, 1297 (1956).

(23) Mechanism is unspecified. Disordering may involve a series of interchanges with a vacancy, a Frenkel defect, a dislocation or some other process.

(24) J. Lulay and C. Wert, *Acta Met.*, **4**, 627 (1956).

(25) V_0 is estimated from the critical temperature using the Bragg-Williams equations.

ADSORPTION FROM LIQUID MIXTURES AT SOLID SURFACES*

By C. G. Gasser and J. J. Kipling

Department of Chemistry, The University, Hull, England

Received May 6, 1959

There are at least four major factors which appear to be important in considering adsorption from the liquid phase onto solids: (a) the thickness of the adsorbed film, (b) the orientation of the adsorbed molecules, (c) the polarity of the solid surfaces, (d) the interaction between the liquid components. These factors probably are relevant in the choice of solutes designed to stabilize dispersions. Adsorption by charcoal from mixtures of benzene with each of the lower aliphatic alcohols is considered in the light of these four factors. Adsorption can be interpreted as being confined to a monolayer, the alcohol molecules being adsorbed with the major axis parallel to the solid surface. The competitive adsorption is affected both by interaction between the liquid components and by strong interaction between the alcohol molecules and oxide complexes on the adsorbing surface.

Introduction

The stabilizing of dispersions of solids in liquid media is usually dependent on the adsorption of a solute from the liquid at the interface. The adsorbed material frequently may be ionic in character, but a number of cases of non-ionized substances (*e.g.*, polyvinyl pyrrolidone, alkylated aromatic hydrocarbons[1]) and of substances with only a small ionic contribution (*e.g.*, gum arabic) are important. Although the adsorption of high molecular weight and especially of polymeric substances may involve factors not present in the adsorption of simpler compounds,[2] we believe the fundamental information which can be obtained from a study of simple systems to be relevant to the question. Bartell and Murray have pointed out the close connection between preferential adsorption from binary mixtures of simple compounds and stability of suspensions.[3]

Consideration of published work on adsorption by solids from binary mixtures of simple non-electrolytes suggests that the following points are important: (1) whether the adsorbed film is one or several molecules thick; (2) the orientation of the adsorbed material at the interface; (3) the polarity of the solid surface; (4) the interaction between the two liquid components; in the case of limited miscibility, the nature of the "solvent."

As yet, the amount of fundamental information of this kind on the more complex systems of practical importance is very small. Increasing attention is being paid, however, to relatively simple systems and it may be hoped that this will provide a basis for understanding the type of adsorption which is important in colloidal and rheological fields. We therefore present results which have been obtained with two-component systems, the two substances being miscible over the entire concentration range. Benzene was used as one component throughout; for the other component the lower aliphatic alcohols were used in turn. The results have some relevance to each of the preceding four points.

Experimental

The adsorbent was a further sample of steam-activated coconut shell charcoal washed with water to remove soluble mineral matter as described previously.[4]

The purification of benzene and of most of the alcohols also has been described.[5,6] The remaining alcohols were treated similarly, and gave $n^{20}\text{D}$ 1.3959 (isobutyl), 1.4100 (n-amyl), 1.4081 (isoamyl).

Adsorption was carried out at 20°, the measurements for liquid-phase adsorption being made refractometrically.[6]

Partial pressure data for 20° were obtained by the method we have used previously.[6]

Results

Results for liquid-phase adsorption are plotted in Fig. 1 (a-d) as composite isotherms (or "isotherms of concentration change"[6]). The concentration axis is in terms of x, the mole fraction of component 1 (the alcohol in each case) in the liquid phase at equilibrium. The ordinates represent $n_0(\Delta x/m)$, where Δx is the decrease in mole fraction of alcohol due to the adsorption which occurs when m g. of solid are brought into contact with a liquid mixture containing a total of n_0 millimoles (alcohol + benzene).

Discussion

The systems which we have examined were investigated previously by Bartell.[7,8] Our composite isotherms follow his as closely as could be expected for two different charcoals. Interpretation of the results has, however, changed since that time, as will appear in the subsequent discussion.

1. **Thickness of the Adsorbed Film.**—In Bartell's work it was accepted that both components of the present type of system are adsorbed. It was, however, postulated that the individual isotherm for adsorption of each component followed a Freundlich equation. This has been shown to be inappropriate for this type of adsorbent,[6] and the results are more satisfactorily interpreted by assuming that the adsorbed phase is confined essentially to a monolayer. There is, as Zettlemoyer has pointed out,[9] no direct method of determining the thickness of the adsorbed layer in such systems. The monolayer model, however, has the advantage that it is the simplest postulate to use, as Guggenheim and Adam suggested in relation to adsorption at the liquid–vapor inter-

---

* Read at the 134th Meeting of the American Chemical Society, September, 1958, Symposium on Stability of Dispersion of Solids in Organic Liquids.

(1) M. van der Waarden, *J. Colloid Sci.*, **5**, 317 (1950).

(2) R. Ullman, J. Koral and F. R. Eirich, "Proc. 2nd International Congress of Surface Activity," Vol. III, p. 485, Butterworths, London, 1957.

(3) F. E. Bartell and C. A. Murray, *Amer. Paint J.*, **23**, 251 (1938).

(4) A. Blackburn and J. J. Kipling, *J. Chem. Soc.*, 4103 (1955).

(5) J. J. Kipling and D. B. Peakall, *ibid.*, 4828 (1956).

(6) J. J. Kipling and D. A. Tester, *ibid.*, 4123 (1952).

(7) F. E. Bartell and C. K. Sloan, *J. Am. Chem. Soc.*, **51**, 1643 (1929).

(8) F. E. Bartell and G. H. Scheffler, *ibid.*, **53**, 2507 (1931).

(9) A. C. Zettlemoyer, 1958 Mattiello Award Lecture.

face.[10] It has provided a satisfactory interpretation of adsorption on a number of solid surfaces from most completely miscible pairs of liquids.[5,6,11–13] It does not apply to systems of limited miscibility as the solubility limit is approached,[14] nor to completely miscible liquids differing so widely in polarity (*e.g.*, *n*-dodecane and ethanol with Graphon as adsorbent[15]) that the system is close to phase separation at the temperature of the experiments; Kiselev's work is particularly relevant to this last point.[16–18] Aqueous mixtures also present a special case.[11]

The present results can be interpreted satisfactorily in terms of the monolayer model. (Adsorption from the same liquid systems on other carbons is more complex, as we hope to report later.[19]) Thus, if it is assumed that the adsorbate always completely covers the surface to the extent of a monolayer, then

$$\frac{n_1^s}{(n_1^s)_m} + \frac{n_2^s}{(n_2^s)_m} = 1$$

where n_1^s and n_2^s are the numbers of millimoles of components 1 and 2, respectively, adsorbed per g. of adsorbent, $(n_1^s)_m$ and $(n_2^s)_m$ being the corresponding monolayer values. It can further be shown on algebraic grounds,[7] without reference to any model for adsorption of this type, that

$$n_0(\Delta x/m) = n_1^s(1 - x) - n_2^s x$$

From these two equations, the isotherms of adsorption of the individual components can be calculated. These will be discussed below.

2. The Orientation of the Adsorbed Molecules.—Again there is no direct evidence as to the orientation of molecules at the interface between a liquid and any other phase. It has seemed simplest to assume that the orientation adopted by a given molecule at the solid–vapor interface is also assumed at the solid–liquid interface unless special factors intervene. We have consequently determined monolayer values from vapor isotherms for each of the alcohols studied; the isotherms were Type I of the B.E.T. classification with an upward turn close to saturation pressures. The results are shown in Table I.

It frequently has been assumed that aliphatic acids and alcohols are adsorbed with the same orientation at solid surfaces as the long-chain homologs show when close-packed on aqueous substrates, *viz.*, with the hydrocarbon chain perpendicular to the surface. If this were so in the present case, *n*-propyl, *n*-butyl and *n*-amyl alcohols would occupy equal molecular areas at the charcoal surface. Ethyl and methyl alcohols would occupy slightly smaller areas as the full effect of the "zig-zag" in the hydrocarbon chain on the cross-sectional area would not be shown. Table I shows that this is not so. The ratio of the molecular areas (referred to that of propyl alcohol for the above reason) would be 1 for the higher normal alcohols, and only slightly less than 1 for ethyl and methyl alcohols. In fact, however, the ratio increases steadily along the homologous series, almost as a linear function of the chain-length.

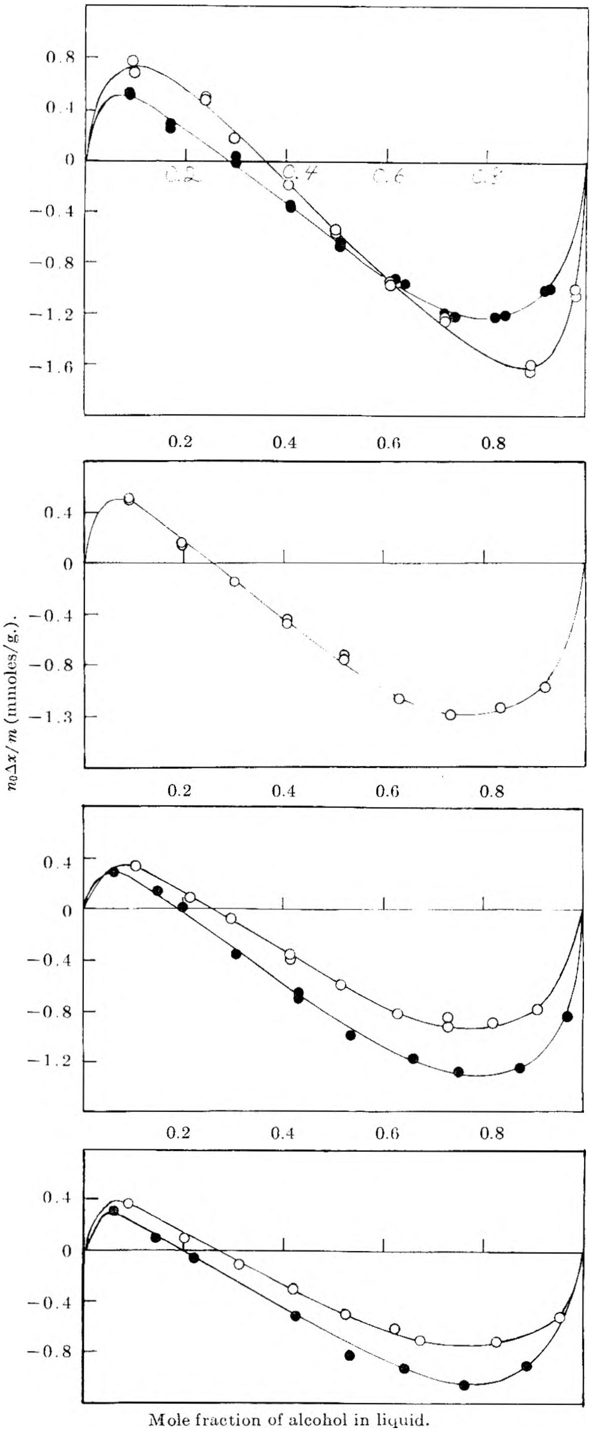

Fig. 1.—Composite isotherms for adsorption from alcohol–benzene systems (starting from top a-d): (a) ○, MeOH–C_6H_6; ●, EtOH–C_6H_6; (b) PrOH–C_6H_6; (c) ○, *n*-BuOH–C_6H_6; ●, *iso*-BuOH–C_6H_6; (d) ○, *n*-AmOH–C_6H_6; ●, *iso*-AmOH–C_6H_6.

---

[10] E. A. Guggenheim and N. K. Adam, *Proc. Roy. Soc. (London)*, **A139**, 218 (1933).

[11] A. Blackburn and J. J. Kipling, *J. Chem. Soc.*, 3819 (1954).

[12] J. J. Kipling, "Proc. 2nd International Congress of Surface Activity," Vol. III, p. 462, Butterworths, London, 1957.

[13] F. E. Bartell and F. C. Benner, THIS JOURNAL, **46**, 847 (1942).

[14] R. S. Hansen and R. P. Craig, *ibid.*, **58**, 211 (1954).

[15] R. S. Hansen and R. D. Hansen, *ibid.*, **59**, 496 (1955).

[16] K. G. Krasil'nikov and A. V. Kiselev, *Doklady Akad. Nauk S.S.S.R.*, **63**, 693 (1948).

[17] K. G. Krasil'nikov and A. V. Kiselev, *ibid.*, **69**, 817 (1949).

[18] A. V. Kiselev and V. V. Kulichenko, *ibid.*, **82**, 89 (1952).

[19] C. G. Gasser and J. J. Kipling, Proceedings of the Fourth Conference on Carbon, Pergamon Press, London, 1960.

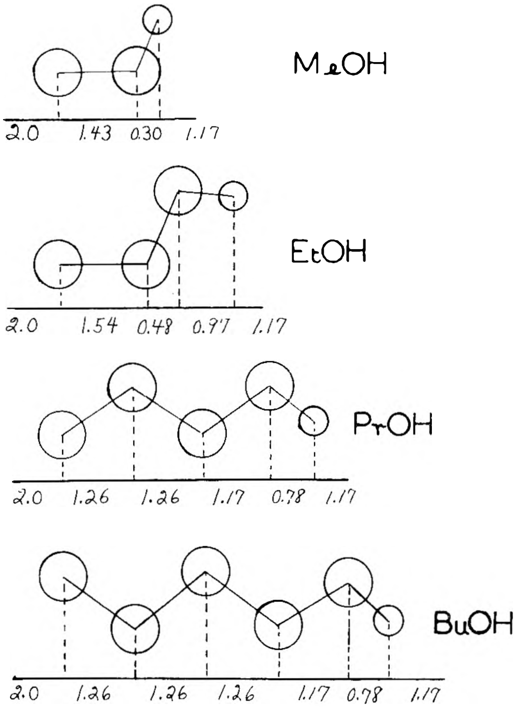

Fig. 2.—Configurations of alcohol molecules (distances in Å.).

Table I

Alcohol	Monolayer value, mmoles/g.	Calcd. molecular area (sq.Å.)	Ratio of calcd. molecular areas	Ratio of exptl. molecular areas	Ratio of molecular vol.[a]
Methyl	7.04	16.7	0.53	0.53	0.54
Ethyl	4.89	25.4	0.81	0.77	0.78
Propyl	3.75	31.4	1.00	1.00	1.00
n-Butyl	3.09	36.6	1.17	1.21	1.22
Isobutyl	2.88	37.8	1.20	1.30	1.24
n-Amyl	2.58	41.8	1.33	1.45	1.45
Isoamyl	2.53	44.5	1.42	1.48	1.46
Benzene	3.05				

[a] Calculated from data given by J. Timmermans, "Physico-Chemical Constants of Pure Organic Compounds," Elsevier, London, 1950.

This suggests that the molecules lie with the hydrocarbon chain parallel (not perpendicular) to the surface of the charcoal. The configurations are shown in Fig. 2. Calculations have been made of the corresponding areas occupied at a surface and are given in column three of Table I. There is a regular increment, corresponding to the addition of each $-CH_2$ group, beyond propyl alcohol, *i.e.*, there is a linear relation between molecular area and chain-length. Methyl and ethyl alcohol however, have slightly narrower molecules and there is consequently a slight departure from this regularity at the beginning of the homologous series. The ratio of these calculated areas agrees very closely with the ratio of the areas found experimentally.

The coincidence of the ratios is not, of itself, sufficient proof that the alcohol molecules are oriented in this way. Gregg and Stock have recently pointed out that for the normal paraffins, there is a linear relation between molecular volumes as well as molecular areas and the number of carbon atoms in the chain.[20] The adsorption might therefore be condensation of the vapor in pores or channels to a liquid-like condition and the data would give no indication of the orientation of these molecules at the solid surface. The adsorption of the hydrocarbons on ammonium phosphomolybdate, although giving Type I isotherms was, in fact, best interpreted in terms of capillary condensation.

For the alcohols, there is also a linear dependence of both molecular area and molecular volume on the number of carbon atoms in the molecule; this relationship, moreover, holds almost as well for the branched-chain as for the straight-chain molecules. In the present case, we think that adsorption is confined to a monolayer except at very high relative pressures. Subsidiary evidence relates to the straight-chain aliphatic acids to which the same arguments apply and for which a similar linear relationship between molecular area occupied on charcoal and number of carbon atoms in the molecule has been found.[21] These acids are probably adsorbed mainly in the dimeric form so that their adsorption is rather less sensitive to the polar nature of the surface than is the adsorption of alcohols. If the acetic and butyric acid vapors are adsorbed on the non-porous carbon black, Spheron 6 (which has a surface chemically similar to that of the charcoal, but probably more highly oxygenated), Type II isotherms are observed, indicative of multilayer adsorption. The monolayer values, however, are in the ratio required for orientation of the molecule with the major axis parallel to the surface (Table II). Moreover, the surface area of the solid calculated on this basis agrees closely (104 sq. m./g.) with the area determined from nitrogen adsorption (110 sq. m./g.).[22] Thus, if the first layer in multilayer adsorption on a non-porous carbon surface has this orientation, it seems highly probable that the only layer in unimolecular adsorption on the porous charcoal has the same orientation of the molecules.

Table II

	Monolayer value, (mmoles/g.)	Calcd. molecular area (sq. Å.)[a]	Ratio of calcd. molecular areas	Ratio of exptl. molecular areas
	Adsorption on Spheron 6			
Acetic acid	0.87[b]	19.6	1.00	1.00
n-Butyric acid	0.54	31.4	1.60	1.61
	Adsorption on charcoal			
Acetic acid	5.65	19.6	1.00	1.00
n-Butyric acid	3.60	31.4	1.60	1.57

[a] Expressed in terms of monomer molecules, although the adsorbate is probably mainly dimer. [b] We are indebted to Dr. A. Blackburn for this result.

In passing, we note that aliphatic compounds are adsorbed on some solids with the hydrocarbon chain perpendicular to the surface (stearic acid on alumina,[23] various fatty acids on anatase,[24] palmitic

---

(20) S. J. Gregg and R. Stock, *Trans. Faraday Soc.*, **53**, 1355 (1957).

(21) A. Blackburn and J. J. Kipling, *J. Chem. Soc.*, 1493 (1955).

(22) R. A. Beebe, J. Biscoe, W. R. Smith and C. B. Wendell, *J. Am. Chem. Soc.*, **69**, 95 (1947).

(23) A. S. Russell and C. N. Cochran, *Ind. Eng. Chem.*, **42**, 1332 (1950).

acid on Raney nickel,[25] though in the last case, at least, it is clear that chemisorption, not physical adsorption, is involved). By contrast, the lower alcohols occupy areas on alumina and anatase[26] which approximate to those given in Table I. It seems, therefore, that the parallel orientation is likely to be adopted on relatively non-polar surfaces, but that the perpendicular orientation may sometimes be adopted on the more polar surfaces.

3. The Polarity of the Surface.—The individual isotherms are presented in Fig. 3. They show that, at high alcohol concentrations, the alcohol competes with benzene for the surface the more effectively, the higher it stands in the homologous series, *i.e.*, the higher the proportion of hydrocarbon to hydroxyl character in the molecule. The iso-alcohols compete less effectively with benzene for the surface than do the *n*-alcohols.

At low alcohol concentrations, the competition is in the reverse order if the adsorption of alcohol is considered in terms of millimoles/g. (or alternatively of mole fraction in the adsorbate) (Fig. 4). Two possible reasons for this are now considered.

The major influence of the polarity of an adsorbing surface is seen by comparing the present results with those obtained for adsorption from the same liquid mixtures on oxide adsorbents.[8,5,27] A highly polar surface adsorbs the more polar component of a mixture (*e.g.*, an alcohol) preferentially to the less polar component (*e.g.*, benzene). Contrary to Bartell and Sloan's generalization,[7] this may occur at all concentrations, giving a composite isotherm which is U-shaped and not S-shaped like those of Fig. 1. A U-shaped isotherm may also be found when the surface is relatively non-polar but homogeneous (methyl alcohol-benzene and *n*-butyl alcohol-benzene with Graphon[19]). Such a situation also pertains for the system ethyl alcohol-benzene at the liquid-vapor interface,[28] where, although there is no solid adsorbent, homogeneous conditions are found. The question, therefore, arises as to whether S-shaped composite isotherms (in particular those for the present liquid mixtures) reflect a heterogeneity of the solid surface.

Few carbons are free from surface hydrogen and oxygen atoms.[29] and analysis of the charcoal used in the present work shows the presence of a significant quantity of oxygen,[30] some if not all of which may be assumed to be present in the surface. Such oxygen complexes are much more polar in character than the rest of the surface which may be regarded as essentially hydrocarbon in nature.

Figure 3 shows that at about 0.1 mole fraction of alcohol, the amount of benzene adsorbed is very nearly the same for all systems. This means that the same area of surface ($^1/_5$ to $^1/_6$ of the total) is available to the alcohol at this mole fraction, whichever member of the series it may be. The decreasing number of millimoles taken up as the

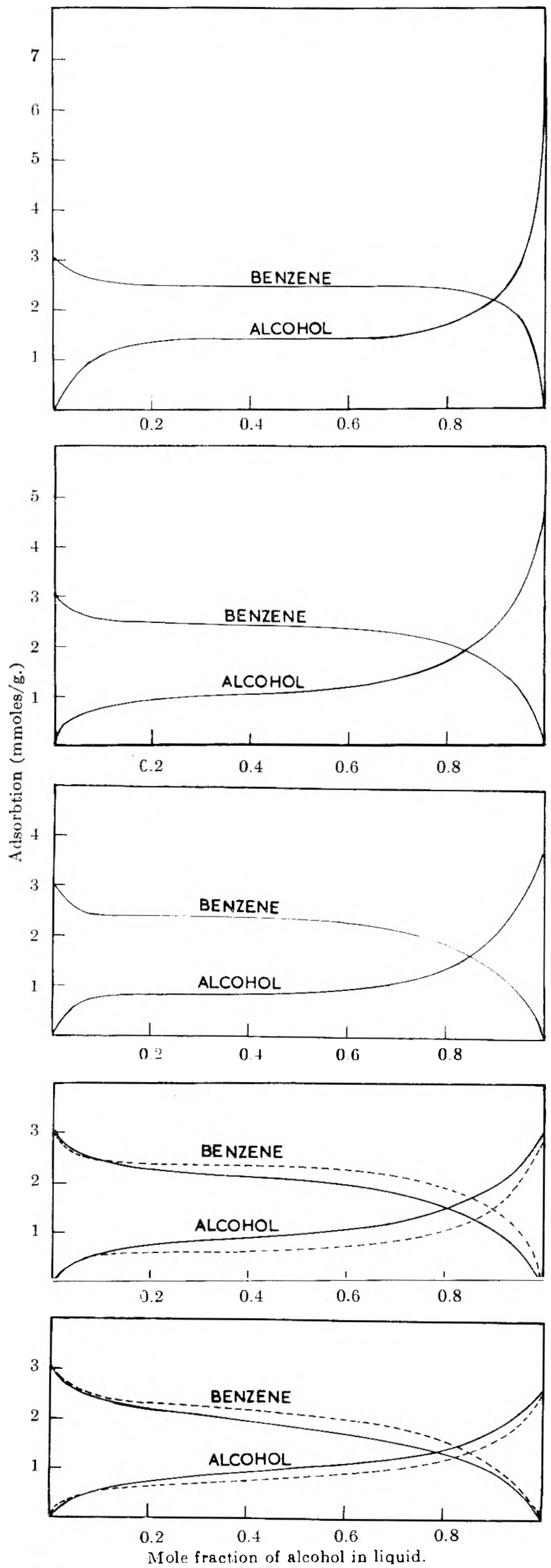

Fig. 3.—Adsorption (individual isotherms, starting from top a-e): (a) MeOH-C_6H_6; (b) EtOH-C_6H_6; (c) PrOH-C_6H_6; (d) ——, *n*-BuOH-C_6H_6; – – –, *iso*-BuOH-C_6H_6; (e) ——, *n*-AmOH-C_6H_6; – – –, *iso*-AmOH-C_6H_6.

---

[24] L. Dintenfass, *Kolloid-Z.*, **155**, 121 (1957).

[25] H. A. Smith and J. F. Fusek, *J. Am. Chem. Soc.*, **68**, 229 (1946).

[26] E. Calvet and B. Astruc, *Mem. Serv. Chim. l'Etat.*, **36**, 401 (1951).

[27] J. J. Kipling and D. B. Peakall, *J. Chem. Soc.*, 4054 (1957).

[28] J. L. R. Morgan and A. J. Scarlett, *J. Am. Chem. Soc.*, **39**, 2275 (1917).

[29] J. J. Kipling. *Quart. Revs.*, **10**, 1 (1956).

[30] A. Blackburn, J. J. Kipling and D. A. Tester, *J. Chem. Soc.*, 2373 (1957).

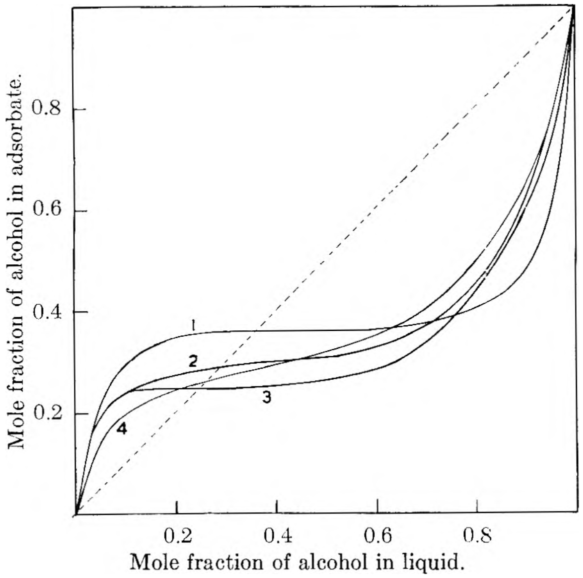

Fig. 4.—Adsorption from alcohol–benzene systems: (1) MeOH–C_6H_6; (2) EtOH–C_6H_6; (3) PrOH–C_6H_6; (4) n-BuOH–C_6H_6.

homologous series is ascended reflects the increase in molecular size.

The preferential adsorption of the alcohols at this concentration may thus be attributed to their specific adsorption at oxygen sites on the surface by which they are more strongly held, possibly by hydrogen-bonding, than is benzene. Over the rest of the surface (the hydrocarbon fraction) benzene can be more strongly held than the alcohols. This phenomenon is the more likely to be noticed at low concentrations because the alcohols then are present to a greater degree as monomeric molecules, having free hydroxyl groups, whereas they exist as dimers or higher polymers at higher concentrations in relatively non-polar solvents,[31] and are presumably less able to form strong bonds at the oxygen sites.

If all the oxygen in the charcoal is present at the surface, it would occupy about $^1/_5$ of the area. It is thus possible that the fraction of the surface occupied by the individual alcohols at 0.1 mole fraction is related to the chance that their molecules are adsorbed at an oxygen site. The chance would be high for methyl alcohol, but would decrease with increase in chain length (assuming that the molecules are oriented as described above) due to overlapping of adjacent sites by the hydrocarbon chains.

4. The Interaction between the Liquid Components.—It is important to consider S-shaped composite isotherms from another standpoint. Jones and Mill[32] have suggested that they reflect gross deviations of the liquid mixture from ideal behavior. S-shaped composite isotherms always imply that the individual isotherms show a point of inflection.[30] Jones and Mill consider that this should not be present if the individual adsorption isotherms are plotted against equilibrium *vapor* mole fractions instead of equilibrium *liquid* mole fractions. They have shown that replotting of isotherms in this way does remove the point of inflection in some cases.

Undoubtedly the present systems do show gross deviations from ideal behavior, as Table III indicates. Replotting the individual isotherms against vapor mole fraction does alter their shape, but appears not to eliminate the point of inflection completely. The departure from ideality of mix-

Table III

Partial Pressures at 20°[a]

(a) Methyl alcohol–benzene

Mole fraction of MeOH	p_{MeOH} (mm.)	$p_{C_6H_6}$ (mm.)
0.000	0.0	74.5
.106	56.1	70.9
.133	60.7	71.8
.196	66.3	71.2
.199	67.4	70.2
.368	69.5	68.6
.408	71.4	66.1
.510	74.2	66.8
.514	75.5	65.5
.633	77.3	62.7
.657	77.3	62.2
.815	83.7	49.1
.851	85.7	45.3
.917	90.8	32.2
1.000	96.0	0.0

(b) n-Propyl alcohol–benzene

Mole fraction of PrOH	p_{PrOH} (mm.)	$p_{C_6H_6}$ (mm.)
0.000	0.0	74.5
.085	6.2	69.8
.118	6.7	71.3
.305	9.9	65.5
.375	10.4	63.6
.564	11.0	58.5
.672	11.0	51.5
.762	12.2	43.9
.855	12.6	33.2
.902	13.2	24.1
1.000	14.3	0.0

(c) n-Butyl alcohol–benzene

Mole fraction of BuOH	p_{BuOH} (mm.)	$p_{C_6H_6}$ (mm.)
0.000	0.0	74.5
.112	2.2	71.0
.118	2.1	68.7
.299	2.6	65.8
.397	2.6	61.6
.500	3.0	58.0
.542	3.5	54.5
.649	3.3	47.7
.731	3.5	44.0
.743	4.1	42.1
.794	4.1	37.7
.843	3.5	29.9
.948	3.6	9.4
1.000	4.5	0.0

[a] Data for the system ethyl alcohol–benzene are given in ref. 6.

---

(31) K. L. Wolf, *Trans. Faraday Soc.*, **33**, 179 (1937); *cf.* W. C. Coburn and E. Grunwald, *J. Am. Chem. Soc.*, **80**, 1318 (1958); E. D. Becker, U. Liddel and J. N. Shoolery, *J. Molecular Spectroscopy*, **2**, 1 (1958).

(32) D. C. Jones and G. S. Mill, *J. Chem. Soc.*, 213 (1957).

tures of the lower alcohols with benzene is so great that it is difficult to plot the curves accurately at low mole fractions, but we are satisfied that there remains a residual inflection which can only be explained in terms of a heterogeneous solid surface.

This is not to minimize the important consideration put forward by Jones and Mill. It is clearly a significant factor in controlling adsorption from the present systems. The added factor of surface heterogeneity, however, makes the total process of adsorption more complex than might have been expected for such relatively simple systems. (Its importance in the chemistry of pigments has been discussed recently by Dintenfass.[24]) Both factors should be taken into account in future work of this kind.

Acknowledgment.—We acknowledge gratefully financial assistance from British Industrial Solvents (a division of The Distillers Company Limited).

KINETICS OF THE THIONINE-FERROUS ION REACTION

By S. Ainsworth[1]

Photosynthesis Project, University of Illinois, Urbana, Illinois

Received August 13, 1959

The initial quantum yield of photoreduction of thionine by ferrous ions and the extent of bleaching in the photostationary state are measured. The data are explained by postulating two mechanisms: in one, a long-lived, excited species of thionine is reduced by encounters with ferrous ions; in the other, an electron transfer, followed by dissociation, occurs on excitation of a complex formed in the dark between thionine and ferrous ions. The first mechanism appears to predominate when $[Fe^{2+}] \leq 10^{-3}\,M$, the second at higher $[Fe^{2+}]$. The finite rate of re-formation of the complex accounts for the phenomenon of light saturation in the $[Fe^{2+}]$-range between 10^{-2} and $10^{-1}\,M$. Ferric ions are found to quench the reaction strongly.

1. Introduction

The reversible photochemical oxidation-reduction system

$$T + nFe^{2+} \underset{\text{dark}}{\overset{\text{light}}{\rightleftarrows}} (S + L) + nFe^{3+}$$

where T is the purple cationic dye thionine, and S and L its colorless reduced forms (the free radical semithionine and the fully reduced leucothionine, respectively) was first described by Weber[2] and by Weiss,[3] and later studied quantitatively by a succession of workers. Rabinowitch[4] measured spectrophotometrically the photostationary concentration $[T_s]$ as a function of the incident light intensity I_0 and the concentrations of T, Fe^{2+}, Fe^{3+} and H^+. He set out the general reaction mechanism

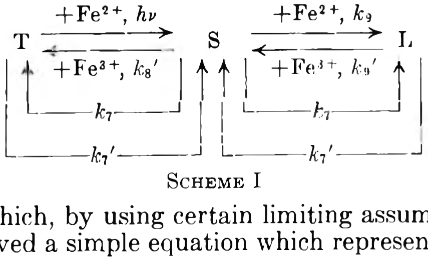

Scheme I

from which, by using certain limiting assumptions, he derived a simple equation which represented the data at [T] below $10^{-5}M$. At higher [T] the extent of photostationary bleaching fell below expectation.

Hardwick[5] and Schlag,[6] in independent studies, concluded that the forward photochemical reaction occurs *via* a reaction between thionine in the triplet state and ferrous ions. They agreed, too, that ferric ions quench excited thionine molecules thus reducing the initial quantum yield, γ_i, of the forward reaction. Schlag also examined the absorption spectrum of a bleached solution of thionine in the photostationary state and found that L formed the predominant part of the reduced dye: this conclusion conflicts with the argument, advanced by Hardwick, that [L] can be neglected compared to [S], both in the initial and the photostationary state.

Havemann and Pietsch[7] measured the quenching of fluorescence of T by ferrous ions as a function of $[Fe^{2+}]$ and temperature. They interpreted their data by assuming the formation of non-fluorescent complexes. Correlation of these results with a few orienting rate measurements led them to conclude that the complex was the photosensitive species. The absorption spectrum of the complex was found to be hardly different from that of the free dye. The results of a later kinetic study by Havemann and Reimer[8] were found to be consistent with the postulate of a photosensitive complex.

The present study included measurements of γ_i, $[T_s]$ and the rate of the back reaction. $[T_0]$ was varied between 2 and $6 \times 10^{-6}M$, that is, below the region where [T] begins to affect the quantum yield. I_0 and $[Fe^{2+}]$ were varied over a wide range. It was concluded that the reaction occurs *via* kinetic encounters of excited thionine molecules with ferrous ions only at $[Fe^{2+}]$ below $10^{-3}M$. At higher $[Fe^{2+}]$, the reaction proceeds mainly through internal electron transfer in $T \cdot Fe^{2+}$ complexes, which are formed at a finite rate in the dark. It was also found that at high $[Fe^{2+}]$, an increase of $[Fe^{2+}]$ diminishes γ_i.

These conclusions are incorporated in Schemes II and III.

---

[1] Now at Sheffield University, Sheffield, England, Chemistry Department.

[2] K. Weber, *Z. physik. Chem.*, **B15**, 18 (1931).

[3] J. Weiss, *Nature*, **136**, 794 (1935).

[4] E. Rabinowitch, *J. Chem. Phys.*, **8**, 551 (1940).

[5] R. Hardwick, *J. Am. Chem. Soc.*, **80**, 5667 (1958).

[6] J. Schlag, *Z. physik. Chem. Neue Folge*, **20**, 53 (1959).

[7] R. Havemann and H. Pietsch, *Z. physik. Chem.* (*Leipzig*), **208**, 98 (1957).

[8] R. Havemann and K. G. Reimer, *ibid.*, **211**, 63 (1959).

Scheme II

(for $[Fe^{2+}] > 10^{-3}\ M$)

$$(1)\quad T + Fe^{2+} \xrightleftharpoons[k_1']{k_1} T \cdot Fe^{2+} \quad (K_1 = k_1/k_1')$$

$$(2)\quad T \cdot Fe^{2+} + h\nu \xrightarrow{2I_0\bar{e}} {}^{*}T \cdot Fe^{2+} \longrightarrow {}^{3}T \cdot Fe^{2+}$$

$$(3)\quad {}^{3}T \cdot Fe^{2+} \longrightarrow T \cdot Fe^{2+} + \text{heat}$$

$$(4)\quad {}^{3}T \cdot Fe^{2+} + Fe^{3+} \longrightarrow T \cdot Fe^{2+} + Fe^{3+}$$

$$(5)\quad {}^{3}T \cdot Fe^{2+} + Fe^{2+} \longrightarrow T \cdot Fe^{2+} + Fe^{2+}$$

$$(6)\quad {}^{3}T \cdot Fe^{2+} \longrightarrow S + Fe^{3+}$$

$$(7)\quad 2S \xrightleftharpoons[k_7']{k_7} T + L$$

$$(8')\quad S + Fe^{3+} \longrightarrow T + Fe^{2+}$$

$$(9')\quad L + Fe^{3+} \longrightarrow S + Fe^{2+}$$

The delay between excitation (2) and electron transfer, involving intermediate formation of the triplet state (6), is discussed below.

Scheme III

(for $[Fe^{2+}] < 10^{-3}\ M$)

$$(10)\quad T + h\nu \xrightleftharpoons{2I_0\bar{e}} {}^{*}T \longrightarrow {}^{3}T$$

$$(11)\quad {}^{3}T \longrightarrow T + \text{heat}$$

$$(12)\quad {}^{3}T + Fe^{3+} \longrightarrow T + Fe^{3+}$$

$$(13)\quad {}^{3}T + Fe^{2+} \longrightarrow S + Fe^{3+}$$

Reactions 7, 8′ and 9′ complete Scheme III. It is assumed that collisional quenching of the excited singlet state does not occur at the low concentrations of reactants employed in these experiments.

II. Experimental

An apparatus for cross illumination of a solution by strong actinic light and a weak scanning beam, was used to determine [T] in the illuminated solution.

The thionine used was Hartmann–Leddon Co. stain, 86% pure according to the manufacturer. It was not further purified. Chromatography suggested the presence of a very minor bluish impurity. [T] was determined spectrophotometrically using an extinction coefficient obtained by Rabinowitch and Epstein[9] with recrystallized material.

Solutions of T, ferrous ammonium sulfate and ferric ammonium sulfate were prepared using de-aerated *p*H 2 buffer (0.2 *M* acetate) as medium and were stored in tonometers under nitrogen atmospheres. Samples to be bleached were prepared by transferring suitable aliquots of the stock solutions to glass photolysis cells. All samples were de-oxygenated by evacuation with a rotary oil pump. The cells were then closed and the solutions studied under vacuum.

Ferric contamination of the ferrous salt was assumed to amount to 0.01% as indicated in manufacturer's specifications.

Measurements of the normal potential of the ferrous–ferric system in 0.2 *M* acetate, gave a value of 0.7 volt as against the known value 0.77 volt in perchlorate.[10] This suggests about 90% complexing of ferric ions by acetate ions (assuming that complexing of ferrous ions is negligible).

The photolysis cell was placed within a Lucite bath through which water from a thermostat was circulated.

Photolyzing light from a 1000 watt projection lamp was passed through a heat filter and the image of a rectangular diaphragm, placed close to the condenser lens, was thrown upon the reaction cell, illuminating its contents uniformly (so-called Köhler optical system). The intensity of the light was controlled by stops at the focus of the condenser lens. In addition, a 600 mμ interference filter was introduced into the optical path when low light intensities were needed. The back of the photolysis cell was silvered to improve the uniformity of illumination throughout the cell, thus increasing the light absorption by a factor of about 2.

Scanning light from a ribbon filament lamp was focussed on the photolysis cell. The intensity was reduced by a variable aperture so as not to cause measurable photolysis. Light transmitted by the reaction solution at 600 mμ was recorded photoelectronically using a Farrand monochromator and a Tektronix 502 oscilloscope.

The intensity of the photolyzing light, after passing through the thermostated bath, was measured with a calibrated Eppley thermopile. The light incident on the thionine solution was obtained from the measured intensity by multiplication with an independently determined factor.

Average decadic molar extinction coefficients $\bar{\alpha}$ and the corresponding natural extinction coefficients $\bar{e}$ of thionine were determined using the thermopile: the values of $\bar{\alpha}$ for white light and for light transmitted by the 600 mμ interference filter were 0.96 and 3.8×10^4, respectively, both relative to the value of 5.7×10^4 given by Rabinowitch and Epstein[9] for monochromatic light of 600 mμ. The relation of optical density to [T] was linear over the range 0–6 $\times$ 10^{-6} *M*, indicating absence of dimerization.

The number of quanta absorbed was calculated from the average frequency of the photolyzing light, assuming the color temperature of the source to be 3000°K. and allowing for the absorption spectra of the filters and of the thionine solution.

The photochemical event was initiated by opening the oscilloscope camera shutter. This was synchronized with a trigger pulse to the oscilloscope and the opening of a shutter at the focus of the condenser lens. The light shutter opened completely in 10 msec., a time about one-tenth as long as the half time of the fastest reaction studied.

Initial quantum yields were obtained by measuring the reaction rate over the first 5–10% of the reaction. The extent of bleaching in the photostationary state was determined by measuring the transmission of thionine in light and dark and calculating the ratio $(OD_0 - OD_s)/OD_s$.

III. General Results

The main observations that suggested modification of earlier reaction schemes were made in measurements of $[T_s]$ as a function of light intensity and of γ_i as a function of $[Fe^{2+}]$.

Figure 1 shows ω[11] (the ratio of bleached to unbleached thionine in the photostationary state) as a function of $I_0\bar{e}$, for different values of $[Fe^{2+}]$. The most striking feature of these curves is that for $[Fe^{2+}]$ between 10^{-2} and 10^{-1} *M* they show clearly the phenomenon of light saturation.

Light saturation suggests that one of the reactants accumulates, in light, in a form in which it cannot undergo the photochemical reaction (or can undergo it only with a much lower quantum yield). Since ferrous ions are present in large excess, the effect must be attributed to thionine. We suggest, as an explanation, that thionine reacts with Fe^{2+} ions with a high quantum yield only if the reactants are combined in a complex, and not (or only with a much lower quantum yield) if they are separated and can react only be kinetic encounters. A further assumption must be made: that when bleached thionine is reoxidized to T, the latter arises in the form of free T, and is complexed at a finite rate—perhaps because T is present as a positive ion and electrostatic repulsion betweeen it and Fe^{2+} must be overcome for the complex to be formed. Light saturation occurs when the rate of complex formation limits the over-all rate of the photochemical reaction.

The disappearance of light saturation at the highest $[Fe^{2+}]$ (in the range of light intensities employed here) can be due, in part, to the increase in rate of complex formation with increasing $[Fe^{2+}]$.

---

(9) E. Rabinowitch and L. F. Epstein, *J. Am. Chem. Soc.*, **63**, 69 (1941).

(10) W. C. Schumb, M. S. Sherrill and S. B. Sweetser, *J. Am. Chem. Soc.*, **59**, 2360 (1937).

(11) More precisely, $\omega \times [Fe^{3+}]$, *cf.* eq. (5) and (7).

Another contributing factor is suggested by measurements of the quantum yield of bleaching as a function of $[Fe^{2+}]$ shown in Fig. 2. Both γ_i, and the quantum yield calculated from stationary state measurements, γ_s, go through a maximum in the region of $[Fe^{2+}] = 4 \times 10^{-2}$ M, indicating that ferrous ions participate in both the forward and back reaction, and that these two reactions are not in direct competition. This effect may be interpreted as a quenching of the excited complex by Fe^{2+} ions, as suggested in Scheme II, eq. (5). Alternatively, it is possible to suppose that quenching is merely due to the ferric impurity in the ferrous salt employed being higher than specified by the manufacturer. Steady-state equations derived by using either assumption suggest that light saturation must disappear at high $[Fe^{2+}]$.

IV. Measurements of the Initial Quantum Yield

From Fig. 1, we can conclude (*cf.* section V) that at $[Fe^{2+}] > 10^{-2}$ M the forward reaction occurs, in the photostationary state, mainly *via* the complex. For the *initial* quantum yield, this should be true down to even smaller concentrations, because the dark equilibrium concentration of the complex prevails during the measurement; while in the photostationary state, this concentration may be considerably depleted. It can be assumed that the measured γ_i is that of the formation of S; for, as long as very little S is present, its dismutation must be negligible. Hence

$$\gamma_i = \frac{\Delta T\alpha}{\Delta t(2I_0\bar{e}[T_0])} \qquad (1)^{12}$$

where $\Delta T\alpha$ is the number of moles/liter of "analytical T" disappearing during the time Δt, when the incident light is I_0 and the rate of light absorption is therefore $2I_0\bar{e}[T_0]$ (the path of light back and forth through the vessel being 2 cm.).

Assuming that the concentration of excited complex obeys the steady-state equation, and that the concentration of complex equals its dark equilibrium concentration, we obtain, from Scheme II

$$\frac{1}{\gamma_i} = \frac{k_3 + k_6 + k_4[Fe^{3+}]}{k_6K_1[Fe^{2+}]} + \frac{k_5 + K_1k_3 + K_1k_6 + K_1k_4[Fe^{3+}]}{k_6K_1} + \frac{k_5[Fe^{2+}]}{k_6} \qquad (2)$$

The corresponding expression for the encounter mechanism III is

$$\frac{1}{\gamma_i} = \frac{k_{11} + k_{12}[Fe^{3+}] + k_{13}[Fe^{2+}]}{k_{13}[Fe^{2+}]} \qquad (3)$$

Dependence of γ_i on I_0 and $[T_1]$.—Equation 1 predicts that plots of $\Delta T\alpha/\Delta t(2I_0\bar{e})$ *vs.* $[T_0]$ and $\Delta T\alpha/\Delta t[T_0]$ *vs.* $I_0\bar{e}$ will be linear. This has been confirmed with good accuracy. Plots of the latter relation were used to calculate γ_i.

Dependence of γ_i on $[Fe^{2+}]$.—Equation 3, for Scheme III, suggests a linear relation between $(\gamma_i)^{-1}$ and $[Fe^{2+}]^{-1}$. In contrast, equation 2, for Scheme II, indicates that $(\gamma_i)^{-1}$ should change linearly with $[Fe^{2+}]^{-1}$ at low ferrous concentrations and with $[Fe^{2+}]$ at higher concentrations, and that the function will have a minimum when

$$\frac{k_3 + k_6 + k_4[Fe^{3+}]}{k_5K_1} = [Fe^{2+}]^2 \qquad (4)$$

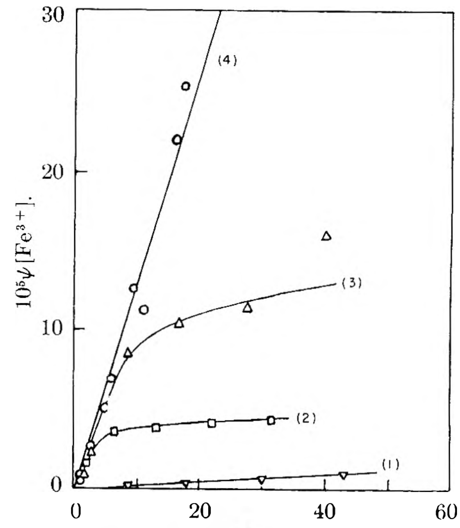

Fig. 1.—Effect of $I_0\bar{e}$ on photostationary bleaching at $[Fe^{2+}]$ = (1) 1×10^{-4}; (2) 3×10^{-2}; (3) 1×10^{-1}; (4) 2×10^{-1} M. $[T_0] = 2 \times 10^{-6}$ M; pH 2; 20°; $[Fe_s^{3+}]$ is taken as the sum of $[Fe^{3+}]$ produced by bleaching, and $[Fe^{3+}]$ introduced as an impurity in the ferrous salt. The light saturation effect was found at the $[Fe^{2+}] = 1 \times 10^{-1}$, 7.5×10^{-2}, 5×10^{-2}, 3×10^{-2}, 2×10^{-2}, 1×10^{-2} M.

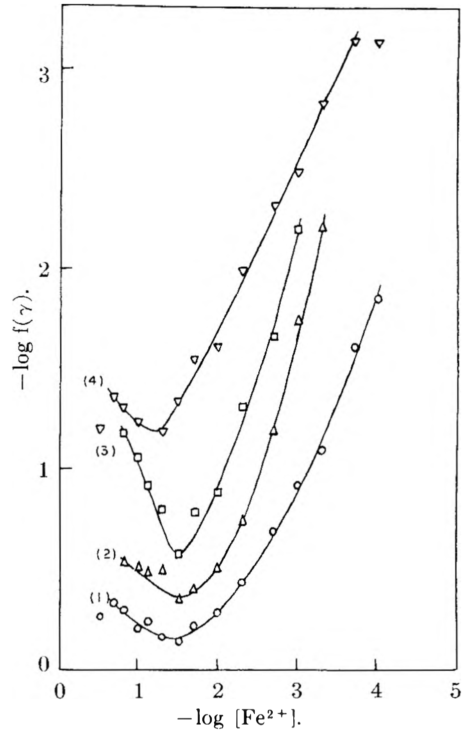

Fig. 2.—Effect of $[Fe^{2+}]$ on quantum yield. The ordinates of the curves are: (1) $-\log \gamma_i - 0.3010$; (no added ferric salt). (2) $-\log \gamma_i - 0.3010$; ($[Fe^{3+}] = 6 \times 10^{-4}$ M). (3) $\log (k_9'/\gamma_s) - 3.00$; ($[Fe^{3+}] = 6 \times 10^{-4}$ M). (4) $\log (k_9'/\gamma_s) - 3.477$; (no added ferric salt). $[T_0] = 2 \times 10^{-6}$ M; pH 2; 20°.

Figure 2 shows two series of relevant experiments. Addition of ferric salt to the reaction solutions (curve 2 *vs.* curve 1) has little influence on the position of the minimum: further, it appears to increase the slope at low $[Fe^{2+}]$, while leaving that at high $[Fe^{2+}]$ unchanged. These relations are expected from equation 2.

---

[12] The optical density of the solution is low enough to assume that the rate of absorption is proportional to $[T_0]$.

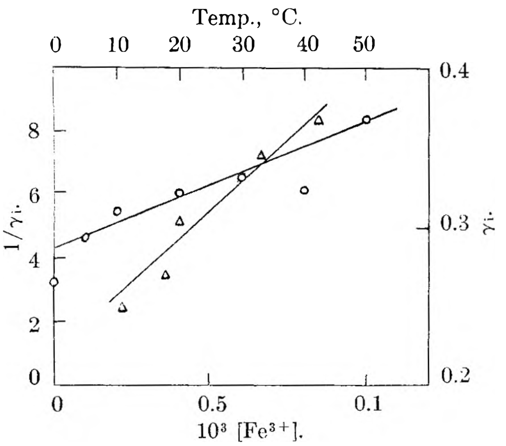

Fig. 3.—Effect of $[Fe^{3+}]$ (triangles) and temperature (circles) on quantum yield: (1) $(\gamma_i)^{-1} = f[Fe^{3+}]$. $[T_0] = 2 \times 10^{-6}$ *M;* $[Fe^{2+}] = 1 \times 10^{-1}$ *M;* *p*H 2; 20°. (2) $\gamma_i = f(\text{temp.})$; $[Fe^{2+}] = 1 \times 10^{-1}$ *M*. $[T_0] = 2 \times 10^{-6}$ *M;* *p*H 2; no added ferric salt.

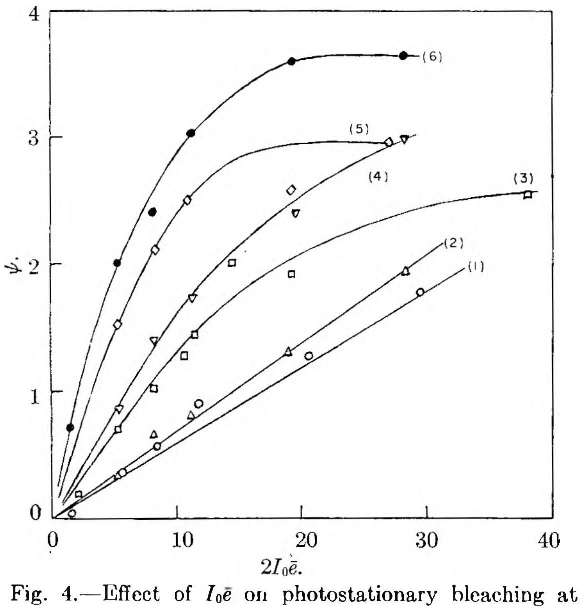

Fig. 4.—Effect of $I_0\bar{e}$ on photostationary bleaching at $[Fe^{3+}]$ = (1) 1×10^{-3}; (2) 8×10^{-4}; (3) 6×10^{-4}; (4) 4×10^{-4}; (5) 2×10^{-4}; (6) 1×10^{-4} *M*. $[T_0] = 2 \times 10^{-6}$ *M*, $[Fe^{2+}] = 1 \times 10^{-1}$ *M*, *p*H 2, 20°.

Plots of $(\gamma_i)^{-1}$ against $[Fe^{2+}]^{-1}$ for low, and against $[Fe^{2+}]$ for high ferrous concentrations are linear as expected from the limiting forms of equation 2.

Dependence of γ_i on $[Fe^{3+}]$.—Equation 2 may be re-arranged to predict a linear relation between $(\gamma_i)^{-1}$ and $[Fe^{3+}]$. This relationship is tested in Fig. 3 for $[Fe^{2+}] = 1 \times 10^{-1}$ *M*.

Dependence of γ_i on Temperature.—Figure 3 shows that γ_i increases linearly with temperature over the range from 10–50°, for experiments with $[Fe^{2+}] = 10^{-1}$ *M*, and without added ferric salt. This is the reverse of the observations of Havemann and Pietsch, who found that the initial rate of bleaching decreases with temperature when $[Fe^{2+}] = 10^{-2}$ *M*.

It will be noted that ours and Havemann's experiments relate to different branches of the curve $(\gamma_i)^{-1} = f[Fe^{2+}]^{-1}$ (Fig. 2) and, therefore, to sets of conditions in which the roles of ferrous ions are essentially different. The effect requires further investigation.

Calculation of Constants.—Ratios of the various constants may be calculated from the data illustrated in Figs. 2 and 3. The only approximation made was to neglect $k_4[Fe^{3+}]$ in experiments where no ferric salt was added to the solution. The ratios often may be evaluated in more than one way, and the resulting agreement confirmed the internal consistency of the data. The only exception was the relation of $(\gamma_i)^{-1}$ to $[Fe^{2+}]^{-1}$ for experiments at $[Fe^{3+}] = 6 \times 10^{-4}$ *M*, where the observed slope was "too great." These data, therefore, were not used in the evaluation of constants. The ratios have been calculated by assuming that S is the predominant reduction product in the initial stages covered by the measurements. The calculated ratios are

$$k_6:k_5:k_4:k_3 = 1:11:4.4 \times 10^3:2$$

$$K_1 = 200 \text{ liter mole}^{-1}$$

The value of $K_1 = 200$ is to be compared with the value of 30 obtained by Havemann and Pietsch by a completely independent method. This indicates that $[T]/[T{\cdot}Fe^{2+}]$ reaches unity at $[Fe^{2+}] = 5 \times 10^{-3}$ *M* (close to the concentration at which the encounter mechanism appears to yield place to the complex mechanism in the photostationary state). The ratio increases to 25 at $[Fe^{2+}] = 2 \times 10^{-4}$ *M;* for this, and lower, concentrations the complex concentration can no longer determine γ_i. However, this does not invalidate the ratios given above since they are derived using only data obtained at the higher $[Fe^{2+}]$.

The ratio of the quenching constants $k_5/k_4 = 2 \times 10^{-3}$ indicates that ferric ions quench the activated complex more efficiently than ferrous ion or, alternatively, that the ferric ion content of the ferrous ammonium sulfate was 0.2%—a content twenty times that specified by the manufacturer.

It is not possible to compare directly the ratios of constants given above with those reported by Hardwick or by Schlag, since they apply to different reaction mechanisms. However, the slope of the plot of $(\gamma_i)^{-1}$ *vs.* $[Fe^{3+}]$, reported by Hardwick, gives $k_4/k_6 = 2.2 \times 10^3$—a value close to that given above. On the other hand, the slope of the plot of $(\gamma_i)^{-1}$ *vs.* $[Fe^{2+}]^{-1}$ for constant $[Fe^{3+}] = 1.9 \times 10^{-4}$ *M* (Hardwick) is greater than expected on the basis of the ratios given above. A similar anomaly in the present experiments was noted earlier. These results relate to conditions where the initial concentration of ferrous ions and, therefore, also that of $T{\cdot}Fe^{2+}$, was low and where $[Fe^{3+}]$ was high enough to de-activate many of the excited complex molecules. Under these conditions, the complex mechanism may cease to be dominant.

V. Back Reaction Measurements

The initial rate of back reaction between reduced thionine and ferric ions in the dark was measured to be $k_9' = 650$ liter mole^{-1} sec.$^{-1}$, in fair agreement with Hardwick's value of about 460 at *p*H 1. Schlag, however, reports a much higher value for experiments at *p*H 2, namely, $k_9' = 2.75 \times 10^3$ liter mole^{-1} sec.$^{-1}$.

VI. Photostationary State

When the photostationary state is established, the rates of formation of T, T·Fe^{2+}, S and L will be equal to those of their disappearance. In order to obtain manageable rate equations, one can try to eliminate the least important reactions from Scheme I. To do this, one must decide whether S or L is the main product, and, if L, by what reactions it is produced and destroyed.

Schlag has concluded that L forms the predominant part of reduced thionine. The same conclusion may be reached in the following way. Parker[13] examined the corresponding methylene blue system and gave $k_8' = 1.8 \times 10^5$ and $k_9' = 30 - 100$. The finding that $k_8' >> k_9'$ is plausible because S is a much stronger reductant than L. The rate constant of recoloration of thionine has a value of about 650. By analogy with the methylene blue system, it seems reasonable to ascribe this value to k_9'. If this is valid, L would become the predominant form of bleached thionine in one photostationary state, since each reduced T molecule would go through the states S and L and dwell much longer in the second one.

Assuming then that L is the predominant species of bleached T in the photostationary state, Scheme I shows that there are four alternative mechanisms for its formation and disappearance. These are described in the following table by their reaction numbers. Each mechanism gives rise to a characteristic equation for ψ as a function of I_0, $[Fe_s^{3+}]$ and $[T_s]$. These are given below

Mechanism	Function
9–9′	$\psi^{-1} \alpha A[Fe_s^{3+}]^2 + B[Fe^{3+}]^3$
7–7′	$\psi \alpha (I_0)^2$
9–7′	$\psi \alpha [T_s]^{-1}$
7–9′	Equation 5

Hardwick's results, together with those of the present author, show that ψ^{-1} is proportional either to $[Fe_s^{3+}]^2$ or to $[Fe_s^{3+}]$, depending on the $[Fe^{2+}]$ values and light intensities used in the measurements. It is also well established that ψ is proportional to I_0 and independent of $[T_s]$. Accordingly, the first three mechanisms must be set aside. The fourth alternative implies the inequalities

$$k_9'[Fe^{3+}] >> k_7'[T]$$

$$k_7[S]\lambda >> k_8'[Fe^{3+}]$$

and hence

$$K_7 = \frac{k_7}{k_7'} >> \frac{k_8'[T]}{k_9'[S]}$$

Assuming, as we did, $k_8' >> k_9'$ and $[T] >> [S]$, we obtain $K_7 >> 10^2$. Michaelis and co-workers[14] have given $K_7 = 10^2$. However, Parker's experiments suggested that Michaelis' value of K_7 for methylene blue is too small and, in a private communication, Parker has stated that the behavior of thionine is qualitatively similar.

It therefore seems reasonable to adopt the fourth mechanism. This leads to a relation which, for Scheme III, has the form

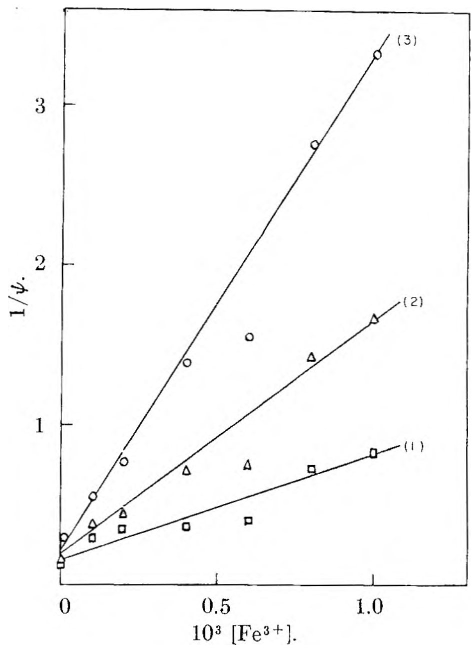

Fig. 5.—Effect of $[Fe^{3+}]$ on photostationary bleaching at $2I_0\bar{e}$ = (1) 20; (2) 10; (3) 5. $[T_0] = 2 \times 10^{-6}$ *M*; $[Fe^{2+}] = 1 \times 10^{-1}$ *M*; *p*H 2; 20°.

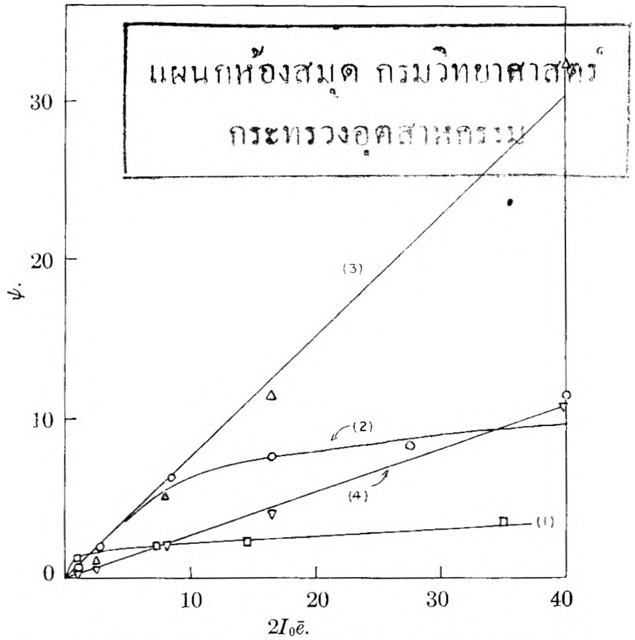

Fig. 6.—Effect of $I_0\bar{e}$ on photostationary bleaching at different temperatures: (1) 11.5°; (2) 20.0°; (3) 33.0°; (4) 43.0°. $[T_0] = 2 \times 10^{-6}$ *M*; $[Fe^{2+}] = 1 \times 10^{-1}$ *M*; *p*H 2; no added ferric salt.

$$\psi = \frac{2I_0\bar{e}\gamma_s}{k_9'[Fe_s^{3+}]} \quad (5)$$

This relation, and the corresponding one derived from Scheme II (equation 7), are found to represent the experimental results. It is concluded, therefore, that leucothionine is formed by dismutation and disappears by oxidation. Such a circular mechanism, inadmissible in true equilibria, is permissible in a photostationary state.

Photostationary State According to Scheme II.—From Scheme II it can be seen easily that in the photostationary state

---

(13) C. A. Parker, THIS JOURNAL, **63**, 26 (1959).

(14) L. Michaelis, M. P. Schubert and S. Granick, *J. Am. Chem. Soc.*, **62**, 204 (1940).

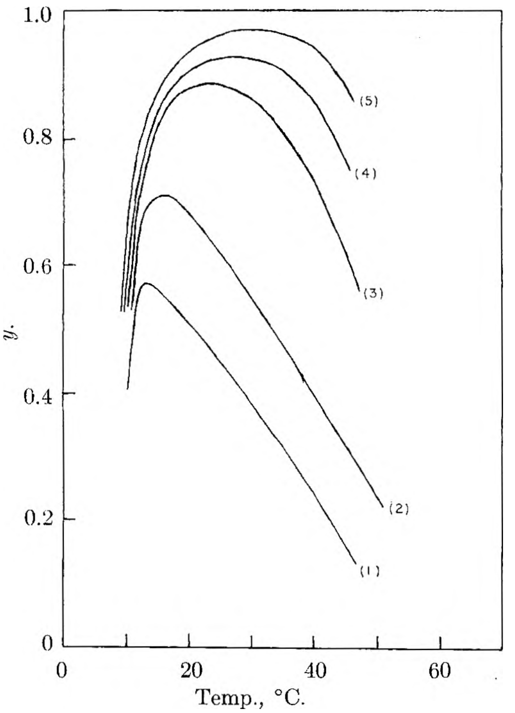

Fig. 7.—Effect of temperature on photostationary bleaching at different relative light intensities: (1) 6; (2) 12; (3) 20; (4) 43; (5) 100, where 100 corresponds approximately to $2I_0\bar{e} = 35$. $[T_0] = 2 \times 10^{-6}\ M$; $[Fe^{2+}] = 1 \times 10^{-1}\ M$; pH 2; no added ferric salt.

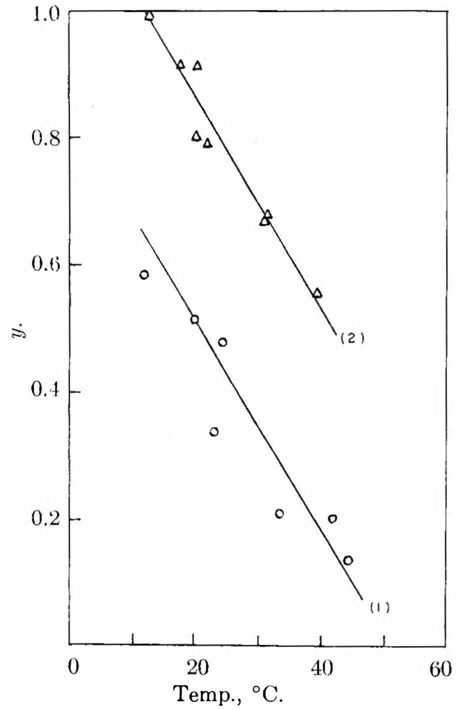

Fig. 8.—Effect of temperature on photostationary bleaching. (1) $[T_0] = 2 \times 10^{-6}\ M$; $[Fe^{2+}] = 1 \times 10^{-6}\ M$; no added ferric salt; pH 2; $2I_0\bar{e} = ca.\ 35$. (2) $[T_0] = 2 \times 10^{-6}\ M$; $[Fe^{2+}] = 1 \times 10^{-1}\ M$; $[Fe^{3+}] = 6 \times 10^{-4}\ M$; pH 2; $2I_0\bar{e} = ca.\ 35$.

$$k_1[T_s][Fe_s^{2+}] = 2I_0\bar{e}\gamma_s\,[T\cdot Fe^{2+}] = k_9'[L_s][Fe^{3+}] \quad (6)$$

and hence

$$\psi = \frac{[L_s]}{[T_s] + [T\cdot Fe^{2+}]} = \frac{2I_0\bar{e}\gamma_s k_1[Fe^{2+}]}{k_9'[Fe_s^{3+}](2I_0\bar{e}\gamma_s + k_1[Fe_s^{2+}])} \quad (7)$$

$$\frac{1}{\psi} = \frac{k_9'[Fe_s^{3+}]}{2I_0\bar{e}\gamma_s} + \frac{k_9'[Fe_s^{2+}]}{k_1[Fe_s^{2+}]} \quad (8)$$

Dependence of ψ on I_0.—The clearest distinction between Schemes II and III lies in the dependence of ψ on I_0. Equation 5, for the encounter mechanism, indicates that ψ is proportional to I_0 at all light intensities. In contrast, equation 7, for Scheme II, shows that ψ is proportional to I_0 only at low light intensities, while at high light intensities ψ reaches a plateau value equal to $k_1[Fe_s^{2+}]/k_9'[Fe_s^{3+}]$. The effect of increasing $[Fe^{2+}]$ is to enhance the rate of complex formation, $k_1[Fe_s^{2+}]$, and also to diminish γ by increasing the velocity of quenching, $k_5[Fe_s^{2+}]$ (see equation 2). Equation 7 shows that both these changes delay the onset of light saturation to higher light intensities. At the lower $[Fe^{2+}]$ the encounter mechanism prevails, resulting in a linear relation between ψ and I_0.

Figure 1 shows plots of ψ $[Fe_s^{3+}]$ *vs.* $I_0\bar{e}$ for a selection from a series of experiments at varying $[Fe^{2+}]$ but where no ferric salt was added to the reaction solutions. At low $[Fe^{2+}]$, the curves intercept the ψ-axis slightly below zero; the cause of this is not known. Hardwick, however, found similar intercepts so the effect may be significant. Another, similar, series of experiments was made, but with $[Fe^{3+}] = 6 \times 10^{-4}\ M$ throughout. In general, plots of ψ *vs.* $I_0\bar{e}$ were linear, but in the range $[Fe^{2+}] = 1.5 \times 10^{-1}$ to $0.75 \times 10^{-1}\ M$, the beginnings of light saturation could be seen. Again, most of the curves showed small negative intercepts on the ψ-axis.

Figure 4 shows that increasing $[Fe^{3+}]$, when $[Fe^{2+}] = 10^{-1}\ M$, delays the onset of light saturation. In part, this reflects the reduction in γ that is brought about by the increased velocity of quenching, $k_4[Fe^{3+}]$ (see equations 2 and 7). However, a second cause can be suggested. Equation 8, for Scheme II, indicates that $(\psi[Fe^{3+}])^{-1}$ is linearly related to $(I_0\bar{e})^{-1}$ with intercept $k_9'/k_1[Fe^{2+}]$. A similar relation is predicted by equation 5 for the encounter mechanism, but without an intercept. On testing the data shown in Fig. 4, no intercept was found until $[Fe^{3+}]$ fell to $4 \times 10^{-4}\ M$; the size of the intercept then increased progressively as $[Fe^{3+}]$ was reduced to $1 \times 10^{-4}\ M$. These changes indicate that increasing $[Fe^{3+}]$ enhances the importance of the encounter mechanism (perhaps because ferric ions quench the excited complex more efficiently than they do the excited thionine molecule) and, in consequence, the light saturation effect is absent or delayed at higher $[Fe^{3+}]$.

Dependence of ψ on $[Fe^{2+}]$.—Equations 5 and 8 predict a linear relation between $(\psi\ [Fe^{3+}])^{-1}$ and $(I_0e)^{-1}$ if γ_s remains independent of ψ, with slope k_9/γ_s. In estimating values of k_9'/γ_s, a correction was made for the negative constant referred to above. Plots of k_9'/γ_s *vs.* $[Fe^{2+}]^{-1}$ are shown in Fig. 2, where data from experiments with and without added ferric salt are illustrated. The minimum on curve 4 appears to be displaced to higher $[Fe^{2+}]$. However, this could well be due to an error in a single point and may not be significant. For a given value of $1/\gamma_i$, the value of k_9'/γ_s for experiments without added ferric salt is about ten times greater than for the corresponding experiments with added ferric salt. It appears, therefore, that the ferric impurity may be about ten times greater than the value specified by the manufacturer.

Values of γ_s may be calculated from the experiments where $[Fe^{3+}] = 6 \times 10^{-4}$ M by taking $k_9' = 650$. The maximum quantum yield occurs when $[Fe^{2+}] = 3 \times 10^{-2}$ M; at this concentration $\gamma_s = 0.17$ and $\gamma_i = 0.22$. The slightly lower value of γ_s is expected since the concentration of complex is lower in the photostationary than in the initial state of the system.

Dependence of ψ on $[Fe^{3+}]$.—If it is assumed that $\gamma_i \simeq \gamma_s$, we can show that for the encounter mechanism

$$\frac{1}{\psi} = \frac{A[Fe^{3+}]}{I_0\bar{e}} + \frac{B[Fe^{3+}]}{I_0\bar{e}[Fe^{2+}]} + \frac{C[Fe^{3+}]^2}{I_0\bar{e}[Fe^{2+}]}$$

The corresponding equation for the complex mechanism is

$$\frac{1}{\psi} = \frac{D[Fe^{3+}]}{I_0\bar{e}} + \frac{E[Fe^{3+}]}{[Fe^{2+}]} + \frac{F[Fe^{3+}]}{I_0\bar{e}[Fe^{2+}]} + \frac{G[Fe^{3+}]^2}{I_0\bar{e}[Fe^{2+}]}$$

(where $A \cdots G$ are ratios of constants). The equations indicate that ψ^{-1} may be proportional to $[Fe^{3+}]^2$ or to $[Fe^{3+}]$ according to the conditions of the experiments. Thus, both equations show that transition from the second power to the first power relationship takes place as $[Fe^{2+}]$ is increased. Further, in the second equation, the fourth term decreases relatively to the second term as I_0 increases. Since this same change is responsible for light saturation, we must always expect a dependence on the first power of $[Fe^{2+}]$ when light saturation occurs.

Hardwick has reported a linear relationship between ψ^{-1} and $[Fe^{3+}]^2$. In contrast, Fig. 5 shows a linear plot of ψ^{-1} *vs.* $[Fe^{3+}]$, with points derived from the results illustrated in Fig. 4. Comparison of the reaction conditions employed in these experiments with those of Hardwick shows that $[Fe^{3+}]$ values were the same over most of the range investigated. On the other hand, the $[Fe^{2+}]$ were 10 times, and the light intensities up to 30 times greater than those employed by Hardwick. Thus, dependence on the first or second power of $[Fe^{3+}]$ is determined by the other variables of the system in the manner predicted.

Dependence of Photostationary Bleaching on [T].—Equation 7 indicates that $[L_s]$ is a function of $([T_s] + [T{\cdot}Fe_s{}^{2+}])$, while equation 5 shows $[L_s]$ to be a function of $[T_s]$, both with zero intercept. Both these relationships have been confirmed by plots of $OD_0 - OD_s$ *vs.* OD_s, and for a range of thionine concentration varying between 0.5 and 4.0×10^{-6} M. No measurements were carried out at the higher values of [T], where Rabinowitch[5] found a strong "quenching" of the bleaching effect.

Dependence of Photostationary Bleaching on Temperature.—The effect of temperature on the photostationary state is illustrated in Figs. 6, 7 and 8. In those figures where temperature is plotted on the abscissa, the photostationary state is described by y, the fractional bleaching: y changes in the same sense as ψ, but more slowly at high values of y.

Figure 6 illustrates data from experiments where no ferric salt was added to the reaction solutions. It can be seen that as the temperature increases, the intensity of light required to bring about saturation increases, and also that ψ passes through a maximum. These changes indicate that both the rate of complex formation and the rate of reoxidation of L increase with temperature, and that the opposing influences of these reactions determine the absolute value of ψ.

These opposing influences are clearly shown in Fig. 7 where y is plotted as a function of temperature for a sequence of light intensities. At low light intensities y depends mainly on the rate of the back reaction: as this increases with temperature, so y decreases. At higher light intensities, the rate of complex formation limits y, until increasing temperature removes this limitation and restores control of y to the back reaction. The resulting maxima, therefore, move to higher temperatures with increasing light intensity. The relative values of the positive and negative slopes in Fig. 7 also indicate that the temperature coefficient of reaction 1 is greater than that of reaction 9′.

Figure 4 shows that light saturation behaviour becomes less important for solutions in which $[Fe^{2+}] = 10^{-1}$ M and $[Fe^{3+}] = 6 \times 10^{-4}$ M. Hence, y can be expected to become more dependent on the rate of the back reaction. Figure 8 shows that y decreases with temperature, and that there is no evidence of a maximum.

Again, the encounter mechanism is believed to predominate at low $[Fe^{2+}]$. Figure 8 shows that at $[Fe^{2+}] = 10^{-5}$ M, y decreases uniformly with temperature.

VII. Complex Formation

The kinetic work described in this paper led to the suggestion, advanced independently by Havemann and Pietsch on the basis of fluorescence data, that the photoreduction of thionine by ferrous ions takes place, to a large extent, by internal electron transfer within a $T{\cdot}Fe^{2+}$ complex. It is interesting that complexing has only a small effect on the absorption spectrum of thionine, but this is not without precedent. Thus Watson[15] and Bannister[16] found it necessary to postulate complex formation between phenylhydrazine (or ascorbic acid) and chlorophyll, without being able to find any changes in the absorption spectrum of the latter. In their studies, as here, the postulate of complex formation was suggested by kinetic evidence which was otherwise difficult to explain.

The fact that thionine molecules and ferrous ions are combined in a complex explains the high quantum yield of bleaching at ferrous concentrations above 10^{-2} M without the necessity of interposing a metastable state between excitation and electron transfer. However, the apparent similarity of the spectra of T and $T{\cdot}Fe^{2+}$ indicates that electron transfer from Fe^{2+} to T is not the direct result of light absorption, but follows the latter with a significant delay. Furthermore, the fact that quenching of the forward reaction by ferric ions is already evident at $[Fe^{3+}] = 10^{-4}$ M suggests that the complex survives, after excitation, at least for a time of the order of 10^{-6} or 10^{-5} second, in some long-

---

(15) W. F. Watson, *Trans. Faraday Soc.*, **48**, 526 (1952).

(16) T. T. Bannister, Thesis, Univ. of Illinois, 1958.

lived state in which it can be de-activated by encounters with ferric ions. The ratio k_3/k_6 shows that, in the absence of quenching by ferric ions, there is one chance in three for the energy of excitation to be utilized for the formation of products, S and Fe^{3+}. It may be, however, that electron transfer always takes place, but is followed, in two events out of three, by an immediate, "first order" back reaction of the semiquinone with the ferric ion in the same complex.

The author is indebted to Dr. E. I. Rabinowitch for his help and stimulating criticism, and to the National Science Foundation for the support of this research.

THERMODYNAMIC PROPERTIES OF ASSOCIATED MIXTURES

By R. P. Rastogi and R. K. Nigam

Department of Chemistry, Punjab University, Hoshiarpur, India

Received September 22, 1959

Phase equilibrium data for benzophenone–diphenylamine and p-nitrotoluene–p-toluidine have been obtained which indicate the formation of compounds with congruent melting point in these mixtures. These and several other mixtures for which the data are available have been subjected to thermodynamic analysis to yield the entropy of fusion. It appears that entropy of fusion of the order of 20 cal./deg./mole is obtained for the compounds which dissociate completely in the liquid state whereas when the entropy of fusion is of the order of 2 cal./deg/mole the compound is very stable in the liquid state. This conclusion has been verified by ultraviolet spectroscopy.

Introduction

Considerable progress has been made in recent years in developing statistical theories of solutions of non-polar species.[1] On account of the obvious difficulties similar progress has not been made for mixtures consisting of polar molecules. Mixtures which involve the formation of complexes of the type A_mB_n from two species A and B are easy to deal with from the theoretical angle. Measurements of heat of mixing and vapor pressures have been made for systems such as ether–chloroform and acetone–chloroform where formation of the complex of the type AB is supposed to occur.[2,3] The systems where the complexes of the type AB_2 are formed also have been subjected to thermodynamic study.[4] Such mixtures have been treated on the basis of an ideal associated solution model where the deviations from ideality arising from the different sizes and shapes of complexes and monomers are neglected. These complexes are formed by forces much weaker than the valence forces which are responsible for the formation of a chemical compound.

The object of the present investigation was to examine the applicability of this model to such systems by utilizing solid–liquid equilibrium data. The entropy of fusion of such complexes has also been studied in order to have an estimate of their stability in the molten state. The systems for experimental study have been chosen in such a way that the size and shape of the components are similar.

Experimental

Materials.—Benzophenone (A.R.), diphenylamine (A.R.), p-nitrotoluene (B.D.H.) and p-toluidine (B.D.H.) were purified by fractional crystallization. Benzophenone was further subjected to vacuum distillation. The purity of these substances was tested by melting point determinations which agreed with the accepted values within ±0.1°. Alcohol for spectrophotometric work was carefully purified. The absorption maxima of these compounds in alcoholic solutions agreed with the literature values further confirming the purity of the materials used in the present study.

Freezing Point Diagrams.—A phase diagram for benzophenone and diphenylamine was obtained by a thaw-melt method as described previously.[5,6] This system has been investigated previously[7] but the detailed data were not available for the region between the two eutectics. Since for thermodynamic analysis this region is more important, the system was reinvestigated. The thaw-melt method gave erratic results for p-nitrotoluene and p-toluidine system. This procedure involved difficulties on account of the fact that mixtures of these compounds have lower melting points than the room temperature. Hence, chilling of a molten mixture even in ice did not produce uniform mixture and the subsequent thaw points and melting points were erratic. Accordingly recourse was taken to the method of thermal analysis. The mixture was taken in a narrow tube which was placed in another wide mouth tube so that there was annular space. The copper–constantan thermocouple was introduced into the innermost tube. Ice made from distilled water was used as a cold junction. The e.m.f. developed was measured by a Pye Precision Vernier Potentiometer. The temperature could be read correct to ±0.02°. The outer jacket along with the inner tube was placed in an ice-bath. Such a device ensured controlled rate of cooling. The results for p-nitrotoluene and p-toluidine are given in Table I and plotted in Fig. 1.

Spectrophotometric Analysis.—The absorption spectrum was investigated by a Unicam Spectrophotometer using 1 cm. silica cells. 10^{-4} to 10^{-5} molar solutions of the substances were made in highly purified ethanol. All the substances were found to obey Beer's law in this concentration range. The preliminary observations showed that the absorption maxima for all these substances occurred in ultraviolet range in ethanol solutions. The molar concentrations were chosen in such a fashion that maximum accuracy could be obtained in measuring optical densities at a certain wave length. Series of readings of optical densities of the same solutions for different wave length were undertaken. The transmission density is plotted against mole fractions in Fig. 4 and Fig. 5. The temperature of spectrophotometric measurements was 21.8°.

Results

The thaw points and melting points are recorded in Tables I and II.

---

(1) I. Prigogine, "Molecular Theory of Solutions," North-Holland Publishing Co., Amsterdam, 1957.

(2) J. H. Hildebrand and R. L. Scott, "Solubility of Non-electrolytes," Reinhold Publ. Corp., New York, N. Y., 1950.

(3) Sarolea-Mathot, *Trans. Faraday Soc.*, **49**, 8 (1953).

(4) M. L. McGlashan and R. P. Rastogi, *ibid.*, **54**, 496 (1958).

(5) R. P. Rastogi and K. T. Rama Varma, *J. Chem. Soc.*, 2097 (1956).

(6) R. P. Rastogi and K. T. Rama Varma, This Journal, **62**, 641 (1958).

(7) "International Critical Tables," McGraw-Hill Book Co., New York, N. Y., 1929.

TABLE I

THAW POINTS AND MELTING POINTS OF MIXTURES OF *p*-NITROTOLUENE AND *p*-TOLUIDINE

Mole fraction of *p*-nitrotoluene	Thaw point, °C.	M.p., °C.
0.0	. . .	43.7
.0514	30.50	39.0
.1003	14.03	33.61
.1898	13.96	25.39
.2521	13.95	20.32
.2791	13.92	27.72
.3059	14.01	28.69
.3317	14.01	29.0
.4242	15.14	23.04
.4722	14.91	19.57
.5253	14.99	22.43
.6384	15.10	31.30
.6910	14.91	35.94
.8091	24.65	44.51
.8690	33.49	45.49
.9528	35.97	49.66
1.0	. . .	51.2

TABLE II

THAW POINTS AND MELTING POINTS OF DIPHENYLAMINE-BENZOPHENONE

Mole fraction of diphenylamine	Thaw point, °C.	M.p., °C.
0.0000	. . .	48.1
.1171	32.4	42.3
.1874	32.4	38.0
.2398	32.4	33.4
.2808	32.3	34.5
.3506	32.4	37.2
.3948	32.3	39.5
.4575	32.4	40.7
.4960	32.4	41.6
.6017	34.4	39.9
.6500	34.4	37.5
.7047	34.4	35.9
.8019	34.4	41.7
.9076	34.4	47.8
1.0000	. . .	53.4

The results for *p*-nitrotoluene-*p*-toluidine are plotted in Fig. 1.

Discussion

From phase diagrams it is proved that a 1:1 compound is formed between benzophenone and diphenylamine and 1:2 compound between *p*-nitrotoluene and *p*-toluidine. The phase diagram simply proves the existence of the compound in the solid phase. It does not necessarily follow that the compound exists in the liquid phase. We shall see below that the entropy of fusion can give a positive indication regarding this.

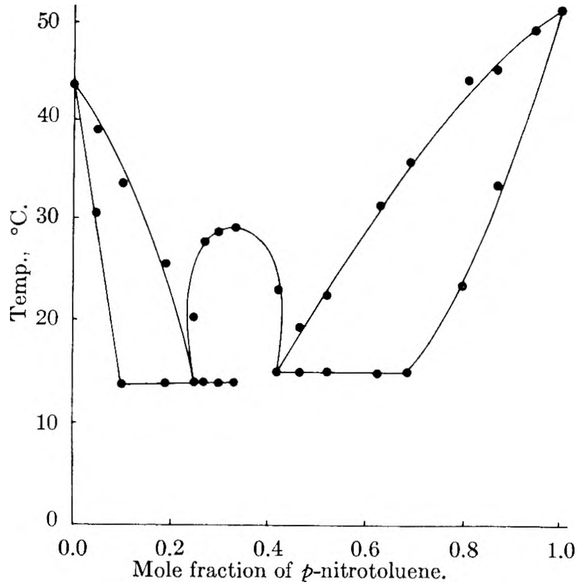

Fig. 1.—Phase diagram of *p*-nitrotoluene-*p*-toluidine mixture.

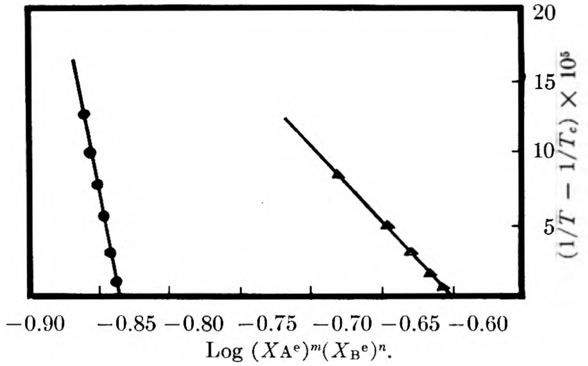

Fig. 2.—Test of eq. 1 and estimation of heat of fusion: ▲, benzophenone-diphenylamine; ●, *p*-nitrotoluene-*p*-toluidine.

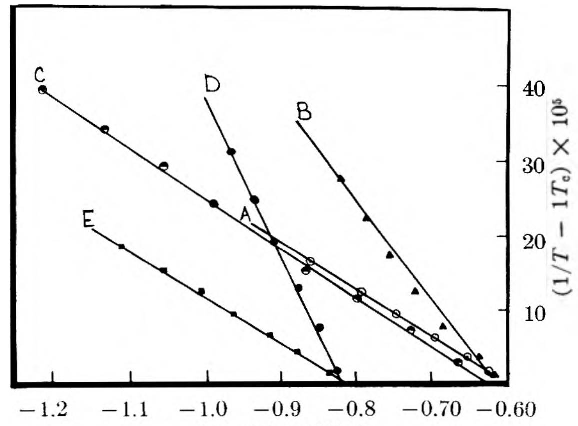

Fig. 3.—Test of eq. 1 and estimation of heat of fusion: (A) ○, 2,4,6-trinitrotoluene-naphthalene; (B) ▲, *m*-dinitrobenzene-α-naphthylamine; (C) ◓, picric acid-phenol; (D) ●, chloroform-dioxane; (E) ■, urea-phenol.

Provided the mixture obeys the ideal associated solution model, thermodynamics yields relation (1) for the region between the eutectic points in the phase diagram.[8]

$$\frac{h_{\mathrm{T,P}}}{R}\left(\frac{1}{T}-\frac{1}{T_{\mathrm{c}}}\right) = -\ln(\xi_{\mathrm{A}}^{\mathrm{l}})^m(\xi_{\mathrm{B}}^{\mathrm{l}})^n + \ln(\xi_{\mathrm{A}}^{\mathrm{l}})_{\mathrm{c}}{}^m(\xi_{\mathrm{B}}^{\mathrm{l}})_{\mathrm{c}}{}^n \qquad (1)$$

where the compound formed has the formula A_mB_n. $\xi_{\mathrm{A}}^{\mathrm{l}}$ and $\xi_{\mathrm{B}}^{\mathrm{l}}$ are the mole fractions of the species A and B, respectively. These would be equal to the stoichiometric mole fractions x_{A} and x_{B} if the compound is completely dissociated in the molten state. The subscript c after the parenthesis represents the corresponding quantities at the congruent melting point. It is evident from

---

[8] I. Prigogine and R. Defay, "Chemical Thermodynamics," Longmans Green and Co., New York, N. Y., 1954.

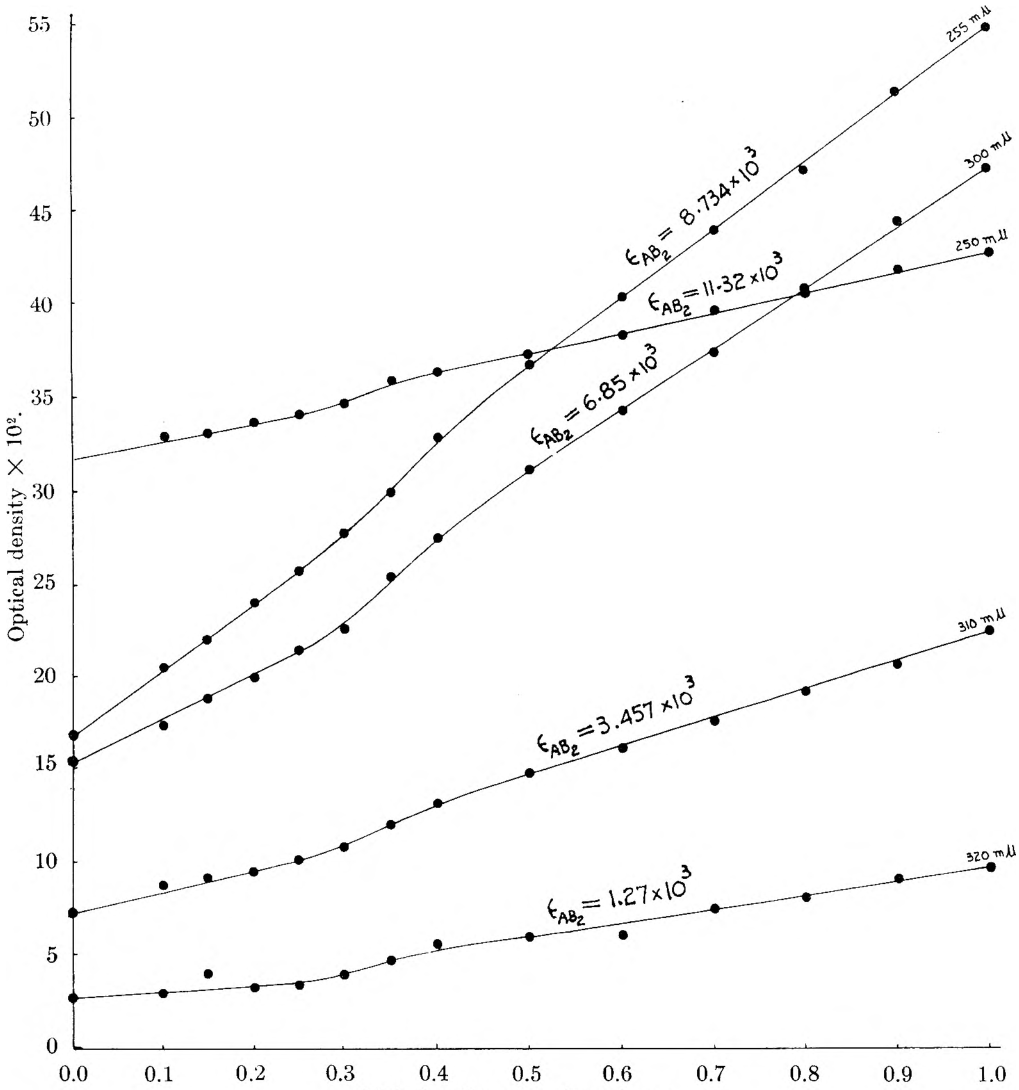

Fig. 4.—Optical density of solutions of *p*-nitrotoluene and *p*-toluidine in alcohol: ●, experimental points; ——, theoretical curve.

equation 1 that in the case of complete dissociation for the molten state the plot of $(1/T - 1/T_c)$ against $\ln(x_A^1)^m(x_B^1)^n$ would be a straight line and the intercept would be equal to $\ln(x_A^1)_c{}^m(x_B^1)_c{}^n$. However, for the case of incomplete or negligible dissociation, one should not expect a straight line if stoichiometric mole fractions are used. In the limiting case the curve may approximate to a straight line and the intercept would be equal to $\ln(x_A^1)^m(x_B^1)^n$. From the slopes of these lines, heat of fusion can be calculated readily and since the melting point of the complex is known from the diagram the entropy of fusion can also be evaluated. In Fig. 2 and Fig. 3, $(1/T - 1/T_c)$ has been plotted against $\ln(x_A^1)^m(x_B^1)^n$ for the two systems studied here and a few more for which the data are available.[7] With the exception of a little scatter in two systems, straight lines are obtained in all cases. In Table III entropies of fusion are recorded for a number of systems. In the last two columns, the value of the constant $-\log(x_A^1)_c\cdot(x_B^1)_c{}^n$ computed from the graph is compared with the constant calculated from the assumed composition of the complex from equation 1. This shows good agreement.

The values of entropies of fusion quoted in Table III are only approximate for those complexes which suffer partial or negligible dissociation. By spectrophotometric study done here it is found that the complex formed between *p*-nitrotoluene and *p*-toluidine is quite stable. Hence the value of the heat of fusion of this complex is only approximate. Nevertheless, the conclusions reached in the present investigation remain unaffected.

Of greater interest is the entropy of fusion of these compounds. This quantity is supposed to be a measure of the change in the internal degrees of freedom on melting. For monoatomic elements the entropy of fusion in general is 2. From the table we find that the entropy of fusion ranges from 2 to 20 cal./deg./mole. For most of the addition compounds investigated here the value is around about 20. The high value of entropy of fusion is generally ascribed to the following factors.[8] (i) the increase in the volume in the liquid phase on account of which the molecules have more room to

TABLE III

ENTROPY OF FUSION AND TEST OF EQUATION 1

System	Type of compd. formed	Heat of fusion (kcal./mole)	Entropy of fusion (cal./mole/deg.)	Constant computed from the graph	Calcd. constant
(1) Chloroform–dioxane	AB_2	2.0	9.6	0.82	0.83
(2) Urea–phenol	AB_2	7.6	22.7	.82	.83
(3) Picric acid–phenol	AB	6.9	19.2	.62	.60
(4) Picric acid–naphthalene	AB	8.4	19.9	.61	.60
(5) 2,4-Dinitrophenol–naphthalene	AB	6.7	18.4	.62	.60
(6) 2,4,6-Trinitrotoluene–naphthalene	AB	7.2	19.6	.60	.60
(7) *m*-Dinitrobenzene–α-naphthylamine	AB	3.5	10.3	.62	.60
(8) 2,4,6-Trinitrotoluene–acenaphthene	AB	7.8	20.3	.58	.60
(9) Dinitrophenol–α-naphthylamine	AB	5.3	14.3	.60	.60
(10) 2,4,6-Trinitrotoluene–phenanthrene	AB	6.9	19.1	.58	.60
(11) Benzophenone–diphenylamine	AB	6.1	19.3	.59	.60
(12) *p*-Nitrotoluene–*p*-toluidine	AB_2	0.73	2.4	.82	.83

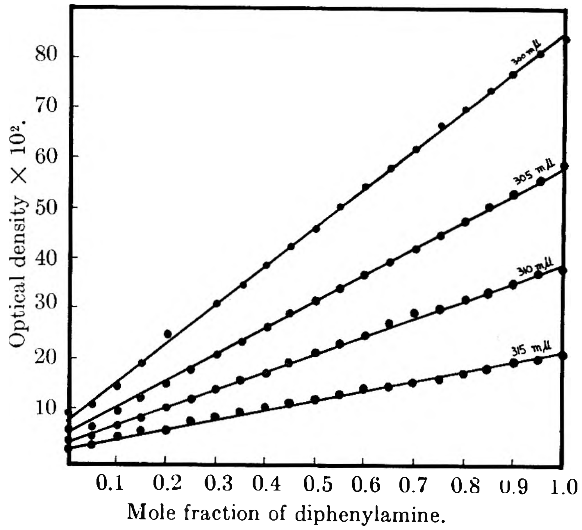

Fig. 5.—Optical density of solutions of benzophenone and diphenylamine in alcohol: ●, experimental points; ——, theoretical curve.

move; (ii) communal entropy; (iii) increases in the number of degrees of freedom on melting. Generally it is found that the third factor is of major importance. In a crystal the surrounding molecules may hinder the rotation to such an extent that it is just a rotatory vibration. Yet in the liquid phase it may have complete freedom of rotation. For such a case, the increase in the freedom of rotation will contribute considerably to the entropy of fusion. In fact, using harmonic oscillator model it can be shown[9] that the molar entropy of fusion $= R + [(E_{\text{int}})^{\text{l}} - (E_{\text{int}})^{\text{s}}]/T_c$. E_{int} is the internal energy. Superscripts l and s refer to liquid and solid phases. It follows from this that the entropy of fusion would be equal to R only when the internal energies are the same in the solid and liquid phases. But this would suggest that about 18 degrees of freedom become free in the molten state for these complexes, which does not appear to be a realistic estimate. Hence, the reason for the very high entropy value must be sought elsewhere. All these considerations ignore the possibility of dissociation of the complex in the molten state. If x' is the degree of dissociation and ΔH is the heat of dissociation in the molten state, the entropy of fusion $\Delta_f S$ should be given by

$$\Delta_f S = \frac{h_{T,P} + x' \Delta H}{T_c} \tag{3}$$

When $x' \rightarrow 0$, $\Delta_f S \rightarrow h_{T,P}/T_c$ and entropy of fusion may become equal to 2. Very large values of entropy of fusion would be obtained when $x' \rightarrow 1$ *i.e.*, when dissociation is complete. We have chosen two mixtures corresponding to these two extreme cases for further analysis.

The mixtures of these substances in ethanol have been subjected to spectrophotometric study. For mixtures of *p*-nitrotoluene and *p*-toluidine, evidence of one compound of the type AB_2 is revealed when the difference of experimental optical density and mixture law optical density is plotted against mole fraction. For a number of wave lengths, the maximum occurs at the stoichiometric composition corresponding to the compound AB_2. A careful analysis of the results was made to detect the existence of any other compound. In the absence of any other compound, the analytical procedure of Vosburgh and Cooper[10] confirms the existence and the formula of the compound. The total optical density of the solution would be made up of the contributions of A, B and AB_2 species. Assuming the validity of the Beer's law for the complex

$$\text{O.D.} = \epsilon_A c_A d + \epsilon_B c_B d + \epsilon_{AB_2} c_{AB_2} d \tag{4}$$

where d is the path length, ϵ is the extinction coefficient and c is the concentration. Our measurements showed that Beer's law is obeyed for all the other species. The subscripts represent the respective species. From the stoichiometry of the reaction and assuming that the compound does not dissociate in the molten state at all, the concentration of AB_2 can be evaluated. Choosing a suitable value of ϵ_{AB_2}, the theoretical optical density can be calculated when the compound is supposed to suffer no dissociation. This is compared with the experimental value in Fig. 4. There is an excellent agreement showing that the compound is very stable. This is in conformity with the finding based on the entropy of fusion.

For a 1:1 compound of benzophenone and diphenylamine the high value of entropy of fusion indicates that the complex is very unstable in the liquid state. No evidence of such a compound is obtained from spectrophotometeric analysis. In Fig. 5, experimental optical densities of the mixture in ethanol are compared with those calculated on the basis that c_{AB} is zero. The agreement is again satisfactory. Hence it appears that the

---

(8) H. Taylor and S. Glasstone, "Treatise on Physical Chemistry," Vol. II, "States of Matter," D. Van Nostrand Co., Inc., New York, N. Y., 1951.

(9) R. H. Fowler and E. A. Guggenheim, "Statistical Thermodynamics," Cambridge University Press, 1939.

(10) W. C. Vosburgh and G. R. Cooper, *J. Am. Chem. Soc.*, **63**, 437 (1941).

entropy of fusion of the addition compound can be a valuable guide regarding its stability in the liquid state.

One of us (R.K.N.) is thankful to the Council of Scientific and Industrial Research for a Junior Research Assistantship. It is a pleasure to acknowledge that the experimental work was done in the chemistry department of Lucknow University.

ORIENTATION POTENTIALS OF MONOLAYERS ADSORBED AT THE METAL-OIL INTERFACE[1]

By FREDERICK M. FOWKES

Shell Development Company, Emeryville, California

Received October 16, 1959

The potential (ΔV) resulting from oriented dipoles in an adsorbed monolayer of surface active material has been measured at the oil–metal interface with the vibrating condenser method, using a thin layer of the oil solution on the metal plate. The potentials of tight-packed monolayers are found to be the same as those of insoluble monolayers on water. Rates of adsorption are easily measured by this method and are found to be slower by a factor of ten to several thousand than calculated for diffusion, the rate depending on the type of surface active material and the type of metal. Equilibrium potentials are often concentration-dependent with the more dilute solutions and the concentration-dependence may be used as an indication of the "strength of adsorption." In cases where strong adsorption was indicated (by little concentration-dependence of ΔV_{eq} except with very dilute solutions) the rates of adsorption were the most rapid. On cold-rolled carbon steel the strength of adsorption (from white oil) is $C_{17}H_{35}CONHCH_2CHOHCH_2NH_2 >> C_{17}H_{35}COOH > C_{18}H_{37}NH_2 >> C_{18}H_{37}OH$. On stainless steel (18-8) the order is $C_{17}H_{35}CH_2NH_2 >> C_{15}H_{31}CH_2OH >> C_{17}H_{35}COOH$; this order indicates that the surface of stainless steel is acidic. On aluminum the order is $C_{17}H_{35}COOH > C_{18}H_{37}NH_2$.

Introduction

The use of surface potentials to measure the concentration and orientation of dipoles in monolayers is well known for insoluble films on the surface of water,[2] adsorbed gases on metal surfaces,[3] and also for films adsorbed from the aqueous phase at the oil–water interface.[4] This paper shows how these potentials may be measured at the oil–metal interface and presents some findings obtained by this method.

Method.—The vibrating condenser method of Zisman and Yamins[5] was adapted to this problem. The reference electrode of gold (12 cm.^{2}) was mounted about a millimeter from a parallel test electrode of somewhat larger size and vibrated at 100–500 c.p.s. by a loud speaker coil (with permanent magnet) energized by an audioöscillator. The resulting alternating potential was detected with an oscilloscope after amplifying the signal through a cathode follower and a high-gain highly-peaked tuned amplifier. The potential between the two plates was compensated with a potentiometer until a null was observed (usually reproducible to within one millivolt). The change of the null potential of the potentiometer for a given metal due to the adsorption of a surface active substance (ΔV) was measured by determining the potential of a metal plate with a thin (0.1 mm.) layer of freshly chromatographed pure oil and then the potential with a similar layer of oil containing the surface-active material. The change in potential ΔV includes the change in potential of the oil-air interface as well as that of the oil–metal interface. The former is minimized by using oils of low enough surface tension (<28 dynes/cm.) so that the additives did not concentrate (by positive adsorption) appreciably at the oil–air interface.[6] Consequently, the observed ΔV is believed to be due almost entirely to the adsorbed dipoles at the oil–metal interface. The stability of the gold reference electrode was checked at least once daily with freshly cleaned metal specimens under clean oil; accidental contamination could be detected in this manner and any drift with time observed. Such drifts were minor during most of these measurements as the humidity was constant, but in later work a dry nitrogen atmosphere was found necessary to minimize drifts. The drifts in potential of the freshly cleaned steel or aluminum plates are ordinarily very marked and the reproducibility of measurements between specimens very poor when potentials of the air–metal interface are investigated; however, the presence of the oil layer in these measurements eliminated nearly all of these difficulties, perhaps by dissolving surface contaminants.

Materials.—The oil used as solvent is the highly refined naphthenic white oil reported in earlier studies[6] which is freshly chromatographed through dry silica gel immediately prior to preparation of the solutions. Reference potentials are measured with freshly chromatographed oil purged with nitrogen. The octadecylamine, stearic acid and octadecanol were highly purified by chemical separations, fractional distillation and recrystallization. Calorimetric melting measurements indicated purities of 99.8% or better. The cetyl alcohol and the condensation product of stearic acid with 1, 3-diaminopropane-2-ol were of lower purity, though fractionally distilled.

The metal plates were sandblasted with clean sand, and then degreased with toluene in a Soxhlet extractor for several hours immediately prior to immersion or coating with oil solutions by the techniques described below. Prior to measuring the plates immersed in oil, most of the oil was wiped off except for a thin layer on the side next to the reference electrode.

Rates of Adsorption.—Measurements of ΔV as a function of time were made by two methods. In one method, the potential was measured immediately after a thin layer of solution was rubbed onto the surface with a glass rod. Similar additions were made at intervals of a few minutes. No changes in potential occurred with the clean oil, but only with oils containing surface-active materials. Such experiments are illustrated in Fig. 1. These curves give the impression that an equilibrium ΔV is nearly reached; however, the 35-minute values are only about 60% of the equilibrium values as shown later. They are characterized by a steep initial rise (before two minutes) in ΔV to about 30% of the equilibrium value. The rapid change during the first two minutes has yet to be explored in detail. In this region adsorption

---

[1] Presented at the Atlantic City Meeting of the American Chemical Society, September, 1959.

[2] N. K. Adam, "The Physics and Chemistry of Surfaces," 3rd Ed., Oxford University Press, New York, N. Y., 1942.

[3] *Cf.* J. P. C. Mignolet, *Rec. trav. chim.*, **74**, 685, 701 (1955).

[4] N. K. Adam, ref. 2, pp. 423–424.

[5] H. G. Yamins and W. A. Zisman, *J. Chem. Phys.*, **1**, 656 (1933).

[6] W. M. Sawyer and F. M. Fowkes, THIS JOURNAL, **60**, 1235 (1956).

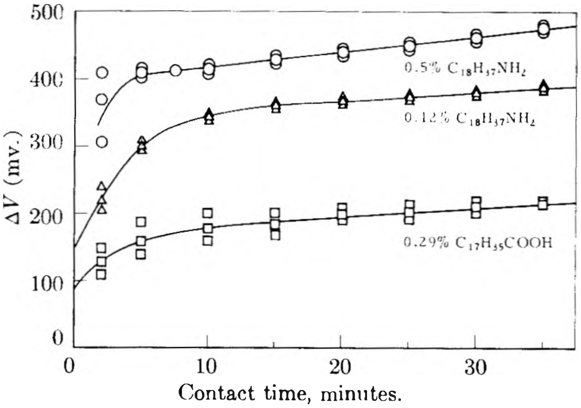

Fig. 1.—Rates of adsorption on steel as indicated by potential measurements.

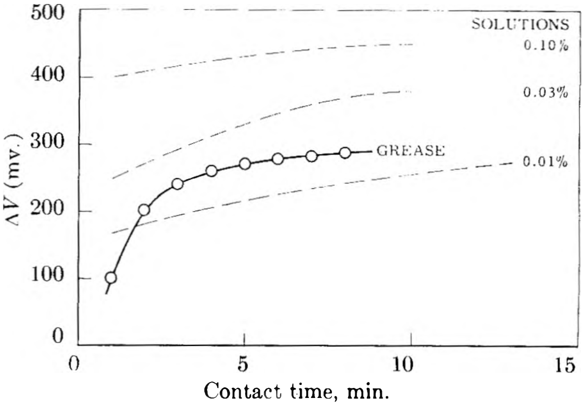

Fig. 2.—Rate of adsorption of amine on steel from grease and from oil solutions.

may be limited only by diffusion initially. The rise in ΔV from 2 to 35 minutes corresponds to a change in ΔV from 30 to 60% of the equilibrium value; this part of the adsorption is very slow compared to diffusion rates. The rate of arrival of stearic acid as indicated by the slope of ΔV *vs.* $\sqrt{t}$ between 2 and 35 minutes is slower by a factor of several thousand than calculated for diffusion-limited adsorption,[7] using the equation

$$\frac{d\Delta V}{d\sqrt{t}} = \frac{2\Delta V_{max} c N \sigma_{min}}{M} \sqrt{\frac{D}{\pi}}$$

where t is time, c is concentration, σ_{min} is the tight-packed area per molecule, and D is the diffusion coefficient (1.5×10^{-7} cm.^{2}/sec. for this system). The octadecylamine adsorbs three or four times faster than the stearic acid but still a thousandth as fast as expected for diffusion-controlled adsorption.

The rate of adsorption in another type of system is illustrated in Fig. 2. Here a silica-based grease with an amine ($C_{17}H_{35}CONHCH_2$-$CHOH$-CH_2NH_2) tightly adsorbed on the silica was rubbed onto a steel plate and the increase in ΔV observed as amine molecules were desorbed from the silica and adsorbed onto the steel. In this case, the concentration of free amine in the oil phase was less than 0.001% (as determined by spreading pressure measurements with the oil phase after centrifuging out the silica),[8] yet the rate of adsorption corresponds to about that found for solutions containing 0.02% of amine (dashed lines). The rate of adsorption of this amine from the more dilute solutions (after one minute) is higher than observed for octadecylamine, but lower by a factor of several hundred than diffusion-controlled adsorption.

Equilibrium Potentials.—In a number of cases equilibrium potentials were obtained in a few hours. Metal plates were immersed in solutions in glass jars and potentials were measured once or twice a day, as described earlier. In the case of the special amine ($C_{17}H_{35}CONHCH_2CH_2OHCH_2$-$NH_2$) solutions with steel plates illustrated by dashed lines in Fig. 2, an equilibrium potential of 570 ± 20 mv. was attained in 17 hours with the 0.3, 0.1 and 0.03% solutions while with the 0.01% solution 530 mv. was attained. Nearly identical potentials and concentration effects were obtained on steel plates with solutions of a long chain quaternary amine, Arquad 2HT. In the case of steel plates with solutions of stearic acid, the potentials level off after a week at 310–330 mv. for solutions of 0.01 to 0.3%, though at 17 hours the spread is from 250 to 305 mv. More concentration dependence of equilibrium potentials was found with steel plates in solutions of octadecylamine; after two days potentials were constant (up through seven days) at 730 mv. for 0.3% solutions, 600 mv. for 0.1% solutions, 520 mv. for 0.033% solutions, and 440 mv. for 0.011% solutions. The most pronounced concentration dependence was observed with octadecanol solutions on steel plates. Though potentials doubled from two to seven days, there was no levelling-off; potentials at seven days were: 0.3%, 300 mv.; 0.1%, 190 mv.; 0.03%, 120 mv.; 0.01%, 90 mv.

Measurements with Different Metals.—Any metal or alloy plate may be used for these measurements. So far only data obtained with cold-rolled carbon steel plates have been presented. A few measurements with 18–8 stainless steel and with aluminum illustrate differences.

In the case of aluminum, 0.3% solutions of stearic acid gave equilibrium values of 350 mv. within a half-hour, while 0.3% solutions of octadecylamine were 460 mv. Here the amine adsorbed about the same as on steel, but the fatty acid adsorbed very much faster on the aluminum.

With stainless steel results similar to those shown for carbon steel in Fig. 1 were obtained with octadecylamine solutions; 30-minute potentials were 450 mv. with 0.3% solutions, 290 mv. with 0.1% solutions, and 200 mv. with 0.03 % solutions. On the other hand, stearic acid showed very little tendency to adsorb on this surface; potentials increased for 30 minutes up to about 30 mv., less than 10% of the equilibrium values on carbon steel or aluminum. Cetyl alcohol solutions on stainless steel gave a potential of 100 mv. in five minutes which remained constant for the next half-hour; this is about one-third of the maximum ΔV observed for alcohols on metals.

Discussion

Several points appear worthy of discussion: the extraordinary lack of potential drift, the mean-

---

[7] F. M. Fowkes, THIS JOURNAL, **57**, 98 (1953).

[8] F. M. Fowkes, G. S. Ronay and M. J. Schick, *ibid.*, **63**, 1684 (1959).

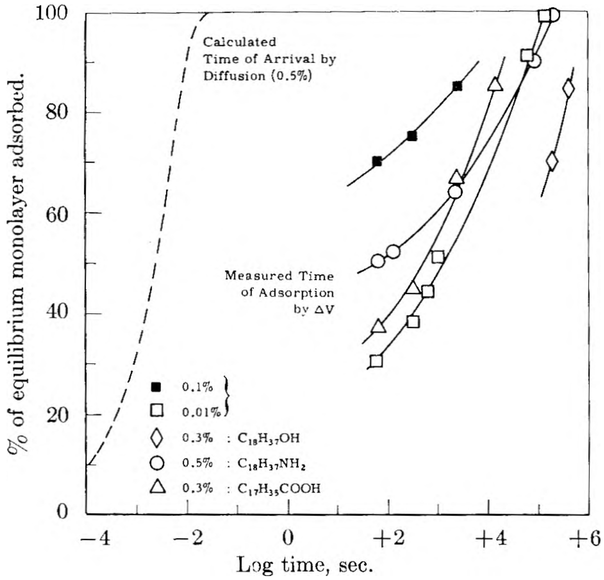

Fig. 3.—Rates of adsorption on steel plates from white oil solution compared with rates of diffusion; for ■ and □, $C_{17}H_{35}CONHCH_2—CHOH—CH_2NH_2$.

ing of the measurements, the slow rates of adsorption, and their utility in demonstrating differences in the tendency of various substances to adsorb on various metals.

We and others have found considerable difficulty in obtaining constant or reproducible potentials between two metal surfaces in air. However, nearly all these difficulties disappear when an oil layer covers the test specimen. This may result from the capacity of the oil to dissolve contaminants which ordinarily would adsorb on the metal surface. The reference electrode was fairly stable (after aging) in air at constant humidity, but better results were obtained in an atmosphere of dry nitrogen.

The equilibrium potentials for the more concentrated solutions are close to those measured for tight-packed insoluble monolayers on the surface of water.[2] For example, with octadecylamine the 750 mv. obtained in these studies checks very closely with the 730–750 mv. measured over neutral substrates with a film balance. With stearic acid the 330 mv. obtained on steel and 350 mv. obtained on aluminum are fairly close to the 380 mv. over acidic or neutral substrates measured with a film balance. Since surface potentials of insoluble films are really not very well understood,[9] we cannot be sure exactly what this new finding means. However, it suggests that either the aqueous substrate has no specific influence on the potential which arises in oriented monolayers, or that enough adsorbed water is present on metals in the laboratory so that the oriented polar groups find themselves in an aqueous environment. If we adopt the principle that monolayers at the metal oil interface have the same potentials as those with equal surface concentration on an aqueous substrate, then the observed values at the metal–oil interface may be used as a measure of packing. Thus a fatty acid film with ΔV = 190 mv. should correspond to half-saturation or about 40 Å.[2] per molecule.

The rates of adsorption may be used to rank additives and interfaces according to tendency to adsorb. Concentration-dependence also is a measure of tendency to adsorb, and, of course, the tightness of packing as indicated by the potential. All three of these measures of tendency to adsorb appear to agree. The conclusions indicated are that on carbon steel the order of adsorption is: $C_{17}H_{35}CONHCH_2CH_2OHCH_2NH_2 >> C_{18}H_{37}NH_2 > C_{17}H_{35}COOH >> C_{16}H_{33}OH$. On stainless steel $C_{18}H_{37}NH_2$ adsorbs about as strongly as on carbon steel but the order is now: $C_{18}H_{37}NH_2 >> C_{16}H_{33}OH >> C_{17}H_{35}COOH$. On aluminum again $C_{18}H_{37}NH_2$ adsorbs about as strongly as on the steels, but $C_{17}H_{37}COOH$ adsorbs more strongly.

The slowness of adsorption at metal–oil interfaces is quite surprising. At liquid interfaces up to 80 or 90% of a monolayer is adsorbed at rates predictable by diffusion,[7] yet at metal–oil interfaces with half a monolayer adsorption is less than a thousandth as fast as is predicted by diffusion (Fig. 3). Furthermore, it appears that the rate of adsorption becomes a smaller and smaller fraction of the calculated rate as the surface concentration of adsorbed molecules increases. This fraction may be called the sticking coefficient and it appears to fall from unity for bare surfaces to as low as 10^{-5} for surfaces at 80% of saturation. This is in sharp contrast to liquid interfaces where the sticking coefficient is unity for all except the nearly saturated surfaces. Perhaps molecules diffusing into a liquid interface can easily push adjacent molecules aside without breaking any adsorption bonds but at a solid interface such a process would require breaking bonds and, consequently, adsorption on a solid surface occurs only when an incoming surface active molecule happens to strike a site with a solvent molecule or when one strikes with sufficient energy to push adjacent adsorbed surface-active molecules aside.

Although others have observed slow rates of adsorption on metals,[10] these are more marked in this study because of using a more viscous solvent (white oil, 27 c.p. at 25°) which results in a considerable reduction in the rate of collisions with the surface. Moreover, it was easier in this study with plane surfaces and no stirring to calculate the diffusion-controlled rate of arrival of surface-active molecules at the surface than in the usual study with stirred metal powders.

---

(9) B. Kamienski, "Proc. Second Int. Congress of Surface Activity," Vol. III, pp. 103 121.

(10) S. G. Daniel, *Trans. Faraday Soc.*, **47**, 1345 (1951).

THE THERMODYNAMICS OF THE MOLTEN SALT SYSTEM KNO_3–$AgNO_3$–K_2SO_4 FROM ELECTROMOTIVE FORCE MEASUREMENTS

BY W. J. WATT[1a] AND M. BLANDER

Oak Ridge National Laboratory,[1b] *Oak Ridge, Tennessee*

Received October 17, 1959

Measurements of the activities of $AgNO_3$ were made in a molten salt concentration cell [A] at 363, 408, 438 and 449° for dilute solutions of Ag^+ and $SO_4^=$ ions ($N_{SO_4^-}$ and $N_{Ag^+} < 0.01$). $\mathrm{Ag}\ \begin{array}{|c||c|} & \mathrm{KNO_3} \\ \mathrm{KNO_3} & \mathrm{AgNO_3} \\ \mathrm{AgNO_3} & \mathrm{K_2SO_4} \end{array}\ \mathrm{Ag}$ [A]. The small negative deviations from ideality which were observed can be attributed to the negative energy of interaction of Ag^+ and $SO_4^=$ ions. Within the experimental precision of about 0.5 mv., $\log \gamma_{AgNO_3}$ is a linear function of $N_{SO_4^-}$, and for a given concentration of $SO_4^=$ ions did not vary measurably with N_{Ag^+}. Although the lattice theory previously proposed[3] strictly applies to mixtures with the cations and the anions, respectively, of the same size and charge, the data are consistent with the form of the equation derived from this theory. For dilute solutions and for small values of β, $\log \gamma_{AgNO_3} = -ZN_{SO_4^-}(\beta - 1)/[2.303(1 + ZN_{Ag^+}\beta)(1 + ZN_{Ag^+})]$ (6a) where Z is the quasi-lattice coördination number, $\beta = e^{-\Delta E/RT}$, and ΔE is the energy of formation of the ion pair Ag^+–$SO_4^=$. The comparison of the data and equation 6a leads to a value for $Z = 6$ of $\beta = 3.0$ and $\Delta E = 1.48$ kcal./mole at 408°.

Introduction

A quasi-lattice model of molten reciprocal salt systems A^+, B^+, C^-, D^- has been described previously.[2] In the model, the two cations and the two anions, respectively, have the same size and charge. It is interesting to test the range of validity of the form of the derived equations in systems which deviate appreciably from the conditions for which the model has been derived. The system KNO_3–$AgNO_3$–K_2SO_4 was convenient for such a study. Measurements in this system should be a stringent test of the range of validity of the equations derived from the model since the sulfate ion has a charge and radius very different from the nitrate ion.

The method of measurement utilized was a concentration cell in which the effect of additions of

$$\mathrm{Ag}\ \begin{array}{|c||c|} & \mathrm{KNO_3} \\ \mathrm{KNO_3} & \mathrm{AgNO_3} \\ \mathrm{AgNO_3} & \mathrm{K_2SO_4} \end{array}\ \mathrm{Ag} \qquad \text{(A)}$$

K_2SO_4 to the right hand half cell upon the total e.m.f. was measured. This effect on the e.m.f., aside from the dilution of the solute, is related to the lowering of the activity of $AgNO_3$ due to the presence of sulfate ions, and is caused by the energetic interaction of Ag^+ and $SO_4^=$ ions.

Experimental Method

The method of measurement has been described in a previous publication.[3] The left hand half cell was a reference electrode consisting of a Pyrex tube $^{11}/_{16}''$ in diameter by 16″ long which dipped into a one liter tall form berzelius beaker containing the molten materials of the right hand half cell. An asbestos fiber was sealed into the bottom of the reference electrode to act as a salt bridge. The reference cell had a tapered joint cap, and was filled with a mixture of $AgNO_3$ and KNO_3 which had been melted and then flushed with oxygen-free helium. A silver wire which dipped into this cell solution was led out through the tapered joint cap. These reference electrodes were found to be stable to 0.5 mv. for several days by comparison with other freshly prepared half cells.

The right hand half cell was a one liter tall form berzelius beaker into which was dipped a bare silver wire. The beaker was set in a 5-inch resistance furnace. KNO_3 was melted and flushed with oxygen-free helium in this beaker and addition of solutes $AgNO_3$ and K_2SO_4 was made as required. The solution in the beaker was well stirred with a Pyrex propeller to achieve uniform temperatures. Temperatures were measured with a Pt–Pt 10% Rh thermocouple set in a Pyrex well. The thermocouple e.m.f. was measured with a Leeds and Northrup portable precision temperature potentiometer connected to the thermocouple through an ice-bath. Temperature control was best achieved by manual adjustment of an autotransformer connected to the furnace. E.m.f. measurements of the cell were made with a Rubicon type "B" potentiometer. RACS grade KNO_3 from Baker and Adamson was melted and flushed with oxygen-free helium in each experiment. Clear crystals of C.P. $AgNO_3$ from Mallinckrodt were selected for use. RACS grade K_2SO_4 from Baker and Adamson was vacuum dried to constant weight.

Discussion of Experiment

The Nernst law has been shown to hold to better than 0.5 mv. for dilute solutions of $AgNO_3$ in pure KNO_3[3]

$$E = \frac{2.303RT}{F} \log \frac{N_{Ag^+}}{N'_{Ag^+}} \qquad (1)$$

where N_{Ag^+} is the positive ion fraction of silver in the right hand cell

$$N_{Ag^+} = \frac{n_{Ag^+}}{n_{Ag^+} + n_{K^+}}$$

and n_i is the number of moles of the ion i in the right hand cell. The ′(prime) as superscript refers to the left hand or reference electrode. If the standard state is chosen such that the activity coefficient of $AgNO_3$ is unity at infinite dilution of all components in the solvent KNO_3 then the activity coefficients are unity in the range of concentrations studied.

At given initial values of the concentration of silver ion, $\bar{N}_{Ag^+}$, K_2SO_4 was added to the right hand cell and the change of e.m.f. measured at concentrations of the ions too low to form any precipitates. Table I gives the measured changes of e.m.f. for several temperatures and several initial values of $\bar{N}_{Ag^+}$ for successive additions of K_2SO_4. The values of the change of e.m.f. are relatively small. The value of the liquid junction potential is probably much smaller than the measured changes of e.m.f. and the measured change of e.m.f. can be directly related to the change of the activity of $AgNO_3$ in the right hand cell.

---

[1] (a) Washington and Lee University, Lexington, Va.; Summer Participant at the Oak Ridge National Laboratory. (b) Operated for the United States Atomic Energy Commission by the Union Carbide Corporation.

[2] M. Blander, THIS JOURNAL, **63**, 1262 (1959).

[3] M. Blander, F. F. Blankenship and R. F. Newton, *ibid.*, **63**, 1259 (1959).

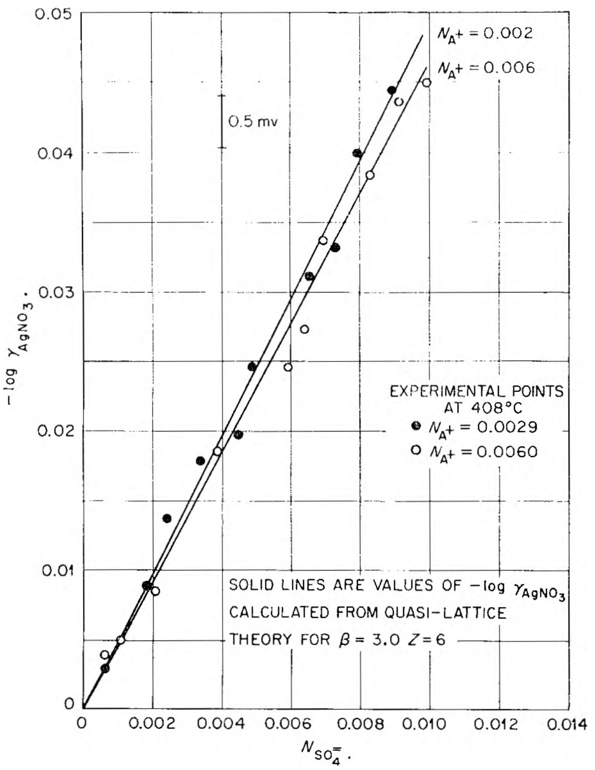

Fig. 1.—The activity coefficient of $AgNO_3$ as a function of SO_4^- concentration.

$$a_{AgNO_3} \equiv N_{Ag^+} N_{NO_3^-} \gamma_{AgNO_3}$$

The lowering of the activity of $AgNO_3$ in these experiments is caused by two effects—one being the dilution effect of the K_2SO_4 which becomes relatively significant at the concentrations studied. The other effect, which is of physical significance, is the lowering of the activity coefficient of $AgNO_3$ due to the physical interaction of Ag^+ and $SO_4^=$ ions. The change of e.m.f. upon adding K_2SO_4 is equal to

$$\Delta E = \frac{2.303RT}{F} \log \gamma + \frac{RT}{F} \ln \frac{N_{Ag^+}}{\bar{N}_{Ag^+}} \frac{N_{NO_3^-}}{\bar{N}_{NO_3^-}} \tag{2}$$

where the $\bar{N}$ are the ion fractions of the ions indicated, before K_2SO_4 addition. As $\bar{N}_{NO_3^-} = 1$, $N_{NO_3^-} = 1 - N_{SO_4^-}$ and $N_{Ag^+} \cong \bar{N}_{Ag^+}/(1 + 2N_{SO_4^-})$ we may approximate the second term on the right-hand side of the equation for small $N_{SO_4^-}$ by $-(3N_{SO_4^-})(RT/F)$ making the approximation that $\ln (1 - N_{SO_4}) \cong -N_{SO_4^-}$ and that $\ln 1/(1 + 2N_{SO_4^-}) \cong -2N_{SO_4}$. Equation 2 then becomes

$$\log \gamma_{AgNO_3} = \frac{-3N_{SO_4^-}}{2.303} + \frac{F\Delta E}{2.303RT} \tag{3}$$

The correction term $-3N_{SO_4}/2.303$ makes the calculated deviations from ideality of the $AgNO_3$ less negative than they would be without it.

In Table I are listed the derived values of $-\log \gamma_{AgNO_3}$ at 363, 408, 438 and 449° for several concentrations of $AgNO_3$ and K_2SO_4. In Fig. 1 are plotted values of $-\log \gamma_{AgNO_3}$ for several values of $N_{SO_4^=}$ and N_{Ag^+} at 408°. Within experimental error, the points fall on a straight line and do not exhibit any measurable dependence on the initial value of the concentration of $AgNO_3$. The values of $\log \gamma_{AgNO_3}$ seem to become more negative with an increase of temperature although the size of the decrease is of the order of the experimental precision and may not be significant.

Comparison of the Experimental Results and the Quasi-lattice Theory

The quasi-lattice theory previously proposed yields the result for the activity coefficient γ_{AD} for the component AD in the system A^+, B^+, C^-, D^- dilute in A^+ ions

$$\gamma_{AD} = \frac{(1 - X)^Z}{N_{D^-}} \left(1 + \frac{X}{\beta(1 - X)}\right)^{Z-1} \tag{4}$$

where X, the fraction of positions adjacent to an A^+ ion occupied by a C^- ion, can be calculated from the distribution function

$$\frac{X}{1 - X} = \left(\frac{N_{C^-} - ZXN_{A^+}}{1 - ZN_{A^+}(1 - X) - N_C}\right) \beta \tag{5}$$

$\beta = e^{-\Delta E/RT}$, ΔE is the energy of formation of the ion pair A^+–C^-, and Z is the quasi-lattice coordination number. Any correspondence of the model to the real system must be a forced one, since the model strictly applies only for cations and anions of the same charge, respectively. The assumption that a doubly charged ion $SO_4^=$ replaces two C^- ions in the quasi-lattice, although difficult to visualize, will lead to a correspondence of the model and the system measured.

Comparison of Methods of Describing Solutions

Three methods of describing thermodynamic behavior in reciprocal molten salt solutions are used. Equations 4 and 5 represent one method which is based on a physical theory. For dilute solutions and small values of β the equations reduce to

$$\log \gamma_{AgNO_3} \cong \frac{-ZN_{SO_4^-}(\beta - 1)}{2.303(1 + ZN_{Ag^+}\beta)(1 + ZN_{Ag^+})} \tag{6a}$$

Equation 6a for small values of $ZN_{Ag^+}\beta$ can be rewritten as

$$\log \gamma_{AgNO_3} = \frac{-ZN_{SO_4^-}(\beta - 1)(1 - ZN_{Ag^+}(\beta + 1))}{2.303} = \frac{-bN_{SO_4^-}}{2.303} \tag{6b}$$

In Table II are listed values of the quantity b obtained by a least squares fit of the data in Table I[4] to equation 6b. In the last column of Table I are listed values of $bN_{SO_4^-}$ which are the least square values of $-\log \gamma_{AgNO_3}$.

From the values of b listed in Table II the quantities $Z(\beta - 1)$, β and ΔE were evaluated for arbitrarily assumed coördination numbers, $Z = 6$ and $Z = 4$. The variation with temperature of b and of the derived values of β may not be significant.[4] An error in b of 10% would lead to an error in ΔE of about 0.13 which is considerably smaller than the variation in ΔE with temperature. Hence the increase of the value of $-\Delta E$ with temperature is probably significant, since the error in b probably is less than 10%.

---

[4] It should be noted that these measurements, in common with most measurements of e.m.f., are subject to non-random errors and hence the least squares treatment is not a valid one. The method of least squares was used to remove some of the subjectivity in treating the data. The calculated standard error in eight of the nine values of b was 2% or less of b. The error in b undoubtedly is larger than this.

TABLE I

E.M.F. CHANGE OF HALF CELLS UPON K_2SO_4 ADDITION AND CALCULATED VALUES OF LOG γ_{AgNO_3}

T, °C.	N_{Ag^+} × 10^3	$N_{SO_4^{--}}$ × 10^3	−Δe.m.f. (mv.)	−log γ_{AgNO_3} Measd.	−log γ_{AgNO_3} Calcd.
363	1.00	0.55	0.43	0.0028	0.0027
		1.76	0.93	.0051	.0086
		3.51	3.54	.0235	.0172
		6.19	4.97	.0313	.0303
		6.94	5.44	.0320	.0340
		7.99	6.14	.0382	.0392
	2.77	0.86	0.68	.0043	.0041
		2.26	1.68	.0104	.0107
		4.00	2.55	.0190	.0190
		5.28	3.65	.0221	.0250
		6.08	4.70	.0294	.0288
		7.53	5.81	.0373	.0357
		9.11	8.89	.0587[a]	
		9.85	9.15	.0598[a]	
	5.95	0.65	0.66	.0044	.0030
		1.08	0.85	.0053	.0050
		2.06	1.43	.0087	.0095
		3.89	2.99	.0187	.0179
		5.94	3.97	.0248	.0273
		6.39	4.51	.0274	.0294
		6.96	5.40	.0338	.0320
		8.30	6.22	.0385	.0382
		9.14	7.01	.0437	.0420
		9.94	7.32	.0451	.0457
408	2.85	0.63	0.52	.0030	.0031
		1.85	1.61	.0090	.0090
		2.37	2.29	.0139	.0116
		3.39	3.02	.0179	.0166
		4.47	3.47	.0199	.0219
		4.90	4.20	.0247	.0240
		6.55	5.37	.0312	.0320
		7.25	5.88	.0332	.0355
		7.92	6.81	.0401	.0387
		8.95	7.59	.0445	.0438
408	5.96	0.81	0.67	.0039	.0039
		1.90	1.75	.0106	.0091
		2.46	2.05	.0120	.0117
		3.48	2.79	.0161	.0166
		4.98	4.11	.0239	.0238
		5.76	4.73	.0275	.0275
		6.81	5.57	.0319	.0325
		8.14	6.69	.0389	.0388
		9.15	7.56	.0440	.0436
		9.47	7.73	.0449	.0452
433	2.80	1.78	1.82	.0107	.0091
		2.74	2.63	.0152	.0139
		4.19	3.88	.0223	.0213
		6.07	5.57	.0320	.0309
		6.51	5.76	.0326	.0331
		6.94	6.17	.0351	.0353
		8.72	7.94	.0454	.0443
		9.34	8.36	.0476	.0475
		9.74	8.39	.0472	.0495
	5.93	2.97	2.67	.0152	.0150
		3.43	3.08	.0175	.0173
		4.91	4.61	.0265	.0248
		5.31	4.81	.0274	.0268
		6.46	6.00	.0344	.0326
		6.99	6.26	.0356	.0352
		8.75	7.36	.0412	.0441
		9.38	7.54	.0416[a]	
		9.86	7.93	.0438[a]	
449	2.99	1.38	0.65	.0037	.0073
		1.96	2.07	.0118	.0104
		4.57	4.30	.0241	.0242
		5.59	5.35	.0300	.0296
		6.58	6.18	.0345	.0348
		7.97	7.38	.0410	.0422
		9.04	8.74	.0492	.0479
	5.94	1.09	0.91	.0049	.0058
		1.74	0.95	.0044	.0093
		4.84	4.63	.0261	.0258
		5.40	5.23	.0296	.0288
		6.27	5.28	.0287	.0334
		7.17	6.82	.0384	.0382
		7.88	7.66	.0432	.0420
		8.67	8.40	.0474	.0462
		9.75	9.46	.0533	.0520

[a] Values omitted in least-squares calculation.

TABLE II

PARAMETER CALCULATIONS FROM THE EXPERIMENTAL RESULTS

			$Z = 6$			$Z = 4$		
T, °C.	N_{Ag^+} × 10^3		Z ($\beta - 1$)	β (av.)	$-\Delta E$	Z ($\beta - 1$)	β (av.)	$-\Delta E$
363	1.00	11.3	11.5	2.9	1.34	11.5	3.9	1.72
	2.77	10.9	11.5			11.4		
	5.95	10.6	12.0			11.8		
408	2.85	11.3	11.9	3.0	1.48	11.8	4.0	1.88
	5.96	11.0	12.3			12.2		
433	2.80	11.7	12.4	3.1	1.58	12.3	4.2	2.00
	5.93	11.6	13.0			13.0		
449	2.99	12.2	13.0	3.2	1.67	12.9	4.3	2.10
	5.94	12.3	13.7			13.7		

The solid lines in Fig. 1 are plots of the theoretical values of log γ_{AgNO_3} at values of N_{Ag^+} of 0.002 and 0.006 for $\beta = 3.0$, and $Z = 6$. The energy of ion pair formation at 408°, ΔE, is -1.4_8 kcal./mole where ΔE represents the exchange of places of two NO_3^- ions adjacent to a silver ion with a sulfate ion.

A crude approximation to ΔE originally proposed by Flood and co-workers[5] is that $\Delta E = 2\Delta H'/Z$ where $\Delta H'$ is the heat change for the metathetical reaction

$$\tfrac{1}{2}K_2SO_4(l) + AgNO_3(l) \rightleftarrows \tfrac{1}{2}Ag_2SO_4(l) + KNO_3(l) \quad (A)$$

Using the data listed in Table III and assuming that the sum of the heat capacities of the reactants and products are the same, a value of −4.0 kcal./mole is obtained for $\Delta H'$ and −1.3 kcal./mole for ΔE if $Z = 6$. This is fortuitously about the same as the value derived from the experimental data at 363 and 408° for a value of $Z = 6$.

Another physical theory, the quasi-thermodynamic theory of Flood, Forland and Grjotheim,[5] leads to the equation

$$\ln \gamma_{AgNO_3} = N_{K^+} N'_{SO_4^-} \frac{\Delta F^0}{RT} \quad (7)$$

where N'_{SO_4} is the equivalent anion fraction of $SO_4^=$, $2n_{SO_4}/(n_{NO_3^-} + 2n_{SO_4^-})$, and where ΔF^0 is the free

---

[5] H. Flood, T. Forland and K. Grjotheim, *Z. anorg. allgem. Chem.*, **276**, 289 (1954).

TABLE III

THERMODYNAMIC DATA[a] FOR CALCULATION OF ΔH

	Heat of formation of solid ΔH_{298} (kcal./mole)	Heat of fusion ΔH_{fus} (kcal./mole)
K_2SO_4	−342.66	10.7
$AgNO_3$	− 29.43	3.42
Ag_2SO_4	−170.50	5.9
KNO_3	−117.76	4.1

[a] "Selected Values of Chemical Thermodynamic Properties," USNBS Circular 500, F. D. Rossini, *et al.*, 1952.

energy change for the metathetical reaction [A]. The form of equations 6 and 7 are essentially the same for dilute solutions of $AgNO_3$. Equation 7 is correct only for $\beta \sim 1$.[2]

The third method of describing the measured solution behavior is a "chemical" method. In the formulation a "complex" species $AgSO_4^-$ is postulated. The activity of the component $AgNO_3$ is attributed to the concentration of "uncomplexed" $AgNO_3$.[6-8] If m_{Ag^+} is the molality of Ag^+ ions, $m_{SO_4^=}$ is the molality of $SO_4^=$ ions and $m_{AgSO_4^-}$ the molality of the associated "complex ion," then an equilibrium constant is written

$$K = \frac{m_{Ag^+}\, m_{SO_4^=}}{m_{AgSO_4^-}} \tag{8}$$

If the total molality of Ag^+ is given by m'_{Ag^+}, of $SO_4^=$ by $m'_{SO_4^=}$, then

$$m_{Ag^+} = m'_{Ag^+}\gamma_1,\ m_{AgSO_4^-} = m'_{Ag^+}(1 - \gamma_1) \text{ and}$$
$$m_{SO_4^=} = m'_{SO_4^=} - m'_{Ag^+}(1 - \gamma_1)^{9}$$

Substituting in (8) and rearranging, the equation

$$\ln \gamma_1 \cong \frac{-m'_{SO_4^=}}{K}\left(1 - \frac{m'_{Ag^+}}{K}\right) \tag{9}$$

is obtained for small values of $(1 - \gamma_1)$. If

$$K \cong \frac{\frac{1000}{M_2}}{Z(\beta - 1)} \tag{10}$$

where M_2 is the molecular weight of KNO_3, then substituting (10) into (9) and approximating $m'_{SO_4^=} \cdot (M_2/1000)$ and $m_{Ag^+}(M_2/1000)$ by $N_{SO_4^=}$ and N_{Ag^+}, respectively, leads to

$$\log \gamma_1 = \frac{-ZN_{SO_4^=}(\beta - 1)(1 - ZN_{Ag^+}(\beta - 1))}{2.303} \tag{11}$$

the data are not good enough to distinguish between equations 6b and 11.

The theory described[2] here contains the implicit assumption that changes of the internal degrees of freedom of the ions involved in the formation of an ion pair can be neglected and that ΔE is a constant. A more general derivation of the theory would lead to the substitution for β by the ratio of the value of the product of the partition functions of the individual ions involved in the formation of an ion pair evaluated after the formation of the ion pair to the value of the product evaluated before the formation of the ion pair. Such a derivation, among other factors, would involve rotational degrees of freedom of the $SO_4^=$ ions. Any discussion of these effects is unwarranted and too speculative to publish at the present state of understanding of molten-salt solutions, but it seems possible that the change of internal degrees of freedom of the ions involved in the formation of an ion pair may be related to the apparent lack of constancy of the parameter ΔE.

Conclusions

The concentration dependence of the deviations from ideality in the KNO_3–$AgNO_3$–K_2SO_4 system can be satisfactorily described in terms of the parameters of the theory based on the quasi-lattice model but the temperature dependence is incorrectly described. The data are also consistent with the "chemical" description. To distinguish between the quasi-lattice description and the "chemical" description, independent measurements of the absolute concentration of Ag^+–$SO_4^=$ pairs would be necessary. The quasi-lattice theory leads to a prediction for the concentration of ion pairs which, for weakly associating ions, is significantly different from that calculated from the mass action law.[2]

Acknowledgments.—The authors wish to thank Drs. F. F. Blankenship and R. F. Newton for many fruitful discussions.

---

(6) This statement is inconsistent with the quasi-lattice theory as discussed previously.[2] This section concerns only the proof of any one description *from the experimental data*. It should be emphasized that the word "chemical" as used here does not imply any special type of bonding, but is used to imply only the use of the mass-action law to describe the data.

(7) F. R. Duke, THIS JOURNAL, **62**, 417 (1958).

(8) E. R. VanArtsdalen, *ibid.*, **60**, 172 (1956).

(9) $\gamma_1 = \gamma_{AgNO_3} N_{Ag^+} N_{NO_3^-}/m'_{Ag^+} \times 1000/M_2$.

DIFFUSION AND SEDIMENTATION OF ELECTROLYTES AND NON-ELECTROLYTES IN MULTICOMPONENT SYSTEMS

BY HANSJÜRGEN SCHÖNERT[1]

Boston University Department of Chemistry, Boston 15, Massachusetts

Received October 29, 1959

The relationship between diffusion coefficients and sedimentation coefficients for any solute species in a multicomponent system containing electrolytes and/or non-electrolytes is derived by the methods of thermodynamics of irreversible processes. For a two component system the relationship reduces to the familiar Svedberg equation. In a case where two electrolytic components have one ionic species in common, the general equation is such that determinations of diffusion and sedimentation coefficients may be used to identify the kind and nature of the dissociation products.

In a recent publication[2] Peller has elucidated the relationships between sedimentation and diffusion coefficients for multicomponent non-electrolyte systems. He also provided a relevant bibliography. Since many such measurements are carried out in buffer solutions,[3] it is desirable to extend the derivation of the Svedberg equation to systems containing electrolytes as well as non-electrolytes.

The Dissipation Function.—Consider a solution of solvent, denoted by 0, non-electrolyte solutes 1, 2, . . ., m, undissociated species of weak electrolytes 1α, 2α, . . ., $i\alpha$, cations $1+$, $2+$, ..., $i+$, and anions $1-$, $2-$, ..., $i-$. It is assumed that the whole system is rotating with constant angular velocity and is kept at a constant temperature T. Then the dissipation function[4] $T\sigma$, where σ is the entropy production per unit volume, may be split into two main parts, $(T\sigma)_1$ and $(T\sigma)_2$, one giving the contributions from the different flows of substances, and the other originating in the chemical reactions between undissociated and dissociated species of the electrolytes. According to the principle that the entropy production of the whole system is the sum of the entropy productions of the various processes,[4] one can write

$$T\sigma = (T\sigma)_1 + (T\sigma)_2 \tag{1}$$

$(T\sigma)_1$ is a specialization of the general formula derived by Hooyman, *et al.*[5]

$$(T\sigma)_1 = \sum_i J_i X_i = J_0 X_0 + \sum_m J_m X_m + \sum_{i\alpha} J_{i\alpha} X_{i\alpha} + \sum_{i+} J_{i+} X_{i+} + \sum_{i-} J_{i-} X_{i-} \tag{2}$$

with J_i as the flow of kind of particle i

$$J_i = \rho_i (v^i - v^a) \tag{3}$$

and X_i as the force of kind of particle i

$$X_i = (1 - \rho v_i) g + e_i E - (\text{grad } \mu_i)_{T,P} \tag{4}$$

The subscript i denotes any kind of particle. Summation over i means summation over all kinds of particles. The symbols have the meanings

ρ_i, density of particle species i (mass per unit volume)
v^i, velocity of particle species i
v^a, reference velocity
$\rho = \sum_i \rho_i$, density of solution
v_i, partial specific volume of particle species i
g, gravitational or centrifugal field strength
e_i, electrical charge of particle species i per unit mass, $e_i = 0$ for $i = 0, m, i\alpha$
E, electrical field strength
μ_i, specific chemical potential of particle species i
p, pressure

In writing equation 4 the condition of electroneutrality has been used

$$\sum_i e_i \rho_i = 0 \tag{5}$$

and terms due to Coriolis forces have been neglected.

The second part of the dissipation function $(T\sigma)_2$ pertaining to the chemical reactions can be written[4]

$$(T\sigma)_2 = \sum_r A_r w_r$$

with A_r as affinity and w_r as reaction velocity of reaction r.

Before setting up the phenomenological equations, one performs a transformation of the set of flows J_i and forces X_i to a new set of flows J_j' and forces X_j'. The transformation may be carried out in such a way that one of the new flows is the electrical current density J and the other flows are those of electrically neutral components.

This is done for these reasons: (1) in a sedimentation and/or diffusion experiment the electrical current density J equals zero and therefore the treatment of these effects is carried through more readily if one takes account of this fact already at this point. Nevertheless, for the sake of generality the term in the equation for the entropy production pertaining to the electrical current density is dropped only in that part of this treatment which deals explicitly with diffusion and sedimentation. (2) The forces X_i depend on $(\text{grad } \mu_i)_{T,P}$. But as the chemical potentials of ions are only meaningful in those combinations which correspond to electrically neutral components, the forces X_i and hence the flows J_i should be transformed to those of the electrically neutral components.

To perform the transformation to the electrical current density, the term $e_i E$ is split out of the force X_i.

---

[1] Monsanto Research Fellow at Boston University. Institut für Physikalische Chemie, Technische Hochschule Aachen, Germany.

[2] L. Peller, *J. Chem. Phys.* **29**, 415 (1958).

[3] T. Svedberg and K. O. Pedersen, "The Ultracentrifuge," Oxford University Press, London, 1940.

[4] S. R. de Groot, "Thermodynamics of Irreversible Processes," North Holland Publ. Comp., Amsterdam The Netherlands, 1951; I. Prigogine, "Etude Thermodynamique des Phénomènes Irreversibles," Ed. Desoer, Liège, Belgium, 1947; R. Haase, *Erg. exakt. Naturw.*, **26**, 56 (1952).

[5] G. J. Hooyman, H. Holtan, P. Mazur and S. R. de Groot, *Physica*, **19**, 1095 (1953).

$$\sum_i J_i X_i = JE + \sum_i J_i \bar{X}_i \tag{6}$$

with

$$\bar{X}_i = (1 - \rho v_i)g - (\text{grad } \mu_i)_{T,P} \tag{6a}$$

where (3) and (4) have been used together with the definition of an electrical current density

$$J = \sum_i e_i J_i \tag{7}$$

To find the number and proper definitions of the flows J_j' it may be useful to consider an example. The kinds of particles present in a buffer solution may be

	ρ_i	J_i
H_2O	ρ_0	$J_0 = \rho_0(v^0 - v^a)$
HOAc	$\rho_{1\alpha}$	$J_{1\alpha} = \rho_{1\alpha}(v^{1\alpha} - v^a)$
H^+	ρ_{1+}	$J_{1+} = \rho_{1+}(v^{1+} - v^a)$
Na^+	ρ_{2+}	$J_{2+} = \rho_{2+}(v^{2+} - v^a)$
OAc^-	$\rho_{1-} + \rho_{2-}$	$J_{1-} = \rho_{1-}(v^{1-} - v^a)$ $J_{2-} = \rho_{2-}(v^{2-} - v^a)$

$$J_{OAc^-} = J_{1-} + J_{2-}$$

where the following notation has been used: The numbers 0, 1, 2 designate the three components water (0), acetic acid (1) and sodium acetate (2), respectively, and α, $+$ and $-$, the undissociated species (α), cations ($+$) and anions ($-$), respectively. The acetate ion is delivered by the dissociation of acetic acid and sodium acetate, therefore its density has contributions from both components. Furthermore as $v^{1-} = v^{2-}$, the addition of J_{1-} and J_{2-} yields the flow J_{OAc^-} of the acetate ion. Hence five flows exist.

The three components correspond to three independent flows J_0', J_1' and J_2'. These flows are connected with those of the particles J_i by

$$\begin{aligned} J_0' &\equiv J_0 \\ J_1' &\equiv J_{1\alpha} + J_{1+} + J_{1-} \\ J_2' &\equiv \phantom{J_{1\alpha} + {}} J_{2+} + J_{2-} \end{aligned}$$

In the general case the number of independent flows J_j' of the components may be found from the following consideration. The solution may have N different species of ions or undissociated electrolytes. Because of the condition of electroneutrality, only $(N - 1)$ of these are independent. Assuming that in a sedimentation or diffusion process, chemical equilibrium locally prevails at any moment between the undissociated species, the number of which may be α, and the ions then $(N - 1 - \alpha)$ independent flows J_j' remain in addition to the flows of the solvent, of the nonelectrolytes, and J. This number of independent flows of components is not necessarily the same as the number of components in equilibrium thermodynamics.[6]

Then when k is the component which dissociates into the ion species $k+$ and $k-$, and the undissociated part is designated $k\alpha$, one can define[7]

$$J_k' \equiv J_{k\alpha} + J_{k+} + J_{k-} \tag{9}$$

Using equation 3 for the flows on the right side of (9), it follows that

$$J_k' = \rho_k'(v^{k'} - v^a) \tag{10}$$

where ρ_k' is the stoichiometric density of component

$$\rho_k' = \rho_{k\alpha} + \rho_{k+} + \rho_{k-}$$

k and $v^{k'}$ is the velocity of the center of mass of component k

$$v^{k'} = (\rho_{k\alpha} v^{k\alpha} + \rho_{k+} v^{k+} + \rho_{k-} v^{k-})/\rho_k'$$

So J_k' has the same meaning for a component k as J_i for a kind of particle i.

This means in the example of the buffer solution

$$\begin{aligned} J_0' &= \rho_0'(v^{0'} - v^a), & \rho_0' &= \rho_0 \\ J_1' &= \rho_1'(v^{1'} - v^a), & \rho_1' &= \rho_{1\alpha} + \rho_{1+} + \rho_{1-} \\ J_2' &= \rho_2'(v^{2'} - v^a), & \rho_2' &= \phantom{\rho_{1\alpha} + {}} \rho_{2+} + \rho_{2-} \end{aligned}$$

where $v^{1'}$ and $v^{2'}$ are the velocities of the center of mass of acetic acid and sodium acetate, respectively.

The forces X_k' which are conjugated to J_k' can be found by the principle of the invariance of the dissipation function against transformations of flows and forces.[4] To perform this transformation several properties of the ions and components have to be used.

The molecular weights M_{k+} and M_{k-} of cation $k+$ and anion $k-$ and their electrochemical valencies z_{k+} and z_{k-} are connected with their charges e_{k+} and e_{k-} by

$$\begin{aligned} e_{k+} M_{k+} &= z_{k+} F \\ e_{k-} M_{k-} &= z_{k-} F \end{aligned} \tag{11}$$

where F is the Faraday constant.

Furthermore, for each neutral component the condition of electroneutrality holds in the form

$$z_{k+} \nu_{k+} + z_{k-} \nu_{k-} = 0 \tag{12}$$

where ν_{k+} and ν_{k-} are the numbers of cations and anions, respectively, into which one component dissociates. To rewrite definition (9), one uses the fact that the new flows J_j' and the electrical current density J are all independent of each other, which means that one can set all J_j' but one, designated by J_k', as well as J equal to zero. Then in the summation

$$J = \sum_i e_i J_i = 0 \tag{13}$$

all terms but those which contain J_{k+} and J_{k-} drop out and one has[8]

$$e_{k+} J_{k+} + e_{k-} J_{k-} = 0 \tag{13a}$$

Using (11), (12) and (13a), equation 9 can be rewritten

$$J_k' = J_{k\alpha} + J_{k+} M_k / \nu_{k+} M_{k+} \tag{14}$$

with

$$M_k = \nu_{k+} M_{k+} + \nu_{k-} M_{k-} \tag{15}$$

as molecular weight of component k.

The invariance of the dissipation function against transformations of flows and forces may be expressed by

$$J_k' X_k' = J_{k\alpha} \bar{X}_{k\alpha} + J_{k+} \bar{X}_{k+} + J_{k-} \bar{X}_{k-} \tag{16}$$

where only the contributions caused by one flow are considered. Eliminating J_k' by means of (14)

---

[6] B. R. Sundheim, *J. Chem. Phys.*, **27**, 791 (1957).

[7] Cases in which a component dissociates into more than two kinds of ions are not included in this treatment, although it can be shown that the final result, equation 22, is the same when such cases are considered.

[8] Equation 13a holds only for the theoretically possible case, that the only component involved in the transport process is component k (see 16). Because of the theoretical independence of all flows of each other this does not affect the final result (22).

and J_{k-} by means of (13a), equation 16 can be rewritten with the help of (11) and (12) into

$$J_{k\alpha}X_k' + J_{k+}M_kX_k'/\nu_{k+}M_{k+} = J_{k\alpha}\bar{X}_{k\alpha} + (\bar{X}_{k+}\nu_{k+}M_{k+} + \bar{X}_{k-}\nu_{k-}M_{k-})\frac{J_{k+}}{\nu_{k+}M_{k+}} \quad (17)$$

The assumption that chemical equilibrium prevails between the undissociated species $k\alpha$ and the ions $k+$ and $k-$ means

$$\nu_{k+}M_{k+}\,(\text{grad }\mu_{k+})_{T,P} + \nu_{k-}M_{k-}\,(\text{grad }\mu_{k-})_{T,P} = M_k(\text{grad }\mu_{k\alpha})_{T,P} = M_k(\text{grad }\mu_k)_{T,P} \quad (18)$$

where μ_k is the specific chemical potential of component k. Likewise it is true that

$$\nu_{k+}M_{k+}v_{k+} + \nu_{k-}M_{k-}v_{k-} = M_kv_{k\alpha} = M_kv_k \quad (19)$$

with v_k as the partial specific volume of component k. Therefore, using (15) and (6a)

$$\nu_{k+}M_{k+}\bar{X}_{k+} + \nu_{k-}M_{k-}\bar{X}_{k-} = M_k\bar{X}_{k\alpha} \quad (20)$$

Inserting this expression into (17) gives

$$X_k' = (1 - \rho v_k)g - (\text{grad }\mu_k)_{T,P} \quad (21)$$

and thus

$$(T\sigma)_1 = JE + J_0X_0 + \sum_m J_mX_m + \sum_k J_k'X_k' \quad (22)$$

As (21) and (10) give, for X_k' and J_k' of the electrolyte components, the same expressions as already found in (4) and (3) for non-electrolyte components, one can drop the different notation and write

$$(T\sigma)_1 = JE + \sum_k J_k'X_k' \quad (22a)$$

where summation over k now means summation over all components.

This set of flows and forces was used previously by Sundheim for the case of diffusion in multicomponent electrolyte systems.[6]

The Phenomenological Equations.—To simplify the calculations in a multicomponent system, the reference velocity v^a may be taken as the velocity $v^{0\prime}$ of the solvent, thus making $J_0' = 0$. For sedimentation and diffusion, the electrical current density J is zero. The condition of local chemical equilibrium ensures that $A_r = 0$ for all r. Therefore the dissipation function takes the form

$$T\sigma = \sum_{i=1}^{n} J_i'X_i'$$

summation i now running over non-electrolyte and electrolyte solute components, but not including the solvent. Thus according to the methods of thermodynamics of irreversible processes[4] the linear phenomenological equations have the form

$$J_i' = \sum_{k=1}^{n} a_{ik}X_k' \quad (23)$$

Relationship between Diffusion and Sedimentation Coefficients.—The diffusion coefficients D_{ik} of such a system are defined[2,7,9] in the absence of a gravitational or centrifugal field by

$$J_i'c_i/\rho_i' \equiv -\sum_{k=1}^{n} D_{ik}(\text{grad }c_k)_{T,P,c}, \qquad g = 0 \quad (24)$$

c_i being the stoichiometric concentration of component i in moles per unit volume. The sedimentation coefficients s_i are defined by[2,10]

$$J_i' \equiv \rho_i'gs_i, \qquad (\text{grad }c_k)_{T,P,c} = 0 \quad (25)$$
$$k = 1, 2, \ldots, n$$

Comparing (24) and (25) with (21) and (23) gives

$$D_{ik} = \frac{c_i}{\rho_i'}\sum_{l=1}^{n} a_{il}(\partial\mu_l/\partial c_k)_{T,P,c} \quad (26)$$

and

$$s_i = \frac{1}{\rho_i'}\sum_{m=1}^{n} a_{im}(1 - \rho v_m) \quad (27)$$

(26) and (27) combine to

$$D_{ik}/s_i = \sum_{l=1}^{n} a_{il}(\partial\mu_l/\partial c_k)_{T,P,c}\,c_i \Bigg/ \sum_{m=1}^{n} a_{im}(1 - \rho v_m) \quad (28)$$

For a two component system (28) reduces to the familiar expression[2,3,11]

$$D_1/s_1 = c_1(\partial\mu_1/\partial c_1)_{T,P,c_0}/(1 - \rho v_1) \quad (29)$$

but now including components like weak, incompletely dissociated acids.

For the general case it is best to follow the method of Peller.[2] Solving (26) for a_{il} gives

$$a_{il} = \frac{\rho_i'}{c_i}\frac{F_{il}'}{G'} \quad (30)$$

with

$$\frac{F_{il}'}{G'} = \frac{\begin{vmatrix} (\partial\mu_1/\partial c_1)_{T,P,c} & \cdots & D_{i1} & \cdots & (\partial\mu_n)/\partial c_1)_{T,P,c} \\ \vdots & & \vdots & & \vdots \\ (\partial\mu_1/\partial c_n)_{T,P,c} & \cdots & D_{in} & \cdots & (\partial\mu_n/\partial c_n)_{T,P,c} \end{vmatrix}}{\begin{vmatrix} (\partial\mu_1/\partial c_1)_{T,P,c} & \cdots & (\partial\mu_l/\partial c_1)_{T,P,c} & \cdots & (\partial\mu_n/\partial c_1)_{T,P,c} \\ \vdots & & \vdots & & \vdots \\ (\partial\mu_1/\partial c_n)_{T,P,c} & \cdots & (\partial\mu_l/\partial c_n)_{T,P,c} & \cdots & (\partial\mu_n/\partial c_n)_{T,P,c} \end{vmatrix}} \quad (31)$$

The derivatives of the chemical potentials in the determinants are those of the specific chemical potentials. Therefore by multiplying the ith row in the determinants with the molecular weight M_i of component i, equation 30 may be rewritten

$$a_{il} = \frac{F_{il}}{G}M_i\frac{\rho_i'}{c_i} \quad (32)$$

where F_{il} and G have the same form as F_{il}' and G', but the chemical potentials $\bar{\mu}_i$ are now taken per mole.

Using (32), equation 27 yields

$$s_i = \frac{1}{c_iG}\sum_{l=1}^{n} F_{il}M_l(1 - \rho v_l) \quad (33)$$

the summation running over all components l = 1, 2, ..., n but not including the solvent 0. Equation 33, valid for non-electrolyte and/or electrolyte components, was derived and discussed by Peller[2] for non-electrolyte components. A

---

(9) R. L. Baldwin, P. J. Dunlop and L. J. Gosting, *J. Am. Chem. Soc.*, **77**, 5235 (1955).

(10) Different authors use different reference velocities in (24) and (25). But one can show that the ratio D_{ik}/s_i is independent of the choice of the reference velocity.

(11) R. Haase, *Koll.-Z.*, **138**, 105 (1954); **147**, 141 (1956).

similar expression for a three component system is given by Baldwin.[12]

Discussion of Special Cases.—Equation 33 may be simplified for special cases of electrolyte solutions in which the concentration of one component goes to zero. In the further treatment some results of Peller[2] are taken over without derivation.

(a) The solution has besides non-electrolyte components one electrolyte, designated by p. The molar chemical potential $\bar{\mu}_p$ is given by

$$\bar{\mu}_p = \bar{\mu}_{p0} + \nu_p RT \ln c_p y_p \qquad (34)$$

where $\nu_p = \nu_{p+} + \nu_{p-}$ is the number of ions into which one molecule dissociates, and c_p and y_p are the mean molarity and mean activity coefficient, respectively. Replacing RT by $\nu_p RT$, formula (25) of Peller holds for electrolyte components in the form

$$s_p = \frac{D_{pp}}{\nu_p RT} \left\{ M_p(1 - \rho v_p) + \sum_{\substack{l=1 \\ l \neq p}}^{n} \frac{G_{pl}}{G_{pp}} M_l(1 - \rho v_l) \right\} \qquad (35)$$

G_{pl} is the cofactor of $(\partial\bar{\mu}_l/dc_p)_{T,P,c}$ in the determinant G. The approximations are for $c_p \rightarrow 0$

$$\lim_{c_p \to 0} D_{pl} = D^0{}_{pl} = 0 \qquad \begin{matrix} l = 1, 2, \ldots n \\ l \neq p \end{matrix} \qquad (36)$$

and

$$\lim_{c_p \to 0} D_{pl} (\partial\bar{\mu}_k/\partial c_p)_{T,P,c} = 0 \qquad \begin{matrix} l,k = 1, 2, \ldots n \\ l \neq p \\ k \neq p \end{matrix} \qquad (36a)$$

and

$$\left|\frac{D^0{}_{pp}}{RT} G_{pl}\right| >> \left|\sum_{\substack{j=1 \\ j \neq p}}^{n} (-1)^{j+l} \left(\frac{\partial D_{pj}}{\partial c_p}\right) (G_{jl})_{pp}\right| \qquad (36b)$$

where $(G_{jl})_{pp}$ is the cofactor of $(\partial\bar{\mu}_p/\partial c_p)_{T,P,c}$ in the determinant $(-1)^{j+l}G_{jl}$. For non-electrolyte components

$$\lim_{c_p \to 0} (\partial\bar{\mu}_k/\partial c_p)_{T,P,c}$$

is finite. Therefore (36) is sufficient to ensure (36a). For electrolytes $\lim\limits_{c_p \to 0} (\partial\bar{\mu}_k/\partial c_p)_{T,P,c}$ may become infinite and thus (36a) is an independent condition.

(b) In the case of two electrolytes p and q with a common anion, for example NaCl and KCl, the molar chemical potentials may be written

$$\bar{\mu}_i = \bar{\mu}_{i0} + RT \ln (c_i\nu_{i+})^{\nu_{i+}}(c_p\nu_{p-} + c_q\nu_{q-})^{\nu_{i-}} y_{i\pm}{}^{\nu_i} \qquad i = p,q \qquad (37)$$

Assuming furthermore the conditions (36), (36a) and (36b) for the components p and q and using (37), equation (33) can be simplified for $c_i \rightarrow 0$, $i = p,q$, to

$$s_i = \frac{D^0{}_{ii}}{\nu_{i+} RT} \left\{ M_i(1 - \rho v_i) + \sum_{\substack{l=1 \\ l \neq i}}^{n} \frac{G_{il}}{G_{ii}} M_l(1 - \rho v_l) \right\} \qquad i = p,q \qquad (38)$$

Equation 38 differs from (35) in the sense that the factor ν_i $(i = p,q)$ reduces to ν_{i+} $(i = p,q)$, thus showing that only those dissociation products of an electrolyte component i make a contribution to the factor $\nu_i(i = p,q)$ which are not already present in the solution. In the case of two electrolytes with a common cation, $\nu_i(i = p,q)$ would reduce to ν_{i-} $(i = p,q)$.

Experimental substantiation for this fact is provided by the measurements of Baker, Lyons and Singer.[13] These authors measured diffusion and sedimentation coefficients of silicotungstic acid, $H_4[SiW_{12}O_{40}]$, and phosphotungstic acid, $H_3[PW_{12}O_{40}]$, in sodium acetate–acetic acid buffer solutions.

If their data are applied to equation 38, the correct molecular weights for the heteropoly compounds may be calculated on the assumption that $\nu_{i-} = 1$ because the cation species H^+ is common to the compounds and to the acetic acid, and because the compounds are monomeric.

Besides this the experiments show that the approximations for $c_i \rightarrow 0$ are justified, and that the second term on the right-hand side of (38) $\Sigma(G_{il}/G_{ii})M_l(1 - \rho v_l)$, is small within the limits of experimental error compared with the first term, $M_i(1 - \rho v_i)$ if no compensation of the different correction terms and approximations has taken place.

(c) If the solution contains three electrolyte components or four different ions, for example NaCl (p), KBr (q) and KCl (r), then a simplification of (33) is no longer possible. To show this one can consider a volume element in a diffusion experiment which in the initial stage of the experiment may contain only two of these components, for example 2 moles of NaCl and 2 moles of KBr. The diffusion in an intermediate stage can exist in principle in the form that 1 equivalent of sodium ions leaves the volume element and 1 equivalent of potassium ions enters it. After this the volume element contains 1 mole NaCl, 2 moles KBr and 1 mole of KCl. This shows that the diffusion of the components p and q may in principle cause a diffusion of component r, even when the concentration of component r in the initial and final stage of a diffusion experiment is zero. Thus the condition of vanishing cross term diffusion coefficients (36) can no longer be assumed to be valid in general.

This is always the case when the number of components in a non-equilibrium process (here three components NaCl, KBr and KCl) is higher than the number of components in the corresponding thermodynamic equilibrium (here two components NaCl and KBr).[6]

The results of diffusion and sedimentation measurements in properly chosen solutions can be used in equation 38 to determine the nature of electrolytic dissociation products. For example, a compound $M_A[W]_B$, where M is a metal ion and W a high molecular weight anion, may be measured (a) in water and (b) in a solution of a salt of M. The results, together with a chemical analysis, would show the magnitudes of the subscripts A and B as well as the molecular weight of the compound. This information would indicate the degree of polymerization of the anion W. Naturally the

---

[12] R. L. Baldwin, *J. Am. Chem. Soc.*, **80**, 496 (1958).

[13] M. C. Baker, P. A. Lyons and S. J. Singer, *J. Am. Chem. Soc.*, **77**, 2011 (1955); THIS JOURNAL, **59**, 1074 (1955).

molecular weight of the compound as a whole must be of such magnitude that the sedimentation coefficient can be measured with reasonable accuracy.

Acknowledgments.—The author wishes to express appreciation to Professor Louis C. W. Baker, in whose laboratory this work was carried out, for helpful discussions and for introduction to problems involving heteropoly electrolytes, which prompted the author to undertake this derivation. He is indebted to Professor R. Haase for advice and critical reading of the manuscript. This research was supported in part by a grant from Monsanto Chemical Company and in part by the U.S. Atomic Energy Commission, through Contract AT(30-1)-1853. The author also wishes to thank the Fulbright Commission for a Travel Grant.

SUBLIMATION PRESSURES OF SOLID SOLUTIONS. I. THE SYSTEMS TIN(IV) BROMIDE-TIN(IV) IODIDE AND TIN(IV) BROMIDE-TITANIUM (IV) BROMIDE. THE SYSTEM TIN(IV) BROMIDE-TIN(IV) IODIDE-CARBON TETRACHLORIDE[1]

BY JAMES J. KEAVNEY[2] AND NORMAN O. SMITH

Contribution from the Department of Chemistry, Fordham University, New York, N. Y.

Received November 6, 1959

A manometer has been designed for measuring vapor pressures of materials the vapor of which slowly interacts with or dissolves in the manometric liquid. It was used to measure the sublimation pressures of pure $SnBr_4$ and $TiBr_4$, of solid solutions of $SnBr_4$ in SnI_4 over a small range of temperature, and of solid solutions of $SnBr_4$ in $TiBr_4$ at 22°. Marked negative deviations from Raoult's law were found in the system $SnBr_4$–SnI_4, interpreted as a tendency toward the formation of mixed halides in the solid state. A supplementary study of the solid–liquid equilibria in the system $SnBr_4$–SnI_4–CCl_4 at 12° was undertaken to examine the distribution of $SnBr_4$ and SnI_4 between solid and saturated liquid solution. The distribution is of Type II in the Roozeboom classification, although it gives some evidence of compound formation. Measurement of the sublimation pressures in the system $SnBr_4$–$TiBr_4$ proved very difficult, and the results, although erratic, showed positive deviations from Raoult's law.

In contrast to liquid solutions comparatively few measurements of the thermodynamic properties of solid solutions, especially non-metallic ones, have ever been made. The e.m.f. approach, used by Wachter[3] for NaCl-AgCl and $PbCl_2$-$PbBr_2$ solid solutions, is not convenient for covalent substances, and what few studies have been made with the latter have been through sublimation pressure. Speranski,[4] and Perlman and Davies[5] measured the vapor pressure of naphthalene in β-naphthol. Speranski[6] and Küster[7] determined the vapor pressures of *p*-dichlorobenzene-*p*-dibromobenzene and of *p*-dibromobenzene-*p*-bromochlorobenzene solid solutions, and Vanstone[8] studied the system borneol-camphor. Hollman[9] measured the dissociation pressure of hydrated salt pairs. In an attempt to add to the limited available data of this kind the present investigation was undertaken. The Group IV tetrahalides were chosen because, in addition to their widespread isomorphism, the tetrahedral structure makes for comparative simplicity in any theoretical treatment that might result. Hildebrand[10] has drawn attention to their approximately spherical symmetry and recommended them for study. The experimental difficulties encountered were formidable, however; the data obtained permit only a qualitative interpretation and so fall short of the original goal of thermodynamic treatment. Among the difficulties may be mentioned the hygroscopic nature of the components, the fact that the pressures to be measured lay in a difficult range (a few tenths of a mm.), and the slowness with which equilibrium is attained.

Pure Components

Experimental—$SnBr_4$ was prepared by the method of Lorenz[11] from reagent grade mossy tin and liquid bromine (N. F.), and distilled from the reaction mixture over a range of 1° and stored in a glass stoppered bottle in a desiccator; m.p. 29.2–29.4°. It was analyzed for tin gravimetrically (ignition to SnO_2) and volumetrically (reduction to stannous ion and titration with KIO_3—KI soln.), and for bromine (potentiometrically with standard $AgNO_3$). Calcd.: Sn, 27.08; Br, 72.92. Found: Sn, 27.14 (grav.), 27.21 (vol.); Br, 72.78. It was distilled as needed into the apparatus described below. SnI_4 was prepared from the elements according to the method of McDermott[12]; m.p. 144–145°. It was analyzed for tin gravimetrically and for iodine volumetrically as above. Calcd.: Sn, 18.95; I, 81.05. Found: Sn, 19.12; I, 79.82. The CCl_4 was obtained from Eastman sulfur-free material by distillation in a 3-ft. column and collection at 75.9–76.1°. $TiBr_4$ was prepared from sugar charcoal and reagent grade TiO_2 by the method of Baxter and Butler[13] in a stream of nitrogen at 450°, and purified by distillation under reduced pressure; m.p. 38.7–39.2°.

The vapor pressures of $SnBr_4$ and $TiBr_4$ were measured using a static method with a liquid manometer. (SnI_4 was assumed to have negligible volatility at all temperatures

---

[1] The material of this paper is taken from a thesis presented by J. J. Keavney for the degree of Doctor of Philosophy at Fordham University, June, 1957. Portions of the work were reported to the Division of Physical and Inorganic Chemistry of the American Chemical Society in New York, September, 1954, and to the New York Section's Meeting-in-Miniature, February, 1954.

[2] National Science Foundation Fellow, 1953–1954.

[3] A. Wachter, *J. Am. Chem. Soc.*, **54**, 919, 2271 (1932).

[4] A. Speranski, *Z. physik. Chem.*, **46**, 70 (1903).

[5] E. P. Perlman and J. H. Davies, *J. Chem. Soc.*, **91**, 1114 (1907).

[6] A. Speranski, *Z. physik. Chem.*, **51**, 45 (1905).

[7] F. W. Küster, *ibid.*, **50**, 65 (1905).

[8] E. Vanstone, *J. Chem. Soc.*, **97**, 429 (1910).

[9] R. Hollman, *Z. physik. Chem.*, **37**, 193 (1901).

[10] J. H. Hildebrand, *J. Chem. Phys.*, **15**, 727 (1947); J. H. Hildebrand and R. L. Scott, "The Solubility of Nonelectrolytes," Reinhold Publ. Corp., New York, N. Y., 1950, pp. 58, 313.

[11] R. Lorenz, *Z. anorg. Chem.*, **9**, 365 (1895).

[12] F. A. McDermott, *J. Am. Chem. Soc.*, **33**, 1963 (1911).

[13] G. P. Baxter and A. Q. Butler, *ibid.*, **50**, 408 (1928).

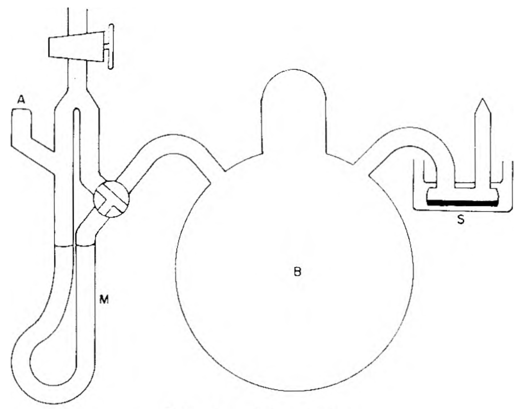

Fig. 1.—Apparatus.

studied.) The low pressures, and the reactivity of the halide vapors with mercury, eliminated its use and the Pyrex apparatus shown in Fig. 1 was designed which would require contact of the vapors with the manometer liquid for only the brief interval of time needed for a measurement. Concentrated sulfuric acid was used for this purpose for the $SnBr_4$, and mineral oil, thoroughly dried by filtering through activated alumina (ignited for an hour), for the $TiBr_4$. The density of the sulfuric acid was taken from the International Critical Tables. The density (d) of the mineral oil, measured with a pycnometer, obeyed the relation $d = 0.8774 - 6.6 \times 10^{-4} (t° - 20)$ g./ml. The manometer M, internal diameter 8 mm., led to an oil diffusion pump, forepump and McLeod gage. The volume of the bulb B was 1 liter. The entire apparatus shown was immersed in a water-bath.

$SnBr_4$ or $TiBr_4$ was introduced into the sample holder S from a small flask (not shown), fitted with a ground glass stopper, sealed onto S, as follows: The stopper was put on and the manometer liquid introduced into M through tube A, which was then sealed off. With the T-bore stopcock in a position 90° to the right of that shown, the system was evacuated for about an hour. During this time the apparatus was flamed in order to remove moisture. After the hour, dry air was admitted slowly through an air leak until the pressure was atmospheric. The stopper of the flask was removed and the $SnBr_4$ introduced into it. The apparatus was then evacuated and ice-water passed through the jacket of S. The sample was distilled from the flask into S and the tube from the flask to S sealed off under vacuum. The T-bore stopcock was turned to the position shown and the stopcock at the top of the manometer closed. The whole apparatus was now allowed to stand overnight in a thermostat at about 40°. During this time gases which had been trapped in the sample slowly escaped. The sample was then frozen by passing ice-water through the holder jacket. $SnBr_4$ supercooled easily and often required considerable time at 0° before solidifying. The bulb was then evacuated until the McLeod gage showed a pressure of 1 μ for 15 min. or more. The thermostat was then set at the desired temperature and the sample allowed to equilibrate. About 30 min. was allowed for this, although a constant reading was obtained after 10 min. The measurement was made as follows: the pump was started and the stopcock at the top of the manometer opened. The pressure was checked with the gage until it reached a constant value of no more than 1 μ. The stopcock was then turned 90° to the left and the difference in the manometer levels measured with a Gaertner cathetometer graduated to 0.01 mm. The stopcock was then returned to its original position and the manometer pumped out. The degassing procedure was repeated and measurements made until the same reading was obtained after two degassings. Once degassing had been completed it was found that readings could be reproduced within 5μ; this indicated that the gases produced by the interaction of the vapor and the monometer liquid did not approach significant amounts. Pressures were reproducible when the equilibrium was approached from both lower and higher temperatures. The pressures recorded below are reduced to 0° and accurate to 1 μ. Any error introduced by allowing the vapor to expand into the evacuated bulb cannot be greater than 0.4%, since the volume of the space between the stopcock and manometer liquid was only 3-4 ml. Bath temperatures were held constant within 0.05° and are accurate to 0.1°, by comparison with a certified N.B.S. thermometer.

Results and Discussion.—Table I gives the measured sublimation pressures for $SnBr_4$ and $TiBr_4$, and includes some values for liquid $SnBr_4$. Figures 2 and 3 show the data plotted as log p-(mm.) *vs.* $1/T$(°K.). Both sets of data were fitted to the equation $\log p = A - B/T$ by the method of least squares, weighting the points as the square of p so as not to overweight the smaller values of p. The following parameters were thus obtained: $SnBr_4$(s) $A = 10.7569$, $B = 3311.19$; $SnBr_4$(l) $A = 8.9702$, $B = 2766.55$; $TiBr_4$(s) $A = 11.0081$, $B = 3538.18$. From the slopes of the lines the heats of vaporization, sublimation and fusion of $SnBr_4$ were found to be 12.65 ± 0.14, 15.13 ± 0.17 and 2.48 ± 0.21 kcal./mole, respectively. The heat of sublimation of $TiBr_4$ is 16.17 ± 0.15 kcal./mole.

TABLE I

SUBLIMATION AND VAPOR PRESSURE OF $SnBr_4$ AND $TiBr_4$

$SnBr_4$		$TiBr_4$	
t, °C.	p, mm.	t, °C.	p, mm.
7.4	0.098	14.4	0.053
9.8	.116	16.0	.060
11.4	.133	17.4	.071
13.4	.149	20.0	.082
15.5	.199	23.0	.116
17.2	.223	24.8	.135
18.6	.254	25.2	.141
21.0	.321	26.9	.165
22.2	.359	26.9	.157
24.6	.424	29.2	.202
25.3	.467	30.2	.235
28.0	.577	30.5	.225
20.5[b]	.359	33.4	.297
20.6[b]	.339	36.4	.376
24.8[b]	.486		
30.7[a]	.746		
31.0[a]	.753		
34.9[a]	.985		
35.8[a]	1.031		
37.4[a]	1.160		
41.4[a]	1.493		

[a] Liquid. [b] Supercooled liquid.

Figure 2 also shows the data of Seki,[14] and of Kabesh and Nyholm[15] ($SnBr_4$(l) only), and Fig. 3 includes the values of Seki.[14] It can be seen that the data of Seki are uniformly higher than those reported here. Recently, Hall, Blocher and Campbell[16] measured the vapor pressure of $TiBr_4$ at temperatures above the melting point. An analysis of their data and Seki's led them to the conclusion that Seki's values were high because of residual moisture and consequent hydrolysis products. Our results confirm this conclusion.

Hall, Blocher and Campbell also calculated the heat of sublimation of $TiBr_4$ at 25°, using their vapor pressure equation and the heat of fusion determined by Kelley,[17] and obtained

---

(14) S. Seki, *J. Chem. Soc. Japan*, **62**, 789 (1941).

(15) A. Kabesh and R. S. Nyholm, *J. Chem. Soc.*, 3245 (1951).

(16) E. H. Hall, J. M. Blocher and I. E. Campbell, *J. Electrochem. Soc.*, **105**, 271 (1958).

(17) K. K Kelley, Quarterly Status Report to ONR from the U. S. Bureau of Mines, Project NR 037-054, October-December, 1955.

16.2 kcal./mole. This is in excellent agreement with our results. In addition, they have calculated the spectroscopic entropy of $TiBr_4$ and, in combination with the entropy of sublimation, find that it agrees with the third law entropy determined by Kelley.[18]

The System $SnBr_4$–SnI_4

This system was chosen because the components are the least sensitive to moisture of the Group IV halides, because it had been demonstrated[19] that they form a complete series of solid solutions, and because one of the components could be considered involatile, thereby avoiding vapor analysis. It was anticipated, however, that the tendency toward chemical interaction, claimed by Raeder[20] to be present in the molten state, would also be shown in the solid.

Experimental.—The apparatus of Fig. 1 was used. Solid solutions were made *in situ* by evacuating and flaming the entire apparatus, introducing solid SnI_4 into S and distilling $SnBr_4$ onto the SnI_4 as described above. Occluded gases were removed by allowing the whole to stand overnight under vacuum at a temperature above the m.p. of the sample. Vibration caused by the bath stirrer homogenized the melt. The sample was now quenched, or supercooled and allowed to freeze suddenly, thus favoring the formation of a homogeneous solid. The system held at 0° was now pumped down to 1μ. The stopcock was then turned to the position shown in Fig. 1, the bath set at the temperature of measurement, and the system allowed to equilibrate. Pressure measurements were made every two days with frequent degassings. After 10–15 days the same pressure was obtained after two successive degassings. Measurements were now made at a new temperature without further degassing, and steady values obtained after 2 days. Values for a given temperature were reproducible within 5μ whether approached from lower or higher temperatures. After a set of pressure–temperature readings had been completed the solid solution was analyzed by dissolving it in water, adding NaOH, heating for several minutes until the color of the SnI_4 disappeared, acidifying with H_2SO_4, and titrating potentiometrically for both iodide and total halide.[21] The latter was necessary since the original sample weight was unknown. The applicability of the method had been demonstrated by analyzing samples of known composition. The mole % SnI_4 as prepared and as found were, respectively, 0.85, 0.93; 15.89, 15.96; 21.45, 21.67; 51.89, 51.67, 51.67; 96.49, 95.55. Thus the analytical compositions are usually accurate to 0.2 mole % or better.

Results and Discussion.—The sublimation pressures of the various solid solutions (I to X) at different temperatures are given in Table II. It is assumed that, in view of the large amount of solid phase compared to that of the vapor, the analytical composition of the former represents that of the solid phase at all temperatures studied with that particular sample. The best straight lines for log P *vs.* $1/T$°K. plots of the data were found for each solution by the method of least squares, and from the slopes the heats of sublimation were calculated. They are discussed below. By interpolation the pressures for each solution were calculated for 17.5° to be as follows: $SnBr_4$ 0.233 mm.; I, 0.212; II, 0.192; III, 0.201; IV, 0.163; V, 0.145; VI, 0.100; VII, 0.145; VIII, 0.055; IX, 0.025; X, 0.021; SnI_4, zero. It may be seen that the system exhibits extreme negative deviations from ideal behavior. A possible explanation is that molecules of the two components interact by exchange of halogen to give compounds such as $SnBr_2I_2$, first proposed by Retgers,[22] but not evident in the melting point diagram determined by Auger[23] and Raeder.[19] Later Raeder,[20] and

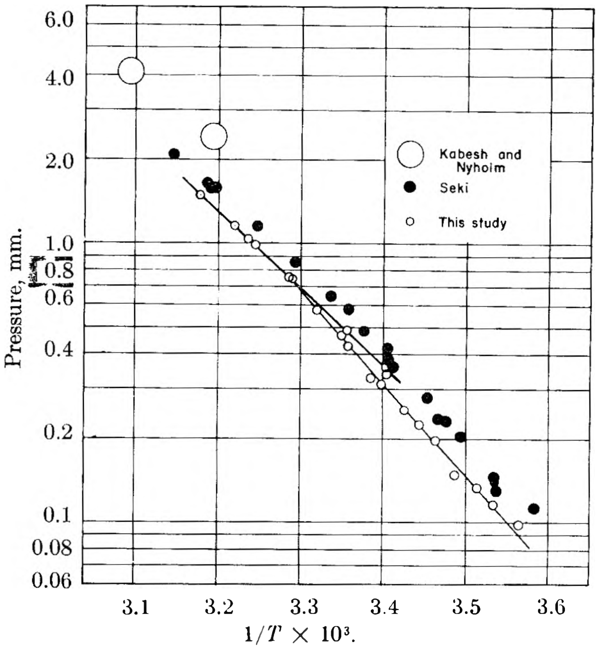

Fig. 2.—Sublimation and vapor pressure of $SnBr_4$.

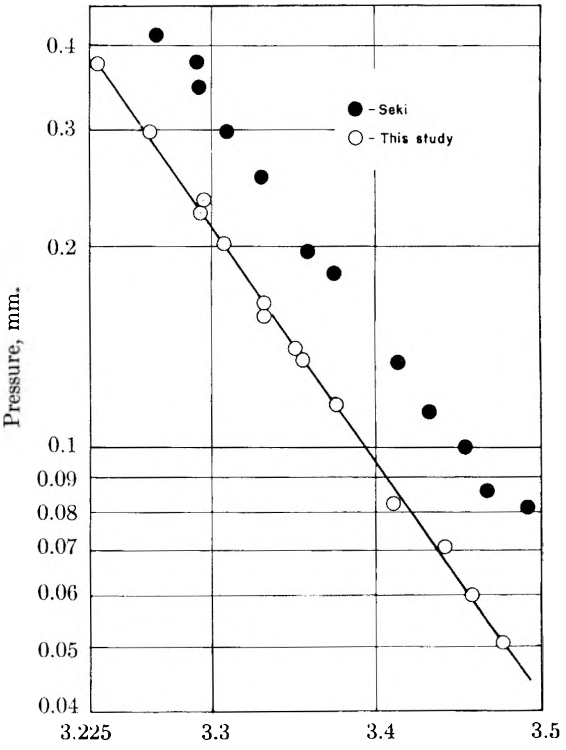

Fig. 3.—Sublimation pressure of $TiBr_4$.

---

[18] K. K. Kelley, ref. 17, July–September, 1955.

[19] M. G. Raeder, *Z. anorg. Chem.*, **130**, 325 (1923).

[20] M. G. Raeder, *K. Norske Videnskab. Selskabs. Skrifter*, **3**, 1 (1929).

[21] A. N. Campbell and L. W. Shemilt, *Trans. Roy. Soc. Can.*, **40**, III, 17 (1946).

[22] J. W. Retgers, *Z. physik. Chem.*, **16**, 577 (1895).

[23] M. V. Auger, *Compt. rend.*, **149**, 860 (1909).

Delwaulle and co-workers[24] presented evidence for many such mixed halides in the liquid state, so it is not surprising that they also appear to be present in the solid state. This led to the suspicion that mixed halides were also present in the vapor, in spite of the non-volatility of SnI_4. In order to determine this a solid solution of about 25 mole % SnI_4 was allowed to equilibrate with its vapor at 15°. The vapor was analyzed and found indeed to contain iodide to the extent of 7 mole % of the total halogen. Unfortunately this means that it is not possible to calculate the activity of $SnBr_4$ in the solid solutions from the data of Table II alone.

TABLE II

SUBLIMATION PRESSURE OF $SnBr_4$–SnI_4 SOLID SOLUTIONS

Temp., °C.	Press., mm.	Temp., °C.	Press., mm.	Temp., °C.	Press., mm.
Soln. I, 1.7 mole % SnI_4		Soln. IV, 12.8 mole % SnI_4		Soln. VII, 27.9 mole % SnI_4	
11.7	0.121	15.9	0.139	8.0	0.061
14.6	.168	16.1	.150	12.5	.089
15.5	.171	17.0	.147	12.9	.092
17.9	.221	19.1	.181	14.0	.105
20.5	.270	19.1	.198	15.4	.120
24.1	.367	20.1	.201	15.8	.125
24.4	.396	21.0	.236	15.8	.126
				18.4	.156
				18.4	.160
Soln. II, 5.6 mole % SnI_4		Soln. V, 15.3 mole % SnI_4			
16.6	0.180	15.0	0.107	Soln. VIII, 42.4 mole % SnI_4	
18.1	.199	17.0	.142		
20.0	.243	17.3	.147	14.5	0.046
22.2	.299	17.9	.151	17.2	.055
		18.2	.155	22.1	.070
		19.1	.169		
Soln. III, 8.3 mole % SnI_4		20.2	.190		
				Soln. IX, 61.2 mole % SnI_4	
4.5	0.057				
7.7	.081	Soln. VI, 27.2 mole % SnI_4		15.4	0.011
9.2	.105			16.8	.018
11.5	.111	13.9	0.062	17.7	.023
12.7	.127	15.7	.087	18.4	.036
13.2	.126	16.1	.081	25.6	.061
13.6	.145	16.5	.092	31.4	.504
15.2	.165	17.7	.095		
15.8	.159	17.7	.091		
16.0	.178	17.9	.108	Soln. X, 76.3 mole % SnI_4	
19.4	.244	18.3	.112		
		19.5	.129	17.6	0.023
				28.0	.053
				34.0	.093

The heats of sublimation, referred to above, for the various solid solutions, I to X, are 15.16, 15.87, 15.17, 16.51, 16.96, 20.45, 15.46, 9.00,19.06, 15.78 kcal./mole vapor formed, respectively. For the reasons given above the exact process to which each refers cannot be stated, but the irregular variation is undoubtedly related to the complex nature of the molecular species present.

The System $SnBr_4$–SnI_4–CCl_4

The above binary study was supplemented by an investigation of the ternary equilibria between solid solutions of $SnBr_4$ and SnI_4 and their saturated liquid solutions in CCl_4. (It was anticipated that CCl_4 would not take part in any halogen exchange with the tin compounds, thus retaining the ternary character of the system.) Such distribution studies, although by themselves not permitting the evaluation of solid state activities, can throw light on the nature of the deviations from ideality which may be present.[25]

Experimental.—Thirteen different mixtures (Table III), each totalling 10-15 g., were weighed into 30-ml. glass tubes containing small glass beads. In samples 2, 4 and 6 the SnI_4 was dissolved in the CCl_4 before adding the $SnBr_4$, and in samples 3, 5 and 7 the $SnBr_4$ was dissolved first. (In samples 2 to 7, and 13, the $SnBr_4$ was added in a dry box, but the conditions under which the subsequent analyses had to be performed indicated that the use of the dry box in the preparation was superfluous, so it was not used for the other samples.) The tubes were then sealed off and allowed to rotate in a thermostat at 12.00 ± 0.05° for over two weeks. (Samples 8 to 12, after sealing, were heated sufficiently to liquefy the contents completely before being placed in the thermostat.) At the end of the period of rotation the contents were allowed to settle, the tubes opened up, and duplicate samples of each liquid phase quickly withdrawn and weighed. In some instances, duplicate samples of wet solid phase also were weighed out. Dry solids were not obtainable from most of the tubes because they melted at room temperature. All the samples were analyzed by dissolving in water, making alkaline, allowing to stand overnight, acidifying, and titrating potentiometrically as described above. CCl_4 was determined by difference.

Results and Discussion.—Table III includes the resulting analytical data. Only the averages of the closely agreeing liquid compositions are given, but

TABLE III

THE SYSTEM $SnBr_4$–SnI_4–CCl_4 AT 12.0°

Sample no.	Total compn. Mole % $SnBr_4$	Total compn. Mole % SnI_4	Liquid compn. Mole % $SnBr_4$	Liquid compn. Mole % SnI_4	Wet solid compn. Mole % $SnBr_4$	Wet solid compn. Mole % SnI_4	Dry solid compn. (extrap., wtd. mean) Mole % $SnBr_4$
1	0	...	0	0.934	0	...	(0)
2	0.29	5.94	0.18	1.33	0.16	8.81	0.98
3	0.53	5.94	0.40	1.62	1.24	23.35	3.90
4	3.90	10.79	3.05	4.08	...	...	13.60
5	4.01	10.75	3.09	4.23	6.01	27.43	13.85
					6.03	26.20	
6	5.98	8.14	5.49	6.08	6.32	9.24	19.33
					7.47	17.31	
7	5.78	8.08	5.17	5.83	7.28	18.91	17.65
					7.00	18.47	
8	..	...	33.55	20.75	36.73	31.89	39.72
					33.44	29.21	
9	..	...	42.98	23.10	45.00	29.56	50.43
					44.77	30.20	
10	..	...	60.58	22.66	62.98	28.30	65.08
					62.29	28.11	
11	..	...	68.61	18.94	71.89	19.43	79.18
					73.35	19.88	
12	..	...	74.31	10.01	84.26	9.52	90.80
13	..	0	73.88	0	...	...	(100)

---

[24] M. L. Delwaulle, *et al.*, *Compt. rend.*, **219**, 64 (1944); *J. Am. Chem. Soc.*, **74**, 5768 (1952); *J. phys. radium*, **15**, 206 (1954).

[25] See, for example, A. E. Hill, G. S. Durham and J. E. Ricci, *J. Am. Chem. Soc.*, **62**, 2723 (1940), for an application to isomorphous salts.

the individual wet solid analyses are presented without averaging. It was assumed that any solid phases would not contain CCl_4, and this was borne out by the presence of no more than 1% CCl_4 in the solid phases from samples 2 to 5 which had also been dried by blotting and analyzed (data not shown). The mole % $SnBr_4$ in the solid phases from each tube was calculated from the liquid and total compositions, and from the liquid and wet solid compositions. Table III records the weighted average of these extrapolated values, in which the weighting was proportional to the difference between the % CCl_4 in the liquid and in the total composition or wet solid.

The consistency of the results, regardless of the method of approach to equilibrium, particularly the agreement between samples 4 and 5, and samples 6 and 7, indicates that the data are essentially those for equilibrium. The solubility of SnI_4 (0.934 mole %) may be compared with the value 0.898 at 10° obtained by Dorfman and Hildebrand.[26] No previous literature values for the solubility of $SnBr_4$ in CCl_4 are available. The dip in the liquidus is to be expected in view of the proximity of the temperature of the isotherm to the minimum melting point in the system $SnBr_4$–SnI_4 (19°).[19] The tendency of the tie lines to converge on this dip is also to be expected for the same reason and, in this case, therefore, is not necessarily indicative of a tendency toward an incomplete series of solid solutions, or positive deviations from Raoult's law. A plot of the mole fraction of the more soluble component ($SnBr_4$) in the liquid, on a solvent-free basis, against the mole fraction in the solid shows that the system belongs to Type II of the Roozeboom classification.[27] It gives no obvious indication of a Type III behavior which compound formation between $SnBr_4$ and SnI_4 might be expected to show, although the tie lines at the high iodide side do suggest the possibility.

It is of interest to apply the approach used by Hill, Durham and Ricci[25] for isomorphous salts, to the present system. They found, for two such salts with a common ion, and water, that the distribution data could be represented well by the relation $\log R_l = \log K + m \log R_s$, where R_l and R_s are the ratio, in liquid and solid phases, respectively, of the two ions with respect to which the salts differ, and m and K are constants. In the present system, letting R_l and R_s stand for the ratio of the molar concentrations of bromide to iodide in each phase, and plotting $\log R_l$ *vs.* $\log R_s$ also reveals a linear relationship in which m is close to 0.5 and K is about 1.9. Considering the supposed complexity of both liquid and solid phases this result is unexpectedly simple and its significance not evident. It is apparent that the two points for highest iodide content fall below the straight line, suggesting an abnormality in this region as pointed out above.

The System $SnBr_4$–$TiBr_4$

In order to eliminate the possibility of halogen exchange a study was made of the system $SnBr_4$–$TiBr_4$ in which a complete series of solid solutions has been demonstrated.[28]

Experimental.—The same general procedure was followed as for the system $SnBr_4$–SnI_4. However, since both components are volatile, it was desirable to analyze the vapors. This necessitated the use of a 2-liter flask at B, Fig. 1, with a small tube sealed on the side into which the vapors could be frozen. The increased size of the apparatus required that the manometer be left outside of the bath so that only the sample holder was thermostated. The latter temperature was 22.00 ± 0.05°, and the room temperature was kept at 26–27°. Prolonged contact of the vapors with lubricants was eliminated by using magnetically operated, unlubricated ground glass valves between B and S, and between B and the stopcock, as all lubricants tried were found to absorb the vapors upon lengthy exposure.

Both components were distilled into S, the sample was allowed to stand molten overnight, and the system, after several degassings, brought to equilibrium during a period of more than two weeks, when the pressure readings became constant. Both solid and vapor samples were then taken and analyzed for bromide potentiometrically as described above, and for tin by a modification of the method of DuPraw[29] as follows: The sample was dissolved in HCl, H_2SO_4 and HBF_4 were added, and the tin reduced by Al in a CO_2 atmosphere. Stannous ion was then titrated with standard KIO_3–KI solution. This method was found entirely reliable by analyzing mixtures of known composition over a wide range.

Results and Discussion.—The results, shown in Table IV, leave much to be desired in spite of the precautions taken. Only the solid phase compositions are given since the vapor compositions were even more erratic. The cause of the irregularity in the results is not known. Perhaps the solid solutions lacked homogeneity. It is possible that the behavior is related to a transparent, non-volatile yellowish film which slowly appeared on the inside of some parts of the apparatus during the equilibration period. Its nature was not determined, but it was water soluble. Conceivably this represented a product of some surface catalyzed decomposition of the $TiBr_4$, but the film was not observed when working with $TiBr_4$ alone, possibly because of the shorter duration of the runs. It seems likely that the values for high $TiBr_4$ content are the more reliable since they are the more consistent. Since all but one of the values lie above those predicted by Raoult's law it appears that the system exhibits positive deviations from ideality.

TABLE IV

SUBLIMATION PRESSURE OF $SnBr_4$–$TiBr_4$ SOLID SOLUTIONS AT 22°

Mole % $TiBr_4$	p, mm.	Mole % $TiBr_4$	p, mm.	Mole % $TiBr_4$	p, mm.
0	0.345	42.6	0.324	73.9	0.171
3.1	.319	44.1	.294	83.3	.153
12.4	.320	57.5	.241	88.5	.140
23.1	.295	70.1	.245	100.0	.105
40.9	.348	71.2	.187		

A comparison of the systems $SnBr_4$–SnI_4 and $SnBr_4$–$TiBr_4$ justifies the conclusion that mixed halides exist in $SnBr_4$–SnI_4 solid solutions. For, if such halides did not exist, one would expect the latter to show even greater positive deviations than the $SnBr_4$–$TiBr_4$ solid solutions, since there is a greater difference in molecular size between $SnBr_4$ and SnI_4 than between $SnBr_4$ and $TiBr_4$, thus

---

(26) M. E. Dorfman and J. H. Hildebrand, *J. Am. Chem. Soc.*, **49**, 729 (1927).

(27) H. W. Bakhuis Roozeboom, *Z. physik. Chem.*, **8**, 504 (1891).

(28) L. N. Eingorn, *Ukrain. Khim. Zhur.*, **16**, 414 (1950).

(29) W. A. DuPraw, *Anal. Chem.*, **26**, 1642 (1954).

introducing a greater amount of strain energy.

Summary.—1. A manometer has been designed for the measurement of pressures of vapors which are slowly reactive toward, or dissolve in, the manometric liquid.

2. The sublimation pressure and vapor pressure of $SnBr_4$ has been measured from 7 to 41° and the results found to be appreciably lower than the literature values. The heats of vaporization, sublimation and fusion are 12.65 ± 0.14, 15.13 ± 0.17 and 2.48 ± 0.21 kcal./mole, respectively.

3. The sublimation pressure of $TiBr_4$ was measured from 14 to 36° and found to be appreciably lower than the literature values. The heat of sublimation is 16.17 ± 0.15 kcal./mole.

4. The sublimation pressures of solid solutions of $SnBr_4$ in SnI_4 have been measured over a range of temperature. Marked negative deviations from ideality were evident and interpreted as a tendency to form mixed halides from the components even in the solid state, for which there had previously been evidence only in the liquid state. This was further substantiated by the finding of volatile iodide in the solutions even though SnI_4 itself is non-volatile at these temperatures.

5. The solid–liquid equilibria in the system $SnBr_4$–SnI_4–CCl_4 were investigated at 12°. Although the system showed a Roozeboom Type II behavior there was some evidence at the extreme iodide side of the diagram of compound formation between $SnBr_4$ and SnI_4.

6. The sublimation pressures of solid solutions of $SnBr_4$ in $TiBr_4$ were measured at 22°. The results were erratic, but they definitely indicated positive deviations from ideality.

SHOCK WAVES IN CHEMICAL KINETICS: FURTHER STUDIES IN THE RATE OF DISSOCIATION OF BROMINE

By DOYLE BRITTON

School of Chemistry, University of Minnesota, Minneapolis, Minnesota

Received November 18, 1959

The rate of dissociation of molecular bromine has been determined in the presence of argon, helium, nitrogen, carbon monoxide, oxygen and carbon dioxide in the temperature range 1300–1900°K. in a shock tube. The general features of the results agree with previous work on iodine dissociation. When the dissociation took place in the presence of N_2, CO or O_2 the vibrational relaxation of the latter gases occurred at about the same rate as the dissociation of the bromine, and complicated the interpretation. There was no evidence for any specific chemical effect with carbon monoxide. Bromine atoms and molecules both appeared to be about ten to twenty times more effective than argon as third bodies.

Introduction

It is possible to cause the dissociation of halogen molecules according to the reaction

$$X_2 + M \underset{k_R}{\overset{k_D}{\rightleftarrows}} X + X + M$$

by passing a shock wave through a mixture of the halogen and a suitable inert gas. By varying the strength of the shock wave it is possible to vary the temperature and the rate of the reaction. The rate of dissociation of molecular iodine in the presence of several inert gases has been measured by Davidson and co-workers.[1,2] The rate of dissociation of bromine has also been studied before by this means,[3,4] but only in the presence of argon. Since flash photolysis experiments[5a,b] at, or just above, room temperature have led to the determination of this dissociation rate in the presence of argon, nitrogen, oxygen and carbon dioxide, it was of interest to extend the shock tube studies to include all of these gases. This has been done, and the work reported here includes a further study on argon as an inert gas plus studies with helium, nitrogen, oxygen, carbon monoxide and carbon dioxide.

The rate constants indicated above are more explicitly defined by

$$\frac{d(X_2)}{dt} = -k_D(M)(X_2) + k_R(M)(X)^2$$

Strictly speaking, this equation should include separate terms for each gas present since k_D and k_R depend upon M. In particular, the possibility that X_2 and X serve in this role should be considered. Both Br_2 and Br are somewhat more efficient as third bodies than the other gases used. Palmer and Hornig[4] concluded that Br_2 was about twice as efficient as argon, while the results obtained in this present work suggest that it might be ten times more efficient. In view of the uncertainty, the rate constants here are reported for the mixture and no correction has been made for the Br_2. This point is discussed further in the section on results, under the heading Bromine. Experimentally k_D is determined but it is often more convenient to discuss k_R. These two constants are related by the equilibrium constant for the dissociation of Br_2 which has been calculated over the temperature range of interest from spectroscopic data.[6] In all of the rate expressions moles/liter was the concentration unit and seconds the time unit. The inert gas

---

(1) D. Britton, N. Davidson and G. Schott, *Disc. Faraday Soc.*, **17**, 58 (1954).

(2) D. Britton, N. Davidson, W. Gehman and G. Schott, *J. Chem. Phys.*, **25**, 804 (1956).

(3) D. Britton and N. Davidson, *ibid.*, **25**, 810 (1956).

(4) H. B. Palmer and D. F. Hornig, *ibid.*, **26**, 98 (1957).

(5) (a) R. L. Strong, J. C. W. Chien, P. E. Graf and J. E. Willard, *ibid.*, **26**, 1287 (1957); (b) W. G. Givens, Jr., and J. E. Willard, *J. Am. Chem. Soc.*, **81**, 4773 (1959).

(6) W. H. Evans, T. R. Munson and D. D. Wagman, *J. Research Natl. Bur. Standards*, **55**, 147 (1955).

present generally will be referred to as the third body, again thinking of the recombination reaction.

Experimental

The Shock Tube.—The experimental apparatus was similar to those which have been described previously.[1,4] The high pressure or driving section of the shock tube consisted of a 240-cm. length of 10-cm. i.d. aluminum pipe. The low pressure section consisted of a 240-cm. length of 10-cm. i.d. aluminum pipe followed by a 240-cm. length of 10-cm. i.d. Pyrex pipe. The two sections were separated by cellulose acetate membranes from 3 to 15 mils in thickness. The driving section was connected to a manifold which allowed for evacuating the tube, filling it with hydrogen (which was the customary driving gas) or nitrogen, and measuring the pressure.

The low pressure section was connected to a vacuum line in which reaction mixtures could be made up and stored. The pumping out of the low pressure system could be done through the vacuum line with a mercury diffusion pump, or directly with a mechanical pump. With the diffusion pump the entire low pressure section could be evacuated to a pressure of 0.1 μ. The pressure in the low pressure section at the start of an experiment was of the order of 10^{-2} atm. After the shock was run it was found very convenient to get rid of the spent reaction mixture and driving gas by flushing the tube out through a stopcock at the down-stream end of the low pressure section with nitrogen admitted at the upstream end of the high pressure section. This was much more rapid than evacuation and just as satisfactory otherwise. After the flushing, the tube was opened and the debris from the broken membrane cleaned out.

Detection and Recording.—The detection system consisted of four stations about 400 cm. downstream from the membrane. The first and third, 40 cm. apart, were used to measure the velocity of the shock wave and to trigger the oscilloscope traces. The second and fourth stations, each 10 cm. from the preceding trigger station, were the actual observation stations.

The light sources for all of the stations were General Electric #1763 6.1-v. instrument lamps. For the trigger stations the lamps were run at 7.5 v. from an a.c. transformer. For the observation stations the lamps were run at 8.0 v. from storage batteries. The optical arrangement at each station is shown in Fig. 1.[7] The use of mirrors gave an effective optical path length of 30 cm. For the trigger stations Corning #5538 glass filters were used to select that wave length region where bromine absorbed strongly. At the observation stations Bausch and Lomb 500 mμ second-order interference filters were used in conjunction with Corning #3385 glass cut-off filters to give light that was approximately monochromatic. For detectors 1P-28 photomultipliers were used. The described arrangement gave a photocurrent of 100 μamp. when the phototubes were operated at 60–70 volts per stage.

The signals from the trigger stations went to an amplifier which fired a thyratron. The thyratron signal triggered the oscilloscope sweep and the timer. The timer, a Model 7360 Universal EPUT and Timer made by the Berkeley Division of Beckman Instruments, measured to the nearest microsecond the time it took the shock wave to pass between the two trigger stations. The signals from the observation stations were displayed on a Tektronix 535 oscilloscope equipped with a type 53/54C dual trace plug-in unit,[8] and were recorded photographically with a Dumont type 2620 Polaroid Land camera. The writing rate of the oscilloscope was chosen so that the observations at the first observation station (recorded on the sweep of the A trace of the dual trace unit) were concluded before observations were begun at the second observation station (recorded on the B trace). The vertical coördinate on the oscilloscope represented the intensity of the light signal and was calibrated with flat traces run at definite, known photocurrents. The horizontal coördinate on the oscilloscope represented the time. It was found that the sweep speed as indicated by the selector switch was uniform and accurate to better than 1% so that no calibration markers were necessary.

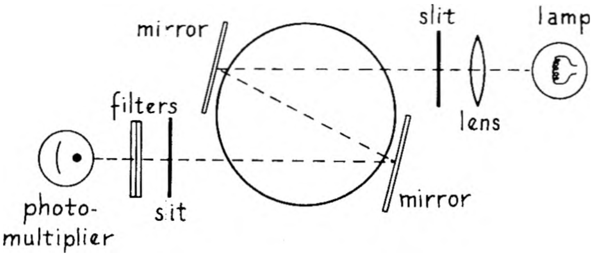

Fig. 1.—The experimental arrangement at each observation station.

The emission was followed by setting the photomultiplier at 180 μamp. photocurrent (this was the value which an original setting of 200 μamp. would drift down to) and then shutting off the light. The sensitivity of the oscilloscope was generally increased by a factor of 2 or 4 since the emission was rather small relative to the absorption.

Chemicals.—The Br_2 was Mallinckrodt Analytical reagent. A bulb-to-bulb distillation was performed in the vacuum line and the middle fraction taken. Argon from Matheson Co., Inc., stated to be 99.9% pure was used without further purification. Helium from the Puritan Co. of unstated purity was passed through a tetratrap[9] at liquid nitrogen temperature before use. Airco dry nitrogen of unstated purity was treated in the same fashion as the helium. Commercial grade carbon monoxide from Matheson stated to be 95.0% pure was purified by passing it through two tetratraps at Dry Ice temperature to remove any impurities condensable at this temperature (in particular H_2O and $Fe(CO)_5$), freezing it in a trap cooled by liquid nitrogen under reduced pressure, allowing it to melt, distilling off and discarding part of the liquid (to remove any H_2), and then using the middle fraction.[10] The last, unused portion of the liquid contained a white solid which probably was CO_2. Airco U.S.P. oxygen was collected in liquid nitrogen and distilled from the liquid. Carbon dioxide of unstated purity from the Liquid Carbonic Co. was condensed in liquid nitrogen, any non-condensable gases present were pumped off, and the carbon dioxide was then sublimed for use.

The reaction mixtures were prepared by placing a known pressure of Br_2 in previously evacuated storage bulbs and then adding inert gas until the total pressure was the desired value. The Br_2 pressure was measured on a butyl phthalate manometer and the total pressure on a Hg manometer. The mixtures were allowed to mix in the bulbs at least 36 hours before use.

Preliminary Calculations.—From a knowledge of the enthalpy functions for the various gases as a function of temperature[11] it is possible to calculate the pressure ratio, density ratio and velocity of the shock wave as a function of the final temperature. A measurement of the velocity then serves to determine all of the remaining properties, in particular the density ratio and temperature. The calculations were made assuming that room temperature was 300° K. The actual value was usually about 301° and the extremes were 5° on either side of this. A 5° error in the assumed room temperature would lead to a 5° error in the calculated high temperature. This was not corrected for. These calculations can be made on the assumption that the gas is vibrationally frozen at its original temperature or that it is vibrationally at equilibrium at the high temperature behind the shock wave. For example, in a shock wave in a 2% Br_2–98% O_2 mixture in which the observed shock velocity was 160 cm./millisec. the temperature at the shock front would be calculated to be 1750°K. if it were assumed that

---

[7] In a few of the early experiments the mirrors were not used. This required the use of higher pressures. The mirror arrangement was instituted after an occasion on which the Pyrex pipe failed to contain the shock wave.

[8] In many of the experiments a type 53/54D high-gain differential plug-in unit was used but the rise time of this unit was several microseconds, and it did not permit the use of two observation stations. The dual trace unit was a late improvement.

[9] W. G. Fately, H. A. Bent and B. Crawford, Jr., *J. Chem. Phys.*, **31**, 204 (1959).

[10] In the first experiments with the CO it was not purified. This resulted in a precipitate forming slowly when it was mixed with bromine. Shocks in this mixture seemed to indicate a very high efficiency for CO as a third body. This probably was due to the presence of hydrogen and the rapid reaction between hydrogen and bromine.

[11] "Selected Values of Chemical Thermodynamic Properties," Series III, Natl. Bur. Stds., Washington, 1954.

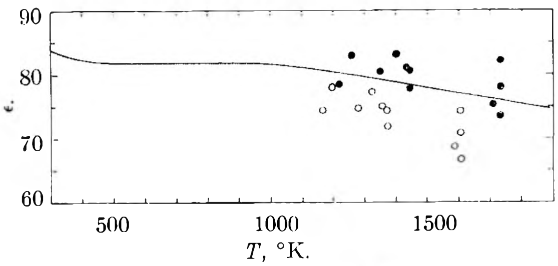

Fig. 2.—Extinction coefficient of Br_2 at 500 mμ: ●, nitrogen assumed vibrationally unrelaxed; ○, nitrogen assumed vibrationally relaxed; ——, theoretical extrapolation from the room temperature value.

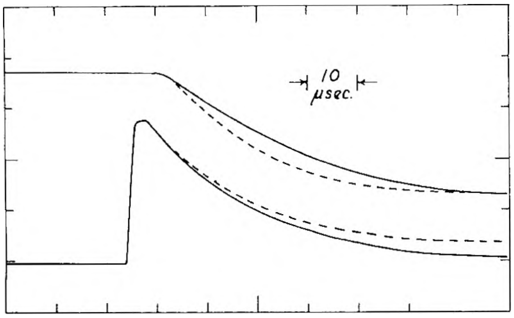

Fig. 3.—Typical oscilloscope trace: upper solid curve, emission (vertical sensitivity 8 × lower trace); upper dotted curve, emission calculated from observed temperature coefficient data; lower solid curve; experimental absorption; lower dotted curve, absorption corrected for emission. This experiment was with 5% Br_2 in Ar. Temperature at the shock front 1848°K. Temperature at equilibrium 1580°K. The rate of emission depends upon the square of the bromine atom concentration and is too low to be observable for the first 10 μsec.

no vibrational relaxation occurred in the shock front, and 1565°K. if it were assumed that complete vibrational relaxation took place. The choice between these two extremes was uncertain for the nitrogen, oxygen and carbon monoxide and had to be decided from the data, as is discussed later. It is also possible to calculate the shock parameters on the assumption that the bromine has dissociated to some definite degree. This was necessary to decide on the equilibrium dissociation in the experiments with emission. All of these calculations are straightforward algebraically, but are tedious. For this reason a Minimatic program was prepared for the Univac Scientific Model 1103 computer and the calculations were made by this means.

Results

Extinction Coefficients.—All of the observations were made at a wave length of 500 mμ, which was chosen for the reason that at this wave length the change of the extinction coefficient with temperature was relatively small. The decadic extinction coefficient for the bromine at room temperature was determined by observing the drop in photocurrent when the apparatus was filled with the reaction mixture. The average of 11 experiments using a 10-cm. light path (*i.e.*, without the mirrors shown in Fig. 1 present) gave $\epsilon = 84 \pm 3$ liter mole^{-1} cm.$^{-1}$. The average of 20 experiments using a 30-cm. light path gave $\epsilon = 86 \pm 4$. The direct measurement of Acton, *et al.*,[12] gave $\epsilon = 77$ at 298°K. The value $\epsilon = 84$ was used as the room temperature value in making calculations throughout this work.

The theory of Sulzer and Wieland[13] was used to calculate the change in ε with temperature. In those cases where the degree of vibrational relaxation was not in question, the high temperature values that were determined in the shock wave experiments agreed with the calculated values within the estimated experimental error which was about 5% at the lower shock temperatures and 10% at the higher. In every case ε was calculated from the change in optical density at the steep rise in the curve, with the assumption that no dissociation had occurred. If the dissociation was so rapid in a particular experiment that no good estimate of the initial rise could be made, that experiment was discarded. Figure 2 shows the experimental values for nitrogen compared with the theoretical curve. The scatter and fit for the unrelaxed points is typical of the results for most of the other gases. These are discussed in detail under the individual cases. Since the theoretical curve seemed to express the data well, it was used to find the temperature coefficient, and no attempt was made to fit some other curve to the experimental points.

Emission.—As soon as bromine atoms are formed emission begins to occur in the same wave length region as the absorption. This has been studied in some detail by Palmer[14] who concluded that it was primarily from two-body radiative recombination. The results here generally agree with his although his observations were made at 3650, 4390 and 5950 Å. and these were made at 5000 Å. The emission was measured at the equilibrium position, corrected for self-absorption, and divided by the square of the bromine atom concentration to obtain an effective rate constant for emission. From the results of ten experiments between 1350 and 1850°K. with argon present as the inert gas, it was possible to obtain an activation energy for the emission process. This was found to be 10.7 ± 0.5 kcal. (= 3750 cm.$^{-1}$).[15] This activation energy was calculated assuming that $k \sim T^{-1/2} \exp(-E/RT)$.[14] Figure 3 shows the oscilloscope trace of a typical emission experiment. Once the effective emission rate constant is known as a function of temperature, it is possible to calculate the appearance the emission curve should have as a function of time. This calculated curve is also shown in Fig. 3. It can be seen that the shape is qualitatively correct but the observed emission is less than the calculated in the intermediate range of dissociation. This was generally the case. It is possible that this was caused by the observation arrangement which had only one slit between the tube and the photocell, so that emission was observed from a wedge-shaped section of the tube. The emission was studied primarily in order to be able to correct the absorption curves, and the fact that the slit arrangement was not ideal for the emission work was overlooked until the work was done. Another more interesting possibility is that the emission is due in part to excited Br atoms and that the excitation process

$$\mathrm{Br}(^2P_{3/2}) + M \xrightarrow{k} \mathrm{Br}(^2P_{1/2}) + M$$

occurs at a rate comparable to the rate of dissocia-

---

[12] A. P. Acton, R. G. Aickin and N. S. Bayliss, *J. Chem. Phys.*, **4**, 474 (1936).

[13] P. Sulzer and K. Wieland, *Helv. Phys. Acta*, **25**, 653 (1952).

[14] H. B. Palmer, *J. Chem. Phys.*, **26**, 648 (1957).

[15] If it is assumed that the radiation process involves one excited bromine atom, this energy becomes 1.6 kcal. (= 550 cm.$^{-1}$).

tion. The rate constant for this reaction can be estimated as $k = PZ \exp(-\Delta\epsilon/kT)$ which at 1600° K. equals $6 \times 10^9\ P$ liter mole^{-1} sec.$^{-1}$ for argon as the colliding atom. For a concentration of 4×10^{-3} mole/liter, this gives a half-life of about 0.03 μsec. if the probability factor $P = 1$, and 30 μsec. if $P = 10^{-3}$. The latter value of P does not seem unreasonably low since the reaction involves a forbidden electronic transition. The details of the emission process here seem worthy of considerable further study.

In the experimental results reported here the emission was found to be sufficiently low below 1900°K. that it could be ignored. Only a few experiments were performed at higher temperatures than this and these have been omitted in this report.

Dissociation.—The rate of dissociation was determined from the initial slope on the oscilloscope trace. (See Fig. 3.) If the angle of this slope away from the horizontal is θ, then this is converted to the change in photocurrent by

$$\frac{di}{d\tau} = \tan\theta\ \frac{\mu\text{amp./cm.}}{\text{sec./cm.}}$$

where the two factors on the right are the oscilloscope scale factors. The intensity of the transmitted light is i, that of the incident light i_0, zero and τ is the apparent time.

$$k_D = \frac{1}{\log i/i_0}\,\frac{d \log i/i_0}{d\tau}\,\frac{1}{\Delta^2 c_1}\left(1 - \frac{d \ln \epsilon}{d\alpha} - \frac{d \ln \Delta}{d\alpha}\right)^{-1}$$

Δ is the density ratio across the shock front, c_1 is the concentration of the unshocked gas, ϵ is the extinction coefficient, and α is the degree of dissociation. It should be recognized that this is not an isothermal system. In a 5% Br_2–95% Ar mixture the temperature would drop 400° as α went from 0 to 1. The observed change in the optical density with time is primarily due to the disappearance of Br_2, but part of the change can be traced to an increase in density which follows from the change in degree of dissociation, and part to an increase in the extinction coefficient which follows from the change in temperature. These latter effects are corrected for by the term in parentheses in the expression for the rate constant. Since the rate constant is ultimately determined by the slope of the optical density curve at a particular point, the changing temperature does not need to be considered other than to use the temperature appropriate to the point at which the slope is measured.

In a few cases the picture was enlarged, the curve measured at many points, and the value of k_D determined by integration (using an integrated expression that allowed for the change of k_D with T during the course of the reaction) or from plots of log log i/i_0 vs. τ, which more nearly gives a straight line. These values probably were more accurate but the scatter from run to run was just as great and there was no consistent difference from the simple method of calculation, therefore the latter was generally used. In the section on the individual third bodies the results have been expressed as $\log k_R = A + B/T$. This is not meant to imply that this is the correct theoretical form to describe the temperature variation of this rate constant, but is merely intended as a convenient way of summarizing the data. The equations were obtained from the experimental points by the method of least squares, simply to have an objective means for this determination. An average value is also given in each case. This is the value at the center of gravity of the experimental points. Figure 4 shows the data for nitrogen, which are typical of the scatter of all data. The estimates of error given are the probable errors.

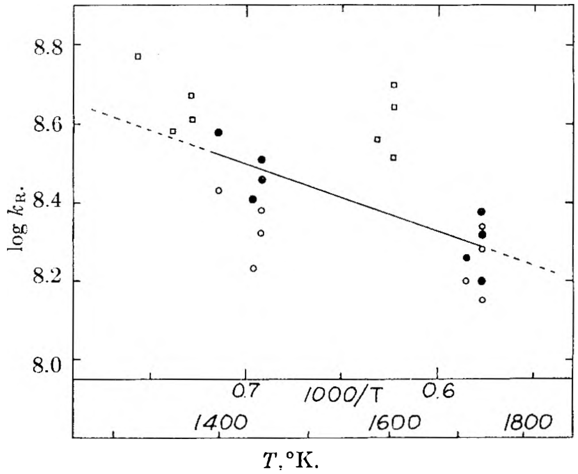

Fig. 4.—Recombination rate constants for N_2 as third body: □, nitrogen assumed vibrationally relaxed; ○ nitrogen assumed vibrationally unrelaxed; ●, nitrogen assumed vibrationally unrelaxed initially, corrected for relaxation. The line is the best straight line through the solid points.

It should be emphasized that k_D is determined experimentally and that $k_R = k_D/K$ is plotted in Fig. 4 and discussed in the various sections.

Argon.—There were no unusual features in any of the argon runs, which serve as a standard of comparison for the others. Nineteen experiments were run in 2% Br_2–98% Ar mixtures at initial temperatures ranging from 1370 to 1880°K. These gave $\log k_R = 7.608 + 1368\ (\pm 196)/T$, and an average value of $\log k_R$ of 8.445 ± 0.012 at 1635°K. Fourteen experiments were run in 5% Br_2–95% Ar mixtures at initial temperatures ranging from 1381 to 1848°K. These gave $\log k_R = 7.619 + 1527\ (\pm 177)/T$, and an average value of $\log k_R$ of 8.545 ± 0.010 at 1649°K. Thirteen more 5% experiments were run at temperatures from 1935 to 2260°K. These gave rate constants which agreed with the values at the lower temperatures, but which are not included since they should have been corrected for emission and the correction seemed rather uncertain. The difference between the 2 and 5% results can be accounted for by a greater efficiency of the Br_2 molecules as third bodies, as is discussed in the section Bromine, however the data show sufficient scatter that this is dubious. Probably the best way to treat the argon data is to combine the 2 and 5% points to obtain $\log k_R = 7.639 + 1388\ (\pm 174)/T$, and an average value of k_R of 8.485 ± 0.010 at 1641°K. Several experiments were run with a defective but identical pair of filters at the two observation stations, in which dissociation was observed at both stations. These are not included in the numerical results, but are worthy of note because it could at least be seen that the extinction coefficients and rate constants were nearly identical at the two stations in a given shock. The difference between them was about one fourth the variations that were found between different shocks. This suggests that attenuation of the shocks between the stations was not significant.

Helium.—Sixteen experiments at temperatures from 1469 to 1915°K. were run in 5% Br_2–95% He mixtures. These gave $\log k_R = 7.409 + 1743\ (\pm 239)/T$, and an average value of $\log k_R$ of 8.459 ± 0.013 at 1661°K. The only unusual feature of these shocks was that observations over a long period of time showed the absorption curve to become eventually concave downward. This cannot be explained.

Nitrogen.—Eight experiments at temperatures from 1400 to 1732°K. were run in a 2% Br_2–98% N_2 mixture. The oscilloscope traces for these experiments were interpreted both on the assumption that the nitrogen was vibrationally unrelaxed and on the assumption that the relaxation took place in the shock front. The calculated extinction coefficients were shown in Fig. 2 for both assumptions, along with the results from three experiments at temperatures too low for a measurable dissociation rate. The extinction coefficients suggest strongly that the nitrogen is not vibrationally relaxed at the shock front. The shape of the curves gives no indication of vibrational relaxation so that it would appear from these data that the nitrogen does not relax vibrationally to any appreciable extent in the time of the experiment. However, shock wave experiments at higher temperatures[16] and acoustical resonance experiments at lower temperatures[17] indicate that the vibrational relaxation times are of the order of the times in this experiment. Values of k_R are shown in Fig. 4 for three assumptions: that there is no vibrational relaxation; that vibrational relaxation is complete in the shock front; that vibrational relaxation is occurring at a rate of the order of the rate of dissociation. The last assumption is believed most likely to be correct, since the results of Blackman, and Lukasik and Young indicate that the rate of relaxation in pure nitrogen is such that this would be true, and the presence of Br_2 can only increase this rate. However, the limiting values of the extinction coefficients show that it has not been increased greatly. The correction to the rate constant calculated from the initial slope has been made according to

$$k_D = k_D{}^* + Qk_\beta$$

$$Q = \frac{1 - \mathrm{d}\ln\Delta/\mathrm{d}\alpha - \mathrm{d}\ln\epsilon/\mathrm{d}\alpha}{\mathrm{d}\ln\Delta/\mathrm{d}\beta + \mathrm{d}\ln\epsilon/\mathrm{d}\beta}$$

$$k_\beta = RT/\tau_0$$

where $k_D{}^*$ is the apparent rate constant for dissociation if it is assumed that there is no vibrational relaxation, α is the degree of dissociation relative to complete dissociation, β is the degree of vibrational relaxation relative to the equilibrium value, and τ_0 is the vibrational relaxation time as normally defined. The corrected results gave $\log k_R = 7.301 + 1705\ (\pm 281)/T$, and an average value of $\log k_R$ of 8.390 ± 0.017 at 1565°K.

Carbon Monoxide.—Several sets of experiments were run involving CO as the inert gas. The first few experiments seemed to indicate that this was an exceedingly efficient third body, perhaps an order of magnitude or more better than nitrogen. This was almost certainly due to a small amount of hydrogen impurity in the CO. However, before it was realized that this might be the explanation, five experiments were run in a 2% Br_2–10% CO–88% Ar mixture, since it was thought the large efficiency of the CO would still lead to a significant increase over the observed dissociation rate in argon. The five experiments gave $\log k_R = 7.418 + 1797(\pm 302)/T$, and an average value of $\log k_R$ of $8.562 + 0.016$ at 1571°K. if the CO was assumed unrelaxed and about 10% higher if it was assumed relaxed. This is about the same as the pure argon. In view of later experiments this is reasonable and simply means that with the 10-fold dilution of the CO the concentration of the H_2 impurity was reduced to such a level that it had little effect. In the most significant set, sixteen shock waves were run in a 2% Br_2–98% CO mixture with the CO carefully purified as described in the section on chemicals. This set gave rate constants about the same as those for N_2 as third body. The interpretation was complicated again by the vibrational relaxation of the CO. In this case there was no question about vibrational relaxation. The extinction coefficients indicated that the CO was vibrationally unrelaxed at the shock front, and at the lower temperatures, 1100 to 1500°K., relaxation was apparent simply from the shape of the dissociation curves. The rate of vibrational relaxation has been studied by shock tube methods at these temperatures and higher by Windsor, Davidson and Taylor,[18] who found that it was lower than N_2, and that it was very sensitive to certain impurities. Very rough estimations of the relaxation times for CO in the experiments reported here give values about one fourth of those in the pure gas. The seven dissociation experiments at the highest temperatures, 1640 to 1910°K., were the only ones in which it was felt that the initial slopes could be determined with any certainty. Table I lists these values and also those obtained using a relaxation time four times that for the pure gas. The corrected values are thought to be the best, but the abnormally high temperature dependence indicates that they are probably not too reliable. The equa-

TABLE I

EFFECT OF VIBRATIONAL RELAXATION IN CO

$k_D{}^*$ = the apparent value from the oscilloscope trace; k_β = the rate of vibrational relaxation from reference 18; $k_D = k_D{}^* + 4\,Qk_\beta$. The units are: k_D, k_β—liter^1 mole^{-1} sec.$^{-1}$; k_R—liter^2 mole^{-2} sec.$^{-1}$

T	$k_D{}^*$	$k_R{}^*$	Qk_β	k_D	k_R
1640	3.0×10^5	1.20×10^8	0.52×10^5	5.0×10^5	2.0×10^8
1748	5.0	0.84	.78	8.1	1.4
1770	5.6	.81	.84	9.0	1.3
1785	6.0	.78	.89	9.6	1.2
1810	7.4	.81	.97	11.3	1.2
1892	14.0	.90	1.23	18.9	1.2
1910	11.2	.64	1.29	16.4	0.9

---

[16] V. H. Blackman, *J. Fluid Mech.*, **1**, 61 (1956).

[17] S. J. Lukasik and J. E. Young, *J. Chem. Phys.*, **27**, 1149 (1957).

[18] M. Windsor, N. Davidson and R. Taylor, "Seventh Symposium (International) on Combustion," London, 1959, p. 80.

tion for these points is log $k_R = 6.222 + 3374 (\pm 40\ 2)/T$.

Oxygen.—Seven experiments were run in 2% Br_2–98% O_2 and twelve in 5% Br_2–95% O_2 mixtures. In the four experiments at the lowest temperatures, 1120 to 1280°K., where negligible dissociation occurred, vibrational relaxation could be seen taking place at times just barely long enough to be detectable. This agrees with the results[16] in pure O_2. The experimental extinction coefficients indicated that in all of the shocks below 1700°K. the relaxation was complete in a time short compared to the reaction time. In four experiments near 1800°K., the extinction coefficients and the shapes of the curves seemed to indicate that these were not completely relaxed at the shock front and that relaxation took place in a time comparable to the experimental time. This conclusion is consistent with the experimental values of the relaxation time for pure O_2 as determined by Blackman.[16] The experimental points in the 2 and 5% mixtures combined (with the omission of the four points near 1800°) gave log $k_R = 7.844 + 1409 (\pm 504)/T$, and an average value of log k_R of 8.835 ± 0.023 at 1422°K. The k_R values for the four points near 1800° agreed with this fairly well if they were corrected for vibrational relaxation.

Carbon Dioxide.—Eleven experiments were run in 2% Br_2–98% CO_2 mixtures. Three of these were at temperatures too low for any appreciable amount of dissociation to take place. The eight others at temperatures from 1380 to 1622°K. gave log $k_R = 7.885 + 1276 (\pm 654)/T$, and an average value of log k_R of $8.686 + 0.030$ at 1474°K. As was the case in the experiments with I_2 in CO_2,[2] the extinction coefficients indicated clearly that the CO_2 was vibrationally relaxed. In the experiments with I_2 it was noticed that the density of the gas behind the shock front was not very smooth and it was suggested that this might be due to the nearness of the cold front to the shock front in the CO_2 shocks, this nearness being a necessary consequence of the high heat capacity of CO_2. This same unevenness was present in all of the experiments reported here where the cold front was two to three times further away. In the I_2 shocks the observations were made 10–12 tube diameters from the membrane. In the present experiments the observations were made about 40 tube diameters from the membrane. Since the two sets were equally uneven this unevenness cannot be attributed to the nearness of the cold front nor to the recentness of the bursting process, although it still may be a consequence of the high heat capacity.

Bromine.—The question of the efficiency of bromine atoms and molecules as third bodies is one which the data reported here do not answer well, since none of the experiments was performed with a large amount of Br_2 relative to the inert gas. However, with both argon and oxygen two sets of experiments were made, one set at 2% Br_2, and the other at 5%. In each case the constants determined in the 5% mixtures were, on the average, higher than those determined in the 2% mixtures, although the spread in the points was such that the two sets overlapped. Using the values from the smoothed curves through the argon data ($k_R = 2.90 \times 10^8$ liter^2 mole^{-2} sec.$^{-1}$ for 2% and 3.74×10^8 for 5%) one finds $k_R = 2.3 (\pm 0.2) \times 10^8$ for argon and $30(\pm 5) \times 10^8$ for Br_2. The ratio $k_{Ar}/k_{Br_2} = 13(\pm 3)$. The errors are estimated from the least squares probable errors and are certainly optimistic. The results of Givens and Willard[5b] gave a ratio of 130 at 300°K., 110 at 350°K. and 90 at 400°K. and would predict a ratio of 40 at 1600°K. if it is assumed the ratio can be written in the form $Ae^{-B/T}$. The shock wave data of Palmer and Hornig gave a ratio of about two at high temperatures. A similar treatment of the oxygen data gives k_R for Br_2 as $44(\pm 36) \times 10^8$ at 1400°K.

If the slope is measured on the optical density curve at some intermediate point in the reaction then it should be possible to find a rough estimate of k_R for Br atoms if they are much more efficient as third bodies. This was done in four shocks at points near 50% dissociation and $k_R = 40(\pm 10) \times 10^8$ was found. The error was estimated from the scatter in the four values. No estimate of this constant has been made at lower temperatures.

The values listed for the various bases in Table II have not been corrected for the extra efficiency of the Br_2 since this correction is at most about 30% and is fairly uncertain. The extra efficiency of the Br atoms would not affect the results, since at the start of the dissociation there are no atoms present, and their later appearance would not affect the initial slope.

Other Gases.—Without giving much thought to the matter, some experiments were run in N_2O as an inert gas.[19] A consideration of the reactions

$$N_2O = N_2 + {}^1/_2O_2$$

and

$$N_2O = N_2 + O$$

would have shown that N_2O is both thermodynamically and kinetically unstable at the temperatures at which the Br_2 dissociation would be expected. The few experiments run show that the Br_2 disappeared at a rate which increased with time. Therefore the N_2O or its decomposition products must react with the Br_2. This is a system that will be looked into further but was postponed for the time since it clearly does not belong with a study of the effect of inert gases.

As part of the series of third bodies discussed here, it was intended to include HBr and HCl. The HBr was also of interest in connection with studies of the H_2–Br_2 reaction.[20] It is not included here since it is not a simple system. In the presence of large amounts of HBr the following series of reactions occur

$$Br_2 + M = 2Br + M$$
$$Br + HBr = Br_2 + H$$
$$H + HBr = H_2 + Br$$

that is, the reverse of the normal H_2–Br_2 reaction. This will be discussed more fully with the H_2–Br_2 studies. A rather similar situation obtains with

---

[19] See Priestley's comment as quoted by J. B. Conant, "Harvard Case Histories in Experimental Science," Vol. I, Cambridge, Mass., 1957, p. 99.

[20] D. Britton and R. M. Cole, unpublished work.

HCl,[21] although the mechanism here has not yet been determined. The net reactions

$$HCl + Br_2 = HBr + BrCl$$

and

$$HCl + BrCl = HBr + Cl_2$$

appear to take place quite rapidly and must be studied before any dissociation studies could be meaningful.

Discussion

Other work on the dissociation of bromine in shock waves has only been with argon as a third body.[3,4] The results here agree with the earlier work within the experimental error. Flash photolysis experiments at or near room temperature[5] showed that the recombination rates at these temperatures were about an order of magnitude larger.

The most likely looking theoretical explanation of the temperature dependence of k_R is that the two reactions occur

$$M + X \rightleftarrows MX \quad (1)$$
$$MX + X \longrightarrow M + X_2 \quad (2)$$

and that the first of these is sufficiently rapid that equilibrium is maintained in this step. This has been developed by Bunker and Davidson[22] from whose work one can write

$$k_R = 3.91 \times 10^6 \sigma_1{}^3\sigma_2{}^2 \left(\frac{\epsilon_0}{k\mu_2}\right)^{1/2} \frac{\epsilon_0}{kT}\left[1 + 0.267\frac{\epsilon_0}{kT}\ldots\right]$$

where σ_1 and σ_2 refer to the collision diameters in Angström units in reactions 1 and 2, ϵ_0 is the depth of the potential minimum in reaction 1, and μ_2 is the reduced mass in molecular weight units for the collision in reaction 2. Table II shows a comparison of the several experimental results with the theory. Values of the various molecular parameters necessary for the theoretical calculations were taken from Hirschfelder, Curtiss and Bird.[23] It will be seen that the agreement is fair. Helium and bromine do not fit well, and oxygen is questionable. As Bunker and Davidson have pointed out, light gases such as He and H_2 do not fit well into their theoretical picture. The bromine may well involve a specific chemical interaction, as was probably the case for iodine recombination in the presence of iodine.

TABLE II

COMPARISON OF EXPERIMENTAL AND THEORETICAL RESULTS

Inert gas	k_R (l.^{2} mole^{-2} sec.$^{-1}$) Experimental	Ref.	k_R (l.^{2} mole^{-2} sec.$^{-1}$) Theoretical
Temperature, 300°K.			
Argon	2.0×10^9	5b	1.9×10^9
Nitrogen	3.4	5a	2.0
Oxygen	7.9	5a	2.1
Carbon dioxide	7.8	5b	5.0
Bromine (molecules)	130	5b	8.0
Temperature, 1600°K.			
Argon	3.2×10^8		3.4×10^8
	3.2	3	
	3.6	4	
Helium	3.2		0.38
Nitrogen	2.3		3.4
Carbon monoxide	2.1		3.7
Oxygen	5.3		3.6
Carbon dioxide	4.2		8.3
Bromine (molecules)	5.4	4	12.4
	30		

Acknowledgments.—I wish to thank Mr. William Streib and Mr. Richard Zuehlke for their help in constructing the apparatus and Mr. Roger Cole for running many of the experiments with argon. I am grateful for the support of the Research Corporation, the Office of Ordnance Research, U.S. Army and the Graduate School of the University of Minnesota.

---

[21] D. Britton and E. Saettler, unpublished work.

[22] D. O. Bunker and N. Davidson, *J. Am. Chem. Soc.*, **80**, 5090 (1958).

[23] J. O. Hirschfelder, C. F. Curtiss and R. B. Bird, "Molecular Theory of Gases and Liquids," New York, N. Y., 1954.

EQUILIBRIA IN THE SYSTEM Rb_2O–Nb_2O_5 AND SEQUENTIAL TRENDS IN OXIDE–OXIDE INTERACTIONS.[1] THE PREDICTION OF COMPOUND RETENTION

BY ARNOLD REISMAN AND FREDERIC HOLTZBERG

Contribution from the Watson Laboratories of International Business Machines, New York, N. Y.

Received November 25, 1959

As part of the general investigation of oxide–oxide interactions, the present study of the congener series Alkali Oxide-Group VB pentoxide was continued with an investigation of the system Rb_2O–Nb_2O_5. Eight compounds have been identified in this system. Three of these, the 1:4, 4:11 and 4:1 members melt congruently at 1315, 1319 and *ca.* 1300°, respectively, the remainder having base to acid ratios of 2:15, 1:2, 2:3, 1:1 and 4:3 melt incongruently at 1351, 1185, 1148, 964 and 830°, respectively. On the basis of the observed liquidus behavior of the several compounds appearing in the sequence of interactions studied, the preliminary model hypothesis previously discussed is expanded upon, and predictions concerning compound repetition in the Cs_2O–Nb_2O_5 interaction are presented.

Introduction

The interactions of the alkali oxides or silver oxide with Nb_2O_5 fall into two groups depending on whether or not the comparative behaviors are similar. Thus, it has been shown that despite large ionic radii variations and normal coördination number differences in the sequence Li^+, Na^+ and Ag^+, the mixed oxide reactions involving these ions

---

[1] This paper was presented in part at the 136th A.C.S. Meeting, September, 1959.

resemble one another. Each of these binary systems generates intermediate members having base to acid ratios of 1:14, 1:4, 1:1 and 3:1, the similarity between the sodium and silver analogs being such that they are isostructural.[2,3] In addition, the compounds $NaNbO_3$ and $AgNbO_3$ exhibit similar dielectric properties even though the covalent character of the Na-O and Ag-O bonds might be expected to be appreciably different.

With the introduction of K_2O,[4] one observes appreciable changes in the gross structure of the phase diagram. While the picture from 50 mole % alkali oxide on is unchanged, the number of intermediate compounds in the range 0-50 mole % increases, and none of the previously encountered ratios reoccur. Furthermore, relatively stable metastable regions tend to form in the latter range, involving, for example, the formation of a 6:7-7:6 join at the expense of the meta-salt fields.[5] The 7:6 ratio is of particular interest since it represents a value frequently reported in aqueous niobate systems, but not observed in the anhydrous counterparts. A feature of further interest in the potassium system is the first appearance of a non-primitive component in the 0-50 mole % region where the 2:3 compound is seen to melt congruently. Related to this, is the melting of the 1:1 salt at a singular point between congruency and incongruency within the limits of experimental uncertainty, as compared to the congruent melting of the lithium and sodium analogs.[6]

These trends prompted an investigation of the phase relationships in the system $Rb_2O-Nb_2O_5$. It was expected that in addition to a further increase in the number of compounds formed, deterioration of model behavior would be detected in the region above 50 mole % base, with the possible formation of a 7:6 member. It was also expected that the trend in meta-salt instability would continue with complete incongruency occurring.

Experimental Procedure

Reagents.—Trona Rb_2CO_3 and Fansteel "High Purity" Nb_2O_5 served as the starting materials for all reactions. The pentoxide was ignited in platinum at 1100° for 24 hours to remove all moisture. The carbonate was reported to assay 99.5%, but analysis of the material showed the presence of from 4-5% iron by weight. Six isothermal recrystallizations from water reduced the iron content to the p.p.m. range, and subsequent conversion of the product to the bicarbonate followed by six further recrystallizations, in which the mother liquor was cooled to *ca.* 2°, and then reconversion to the dry carbonate at 285° yielded a chemical assaying *ca.* 99.8% on the basis of X-ray fluorescence analysis. Traces of K and Na were the only detectable impurities.

Sample Preparation.—Specimens for X-ray, density and heating curve studies were prepared by the reaction of mixtures in platinum crucibles at 10-20° below the appropriate solidus temperatures as determined in pre-runs. In order to ensure completeness of reaction, the firing procedure, with intermediate grindings, was repeated three times. Each firing was monitored with X-rays and in most cases no change in diffraction pattern was detected after the second heat treatment.

Samples for cooling curve analysis were prepared by mixing the powdered reactants in a rotating glass vial, and then slowly heating them *in situ* until they melted.

Density Analysis.—In an earlier paper,[7] the powder density measuring technique utilized in resolving compound ratios was referred to, but not adequately described. Since the method has been an invaluable adjunct in phase rule and crystallographic studies, and is now employed as a standard tool in this Laboratory, its detailed description is of value.

Frequently, single crystals large enough for density evaluation by the Archimedes technique are not available, and one must determine the density of powders. Such an approach has been unsatisfactory, because of the difficulties in avoiding significant air inclusions in the samples, and adsorbed air bubbles on their surfaces which lead to low density values, frequently in error in the non-decimal or at best in the first decimal position. The usefulness of such data for any but the grossest approximations is nil. Air inclusions can be avoided if density specimens are prepared *via* reaction in the solid state, rather than from previously melted polycrystalline agglomerates, or in cases where the densities of starting reagents are desired, from samples sintered several times beneath their melting points. Surface adsorbed air can be removed by boiling the standard liquid, powder slurry for several hours.

Using the pycnometer described in ref. 7, the masses empty and with water, trichloroethylene, or some other suitable liquid are determined at the working temperature. From 10-20 g. of powder is then introduced into the empty pycnometer bulb, the combined mass is determined, and approximately half the required volume of liquid is added. The slurry is simmered for 3-4 hours, and the pycnometer is then equilibrated at temperature for two hours. A supply of the standard liquid normally is equilibrated along side of the sample, and when the latter has attained constant temperature the liquid level is filled to mark, while still in the water-bath, using a long medicine dropper. This technique obviates possible difficulties arising with the use of a standard liquid having a high thermal coefficient of expansion. Once filled to mark, the pycnometer is stoppered, removed from the bath, dried, equilibrated with the ambient atmosphere to avoid condensate accumulation on the outside walls, if the bath temperature is lower than the surroundings, and weighed.

Depending on the precision required, and on the thermal coefficient of expansion of the standard liquid, the temperature of the constant temperature bath must be maintained within certain limits. For water ±0.1°, and for trichloroethylene ±0.05° variations will yield an error in the third decimal position.

Based on hundreds of evaluations, using a variety of materials measured in either water or trichloroethylene, the method has been found reproducible to better than ±0.005 g./cm.^{3} at 20°. When used for obtaining densities of liquids, as is the case during calibration of the pycnometer, the method is reproducible to ±0.0002 g./cm.^{3} at 20°. Comparison of measured densities with X-ray derived densities of materials whose lattice constants have been reproduced in this Laboratory and others, has shown the powder density technique to be in agreement to at least ±0.02 g./cm.^{3}, and generally to ±0.01 g./cm.^{3} or better. Significantly, the measured densities have in all cases been lower than calculated densities. As the measured values would reflect crystal imperfections, the slightly low results are probably indicative of such imperfections.

While the method has been extremely powerful in phase rule investigations, it has been equally effective in evaluating X-ray data. In all cases where deviation from a calculated density has exceeded 0.02-0.05 g./cm.^{3}, the deviation has been attributable to improper indexing of the material. In the one instance where measured densities have been compared with calculated values over a series of solid solution compositions, the agreement has been excellent[8]

---

[2] A. Reisman, F. Holtzberg and E. Banks, *J. Am. Chem. Soc.*, **80**, 37 (1958).

[3] A. Reisman and F. Holtzberg, *ibid.*, **80**, 6503 (1958).

[4] A. Reisman and F. Holtzberg, *ibid.*, **77**, 2115 (1955).

[5] A. Reisman, F. Holtzberg and M. Berkenblit, *ibid.*, **81**, 1291 (1959).

[6] Since the melting diagram of the system $Ag_2O-Nb_2O_5$ is unknown, nothing can be said of the melting behavior of the compound $AgNbO_3$.

[7] A. Reisman, F. Holtzberg, M. Berkenblit and M. Berry, *ibid.*, **78**, 4514 (1956).

[8] A. Reisman and E. Banks, *ibid.*, **80**, 1877 (1958), Fig. 4, 5. See also G. Shirane, R. Newnham and R. Pepinsky, *Phys. Rev.*, **96**, 581 (1954).

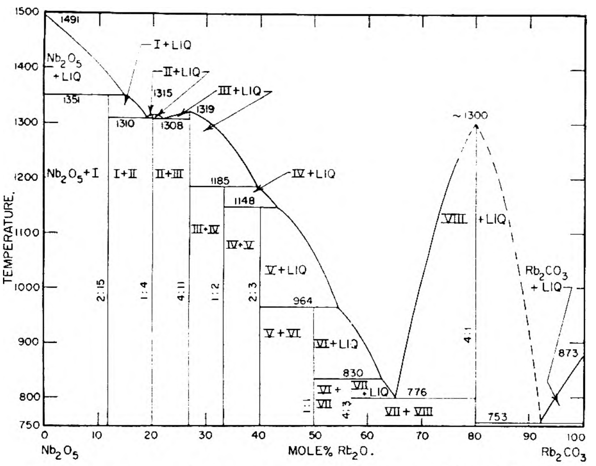

Fig. 1.—Thermal diagram of the system $Rb_2O-Nb_2O_5$.

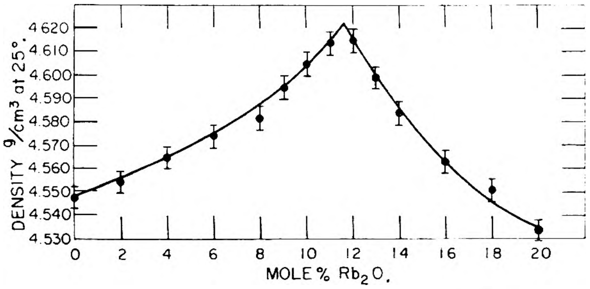

Fig. 2.—Partial density diagram of the system $Rb_2O-Nb_2O_5$.

despite the use of a system in which phase equilibrium is difficult to achieve.

Differential Thermal Analysis.—Three types of furnace design were utilized in the present study because of the wide temperature interval surveyed. Cooling studies were performed in a modified furnace based on that described in ref. 4. The modification consists of a second platinum–10% rhodium winding concentric with the inner core. Heating studies in the range r.t.—1000° were conducted in the barrel loaded furnace described in ref. 9, and in the range 1000° to the melting point, a platinum–10% rhodium double core modification of this design was employed. Exact details of construction of the three furnaces are given in ref. 10.

Cooling curve samples were of the order 7–10 g. and heating curve samples of the order 0.5–1.0 g. Heating and cooling rates were varied between 2–3° minute, and the charges used in cooling analysis were stirred with oxygen, and seeded through the final solidifications, except in special cases discussed in the final section. All experiments were conducted in platinum or gold–20% palladium crucibles.

Temperatures and temperature differentials were measured with platinum–10% rhodium couples using the shielded construction described in ref. 10. Alundum powder served as a ballast and the traces were recorded on an L and N X-Y recorder using a differential sensitivity of 5 μv./inch in heating experiments and 15 μv./inch in cooling analysis.

X-Ray Analysis.—Powder studies were made with a Debye–Scherrer camera using Ni filtered Cu radiation generated at 40 kv. and 20 ma. All samples were loaded in a dry box and capillaries were sealed with plastic putty.

TABLE I

THERMAL DATA FOR THE SYSTEM $Rb_2O-Nb_2O_5$

Rb_2O, mole %	Nb_2O_5, mole %	Liquidus	Solidus	Transition	Primary phase
0.0	100.0	1491	1491		Nb_2O_5
2.0	98.0	1475	1324		Nb_2O_5
5.0	95.0	1456	1337		Nb_2O_5
7.5	92.5	1435	1349		Nb_2O_5
10.0	90.0	1405	1351		Nb_2O_5
13.0	87.0	1371	1304	1350	Nb_2O_5
15.0	85.0	1351	1308		I
16.0	84.0	1347	1310		I
17.0	83.0	1340	1309		I
17.5	82.5	1336	1312		I
18.0	82.0	1332	1312		I
19.0	81.0	1311	1311	eutectic lies in this interval	I + II
19.5	80.5	1311	1311		I + II
20.0	80.0	1315	1315		II
20.5	79.5	1312	1264		II
21.0	79.0	1311	1291		II
21.5	78.5	1312	1291		II
22.0	78.0	1312	1312	eutectic lies in this interval	II + III
22.5	77.5	1308	1308		II + III
23.0	77.0	1311	1302		III
23.5	76.5	1315	1305		III
24.0	76.0	1316	1303		III
24.5	75.5	1317	1303		III
25.0	75.0	1318	1292		III
25.5	74.5	1316	1297		III
26.0	74.0	1318	1267		III
26.5	73.5	1319			III
27.0	73.0	1318	1124		III
27.5	72.5	1314	1151		III
28.5	71.5	1312	1146		III
29.0	71.0	1311	1138		III
30.0	70.0	1307	1172		III
33.33	66.67	1277	1179		III
33.5	66.5	1274	1135	1180	III
34.0	66.0	1271	1140	1181	III
35.0	65.0	1260	1140	1182	III
36.0	64.0	1242	1144	1181	III
37.5	62.5	1222	1142	1185	III
40.0	60.0	1172	1146		IV
40.5	59.5	1170	910	1148	IV
41.5	58.5	1164	921	1148	IV
42.0	58.0	1159	935	1148	IV
44.0	56.0		950^a		V
45.0	55.0	1130	932		V
46.0	54.0		959^a		V
48.0	52.0		955^a		V
50.0	50.0	1067	959		V
50.5	49.5		823^a		V
52.0	48.0		816	970	V
52.5	47.5	1018		964	V
54.0	46.0		824^a		V
56.0	44.0		826^a		VI
57.0	43.0	936	818		VI
58.0	42.0		769	834	VI
60.0	40.0		776	835	VI
62.0	38.0	835	776	830	VI
62.5	37.5	825	776		VII
65.0	35.0	774	774		VII + VIII
67.5	32.5	903	775		VIII
70.0	30.0	1043	754		VIII
72.5	28.5	1152	761		VIII
75.0	25.0	1237	755		VIII
95	5.0	838	753		Rb_2CO_3
100.0	0.0	873	873		Rb_2CO_3

[a] Heating curve data only.

---

(9) F. Holtzberg, A. Reisman, M. Berry and M. Berkenblit, *J. Am. Chem. Soc.*, **79**, 2039 (1957).

(10) A. Reisman, Ph.D. Thesis, Polytechnic Inst. of Brooklyn, 1958, Univ. Mic. #58-2876 Chem. Phys.

Discussion of Experimental Results

Tables I and II list the results of thermal, density and X-ray studies from which the proposed phase diagram, Figs. 1 and 2, is constructed. The data indicate the existence of 8 intermediate compounds having base to acid ratios of 2:15, 1:4, 4:11, 1:2, 2:3, 1:1, 4:3 and 4:1. Three of these, the 1:4, 4:11 and 4:1 members melt congruently at 1315, 1319 and *ca.* 1300°, respectively, while the remaining intermediates, those having compositions of 2:15, 1:2, 2:3, 1:1 and 4:3, become unstable below their melting points and decompose yielding two phase mixtures at 1351, 1185, 1148, 964 and 830°, respectively.

The use of X-rays in resolving the several compound formulas was severely restricted for two reasons. Some 90 specimens produced in the solid state were subjected to powder diffraction analysis, and it was found that after a certain composition had been reached, in each two phase region, the lines of the disappearing phase were no longer visible. Since no new set of diffraction lines was observed following the disappearance of a solute phase, most compounds could not be bracketed with X-rays to better than ±2–3 mole %.[11] Contributing to the difficulty of X-ray resolution of compound compositions was the fact that the diffraction patterns of adjacent compounds exhibited a great deal of superposition of lines. Since the superimposed maxima generally comprised the strongest reflections, the two phenomena were additive leading to rather poor bracketing. In the case of the 2:3 compound, however, neither effect was serious and this proportion was amenable to X-ray resolution to within ± 1 mole %. One further factor making X-ray techniques suitable for gross approximation only is the close proximity of compounds in the region 0–50 mole % Rb_2O. In some regions, a one mole % variation in terms of the primitive end members corresponds to *ca.* 10–20 mole % variation in terms of the nonprimitive solid phase end members which is probably the cause of the rapid dropping off in diffraction intensity. Consequently, X-ray analysis resulted in uncertainty ranges bounded by 10–14 mole % Rb_2O in the case of compound I, 18.5–20.5 mole % for compound II, 24–30 mole % for Compound III, 32–34.5 mole % for compound IV, 39–41 mole % for Compound V, 49–51.5 mole % for compound VI, 54–60 mole % for compound VII and between 70 and 85 mole % for compound VIII. The very wide range for the last compound is due partly to the difficulty in achieving completeness of reaction below the 776° eutectic and partly because of the poor diffraction pattern given by this material.

TABLE II

DENSITY DATA FOR THE SYSTEM Rb_2O–Nb_2O_5

Rb_2O, mole %	Nb_2O_5, mole %	Density, g./cm.^{3} 20°	Av.
0	100	4.548	4.548
2	98	4.557, 4.551	4.554 ± 0.003
4	96	4.565, 4.565	4.565 ± .000
6	94	4.574	4.574
8	92	4.582, 4.581	4.582 ± .0005
9	91	4.597, 4.593	4.595 ± .002
10	90	4.607, 4.602	4.605 ± .0025
11	89	4.614	4.614
12	88	4.607, 4.622, 4.615	
13	87	4.599	4.599
14	86	4.584	4.584
16	84	4.563	4.563
18	82	4.555, 4.547	4.551 ± .004
20	80	4.533, 4.534	4.534 ± .0005

The precise location of compound I was effected with the powder density measuring technique, and as seen from Fig. 2 the intersection of the density arms occurs at about 11.5 mole % Rb_2O. Within the limits of error, the smallest whole number ratio corresponds to 2:15. Density measurements made at more widely spaced intervals up to 44 mole % base, showed breaks at approximately 20, 27, 33.5 and 40 mole % base. Since these data were not taken at sufficiently close intervals, and were not repeated, they were considered only approximate, especially the rather odd value at 27 mole %. The densities corresponding to each of these breaks are 4.535 ± 0.01, 4.400 obtained by extrapolation, 4.495 obtained by extrapolation and 4.448. The precise locations of these compounds were actually determined thermally *via* cooling and heating studies. From Fig. 1 it is seen that the melting point of the congruently melting compound II is not very different from the eutectic temperatures on either side. If the samples were cooled with seeding through the final solidifications, the net effect was a swamping out of the solidus halts by the liquidus effects. It was found, however, that if seeding was dispensed with, after the liquidus crystallizations had commenced, both the 1310 and 1308° eutectics tended to supercool markedly, and the eutectic halts were observable to within 0.5 mole % on either side of the compound line. The same procedure was also successful with compound III, the last appearance of the 1308° eutectic occurring at 26 mole %, and the first appearance of the 1185° solidification occurring at 27 mole %. Within the limits of experimental error, the compositions of III was chosen as 4:11 corresponding to 26.67 mole % Rb_2O, in good agreement with the approximate density locations.

The component ratios in IV, V, VI and VII could not be satisfactorily established using cooling techniques because of the succession of incongruent halts. These ratios were resolved *via* heating curves on solid state prepared samples. Based on the first appearance of the 1148° reaction at 33.5 mole % coupled with the X-ray and density data, IV was assigned a proportion of 1:2. The first appearance of the 964° reaction at 40.5 mole % fixed the composition of V at 2:3. This compound was found to be isostructural with the potassium analog. In a similar manner VI and VII were readily located.

Compound VIII was resolved using both the heating technique and chemical analysis. Cooling

---

(11) It is not pertinent whether this phenomenon is due to a slight degree of solid solubility since the net effect is to limit the X-ray approach. Subsequent experiments, described below, proved the absence of fields of solid solubility, at least within the limits of experimental error.

methods were of no value since the high liquidus temperatures coupled with the high base content caused severe attack of the platinum containing vessels. Even gold–20% palladium vessels were of little value because of the rather high melting point of VIII. The heating curve samples showed disappearance of the 776° heat effect at approximately 78–78.5 mole %. It was found, however, that in the range from 70 mole % base on, the solid state reactions were not going to completion even after five heat treatments, as evidenced by the appearance of faint Rb_2CO_3 diffraction maxima in the X-ray photographs. Consequently, samples containing from 70–85 mole % were fused quickly in platinum, quenched and then tested for the presence of carbonate. Since carbonate can only occur in the join, compound VIII–Rb_2CO_3, its presence served to disclose first entry into this join. The first trace of carbonate at 80.5 mole % indicates that the composition of VIII is 4:1.

It is interesting that all similarity with the lower molecular weight interactions has ceased (see Table III), the breakdown being most evident in the regions containing more than 50 mole % base where the persistant 3:1 ratio is displaced by the 4:1 value. Instead of the expected 7:6 composition, one of 4:3 is present. It has been pointed out in an earlier paper[5] that the 4:3 ratio appears to be metastable with respect to the 7:6 composition in the aqueous potassium system and is unquestionably metastable in the anhydrous potassium system.

TABLE III

M_2O/Nb_2O_5 RATIO IN COMPOUNDS

i denotes incongruently melting; c, congruently melting; i, c just incongruently or just congruently melting.

	Li_2O	Na_2O	Ag_2O	K_2O	Rb_2O
1/14	i	i	?		
2/15					i
3/22				i	
1/4	i	i	?		c
1/3				i	
4/11					c
1/2					i
2/3				c	i
1/1	c	c	?	i, c	i
4/3					i
3/1	c	c	?	c	
4/1					c

Each of the intermediate members from the 2:3 to the 4:1 compositions inclusive were found to be moisture sensitive. None of these except the latter appeared to be water soluble to any extent, tending in all cases to hydrolyze extensively. High gain DTA studies of the several compounds failed to reveal any first-order anomalies in the interval room temperature to the melting points.

Because of the presence of nine separate phases in the oxide portion of the diagram, the possibility of solid solubility between adjacent compounds was considered. While the X-ray photographs evidenced a great deal of line superposition, the pattern of each phase was quite distinct. Within the limits of error, thermal methods failed to reveal any regions of solid solubility, and one can deduce from this that the structures of adjacent members are not isomorphic. These results were to be expected since any attempt at relating compound and solid solution diagrams overlooks one irreconcilable distinction between the two, namely, the question of ordering. Since a solid solution must exhibit random distribution of substituted ions, such an interaction can never be ordered. On the other hand, the necessity of preserving a unique chemical structure requires that each compound formed be ordered, regardless of the number formed.

Compound Repetition in Oxide Congener Interactions.—While there is no way of predicting the number and combining ratios of compounds formed in the first member of a congener series of interactions, certain trends are becoming evident which appear to enable qualitative attempts at predicting compound repetition, given the first of the interactions, in alkali oxide systems at least. Unfortunately, nothing can be said as yet concerning compounds which have not previously appeared.

It is significant that aside from retention of a 1:1 ratio the only other similarity between the rubidium and potassium systems is the occurrence of 2:3 analogs in both. The nature of the liquidus fields follows the same pattern for both ratios, namely, increasing submergence with increasing alkali metal atomic weight. Since one would expect an increasing ionicity in a periodic group with increasing atomic weight, it is not unwarranted to assume that the order of liquidus stability of alkali metaniobates is $NaNbO_3 > KNbO_3 > Rb_2NbO_3 > CsNbO_3$ and similarly for other analogs. Since an undissociated compound cannot melt incongruently, it is to be expected that the sequence of melting for repeated compounds would always tend from complete congruency to complete submergence. In the case of the 1:1 ratio, the value most likely to appear in a given interaction, the trend toward submergence is striking. In the case of the 2:3 ratios it is again apparent. In no case has the reverse trend been observed.

If we now consider the total picture of compound retention exhibited by all of the systems studied, two factors appear significant: (1) melting point stability, (2) interoctahedral coördination. Thus one might expect repetition of compounds meeting the first requirement until the size of the alkali ion approximates that of the oxygen ion, at which point the interoctahedrol coördination changes markedly. As a result, the potassium system should bear certain resemblances to both the lower and higher weight systems. This is seen in the niobate series, where, aside from the persistent 1:1 ratio, the only repetition in the rubidium interaction is that of the congruently melting analog. The repetition of rubidium analogs in the cesium system should then be governed, primarily, by the first factor.

From these observations we infer that the 2:15 ratio present in the rubidium system will reoccur in the cesium interaction since its liquidus field is quite large. The 1:4 ratio should not reappear since even though congruently melting, its liquidus field is almost completely submerged. Since any cesium analog would be expected to be more dissociated, such a ratio is not likely to reappear heterogeneously. The 4:11 ratio which exhibits a large liquidus field is expected to reoccur while the 1:2 value may or may not reoccur since its field is small, even though the liquidus slope does not indicate a high degree of dissociation in the liquid state. The 2:3 ratio is most certainly expected to appear, with greater submergence of the field, however. The 1:1 ratio also exhibiting a slightly submerged field is expected to repeat in a similar manner, but the 4:3 compound whose liquidus field is practically suppressed should not reoccur. From examination of Fig. 1 it is apparent that the 4:1 ratio should repeat.

In order to further expand on these considerations concerning compound retention, studies of the systems Cs_2O-Nb_2O_5 and M_2O-V_2O_5 have been initiated and will be discussed at some later date.

Acknowledgment.—The authors wish to thank Miss B. Agule for performing the density measurements, Mrs. J. Mineo for assisting with the thermal evaluations, Mrs. C. Pfister for taking the powder photographs, Philips Electronics for making fluorescence analysis equipment available and Miss M. Berry of this Laboratory for performing the fluorescence analysis.

ON THE DEFINITION OF COMPONENTS IN SOLUTIONS CONTAINING CHARGED MACROMOLECULAR SPECIES[1]

BY EDWARD F. CASASSA AND HENRYK EISENBERG

Mellon Institute, Pittsburgh, Pennsylvania

Received November 30, 1959

The choice of electrically neutral components in a three-component solution containing a macromolecular ionic species and a diffusible salt (*e.g.*, protein, sodium chloride, water) is discussed. The definition obtained by equating inner and outer salt concentrations in a dialysis experiment is shown to offer considerable advantage in the interpretation of data from light scattering and equilibrium ultracentrifugation.

In any study of the equilibrium properties of multicomponent solutions containing charged macromolecules and small ions, the problem of a suitable definition of independent components must be considered. Since it has not always been recognized that the well known relations developed for two-component systems cannot be applied arbitrarily to multicomponent systems, interpretations of experimental data have sometimes been subject to error or ambiguity, particularly in connection with the definition of components. One calls to mind, for example, discussions of hydration in the earlier literature on the ultracentrifugation of proteins. Although misconceptions still appear occasionally, analyses of osmotic pressure,[2] light scattering[3-7] and equilibrium sedimentation,[8] based on rigorous thermodynamic and statistical mechanical reasoning, now provide an adequate basis for design and interpretation of experimental studies. Since all that is required thermodynamically of an independent component is that it be electrically neutral, one is obviously left with a wide range of correct definitions, some of which may, however, be more useful or convenient than others in particular circumstances. It is the purpose of this note to point out the consequences, in the thermodynamic treatment of light scattering and sedimentation equilibrium, of a particularly useful choice of components for a three-component system of a type ordinarily encountered in studies of proteins and polyelectrolytes: a solvent 1, a solute component 2 containing a macromolecular ionic species, a salt 3. Only small ions common with those of component 3 appear in the formulation of component 2.

We can express the activities a_2, a_3 of the solute components in Scatchard's formalism[2]

$$\ln a_2 = \ln m_2 + \sum_i \nu_{2i} \ln m_i + \beta_2 \tag{1}$$

$$\ln a_3 = \sum_i \nu_{3i} \ln m_i + \beta_3 \tag{2}$$

where concentrations m are conveniently taken as molalities. The subscripts i refer to the ion species comprising component 3, and the ν_{2i} and ν_{3i} are the numbers of moles of these species included in one mole of electrically neutral components 2 and 3. It follows that

$$m_i = \nu_{3i}m_3 + \nu_{2i}m_2$$

Differentiation of equations 1 and 2 gives

$$a_{22} \equiv (\partial \ln a_2/\partial m_2)_{P,T,m_3} = 1/m_2 + \sum_i (\nu_{2i}^2/m_i) + \beta_{22} \tag{3}$$

$$a_{23} \equiv (\partial \ln a_2/\partial m_3)_{P,T,m_2} = (\partial \ln a_3/\partial m_2)_{P,T,m_3} = \sum_i (\nu_{2i}\nu_{3i}/m_i) + \beta_{23} \tag{4}$$

$$a_{33} \equiv (\partial \ln a_3/\partial m_3)_{P,T,m_2} = \sum_i (\nu_{3i}^2/m_i) + \beta_{33}$$

in which the derivatives $\partial\beta_j/\partial m_k$ are denoted by β_{jk}.

A Definition of Components from Osmotic Equilibrium.—The equilibrium pressure $P = \Pi + P'$ of the three component system sepa-

---

[1] This work was supported in part by a grant (NSF-G7608) of the National Science Foundation.

[2] G. Scatchard, *J. Am. Chem. Soc.*, **68**, 2315 (1946).

[3] H. C. Brinkman and J. J. Hermans, *J. Chem. Phys.*, **17**, 574 (1949).

[4] W. H. Stockmayer, *ibid.*, **18**, 58 (1950).

[5] J. G. Kirkwood and R. J. Goldberg, *ibid.*, **18**, 54 (1950).

[6] H. Shogenji, *Busseiron Kenkyu*, **62**, 1 (1953).

[7] T. Ooi, *J. Polymer Sci.*, **28**, 459 (1958).

[8] R. J. Goldberg, THIS JOURNAL, **57**, 194 (1953).

rated from a salt solution phase at fixed pressure P' and composition m_3' by a membrane impermeable only to component 2, can be derived from the Gibbs–Duhem relation which, with the temperature and the chemical potentials μ_1, μ_3 held constant, reduces to

$$V_m \mathrm{d}P = m_2 \mathrm{d}\mu_2$$

where V_m is the volume of the system containing one kilogram of component 1. Writing ln a_2 as a function of m_2 and m_3 we obtain

$$\frac{V_m}{RTm_2}\left(\frac{\partial \Pi}{\partial m_2}\right)_{\mu_3} = a_{22} + a_{23}\left(\frac{\partial m_3}{\partial m_2}\right)_{\mu_3} = a_{22} - \frac{a_{23}^2}{a_{33}} \quad (5)$$

We are free to define components in such a way that a_{23} vanishes and equation 5 becomes formally equivalent to the result for a two-component system. Since $a_{23}/a_{33} = -(\partial m_3/\partial m_2)_{\mu_3}$ and m_3 must approach m_3' as m_2 approaches zero, the appropriate definition is obtained by letting $m_3 = m_3'$ and adjusting the ν_{2i} to account for any excess or deficiency of diffusible ionic species in the three-component system.[9] The definition is most useful if $(m_i - m_i')/m_2$ does not depend sensibly on m_2; for then the resulting ν_{2i}^* (we shall designate by an asterisk all quantities consistent with $a_{23} = 0$) remain constant as component 2 is diluted with m_3' constant. Experimentally it has been found[10] in protein solutions that $\ln(m_i/m_i')$ is proportional to m_2 and approximately inversely proportional to m_3'. Since expansion of the logarithm gives

$$\ln\frac{m_i}{m_i'} = \ln\left(1 + \frac{m_i - m_i'}{m_i'}\right) = \frac{m_i - m_i'}{m_i'} + \ldots$$

these two conditions are consistent at low solute concentration. The constancy of $(m_i - m_i')/m_2$ has been found also in solutions of synthetic polyelectrolytes.[11,12]

A sufficient (though not necessary) condition for a_{23} to vanish with ν_{2i}^* independent of m_2 is that $\Sigma\nu_{2i}^*/m_i$ and β_{23} be individually invariant with m_2. The first requirement is met if $\nu_{2i}^* m_2/m_3$ is negligible compared to unity while the range of conformity with the second must be established empirically. These stipulations would in principle constitute a restriction to limiting relations for m_2 approaching zero; but in practice they should be applicable to the solutions, dilute in component 2 but moderately concentrated in salt, ordinarily employed in light scattering and ultracentrifuge studies. In any case, extrapolation procedures could presumably be devised to determine limiting behavior.

Light Scattering.—For the three-component system of concern here, Stockmayer's treatment[4] of Rayleigh scattering from multicomponent systems (which is equivalent to a development by Kirkwood and Goldberg[5]) gives

$$\frac{\psi_2^2 H' V_m}{RT\Delta\tau} = \frac{a_{22} - a_{23}^2/a_{33}}{D^2} \quad (6)$$

$$D = 1 - a_{23}\psi_3/a_{33}\psi_2$$

where $\Delta\tau$ is the difference between the turbidities of the three-component system and the two-component system remaining upon removal of component 2. The factor H'/RT depends only on optical and geometrical quantities. The molar refractive index increments $(\partial n/\partial m_j)_{P,T,m}$ are designated ψ_2, ψ_3. Since the most common purpose of the measurement is the determination of the unknown molecular weight M of component 2, equation 6 is usually cast into a more familiar form with concentration c in terms of weight of component 2 (here per kg. of component 1) and, correspondingly, with the refractive index increment as $(\partial n/\partial c)_{m_3}$

$$\left(\frac{\partial n}{\partial c}\right)_{m_3}^2 \frac{H' V_m c}{RT\Delta\tau} = \frac{1}{MD^2} + \frac{c}{M^2 D^2}\left[\Sigma\frac{\nu_{2i}^2}{m_i} + \beta_{22} - \frac{a_{23}^2}{a_{33}}\right] \quad (7)$$

Although it has been commonly assumed that D does not differ significantly from unity when c is expressed as a weight of polymer in the absence of salt (*e.g.*, of the protein remaining after exhaustive dialysis against water) this is not always true for protein systems and may be grossly incorrect in the case of synthetic polyelectrolytes with very high charge density and correspondingly strong interaction between polymer and salt. Thus, even self-consistent definitions of the quantities entering into equations 6 and 7, when coupled with the approximation that D is unity, may lead to incorrect molecular weights.[13-15]

If we define components as suggested by membrane equilibrium so as to make a_{23} vanish, then D becomes unity and the right-hand side of equation 6 reduces simply to a_{22}^* in complete analogy with the osmotic pressure result. Now, $\mathrm{d}n/\mathrm{d}c^*$, M^* and c^* all refer to a component 2 including an amount of salt unknown except by reference to independent measurements of the distribution of ionic species by dialysis equilibrium. We wish to point out, however, that a precisely defined molecular weight can in fact be determined from light scattering even in the absence of distribution data. For concreteness we shall imagine that a protein is dissolved and equilibrated by dialysis against salt solution of concentration m_3'. The procedure is repeated for several protein concentrations (or at low concentration of component 2 the dialyzed solution may equivalently be diluted with more salt solution of concentration m_3'). The refractive index and turbidity differences between the equilibrated protein solutions and the salt solution are measured. It is possible to determine the protein concentration (*e.g.*, from nitrogen analysis or ultraviolet light absorption) in terms of weight c of the *isoionic protein*. The weight concentration of component 2 is not c but $c^* = \epsilon c$, and the molecular weight M^* of component 2 also differs from M by the same factor ϵ. The measurements of refractive index and concentration clearly lead not to $(\partial n/\partial c^*)_{m_3}$ but to $(\partial n/\partial c)_{\mu_3}$. If we write equation 7 correctly for our definition of components and sub-

---

(9) G. Scatchard, A. Gee and J. Weeks, THIS JOURNAL, **58**, 783 (1954).

(10) G. Scatchard, A. C. Batchelder and A. Brown, *J. Am. Chem. Soc.*, **67**, 2320 (1946).

(11) U. P. Strauss and P. Ander, *ibid.*, **80**, 494 (1958).

(12) H. Eisenberg and E. F. Casassa, paper presented at the 137th meeting of the American Chemical Society, Cleveland, Ohio, April 5–14 1960.

(13) G. Ehrlich, THIS JOURNAL, **58**, 769 (1954).

(14) E. F. Casassa, *ibid.*, **60**, 926 (1956).

(15) U. P. Strauss and P. L. Wineman, *J. Am. Chem. Soc.*, **80**, 2366 (1958).

stitute into it the experimentally accessible quantities, we find

$$\left(\frac{\partial n}{\partial c^*}\right)^2_{m_3} \frac{H'V_m{}^*c^*}{RT\Delta\tau} = \left(\frac{\partial n}{\partial c}\right)^2_{\mu_3} \frac{H'V_mc}{RT\Delta\tau} = 1 + \frac{c}{M}\left[\sum_i \frac{\nu_{2i}{}^{*2}}{m_i} + \beta_{22}{}^*\right] \quad (8)$$

i.e., the factors ϵ all cancel out and the correct molecular weight *for the salt-free protein* is obtained by the familiar extrapolation of $c/\Delta\tau$ to $c = 0$. The laboratory operations described above will be recognized as forming a typical procedure in the investigation of a protein. Consequently we arrive at the rather paradoxical conclusion that though many experiments have been undertaken in ignorance of the fact that expressions valid for two component systems no longer hold generally in more complex situations, correct molecular weights may none the less still have been obtained. It is evident from equation 8 that the correct value of $a_{22}{}^*$ is also found in the experiment just described. The crucial factor is, of course, the equilibration of the protein with the salt solution. For this argument to be rigorous we should require that light scattering measurements be carried out under a hydrostatic pressure equal to the osmotic pressure of the solution; but the approximation that the turbidity is independent of pressure is surely trivial in the present instance.

We have taken equation 6 as the point of departure for our discussion of light scattering since the formulation of which this is a special case has ordinarily been used in the analysis of multicomponent systems. Equation 8 can, however, be obtained directly from the results of Shogenji[6] and Ooi,[7] who employed the appropriate grand canonical ensemble to derive the analog of equation 6 with refractive index increments taken at fixed chemical potentials of diffusible components.

Sedimentation Equilibrium.—For the three-component system at equilibrium in the ultracentrifuge, the simultaneous equations[8]

$$M_2L_2\mathrm{d}x^2 = a_{22}{}^{(x)}\,\mathrm{d}m_2 + a_{23}{}^{(x)}\,\mathrm{d}m_3$$
$$M_3L_3\mathrm{d}x^2 = a_{23}{}^{(x)}\,\mathrm{d}m_2 + a_{33}{}^{(x)}\,\mathrm{d}m_3$$

where $L_j = (1 - \bar{v}_j\rho)\omega^2/2RT$, must hold at each level x in the cell measured from the center of rotation. The partial specific volumes $\bar{v}_2$, $\bar{v}_3$ and the solution density ρ are assumed to be independent of x, and the angular velocity is given by ω. Eliminating $\mathrm{d}m_3$ we find

$$\left(M_2L_2 - M_3L_3\frac{a_{23}{}^{(x)}}{a_{33}{}^{(x)}}\right)\frac{\mathrm{d}x^2}{\mathrm{d}m_2} = a_{22}{}^{(x)} - \frac{a_{23}{}^{(x)2}}{a_{33}{}^{(x)}}$$

and then, by defining components so as to make a_{23} zero

$$M_2{}^*L_2{}^*/(\mathrm{d}m_2/\mathrm{d}x^2) = a_{22}{}^{*(x)} \quad (9)$$

provided that the dependence of m_2 and m_3 on x does not require a variation in the ν_{21}; for then the molecular weight $M_2{}^*$ would be a function of x. As we have already mentioned, the ν_{2i} are ordinarily found to be independent of m_2. Since the redistribution of salt alone should be very slight in the centrifugal fields required for equilibrium sedimentation measurements of typical proteins and polyelectrolytes with molecular weights of the order of 10,000 or higher, the effect of variation of m_3 with x usually can be ignored if the components are defined as here proposed so that there is no interaction between salt and component 2. As before, we assume that solutions are dilute so that $\nu_{2i}m_2/m_3 << 1$. Under these conditions, and with the assumption that hydrostatic pressure effects are negligible, $a_{22}{}^*$ is a function of x only through the linear dependence on $1/m_2$ in equation 3.

From equation 9 we obtain

$$M_2{}^*L_2{}^*(\mathrm{d}\ln m_2/\mathrm{d}x^2)^{-1} = 1 + m_2\left(\sum_i \nu_{2i}{}^{*2}/m_i + \beta_{22}{}^*\right)$$

If experiments are carried out at sufficiently low concentration of component 2, the determination of molecular weight depends on the ratio of the concentration gradient to the concentration at any point x, hence only a property proportional to concentration c^* need be measured. The molecular weight obtained in a sedimentation equilibrium experiment is thus automatically that of component 2 as defined by letting $m_3 = m_3'$ in dialysis equilibrium. Experimentally, one determines in the centrifuge the difference between the refractive index or refractive index gradient at each point x in the three-component system and that at the same point in an equivalent column of salt solution. From the foregoing discussion it is obvious that the measured difference is proportional to c^* or $\mathrm{d}c^*/\mathrm{d}x$ only if the reference solution has been equilibrated with the polymer solution by dialysis.

The partial specific volume which enters into $L_2{}^*$ is, of course, defined by reference to the process of adding one gram of component 2 to a large volume of solution in equilibrium with salt of concentration m_3'. In practice one would ordinarily compare the density of the three-component system at concentration c^* with that of the equilibrated salt solution. The circumstance that only c, not c^*, can be measured directly, imposes the difficulty that the correct partial specific volume for component 2 cannot be determined without independent information on distribution of diffusible species in dialysis.

Conclusion

The derivations given here serve to emphasize that the three experimental methods considered do not automatically yield the same molecular weight even though component 2 is monodisperse. As is well known, the osmotic pressure, as a property relating to the concentration of non-diffusible particles present, always gives the molecular weight corresponding to whatever definition is adopted in determining the weight concentration of the non-diffusible component. The same molecular weight may be obtained by light scattering if self-consistent values of weight concentration and refractive increments of components 2 and 3 are combined with distribution data in equation 7; but if the solutions for light scattering are equilibrated by dialysis against the diffusible components, an explicitly defined molecular weight can still be obtained without distribution analysis. In equilibrium sedimentation the molecular weight measured is naturally that for the component 2 defined by setting salt concentrations equal on both sides of a dialysis membrane. These considerations all apply, of course, in similar fashion to any three-component system, whether or not ionic species are present.

Scatchard[2] has chosen the polymeric component in such a way that one mole of neutral component contains one mole of particles with the advantage that the change of chemical potential upon addition of one mole of solute to the system does not reflect primarily the addition of many moles of diffusible ions. For a polymeric ion P^Z of valence Z in the presence of a uni-univalent electrolyte, Scatchard's definition requires simply that component 2 be formulated as including one mole of P^Z ions, $-Z/2$ moles of univalent cations, and $Z/2$ moles of univalent anions. This definition has been utilized in discussions of light scattering by Edsall, *et al.*,[16] and Doty and Edsall,[17] and of sedimentation equilibrium by Johnson, Kraus and Scatchard.[18,19] For a solution in which β_{23} of equation 4 is zero, Scatchard's definition of component 2 and that proposed here become equivalent in the limit as Zm_2/m_3 approaches zero. For example in the case that component 3 is a uni-univalent electrolyte, these conditions give

$$a_{23} = \sum_i \nu_{2i}/m_3$$

Electroneutrality and our requirement that a_{23} be zero are then satisfied by values of $-Z/2$ and $Z/2$ for the moles of salt cations and anions included in a mole of component 2.

The generalization of the relations presented here to systems containing more than one macromolecular component is readily effected. As in the three-component system, interactions between all the non-diffusible solutes and component 3 can be eliminated with the choice of components suggested by dialysis equilibrium. The equations resulting are completely analogous formally to those obtaining for a mixture of macromolecular components in a single solvent[2,5,8] and their application involves the same problems.

Note added in Proof.—An article by Scatchard and Bregman [G. Scatchard and J. Bregman, *J. Am. Chem. Soc.*, 81, 6095 (1959)] published after this paper was submitted is pertinent to our work. In connection with their light scattering study of bovine serum albumin in sodium chloride solutions, they now define the protein component as $Na_{(\nu-h)/2}[H_hPCl_\nu]Cl_{(h-\nu)/2}$, where P represents isoionic protein and h and ν are, respectively, the numbers of protons and chloride ions "bound." Although we have preferred to omit explicit introduction of ion binding, this definition is the same as ours in the particular instance that ν is defined by membrane equilibrium and HCl is not regarded as a diffusible component. It differs from Scatchard's older definition by addition of $\nu/2$ moles of salt. However, since Scatchard and Bregman have formulated activities and refractive index increments differently than we suggest, they arrive at an analog of our equation 8 only by making approximations (justified for their system) which are not required in our derivation.

---

(16) J. T. Edsall, H. Edelhoch, R. Lontie and P. R. Morrison, *J. Am. Chem. Soc.*, **72**, 4641 (1950).

(17) P. Doty and J. T. Edsall, "Advances in Protein Chemistry," Vol. VI, Academic Press, New York, N. Y., 1951, p. 35.

(18) J. S. Johnson, K. A. Kraus and G. Scatchard, This Journal, **58**, 1034 (1954).

(19) J. S. Johnson, G. Scatchard and K. A. Kraus, *ibid.*, **63**, 787 (1959).

AN ELECTRON DIFFRACTION INVESTIGATION OF THE MOLECULAR STRUCTURE OF METHYL AZIDE[1]

By R. L. Livingston and C. N. Ramachandra Rao[2]

Contribution from the Department of Chemistry, Purdue University, Lafayette, Indiana

Received November 30, 1959

The molecular structure of methyl azide has been studied by the sector-microphotometer and the sector-visual methods of electron diffraction and the parameters determined as follows: C–N = 1.47 ± 0.02 Å., N_1–N_2 = 1.24 ± 0.01 Å., N_2–N_3 = 1.12 ± 0.01 Å. and <CNN = 120 ± 2°.

Early electron diffraction work[3] on methyl azide was done by the visual method which employed non-sectored photographs with data extending to a q-value of 55. It was decided to reinvestigate the structure of this molecule by the more refined techniques now available. Of particular interest were the C–N distance and the two N–N distances.

Experimental

Methyl azide was prepared by the dropwise addition of dimethyl sulfate to a basic solution of sodium azide heated to about 80° under constant stirring.[4,5] The vapors were passed through a water condenser and over anhydrous calcium chloride and collected in a Dry Ice–trichloroethene trap. The yields were about 80%. The product, after a few vacuum distillations, gave acceptable elemental analysis and the boiling point was found to be about 21°. The infrared spectrum of the vapor showed no obvious impurities.

Electron diffraction photographs of methyl azide were taken using an r^3-sector and Kodak Lantern Slide contrast plates. The patterns were taken both at a short (10.19 cm.) and a long (25.10 cm.) camera distance. A sample pressure of about 25 mm. was found to be adequate. The electron wave length was 0.05452 Å., obtained by applying an accelerating potential of 48.322 kv. This voltage was measured by determining the potential drop across an accurately known portion of a resistance which itself is across the entire accelerating potential; the results obtained in this manner have been checked against zinc oxide patterns.

---

(1) Contains material from the doctoral dissertation of C. N. R. Rao. Presented at the 135th meeting of the American Chemical Society, Boston, Mass., April, 1959.

(2) Purdue Research Foundation Fellow, 1956–1957; Standard Oil Foundation Fellow, 1957–1958. Indian Institute of Science, Bangalore, India.

(3) L. Pauling and L. O. Brockway, *J. Am. Chem. Soc.*, **59**, 13 (1937).

(4) O. Dimroth and W. Wislicenus, *Ber.*, **38**, 1573 (1905).

(5) O. Mandela and G. Caronna, *Gazz. chim. ital.*, **71**, 182 (1941).

A visual intensity curve was obtained from these sectored plates. The resulting sector-visual data extend from $q = 20$ to $q = 90$ and the visual intensity curve is shown in Fig. 1.

Microphotometer traces of several plates were taken on a Leeds and Northrup microphotometer while spinning the plates at a high speed. The transmittancies were converted to arbitrary intensity units over a total range extending from $q = 18$ to $q = 75$. The total intensity data were converted to the molecular intensity data by the equation

$$I_m(q) = qK\left[\frac{I_t(q)}{I_b(q)} - 1\right] \qquad (1)$$

where $I_m(q)$ is the molecular structure scattering function to be compared with the calculated intensity curves, $I_t(q)$ is the total intensity, $I_b(q)$ is the (estimated) background intensity and K is a constant.

Radial distribution curves were calculated using the equation[6]

$$rD(r) = \sum_{q=1,2,3\ldots}^{q_{\max}} I_m(q)\exp(-bq^2)\sin\frac{\pi qr}{10} \qquad (2)$$

where $rD(r)$ is the radial distribution function, r is the internuclear separation and $\exp(-bq^2) = 0.10$ at $q = q_{\max}$. In each case the intensity data for the inner part of the pattern were obtained from a theoretical intensity curve calculated by means of the equation[6]

$$I_m(q) = \sum_i\sum_j \frac{Z_iZ_j}{r_{ij}}\exp(-b_{ij}q^2)\sin\frac{\pi q r_{ij}}{10} \qquad (3)$$

using punched cards.

The first radial distribution curve calculated from the sector-microphotometer data showed some fairly large negative areas and other extraneous features. By making successive improvements in the background line, the final radial distribution curve shown in Fig. 2 was obtained. The final experimental intensity curve is shown in Fig. 1.

Results and Discussion

The sector-microphotometer radial distribution curve for methyl azide

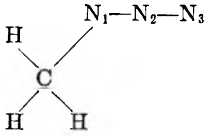

shows four peaks. The first peak has a prominent shoulder on the right side, presumably due to the C–N$_1$ distance. The remainder of the peak should, therefore, be due to the two N–N distances and the C–H distance. This peak was analyzed by the resolution procedure described by Karle and Karle.[7] The shoulder to the right of the first peak was fitted by the Karles' method assuming that the right side of the shoulder did not have any contribution from any other distance. Similarly, assuming that the right side of the peak is not affected by the C–H distance, the area was fitted by trial and error with the Karles' function for the two N–N distances. The areas of the three peaks were subtracted from the total area of the first peak and the remaining area formed a smooth curve about $r = 1.09$ Å., which was attributed to the C–H distance.

The second peak was decomposed in a similar fashion taking the N$_1$–N$_3$ distance as the sum of the N$_1$–N$_2$ and N$_2$–N$_3$ distances from the decomposition of the first peak and assuming that the N$_1$–H distance did not affect the right side of the peak.

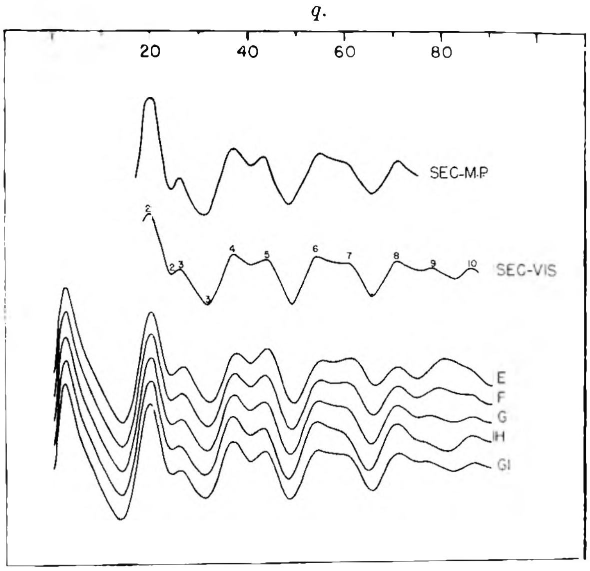

Fig. 1.—Observed and calculated intensity curves for methyl azide.

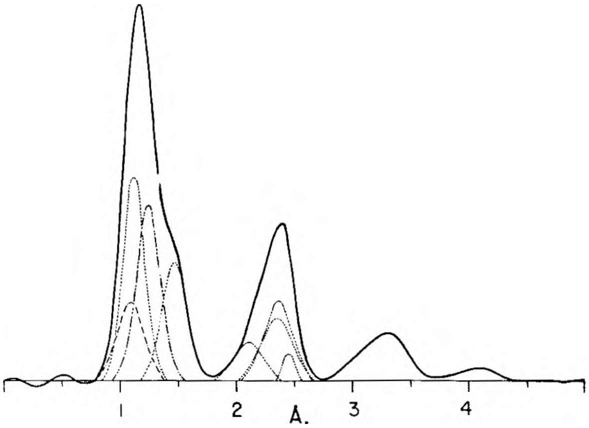

Fig. 2.—The radial distribution curve for methyl azide.

After obtaining the C–N$_2$ and N$_1$–N$_3$ distances, the N$_1$–H distance was fitted at the left side of the peak. The area obtained by subtracting the areas of C–N$_2$, N$_1$–N$_3$ and N$_1$–H peaks agreed well with the area expected for the N$_2$–H$_1$ distance and formed a smooth curve about 2.45 Å. (In interpreting the radial distribution curve and in calculating theoretical models, C_{3v} symmetry was assumed for the methyl group with the hydrogen atoms oriented so as to give one short N$_2$–H distance (N$_2$–H$_1$) and two longer N$_2$–H distances (N$_2$–H$_2$).)

The third peak could be decomposed by assuming that the right side of the peak was mainly due to the C–N$_3$ distance and was not greatly affected by the other distances. The area obtained by subtraction of the C–N$_3$ peak area was comparable to the expected area due to N$_2$–H$_2$ and N$_3$–H$_2$ distances. The fourth peak represented only the N$_3$–H$_2$ distance and although no attempt was made to fit it exactly with the Karles' function, the observed area corresponded closely to the expected area for this distance. The results of the radial distribution curve are summarized in Table I. In general, the areas under the peaks are in good

(6) P. A. Shaffer, Jr., V. Schomaker and L. Pauling, *J. Chem. Phys.*, **14**, 659 (1946).

(7) I. L. Karle and J. Karle, *ibid.*, **18**, 963 (1950).

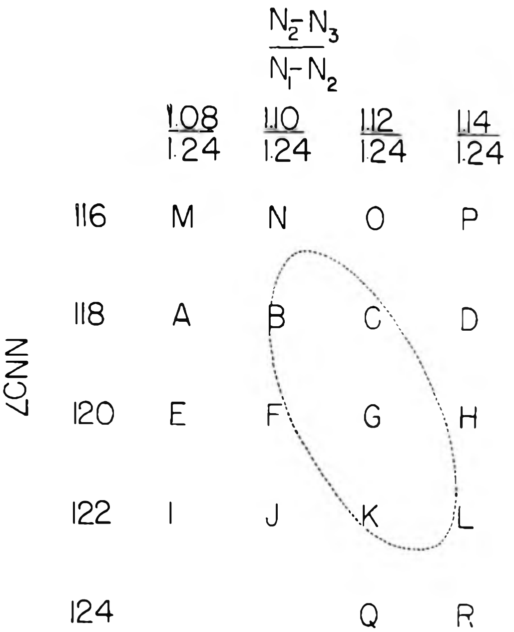

Fig. 3.—Parameter field used for calculations of intensity curves for methyl azide. The principal plane had C–N = 1.47 Å. Models A 1, B 1, C 1, etc., were in the plane C–N = 1.45 Å. and models A 2, B 2, C 2, etc., were in the plane C–N = 1.49 Å.

agreement with the expected values of nZ_iZ_j/r_{ij}, even for distances involving the hydrogen atoms. The values of the root mean square amplitudes of vibration, Δr_{ij}, for the distances involving hydrogen atoms cannot be determined with much certainty since small oscillations in the zero line of the radial distribution curve can change the shape of these small peaks considerably. The values of the interatomic distances obtained by the radial distribution method correspond to a linear geometry for the azide group, C_{3v} symmetry for the CH_3 group and 120° for the CNN angle.

Table I

Results of the Radial Distribution Curve for Methyl Azide by the Sector-microphotometer Method

Distance	r_{ij}, Å.	Δr_{ij}	Peak area	nZ_iZ_j/r_{ij}
C–H	1.09	0.075	45.9	46.6
N_2–N_3	1.12	.05	90.1	89.8
N_1–N_2	1.24	.04	100	100
C–N_1	1.47	.06	64.3	64.8
N_1–H	2.10	.10	25.0	27.3
C–N_2	2.35	.10	41.1	40.9
N_1–N_3	2.36	.08	47.3	47.7
N_2–H_1	2.45	..	7.3	8.2
N_2–H_2	..	..	18.2	12.5
N_3–H_1	..	..		6.8
C–N_3	3.35	.14	26.2	28.4
N_3–H_2	..	..	10.1	10.2

The radial distribution curve calculated from the sector-visual data showed four peaks and resembled the sector-microphotometer curve rather closely. In spite of a few negative regions, the areas of the peaks agreed well with the expected results; these areas had observed values of 67.3, 27.9, 10.0 and 2.4 compared with the expected values (nZ_iZ_j/r_{ij}) of 63.1, 28.3, 10.0 and 2.1, respectively. No attempt was made to decompose the composite peaks in order to obtain the individual distances.

In order to determine the ranges of uncertainty for the various parameters, a correlation procedure was carried out. The sector-microphotometer and the sector-visual intensity curves resembled each other closely and so the correlation procedure has been carried out using the sector-microphotometer data between $q = 17$ and $q = 75$ (Fig. 1) and sector-visual data from $q = 75$ to $q = 87$. Several theoretical intensity curves were calculated keeping the N_1–N_2 distance constant at 1.24 Å. The parameter field chosen in the C–N_1 = 1.47 plane is shown in Fig. 3.

Curves for models M, A, E and I show obvious faults in maxima 5, 7, 9 and 10 as illustrated by curve E in Fig. 1. Curves F and J show similar faults in maxima 5 and 10; curve F is illustrated. These faults are present but not as serious in curve B and the model for this curve is accepted as a borderline case. In curve N, maximum 7 is too low. In curves O, P and D, maxima 5 and 7 are too weak. In curves H, L and R, the main fault lies in maximum 9 as is illustrated by curve H in Fig. 1; in addition, these curves show some faults in the region of maxima 5 and 7. Max 3 is not well-defined in curves L, R and Q; in addition, maxima 5 and 7 are somewhat too high. Model G, which corresponds exactly to the radial distribution curve is, of course, acceptable and gives the best qualitative curve of those calculated. Curves C and K are acceptable but somewhat less satisfactory than G. The acceptable parameter field in the C–N_1 = 1.47 Å. plane is shown by the dotted line in Fig. 3.

Several models were also calculated in two planes, one 0.02 Å. below (X1 plane) and the other 0.02 Å. above (X2 plane) the C–N_1 = 1.47 Å. plane. In the C–N_1 = 1.45 Å. plane, model G1 is barely acceptable and C1 is an extreme borderline case. In the C–N_1 = 1.49 Å. plane, model G2 is barely acceptable and model K2 is a borderline case. All other models in these two planes were regarded as unacceptable.

The observed q-values by the sector-microphotometer method and the $q_{\text{calc}}/q_{\text{obs}}$ ratios for the acceptable models are listed in Table II. The principal parameters calculated for the acceptable models are given in Table III. The radial distribution values are taken as the final results with uncertainties established by the correlation procedure

$$\text{C–N}_1 = 1.47 \pm 0.02 \text{ A.}$$
$$\text{N}_1\text{–N}_2 = 1.24 \pm 0.01 \text{ Å.}$$
$$\text{N}_2\text{–N}_3 = 1.12 \pm 0.01 \text{ Å.}$$
$$\text{and} <\text{CNN} = 120 \pm 2°$$

Also given in Table II are the quantitative results for model G obtained from the visual-sector data. It seemed quite apparent that model G would have been the best model had only the visual-sector data been considered. It is also true that this method would have led to the assignment of slightly larger uncertainties on each molecular parameter. The present work constitutes one additional example of the "calibration" of the sector-visual method.

TABLE II

QUANTITATIVE ELECTRON DIFFRACTION DATA FOR METHYL AZIDE

Max.	Min.	q_{obs}	Sector-microphotometer method						Sector-visual method G
			q_{calc}/q_{obs}						
			B	C	G	K	G2	G1	
2		20.0	0.999	0.997	0.994	0.984	0.984	0.993	1.013
	2	24.2	1.010	1.009	1.006	1.007	1.002	1.012	...
3		26.0	1.021	1.015	0.999	0.979	0.995	1.004	1.005
	3	31.2	1.013	1.006	1.007	1.009	1.010	0.998	0.991
4		37.1	1.009	1.005	0.998	0.991	1.001	.997	1.001
	4	40.7	0.998	0.998	0.993	.986	0.989	.999	0.997
5		43.0	1.013	1.007	1.002	.994	.995	1.013	.986
	5	48.5	1.013	1.003	1.001	1.001	.999	1.003	.988
6		55.0	1.004	0.998	0.993	0.992	.991	...	1.010
	7	65.6	1.005	1.000	.999	.995	.991	1.001	1.000
8		70.9	1.005	1.004	1.001	.999	.994	1.008	1.005
	8	..	...	...	...	...	...	...	0.999
9		..	...	...	...	...	...	...	.993
	9	..	...	...	...	...	...	...	.999
10		..	...	...	...	...	...	...	1.006
		Mean	1.008	1.004	0.999_4	0.994	0.996	1.003	0.999_5
Av. dev. from the mean			0.005	0.004	.004	.007	.006	0.005	.006

TABLE III

PRINCIPAL PARAMETERS FROM ACCEPTABLE MODELS FOR METHYL AZIDE

	B	C	G	K	G1	G2
∠CNN°	118	118	120	122	120	120
C–N_1	1.482	1.476	1.469	1.461	1.484	1.454
N_1–N_2	1.250	1.245	1.239	1.233	1.235	1.244
N_2–N_3	1.109	1.124	1.119	1.113	1.116	1.123
C–N_2	2.349	2.339	2.348	2.356	2.361	2.337
C–N_3	3.326	3.323	3.347	3.360	3.347	3.340

The results of this investigation may be explained by the resonance theory and they are consistent with the adjacent charge rule of Pauling.[8] The observed C–N_1 distance of 1.47 Å. is exactly equal to the sum of the single bond radii of C and N just as in methylamine. The present results are in general agreement with the earlier investigation,[3] in which the C–N_1 distance was assumed to be 1.47 Å. They are more reliable, however, by virtue of the greater accuracy of the methods employed and the larger amount of data available.

---

(8) L. Pauling, "The Nature of the Chemical Bond," Cornell University Press, Ithaca, N. Y., 1940.

INFRARED ABSORPTIONS OF THE COPPER(II) SALTS OF SOME α,ω-DICARBOXYLIC ACIDS

By YOKO KURODA AND MASAJI KUBO

Chemical Department, Nagoya University, Chikusa, Nagoya, Japan

Received December 5, 1959

The infrared absorptions of copper(II) α,ω-dicarboxylates were recorded in the rock-salt region and compared with those of the corresponding sodium salts. The spectrum of copper(II) malonate is almost identical with that of sodium malonate as expected from the normal magnetic moment of the former compound. The spectral features of copper(II) salts beyond the succinate are more complicated than those of the corresponding sodium salts. The band progression observed for some of the sodium salts was not discernible in the spectra of the copper(II) salts. These facts support the conclusion derived from magnetic measurements that the formation of pairs of copper atoms leads to the distortion of methylene chains in crystalline copper(II) α,ω-dicarboxylates beyond the succinate. The difference between the antisymmetric COO stretching frequency of the copper(II) salt of this series and that of the corresponding sodium salt shows nearly the same dependence upon the number of carbon atoms in the acid radicals as does the deviation of the magnetic moments of the copper(II) salts from the theoretical spin-only moment for one odd electron, revealing an intimate relationship existing between these two quantities.

Introduction

This paper embodies an attempt to lend support to the conclusions derived from magnetic measurements on the structure of some copper(II) α,ω-dicarboxylates by means of the measurements of infrared absorptions. One of the present writers and collaborators[1] have found that, with a single exception of copper(II) malonate, the copper(II) salts of α,ω-dicarboxylic acids, $HOOC(CH_2)_{n-2}COOH$ with n = 2–10, show subnormal magnetic moments, *i.e.*, moments smaller than the spin-only moment, 1.73 B.M., for a single unpaired electron. Accordingly, structural units involving two copper atoms as are present in the crystals of copper(II) acetate monohydrate[2] are presumed to exist in crystalline copper(II) α,ω-dicarboxylates,

---

(1) O. Asai, M. Kishita and M. Kubo, *Naturwiss.*, **46**, 12 (1959); THIS JOURNAL, **63**, 96 (1959).

(2) J. N. van Niekerk and F. R. L. Schoening, *Nature*, **171**, 36 (1953); *Acta Cryst.*, **6**, 227 (1953).

except in copper(II) malonate crystals in which copper forms no pair of atoms undergoing spin coupling due to exchange interaction.[3]

The presence of structural units characteristic of some of the copper(II) salts showing subnormal magnetic moments such as copper(II) acetate monohydrate along with the experimentally confirmed planar structure[4,5] of oxalate radicals has led to the conclusion that the crystals of copper(II) oxalate comprise infinitely extending two-dimensional network structures involving coördination links rather than separate molecules having a single copper atom or dimer molecules as in copper(II) acetate monohydrate crystals. Analogous network structures are conceivable for the copper(II) salts of α,ω-dicarboxylic acids having an even number of carbon atoms.

For the malonate, the turning of chains at the central carbon atoms renders the formation of such network structures impossible, and for other members of the odd series the flexibility of carbon chains must take part in bringing copper atoms together in pairs. In fact, it has been found that the effective magnetic moment per one copper atom of the copper(II) salts of the odd series decreases with increasing length of carbon chains of the acids.

The restraint imposed by the formation of these structures will be revealed by infrared spectra. We have therefore recorded the infrared absorptions of these copper(II) salts, attention being focused mainly on CH_2 rocking and C=O stretching vibrations. The absorptions of the corresponding sodium salts and the free acids also were studied for reference.

Preparation of Materials.—The sources of acid samples employed as well as the method of preparation of copper(II) salts have been described in a preceding report.[1] The sodium salts were prepared from the same acid samples.

Experimental Method and Results.—The infrared spectra were recorded by means of a spectrometer of type H-800 from Hilger. The absorption measurements were made at room temperature with a rock-salt prism in the wave number range covering 700–1700 cm.$^{-1}$. Some of the results, for which fairly complete assignments were feasible, are shown in Table I. All these data were obtained by KBr disk method and checked using Nujol mulls. The salts of homologous acids, except a few lower members, showed absorption curves bearing some resemblance to each other and showing a progressive change.

Discussion

The CH_2 rocking vibrations are known to be particularly sensitive to the configuration of linear chains.[6,7] In fact, Corish and Davison[8] have already recorded the infrared absorptions of a number of α,ω-dicarboxylic acids, and found that the bands due to the CH_2 rocking vibrations of these compounds are similar to those of the corresponding paraffins having a polymethylene chain of the same length. The X-ray analysis by Morrison and Robertson[9] has revealed the existence of extended zigzag chains resulting from the *trans* configuration about single bonds in these compounds. This affords a means for the structural elucidation of polymethylene chains by means of infrared spectroscopy.

TABLE I

INFRARED SPECTRA OF COPPER(II) AND SODIUM α,ω-DICARBOXYLATES[a]

Wave number, cm.$^{-1}$		
Cu oxalate	Na oxalate	Interpretation
	774s	In-plane COO deformation
823s	781sh	
1321s	1319s	Sym. COO stretching
1365s	1334s	
1420w	1412w	
1665vs	1635vs	Antisym. COO stretching
Cu malonate	Na malonate	
738s	700s	COO deformation
811m	789s	CH_2 rocking (tentative)
941sh	921m	CC stretching
967m	958m	
.. sh	973m	
1166w		
1184w	1182m	CH_2 twisting
1273m	1266s	CH_2 wagging
1371s	1381s	Sym. COO stretching
1429s	1426s	CH_2 bending
1595vs	1595vs	Antisym. COO stretching
	1643vs	
Cu succinate	Na succinate	
730w	Below 700	COO deformation
881m	808s	CH_2 rocking
893m		
985m	925m	CC stretching
1002m		
1055w		
1186s	1176m	CH_2 twisting and wagging
1223w	1226s	
1301s		
1332s		
1404s	1412sh	CH_2 bending and sym. COO stretching
1432vs	1438vs	
1608vs	1567vs	Antisym. COO stretching

[a] Intensities are graded by vs (very strong), s (strong) m (medium), and w (weak): sh stands for shoulders.

The infrared absorption spectra of the lower members of the sodium salts, from the oxalate to pimelate, observed in the present study were compared with those published by Childers and Struthers.[10] Good agreements were obtained between these two sets of investigations in the region 700-1350 cm.$^{-1}$, for which reference charts were available.

The infrared spectra of sodium α,ω-dicarboxylates can be interpreted in terms of the vibrations of dicarboxylate ions. Provided that the chains assume extended structure, the ions of the even series have C_{2h} symmetry while those of the odd series correspond to C_{2v}. Owing to the presence

---

(3) B. N. Figgis and R. L. Martin, *J. Chem. Soc.*, 3837 (1956).

(4) J. M. Robertson and I. Woodward, *ibid.*, 1817 (1936); J. D. Dunitz and J. M. Robertson, *ibid.*, 142 (1947).

(5) S. Shibata and M. Kimura, *Bull. Chem. Soc. Japan*, **27**, 485 (1954).

(6) J. K. Brown and N. Sheppard, *Trans. Faraday Soc.*, **48**, 128 (1952).

(7) Y. Kuroda and M. Kubo, *J. Polymer Sci.*, **26**, 323 (1957); **36**, 453 (1959).

(8) P. J. Corish and W. H. T. Davison, *J. Chem. Soc.*, 2431 (1955).

(9) J. D. Morrison and J. M. Robertson, *ibid.*, 980, 987, 993, 1001 (1949).

(10) E. Childers and G. W. Struthers, *Anal. Chem.*, **27**, 737 (1955).

of the center of symmetry in the dicarboxylate ion of the even series, vibrations that are symmetric across the center are forbidden in the infrared spectra, rendering the absorption curves simple to a considerable extent. For instance, sodium succinate shows a peak at 1438 cm.$^{-1}$ and a shoulder on its longer wave length side. They are attributable to CH_2 bending and symmetric COO stretching vibrations. Two sharp peaks at 1176 and 1226 cm.$^{-1}$ are assigned to CH_2 twisting and wagging frequencies, respectively. A peak at 925 cm.$^{-1}$ having a hump on the longer wave length side is attributable to the CC stretching vibrations. The CH_2 rocking vibration absorbs at 808 cm.$^{-1}$ in good agreement with 804 cm.$^{-1}$ observed for succinic acid. Thus, all bands observed in the wave number range investigated could be explained in terms of a succinate ion belonging to the point group C_{2h}, indicating the *trans* configuration of the carbon chain.

The number of absorption peaks increases with increasing length of a carbon chain in the dicarboxylate ion of the even series. Owing to the absence of the center of symmetry, the spectra of sodium α,ω-dicarboxylates of the odd series are in general slightly more complicated than those of the salts of the even series having nearly the same number of carbon atoms in a chain. For these reasons, the complete assignment is feasible with difficulty and therefore was not attempted in this study. However, it is noteworthy that each of the sodium salts of both even and odd series shows a sharp band attributable to the CH_2 rocking mode at a wave number practically coincident with that of the corresponding acid. This suggests that the *trans* configuration is realized or at least predominant about single bonds in the carbon chains.

Another evidence in support of the *trans* configuration is afforded by a prominent spectral feature in the wave number range covering 1100–1300 cm.$^{-1}$, where a group of bands known as a band progression[11] appears with more or less regular spacings, notably in the spectra of higher members beyond sodium pimelate. Analogous regular series of bands have been observed in the spectra of various long-chain compounds, such as paraffins, alkyl bromides, fatty acids, glycerides, sodium soaps, etc.[12] The number of bands in a series bears some relationship to the number of carbon atoms in a methylene chain: it is equal to or greater by $^1/_2$ than half the number of carbon atoms depending upon whether the latter number is even or odd, although certain anomalies to this relationship have been reported. It is presumed that these sets of absorption bands arise from CH_2 wagging and twisting modes coupled with the skeletal vibrations of extended zigazg carbon chains.[13]

The structure of methylene chains in copper(II) α,ω-dicarboxylates can now be discussed on the basis of the information obtained for the corresponding sodium salts. In general, the spectral features of copper(II) salts beyond the succinate are more complicated than those of the corresponding sodium salts. For instance, the absorption bands of copper(II) succinate in the wave number range investigated are more numerous than those of sodium succinate, indicating that some of the vibrational modes forbidden in the spectrum of the sodium salt are allowed in the case of the copper(II) salt. In addition, a band attributable to the CH_2 rocking mode shifts from its normal position at about 808 cm.$^{-1}$ for sodium succinate to the higher wave number side and is split into two peaks at 881 and 893 cm.$^{-1}$. This suggests that the structure of succinate ions in the copper(II) salt is distorted to some extent, in good agreement with the conclusion already advanced from magnetic measurements.[1]

The higher members of the copper(II) salts also show complicated spectral patterns quite different from those of the corresponding sodium salts, the band progression mentioned above being hardly discernible in the spectra of the copper(II) salts. With increasing chain length, however, a peak at about 730 cm.$^{-1}$ to be assigned to the CH_2 rocking mode resumes its normal position and almost coincides in its wave number with the corresponding peak of the acids, indicating that the *trans* configuration is predominant. In the intermediate stage, *i.e.*, in the case of copper(II) glutarate and adipate, a few sharp peaks of comparable intensities rather than a single peak appear in the frequency range of CH_2 rocking vibrations. These facts seem to support the conclusion derived from magnetic measurements[1] that the formation of pairs of copper atoms leads to the distortion of methylene chains to some extent in crystalline copper(II) α,ω-dicarboxylates.

Copper(II) oxalate has no methylene group and hence discussions in terms of CH_2 rocking vibrations are not feasible. Its infrared spectrum in the wave number range investigated is very similar to that of sodium oxalate. This is quite understandable, because although copper(II) oxalate shows a subnormal magnetic moment per copper atom and accordingly pairing of copper atoms is surely present in the crystals, two-dimensional network structure is conceivable without any appreciable distortion of oxalate radicals.[1]

The spectrum of copper(II) malonate is almost identical with that of sodium malonate, save that the former is simpler than the latter in having a single peak at 1595 cm.$^{-1}$ attributable to the C=O stretching mode rather than a band split into two peaks as in the sodium salt. Copper(II) malonate is exceptional among its homologs in that its magnetic moment is normal, *i.e.*, close to the spin-only moment, 1.73 B.M., for one unpaired electron.[1] This suggests no pairing of copper atoms taking place in the crystals. Since no restriction due to the formation of pairs of copper atoms is imposed upon malonate radicals in the crystals, it is natural that the spectrum of copper(II) malonate is as simple as that of sodium malonate.

The CO stretching frequencies also provide a very important clue to the elucidation of structures. The antisymmetric COO stretching fre-

---

[11] L. J. Bellamy, "The Infra-red Spectra of Complex Molecules," Methuen & Co., London, 2nd ed., 1958, p. 173.

[12] D. Chapman, *J. Chem. Soc.*, 784 (1958).

[13] R. N. Jones, A. F. McKay and R. G. Sinclair, *J. Am. Chem. Soc.*, **74**, 2575 (1952).

quency is known to be sensitive to the electronic environment of a carboxylate ion. For instance, Kagarise[14] has shown for the salts of phenylstearic acid that a linear relationship exists between the antisymmetric COO stretching frequency and the electronegativity of the metal constituent of the molecule. Accordingly, if the two-dimensional network structure as suggested by magnetic measurements is present in the crystals of some copper(II) α,ω-dicarboxylates, it is expected that the antisymmetric COO stretching frequency is shifted to some extent from its normal position, which may be presumed to be represented by the corresponding frequency observed for sodium salts. Table II gives the antisymmetric COO stretching frequencies observed for both copper(II) and sodium salts of various α,ω-dicarboxylic acids. If the difference between the COO frequencies of the copper(II) and sodium salts, which difference is practically zero for copper(II) malonate showing a normal magnetic moment, is plotted against the number of carbon atoms in an acid radical, the graph bears a fairly close resemblance in shape to that of the magnetic moment of the copper(II) salts per one copper atom plotted against the same abscissa.[1] In other words, the dependence of the shift of the antisymmetric COO stretching frequency of the copper(II) salts from the normal position is similar to that of the deviation of the magnetic moment of the copper(II) salts from the theoretical spin-only moment for one odd electron. This striking parallelism in these two quantities suggests that wherever the truth lies in this debatable problem, there can be no doubt that these two quantities are intimately related to each other and have their origin in common. Presumably, the electronic structure about a copper atom or a pair of copper atoms is responsible for the similadependence of the two quantities upon the numrber of carbon atoms in the acid radical.

Table II

Antisymmetric COO Stretching Frequencies of the Copper(II) α,ω-Dicarboxylates, $(CH_2)_{n-2}(COO)_2Cu$ and the Corresponding Sodium Salts in Cm.$^{-1}$ and the Magnetic Moments of the Copper(II) Salts in Bohr Magnetons

n	Cu salt	Na salt	Difference	μ
2	1665	1635	30	1.20
3	1595	1595	0	1.76
4	1608	1567	41	1.40
5	1590	1583	7	1.45
6	1582	1567	15	1.33
7	1592	1565	27	1.41
8	1595	1559	36	1.44
9	1595	1566	29	1.41
10	1595	1564	31	1.44

[14] R. E. Kagarise, This Journal, **59**, 271 (1955).

A STANDARD FLUORESCENCE SPECTRUM FOR CALIBRATING SPECTRO-FLUOROPHOTOMETERS

By W. H. Melhuish

Contribution No. 73 from the Institute of Nuclear Sciences, Department of Scientific and Industrial Research, Lower Hutt, New Zealand

Received December 14, 1959

The energy and quantum fluorescence spectrum of quinine bisulfate in N H_2SO_4 has been measured. The energy at each wave length (joules sec.$^{-1}$ cm.$^{-1}$ mμ^{-1}) was determined by comparison with a tungsten lamp of known color temperature. The quinine bisulfate fluorescence spectrum is proposed as a standard for calibrating monochromators to be used for measuring fluorescence or phosphorescence spectra.

Introduction

Fluorescence spectra have important applications in physical chemistry especially in such studies as fluorescence quenching, transfer of electronic excitation energy between molecules, the measurement of fluorescence efficiencies and in fluorescence analysis. Previous workers have measured fluorescence spectra by visual, photographic or photoelectric methods. The observed spectrum was usually compared with the spectrum of a tungsten lamp of known color temperature measured in the same apparatus, to obtain the relative energy or number of quanta emitted at each wave length. The energy or quanta emitted by the filament at different wave lengths was either measured with a thermopile or calculated from Planck's law (or Wien's law if extreme accuracy was not required).

In order to avoid the necessity of calibrating the monochromator with a tungsten lamp, Kortüm and Finckh[1] suggested that the fluorescence spectrum of quinine sulfate in M H_2SO_4 be used as a transfer standard. These authors determined the energy fluorescence spectrum of quinine sulfate by a photographic method and obtained the spectrum shown in Fig. 1.

Work in this Laboratory has thrown some doubt on the correctness of the spectrum published by Kortüm and Finckh.[1] The quantum fluorescence spectrum of anthracene in benzene given by Melhuish[2] was determined with a Beckman DU spectrophotometer used as a monochromator, calibrated with the quinine sulfate spectrum of Kortüm and Finckh.[1] This spectrum differed considerably from the quantum fluorescence spectrum given by Cherkasov, *et al.*[3] (see Table II). It was therefore decided to redetermine the fluores-

[1] G. Kortüm and B. Finckh, *Spectrochim. Acta*, **2**, 137 (1941–1944).

[2] W. H. Melhuish, *N. Z. J. Sci. and Tech.*, **37.2B**, 142 (1955).

[3] A. S. Cherkasov, B. Ya. Sveshnikov and G. A. Tishchenko, *Optika i Spekt.*, **4**, 631 (1958).

cence spectra of quinine bisulfate and anthracene using a photoelectric method similar to that described by Burdett and Jones,[4] employing a photomultiplier in place of the photocell.

Experimental

Quinine bisulfate was obtained from two sources; Carnegie Bros., London, (B.P. grade) and British Drug Houses. Both were recrystallized from water and dried at 100°. The absorption spectra of both samples in N H_2SO_4, measured with a Unicam spectrophotometer, were found to coincide. The spectrum agreed closely with that published by Grant and Jones.[5] Anthracene was purified by chromatography on alumina followed by sublimation in a nitrogen atmosphere.

A Hilger constant deviation spectrometer was set up with a 931-A photomultiplier at the exit slit. The fluorescent solutions were held in a disc-shaped cuvette kept at a constant temperature (25 ± 0.1°) by means of water circulated from a thermostat. Radiation from a mercury lamp ("black lamp") was focussed on the front face of the cuvette and the fluorescence from the same face focussed into the spectrometer. Intensity measurements were made by a potentiometric method using a helipot slide wire and a d.c. amplifier as a null detector. The linearity of the helipot (50,000 ohm, manufactured by P. X. Fox Ltd., England) was tested and found to be better than ±0.3% from 200 to 990 divisions and ±1% from 20 to 200 divisions. The 125 watt high pressure mercury lamp was regulated by placing barretters in series with it and running the unit from a constant voltage transformer. The wave length markings on the spectrometer drum were checked with the lines from mercury and neon discharge lamps.

For the spectral energy calibration, a small coiled filament tungsten lamp (8 volts, 1 watt) was set in place of the sample. The brightness temperature of the filament was measured with a calibrated optical pyrometer and the color temperature obtained from tables. The color temperature was 2,200 ±50°K. and the spectral energy distribution was assumed to be that of a black body at this temperature. Forsythe and Adams[6] have shown that this procedure produces errors no greater than 1% in the wave length range 350 to 600 mμ. The transmission of the envelope of the tungsten lamp was assumed to be constant over the range 380 to 600 mμ. This procedure for calibrating the monochromator-photo-multiplier combination allows for changes in the energy transmitted with wave length (at constant slit width) and for the selective response of the photomultiplier (see Burdett and Jones[4]). Variation in absorption by the wall of the cuvette and the lenses in the optical system with wave length, is also included in the calibration.

The intensity of fluorescence of quinine bisulfate (5×10^{-5} to 5×10^{-3} M in 0.05, 0.5 and 2.5 M H_2SO_4) was measured as a function of wave length and the fluorescence energy spectrum determined (Fig. 1 and Table I).

Two sets of measurements made with slit widths of 0.1 and 0.2 mm. differed by less than 1%. These measurements were corrected with the aid of the tungsten lamp data, to the energy fluorescence spectrum (relative joules sec.$^{-1}$ cm.$^{-2}$ mμ^{-1}) or the quantum fluorescence spectrum (relative quanta sec.$^{-1}$ cm.$^{-2}$ mμ^{-1}) making the maximum of the spectrum 1.0. The units used for the ordinate must be definitely stated as the positions and relative heights of the maxima of the spectrum depend on these units. This is clearly illustrated in Fig. 2 where the quantum spectrum of anthracene in benzene is plotted using for the ordinate relative quanta per unit wave length interval (full line) and relative quanta per unit frequency interval (dotted line).

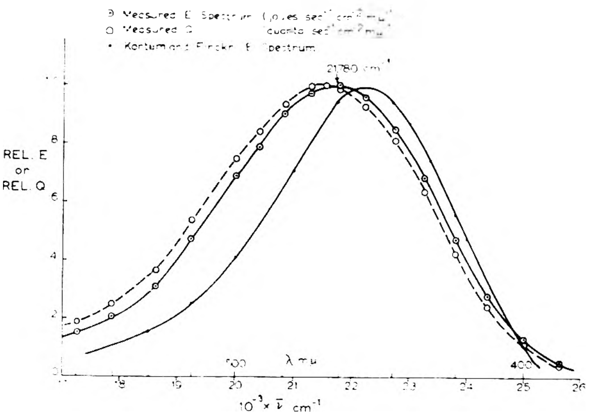

Fig. 1.—Fluorescence spectrum of quinine bisulfate, 5×10^{-3} M in N H_2SO_4.

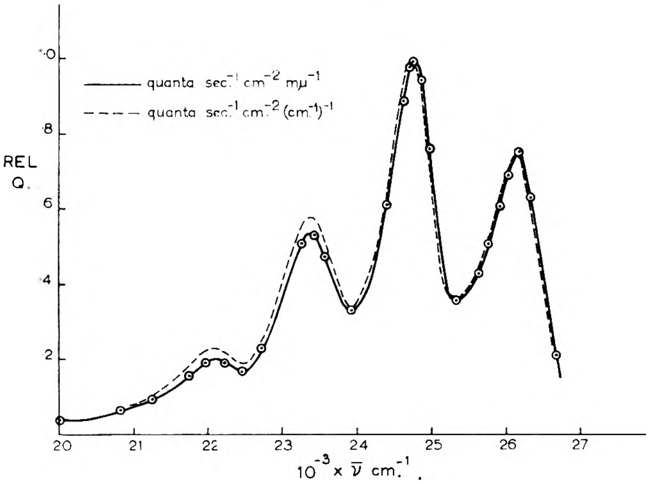

Fig. 2.—Anthracene-benzene, $10^{-5}M$, 25°.

Table I

Calibration of Spectro-fluorophotometer with a Tungsten Filament at a Color Temperature of 2200°K.

	Tungsten lamp		Quinine bisulfate, 5×10^{-3} M		
λ, mμ	Obsd.[a] int.	Planck's Law[b]	Obsd.[a] int.	Energy spectrum	Quantum spectrum
380	15.0	0.170	...	...	...
390	40.0	.231	14.5	0.046	0.039
400	82.5	.309	60.0	.126	.110
410	132.5	.406	158	.272	.242
420	186	.526	297	.469	.425
430	250	.670	456	.683	.636
440	322	.843	583	.853	.812
450	403	1.046	666	.963	.930
460	498	1.285	694	1.000	.994
465	...	...	...	...	1.000
470	592	1.560	664	0.976	0.993
480	685	1.870	593	.905	.937
490	777	2.225	499	.798	.846
500	866	2.625	409	.690	.750
520	1001	3.56	240	.477	.536
540	988	4.69	118	.313	.365
560	838	6.01	51.5	.206	.250
580	654	7.53	23.5	.151	.187
600	475	9.24			

[a] Helipot reading. [b] Calculated relative energy flux per mμ.

Results and Discussion

The fluorescence from quinine bisulfate extends over the range 390 to 580 mμ and is therefore eminently suitable for calibrating spectrofluorophotometers, in the visible region, which are to be used

---

(4) R. A. Burdett and L. C. Jones, *J. Opt. Soc. Am.*, **37**, 554 (1947).

(5) H. S. Grant and J. H. Jones, *Anal. Chem.*, **22**, 679 (1950).

(6) W. E. Forsythe and E. Q. Adams, *J. Opt. Soc. Am.*, **35**, 108 (1945).

for quantitatively measuring fluorescence or phosphorescence spectra. A solution of quinine bisulfate has other advantages; it is reasonably stable to visible and near ultraviolet radiation, reabsorbs very little of its own fluorescence, is not quenched by dissolved air and has a high ($Q = 0.52$) quantum fluorescence efficiency. Varying the acid concentration from 0.05 to 2.5 M H_2SO_4 did not cause more than a 2% change at any point in the fluorescence spectrum. No change in the shape of the spectrum could be detected when the concentration was progressively altered from 5×10^{-3} to 5×10^{-5} M. This is consistent with the fact that overlap between the absorption and fluorescence spectra of quinine bisulfate in acid solution is small.

The maximum of the energy fluorescence spectrum of quinine bisulfate falls at about 21,780 cm.$^{-1}$ which differs considerably from the figure 22,225 cm.$^{-1}$ given by Kortüm and Finckh.[1] It is difficult to attribute this disagreement to differences in experimental technique for both methods use a tungsten lamp as a standard source. The wave length of the maximum found in this work is nearer to that recorded (466 mμ) by Pringsheim.[7] This difference might be due to the source or past history of the quinine bisulfate, for Pringsheim[7] notes that a change in the fluorescence color is produced by heating the salt before dissolving it in water. In view of the very large difference between the spectrum published by Kortüm and Finckh[1] and that reported here, an independent check by another worker would be very desirable. The author is willing to supply a sample of the quinine bisulfate used in the present calibration.

TABLE II

RELATIVE PEAK HEIGHTS OF THE BANDS IN THE FLUORESCENCE SPECTRUM OF ANTHRACENE

Solvent benzene except where otherwise stated

Peak						
1 26130	2 24480	3 23350	4 21950 cm.$^{-1}$	Units[c]	Concn., mole/l.	Ref.
0.79	1.00	0.49	0.15	E	..	8
.71	1.00	.29	..	E	10^{-5b}	1
.79	1.00	.41	.08	Q	10^{-4}	2
.43	1.00	.55	.19	Q	10^{-3}	3
.47	1.00	.50	.16	E	10^{-3}	[a]
.805	1.000	.502	.173	E	10^{-5}	[a]
.44	1.00	.53	.18	Q	10^{-3}	[a]
.750	1.000	.537	.195	Q	10^{-6}	[a]

[a] Present work. [b] Solvent, p-dioxane. [c] E = rel. energy sec.$^{-1}$ mμ^{-1}. Q = rel. quanta sec.$^{-1}$ mμ^{-1}.

The spectrum of anthracene in benzene (Fig. 2 and Table II) measured in the same apparatus, agrees well with the spectra published by Cherkasov, *et al.*,[3] and Wolfsohn and Sambursky[8] but not with that given by Kortüm and Finckh,[1] although it is known[8] that the solvent has very little effect on the relative heights of the fluorescence maxima.

---

[7] P. Pringsheim, "Fluorescence and Phosphorescence," Interscience Publishers, New York, N. Y., 1949 p. 419.

[8] G. Wolfsohn and S. Sambursky, *Trans. Faraday Soc.*, **36**, 427 (1940).

THE DETERMINATION OF PARTIAL PRESSURES FROM TOTAL VAPOR PRESSURE-LIQUID COMPOSITION DATA

By SHERRIL D. CHRISTIAN

The University of Oklahoma, Norman, Okla.

Received December 18, 1959

A digital computer method has been developed for calculating the partial pressures of components in binary mixtures of volatile non-electrolytes from total pressure–liquid composition data. The constant temperature, constant pressure form of the Gibbs–Duhem equation has been applied, and the assumption has been made that species in the vapor phase follow the ideal gas law. The computer program is applicable to systems in which neither component associates in the vapor phase and also to systems in which one component dimerizes and the other does not. The method has been applied to six systems for which previous workers have reported both total and partial pressures, and a graphical comparison of experimental and calculated results has been made. The program used here is available to any worker in the field of solution chemistry through the University of Oklahoma Computer Laboratory.

Introduction

During the past few years a number of techniques have been proposed for determining partial pressures of components in binary liquid mixtures by measurement of total pressures and solution mole fractions alone. In general, these methods involve the simultaneous solution of the constant temperature form of the Gibbs-Duhem equation

$$-v\,dp + RT\,[x_1\,d\ln f_1(p_1,p_2) + x_2\,d\ln f_2(p_1,p_2)] = 0 \qquad (1)$$

and the total pressure expression

$$p = p_1 + p_2 \qquad (2)$$

where p_1 and p_2 are partial pressures of components 1 and 2, f_1 and f_2 are fugacities of the components, x_1 and x_2 are liquid mole fractions of the components, p is the total vapor pressure and v is the molal volume of the solution. Several such methods, notably those described by Scatchard,[1] Redlich and Kister[2] and Barker,[3] have been used in the calculation of activity coefficients and thermodynamic functions for non-electrolyte solutions.

During the course of an intensive study in this Laboratory of liquid-vapor equilibrium of systems involving organic acids and alcohols in non-polar solvents, it appeared desirable to develop an accurate and rapid method for calculating activities and

---

[1] G. Scatchard, *Ann. Rev. Phys. Chem.*, **3**, 269 (1953).

[2] O. Redlich and A. T. Kister, *Ind. Eng. Chem.*, **40**, 341 (1948).

[3] J. A. Barker, *Aust. J. Chem.*, **6**, 207 (1953).

activity coefficients from total pressure–composition data. The use of an IBM 650 or similar computer, available to most researchers in the field of solution chemistry, was contemplated. It was decided to avoid the use of mathematical techniques involving the determination of limiting slopes of pressure plots and instead, to use as input to the computer only total pressure–liquid composition data.

Theory

Following the treatment of Hildebrand and Scott,[4] it may be shown that the activity coefficients of components in binary mixtures are expressible in power series of the liquid mole fraction. Thus

$$\ln \gamma_1 = (1 - x_1)^2(A + Bx_1 + Cx_1^2 + \ldots)$$

and

$$\ln \gamma_2 = x_1^2\,[(A - B/2) + (B - 2C/3)x_1 + (C - 3D/4)x_1^2 + \ldots] \quad (3)$$

where γ_1 and γ_2 are the activity coefficients of the components and $A, B, C, D, \ldots$ are the empirical constants, chosen consistent with the Gibbs–Duhem equation. (Note that $\gamma_1 = f_1/x_1f_1^0$ and $\gamma_2 = f_2/x_2f_2^0$.)

Assuming ideality of the vapor phase and neglecting higher coefficients in the power series expansions, equations 2 and 3 may be combined to give

$$p = x_1p_1^0 \exp(1 - x_1)^2(A + Bx_1 + Cx_1^2) + (1 - x_1)p_2^0 \exp(x^2[(A - B/2) + (B - 2C/3)x_1 + Cx_1^2] \quad (4)$$

where p_1^0 and p_2^0 are the vapor pressures of pure liquids 1 and 2. Thus, fitting total pressure as a function of x_1 in this form, the constants A, B and C, and hence activity coefficients may be determined. It should be noted that in this treatment the $-v\,\mathrm{d}p$ term of equation 1 is neglected.

Limiting the expansions in equations 3 to three terms will in general not prove overly restrictive. In many non-electrolyte systems one or two coefficients have been shown to be sufficient for fitting ln γ data over the entire concentration range.

The assumption of vapor phase ideality is somewhat more restrictive. For example, in the case of solutions in which one or both of the components dimerize in the vapor phase, ideality is not approximated even at low pressures. Also, even non-associating components may have fugacities differing from partial pressures by a few per cent. at total pressures of several atmospheres.

The method given below allows the calculation of activity coefficients of binary systems in which no dimerization occurs in the vapor phase or systems in which only one of the two components dimerizes. The assumption is made throughout that dimers and monomers, once formed, obey the perfect gas law. Corrections for the deviation of non-associating components from ideality have not been undertaken.

Method of Calculation

Equation 4 may be extended to systems in which one component dimerizes by rewriting it in the form

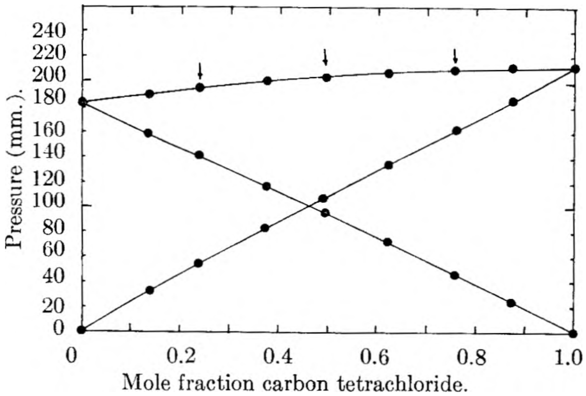

Fig. 1.—Partial and total pressures for the system carbon tetrachloride—benzene at 40°. Curves are calculated points are experimental.

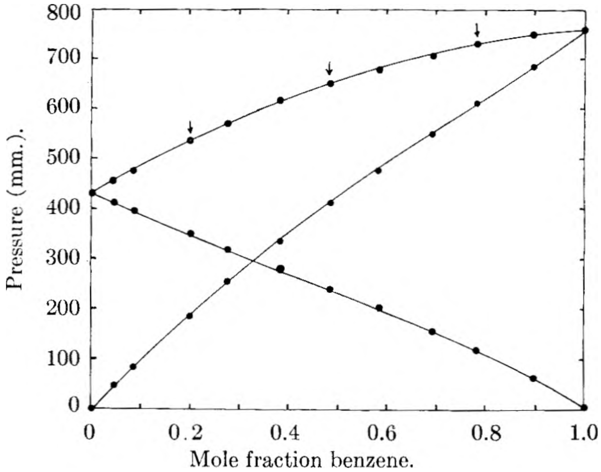

Fig. 2.—Partial and total pressures for the system benzene–n-heptane at curves are calculated, points are experimental.

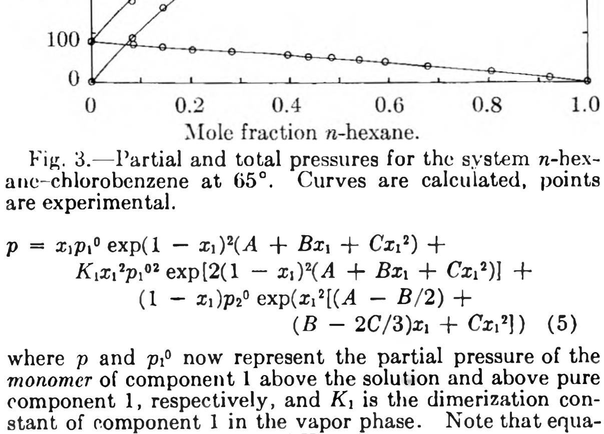

Fig. 3.—Partial and total pressures for the system n-hexane–chlorobenzene at 65°. Curves are calculated, points are experimental.

$$p = x_1p_1^0 \exp(1 - x_1)^2(A + Bx_1 + Cx_1^2) + K_1x_1^2p_1^{02} \exp[2(1 - x_1)^2(A + Bx_1 + Cx_1^2)] + (1 - x_1)p_2^0 \exp(x_1^2[(A - B/2) + (B - 2C/3)x_1 + Cx_1^2]) \quad (5)$$

where p and p_1^0 now represent the partial pressure of the *monomer* of component 1 above the solution and above pure component 1, respectively, and K_1 is the dimerization constant of component 1 in the vapor phase. Note that equation 5 reduces to equation 4 if $K_1 = 0$.

The following procedure was used in reducing experi-

---

[4] J. H. Hildebrand and R. L. Scott, "The Solubility of Non-Electrolytes," 3rd ed., Reinhold Publ. Corp., New York, N. Y., 1950.

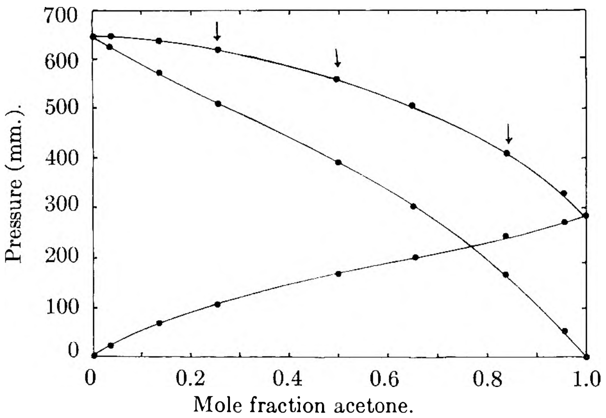

Fig. 4.—Partial and total pressures for the system acetone–diethyl ether at 30°. Curves are calculated, points are experimental.

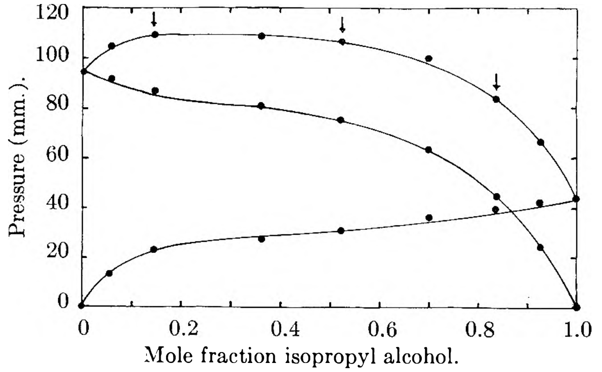

Fig. 5.—Partial and total pressures for the system isopropyl alcohol–benzene at 25°. Curves are calculated, points are experimental.

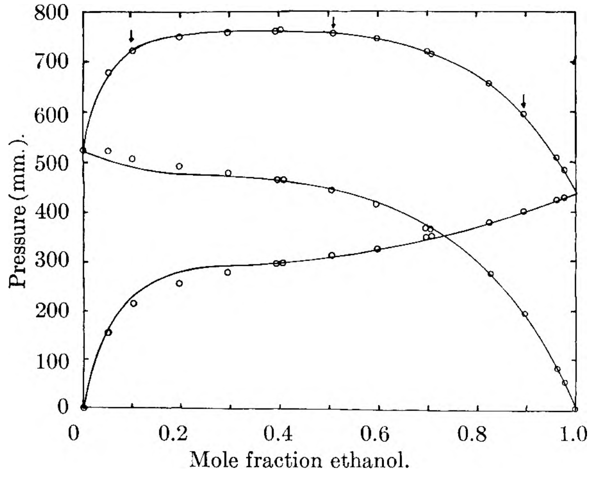

Fig. 6.—Partial and total pressures for the system ethanol–carbon tetrachloride at 65°. Curves are calculated, points are experimental.

mental data prior to solving equation 5 with the computer. First, a plot of total pressure *vs.* liquid mole fraction was constructed. Second, three total pressure points were chosen from the smoothed curve, or, if the total pressure data appeared sufficiently precise, three actual data points were selected. These three points, plus K_1, p_1^0 and p_2^0, constituted the only data input to the computer.

The iterative method used for computing A, B and C from these data was the following. The first data point (total pressure, mole fraction) was forced to fit equation 5 by choosing B and C zero and solving for A by Newton's method. Then, the second data point was fit using the value of A so obtained, choosing C zero and solving similarly for B. The third data point was fit using the values of A and B so determined and solving for C. These values of A, B and C were used to calculate a value of the error function

$$\Delta = (p^{\rm I} - p_{\rm calcd}{}^{\rm I})^2 + (p^{\rm II} - p_{\rm calcd}{}^{\rm II})^2 + (p^{\rm III} - p_{\rm calcd}{}^{\rm III})^2 \qquad (6)$$

where $p^{\rm I}$, $p^{\rm II}$ and $p^{\rm III}$ represent the three measured total pressures and $p_{\rm calcd}{}^{\rm I}$, $p_{\rm calcd}{}^{\rm II}$ and $p_{\rm calcd}{}^{\rm III}$ the values calculated from equation 5 using the constants A, B and C obtained above together with the experimental liquid mole fractions. The magnitude of Δ was, of course, a measure of how closely the A, B and C values fit all three data points. If Δ had a value smaller than a pre-specified arbitrary amount, the problem was considered solved, and partial pressures, total pressures, activities and activity coefficients were calculated. If it did not, the procedure above was repeated using, instead of the initial zeroes, the values of A, B and C just determined. Thus, by a repetitive computational process, the three total pressure data points were fit to within the desired limit, yielding A, B and C and the derived quantities in tabular form.

Results

A series of six binary organic systems was selected for the purpose of testing the computational method. These systems have been previously reported by various workers in the field of solution chemistry, and both total and partial pressures are available. The systems range from those deviating only slightly from Raoult's Law to those which form azeotropes and are far from ideal.

The system carbon tetrachloride–benzene, reported by Scatchard, Wood and Mochel,[5] is shown in Fig. 1. Experimentally determined total pressure and partial pressure values are plotted, along with the curves calculated from equation 5 by the method outlined above. Arrows indicate the three points selected for the curve-fitting process.

The system benzene–*n*-heptane, reported by Brown and Ewald[6], is similarly treated in Fig. 2. The systems *n*-hexane–chlorobenzene, reported by Brown[7]; acetone–diethyl ether, by Sameshima[8]; isopropyl alcohol–benzene, by Olsen and Washburn[9] and ethanol–carbon tetrachloride, by Barker, *et al.*,[10] are shown in Figs. 3 through 6. None of these systems contain dimerizing components; hence, K_1 was taken as zero in solving equation 5. Values of the constants A, B and C calculated for the systems are given in Table I.

TABLE I

VALUES OF THE CONSTANTS A, B AND C

System					
Component 1	Component 2	t, °C.	A	B	C
Carbon tetrachloride	Benzene	40	0.107	0.010	0.000
Benzene	*n*-Heptane	80	.300	.230	.302
n-Hexane	Chlorobenzene	65	.619	− .098	− .051
Acetone	Diethyl ether	30	.800	− .504	.368
Isopropyl alcohol	Benzene	25	2.049	−2.319	1.923
Ethanol	Carbon tetrachloride	65	2.365	−3.210	2.450

Discussion

The agreement between experimentally deter-

---

(5) G. Scatchard, S. E. Wood and J. M. Mochel, *J. Am. Chem. Soc.*, **62**, 712 (1940).

(6) I. Brown and A. H. Ewald, *Aust. J. Sci. Res.*, **A4**, 198 (1951).

(7) I. Brown, *ibid.*, **A5**, 530 (1952).

(8) J. Sameshima, *J. Am. Chem. Soc.*, **40**, 1489 (1918).

(9) A. L. Olsen and E. R. Washburn, THIS JOURNAL, **41**, 457 (1937).

(10) J. A. Barker, I. Brown and F. Smith, *Disc. Faraday Soc.*, **15**, 142 (1953).

mined partial pressure values and those calculated by the total pressure method outlined above is quite satisfactory. Calculated results generally agree with experimental results more closely for systems deviating only slightly from ideality than for those systems which are extremely non-ideal. It should be mentioned, however, that experimental difficulties often are greater for systems showing large positive deviations from Raoult's Law, and it is possible that part of the discrepancy is a result of experimental error. It is well known that total pressure measurements can be made with greater accuracy than partial pressure measurements.

The system ethanol–carbon tetrachloride (shown in Fig. 6) is of special interest. If the experimental results are correct, it would appear that the carbon tetrachloride does not approach Raoult's Law as a limiting law. This could be interpreted as indicating the formation of aggregates of ethanol molecules, even at low ethanol concentrations. Experiments are being undertaken to check both partial and total vapor pressure results for the ethanol–carbon tetrachloride system and other alcohol–non-polar solvent systems.

The above method, in addition to yielding accurate partial pressure values, is extremely rapid and easy to use. It is believed that wide-spread use of a convenient total pressure method, such as the one presented here, will ultimately lead to the accumulation of a much greater volume of accurate thermodynamic data for solutions than would be possible using the more difficult conventional total pressure–partial pressure techniques.

The program developed here is available to any worker in the field through the University of Oklahoma Computer Laboratory. IBM 650 computing time for the systems reported ranged from less than five minutes to a maximum of about 12 minutes. Although no results are given here for systems in which one of the components dimerizes in the vapor phase (acetic acid–carbon tetrachloride, for example), the program has been applied successfully to such systems. These results will be reported in a forthcoming paper. In addition, the program is being modified to allow calculation of partial pressures for systems in which both components dimerize in the vapor phase and in which cross dimerization occurs also.

Acknowledgments.—The author is indebted to Professor William Viavant and Mrs. Margaret Crawley of the University of Oklahoma Computer Laboratory for their advice and assistance in developing the method of computation. The many hours of IBM 650 computer time donated by the Laboratory made this study possible. In addition, the author wishes to express his appreciation for the financial aid given him by the National Science Foundation during the early phases of this work.

PROTON MAGNETIC RESONANCE STUDIES ON INTRAMOLECULAR HYDROGEN BONDING IN MONO-ANIONS OF STERICALLY HINDERED SUCCINIC ACIDS

By L. EBERSON AND S. FORSÉN[1]

Department of Organic Chemistry, Chemical Institute, University of Lund, and Research Group for Nuclear Magnetic Resonance Division of Physical Chemistry, The Royal Institute of Technology, Stockholm 70, Sweden

Received December 3, 1959

The proton magnetic resonance spectra of the monopotassium salts of certain alkyl-substituted succinic acids have been investigated. The results obtained indicate that there is a strong intramolecular hydrogen bond in the mono-anions of those dicarboxylic acids which exhibit anomalously high ratios between their first and second dissociation constants.

Introduction

It is generally accepted[2] that the high K_1/K_2 ratio of maleic acid is due to the formation of a strong intramolecular hydrogen bond in its mono-anion. Infrared,[3] X-ray[4] and neutron diffraction[5] studies have shown unequivocally that there is a short ($O \ldots H \ldots O' = 2.42$–$2.44$ Å.) and, at least statistically, symmetrical intramolecular hydrogen bond in solid monopotassium maleate. Proton magnetic resonance (p.m.r.) studies on monosodium and monopotassium maleate in dimethyl sulfoxide (DMSO) solution[6] have shown proton signals at very low fields ($\delta = -15.03$ and -15.40, respectively, referred to external water standard) which were ascribed to the internal hydrogen bond.

Recently, Eberson[7] has described a number of *rac*-α,α'-dialkyl- and tetraalkylsuccinic acids with extremely high K_1/K_2 ratios (in 50% aqueous ethanol by weight), which were explained in the same way as the maleic acid ratio. However, as infrared data[8] were not quite decisive on this point, it was hoped that p.m.r. studies would give further evidence.

Experimental

The p.m.r. measurements were made with a Varian V-4300 spectrometer operating at a fixed frequency of 40 Mc./sec. and equipped with a Varian V-K 3506 Super Stabilizer.

---

[1] Atomic Energy Department, ASEA, Västerås, Sweden.

[2] H. C. Brown, D. H. McDaniel and O. Häfliger in E. A. Braude and F. C. Nachod, "Determination of Organic Structures by Physical Methods," Academic Press, Inc., New York, N. Y., 1955.

[3] H. M. E. Cardwell, J. D. Dunitz and L. E. Orgel, *J. Chem. Soc.*, 3740 (1953).

[4] S. Darlow in D. Hadzi and H. W. Thompson, "Hydrogen Bonding," Pergamon Press, London, 1959.

[5] S. W. Peterson and H. A. Levy, *J. Chem. Phys.*, **29**, 948 (1958).

[6] S. Forsén, *ibid.*, **31**, 852 (1959).

[7] L. Eberson, *Acta Chem. Scand.*, **13**, 211 (1959).

[8] L. Eberson, *ibid.*, **13**, 224 (1959).

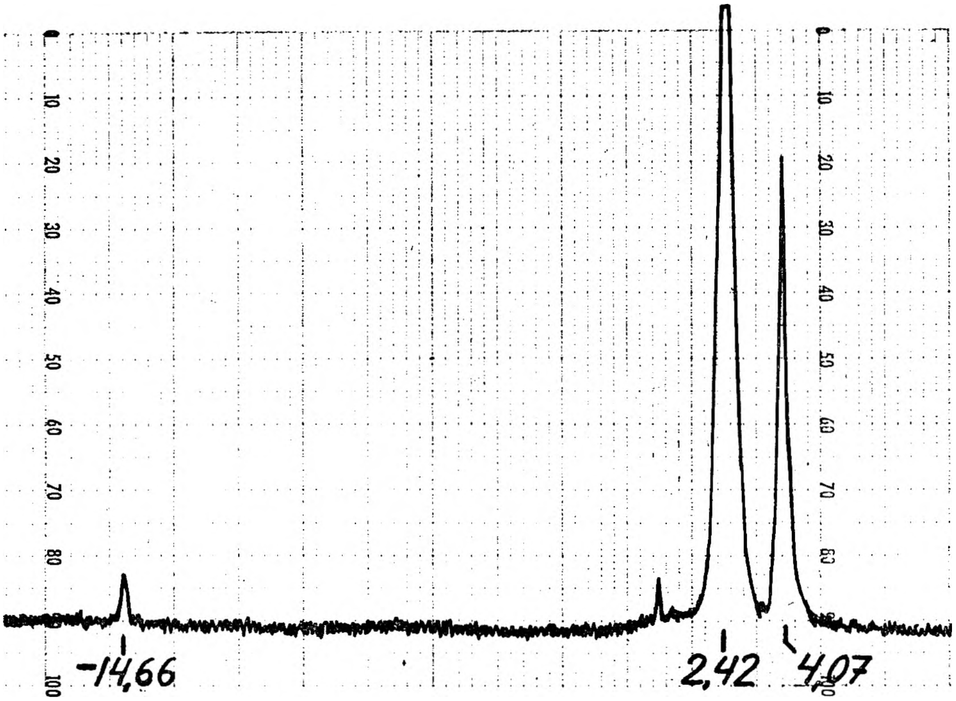

Fig. 1.—P.m.r. spectrum of a solution of the monopotassium salt of *rac*-α,α'-di-(t-butyl)-succinic acid (II) in DMSO (mole fraction 0.13). The shifts are given relative to external water. The assignments are: $\delta = -14.66$, proton in a strong intramolecular hydrogen bond; $\delta = 2.42$, the solvent signal; $\delta = 4.07$, the protons of the t-butyl groups. The small peak close to the solvent signal is one of the $C^{13}H_3$-satellites surrounding the strong methyl signal.

TABLE I

CHEMICAL SHIFTS (δ) IN MONOPOTASSIUM SALTS OF SUBSTITUTED SUCCINIC ACIDS IN DMSO SOLUTION (EXTERNAL WATER STANDARD)

			Assignment of signals		
Salt (x = mole fraction solute)	No.	ΔpK[a]	δ for proton in an internal hydrogen bond	δ for proton not involved in an internal hydrogen bond	δ for DMSO
Monopotassium maleate ($x = 0.06$)[6]		6.60	−15.40		2.42
Monopotassium fumarate[b]		1.82			
Monopotassium *rac*-α,α'-diisopropylsuccinate ($x = 0.1$)	I	7.78	−14.42		2.42
Monopotassium *rac*-α,α'-di-(t-butyl)-succinate ($x = 0.1$)	II	9.54	−14.66		2.42
Monopotassium *rac*-α,α'-dicyclohexylsuccinate ($x = 0.1$)	III	7.76	−14.42		2.42
Monopotassium tetraethylsuccinate ($x = 0.1$)	IV	6.64	−15.02		2.42
Monopotassium *meso*-α,α'-diisopropylsuccinate ($x = 0.04$)	V	2.12		0.75 (broad)	2.42
Monopotassium *meso*-α,α'-di-(t-butyl)-succinate ($x = 0.04$)	VI	1.86		0.75 (broad)	2.42
Monopotassium *meso*-α,α'-dicyclohexylsuccinate ($x = 0.03$)	VII	2.29		0.75 (broad)	2.42

[a] In 50% aqueous methanol by weight.[7] [b] Insoluble in DMSO.

The sample cells used were thin-walled glass tubes with a good filling factor. Measurements against an external water standard were made in a cell made of two coaxial glass tubes containing water in the narrow annular space and the solution to be measured in the central tube.[9] The resonance shifts were determined in c./sec. by the audio-frequency sideband method using a Hewlett-Packard 200 CD Audio Oscillator. The shift measurements were usually reproducible to within ±1 c./sec. The resonance shifts were transferred to the field independent unit δ defined by the expression

$$\delta = 10^6 \times \frac{H_{\text{sample}} - H_{\text{ref}}}{H_{\text{ref}}}$$

The sample temperature was 25 ± 1°. No attempt was made to make corrections for the macroscopic susceptibility effect, as no reliable value for the susceptibility of DMSO could be obtained.

Materials.—The DMSO was purified by freezing out a 99.5% pure stock three times. The monopotassium salts were prepared as described earlier.[8] The solubilities of the potassium salts of the *meso* acids are much less than those of the corresponding *racemic* acids which readily could be obtained in solutions with mole fractions of 0.1–0.2.

Results and Discussion

The monopotassium salts of four acids with very high K_1/K_2 ratios, *viz.*, *rac*-α,α'-diisopropyl-, *rac*-α,α'-di-(t-butyl)-, *rac*-α,α'-dicyclohexyl- and tetraethylsuccinic acid (I–IV) were chosen for measurement and the monopotassium salts of the corresponding *meso* acids (V–VII) were included for comparison (the *meso* acids have normal K_1/K_2 ratios, which are in approximate agreement with those calculated by the Kirkwood–Westheimer method[7]). The results of the p.m.r. measurements on DMSO solutions of the salts are summarized in Table I and a typical spectrum is shown in Fig. 1.

P.m.r. spectra also were run on water and methanol solutions of compounds I–IV, but no signals on the low-field side of the solvent signal

---

(9) Wilmad Glass Co., Landisville, N. J., U. S. A.

could be detected. This does not, however, rule out the possibility that an intramolecular hydrogen bond persists to some extent in these media as a rapid proton exchange between solvent and solute would be expected to broaden and flatten the proton signal from the intramolecular hydrogen bond with a simultaneous merging with the solvent signal.

The corresponding free acids of I–IV in DMSO gave rise to a very broad band at about $\delta = -5.0$, and accordingly any internal hydrogen bond that might have been present must be disrupted in this solvent (*cf.* ref.[6])

It is widely accepted that the position of a proton resonance signal is shifted toward lower applied fields when the hydrogen atom takes part in a hydrogen bond.[10] The magnitude of the shift can be taken as a rough measure of the hydrogen bond strength.[10] The difference in the behavior of the *racemic* and *meso* acid salts and an observed constancy of the alkyl proton shifts on passing from the free acid to the monopotassium salt indicates that in the present case no anomalous effect arises from the presence of the cation. One would therefore expect that the proton resonance shift of $\delta = -15.40$ in potassium hydrogen maleate should be very close to the "lower limit" for O....H....O′ hydrogen bonds. Accordingly, the intramolecular hydrogen bond in the salts I-IV should be comparable in strength to that of the maleate mono-anion. The slightly smaller shifts in the case of I-IV as compared with potassium hydrogen maleate may be an indication that these hydrogen bonds are not symmetrical, but further information is needed to obtain full evidence on this point, *e.g.*, by neutron diffraction data.

It is interesting to note that short, strong hydrogen bonds can be formed in suitably substituted saturated dicarboxylic acids without there being any other path connecting O and O′ through which migration of electrons can take place as in the maleate and phthalate mono-anion.[11] However, some sort of O=C—C=C—C=O conjugation may be necessary for the formation of a *symmetrical* hydrogen bond.

Acknowledgments.—The authors would like to thank Dr. E. Forslind for his kind encouragement and generosity in including this work in the general research program of the NMR-group. Thanks are also due to Dr. B. R. Thomas for valuable linguisitic criticism and to Statens Råd för Atomforskning, Statens Naturvetenskapliga Forskningsråd and Statens Tekniska Forskningsråd which have provided financial support for the NMR-group. The cost of the NMR apparatus has been defrayed by grants from Knut and Alice Wallenbergs Stiftelse.

---

(10) J. A. Pople, W. G. Schneider and H. J. Bernstein, "High-resolution Nuclear Magnetic Resonance," McGraw-Hill Book Co., New York, N. Y., 1959.

(11) See ref. 4, p. 344.

A GAS CHROMATOGRAPHIC STUDY OF THE CATALYTIC ISOMERIZATION OF CYCLOPROPANE[1]

BY D. W. BASSETT[2] AND H. W. HABGOOD

Research Council of Alberta, Edmonton, Alberta, Canada

Received December 23, 1959

The general case of a first-order catalytic reaction occurring during elution of a reactant through a chromatographic column is discussed. Under conditions of low reactant partial pressure and rapid adsorption relative to the rate of the surface reaction, the fractional conversion of a pulse of reactant passed through a chromatographic column is given by an equation analogous to that for the conversion under similar conditions in a steady-state flow reactor. A major advantage of the chromatographic technique is that it permits a determination of the extent of adsorption under reaction conditions, and thus of the rate constant for the reaction on the catalyst surface. The method is illustrated by a gas chromatographic study of the catalytic isomerization of cyclopropane on Linde Molecular Sieve 13X. The rate constant of the surface reaction was found to be $k = 1.3 \times 10^{10} \exp(-30{,}000/RT)$ sec.$^{-1}$. The heat of adsorption of cyclopropane under reaction conditions was 11.0 kcal. mole^{-1}.

Introduction

In recent years, the techniques of gas chromatography have been increasingly applied to the study of heterogeneous catalytic reactions These applications are of two distinct types: those in which gas chromatography is used only as an analytical tool, and those in which gas chromatographic techniques are an integral part of the reaction study. Apart from observations of catalytic reactions occurring during analyses by gas chromatography,[3] reported experiments of the second type[4–9] have all been car-

---

(1) Contribution No. 110 from the Research Council of Alberta. Presented at the Division of Analytical Chemistry Symposium on Gas Chromatography, 137th National Meeting of the American Chemical Society, Cleveland, Ohio, April, 1960.

(2) Research Council of Alberta Post-doctoral Fellow.

(3) (a) B. A. Kazanskiĭ, V. T. Aleksanyan, M. Yu. Lukina, A. I. Malyshev and Kh. E. Sterin, *Izvest. Akad. Nauk S.S.S.R., Otdel. Khim. Nauk*, 1118 (1955); (b) S. A. Greene and H. Pust, *Anal. Chem.*, **30**, 1039 (1958).

(4) (a) R. J. Kokes, H. Tobin, Jr., and P. H. Emmett, *J. Am. Chem. Soc.*, **77**, 5860 (1955); (b) W. Keith Hall and P. H. Emmett, *ibid.*, **79**, 2091 (1957); (c) THIS JOURNAL, **63**, 1102 (1959); (d) P. H. Emmett, *Am. Chem. Soc. Div. Petrol. Chem. Preprints*, **4**, No. 2, C-79 (1959).

(5) W. Keith Hall, D. S. MacIver and H. P. Weber, *ibid.*, **4**, No. 2, C-89 (1959).

(6) K. Stein, J. Feenan, G. P. Thompson, J. F. Shultz, L. J. E. Hofer and R. B. Anderson, *ibid.*, **4**, No. 2, C-115 (1959).

(7) A. G. Goble and Rosemary S. Smith, *ibid.*, **4**, No. 2, C-141 (1959).

(8) S. A. Greene, *J. Chem. Ed.*, **34**, 194 (1957).

(9) A. I. M. Keulemans and H. H. Voge, THIS JOURNAL, **63**, 476 (1959).

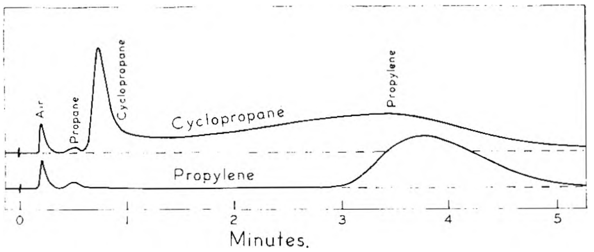

Fig. 1.—Chromatograms for cyclopropane and propylene on 4.177 g. of Ni Zeolite (Linde Molecular Sieve 13X exchanged with Ni^{++}) at 225°; flow 1.32 ml. sec.$^{-1}$ (0°) helium.

ried out by the micro-catalytic technique developed by Kokes, Tobin and Emmett,[4a] and are comparative or qualitative studies of the properties of a number of different catalysts. None of this work has fully explored the chromatographic nature of the process and its power to yield quantitative results. The chromatographic method is of particular importance as it permits measurement of the extent of adsorption and of the heat of adsorption of the reactant under reaction conditions. The activation energy of a surface reaction may therefore be determined. Tamaru[10] has shown that adsorption under reaction conditions may be measured by gas chromatography, but has not used the chromatographic method for direct rate measurements.

This paper presents a brief analysis of the kinetics of a first-order, surface catalyzed reaction, occurring under conditions of chromatographic elution. The quantitative treatment is limited to the case when the partial pressure of reactant is low and the surface reaction is the rate-controlling step. These conditions appear to be fulfilled in the catalytic isomerization of cyclopropane on Linde Molecular Sieve 13X, a crystalline sodium alumino-silicate, which is reported here. Roberts[11] has recently studied this reaction on a variety of catalysts using a conventional steady-state flow reactor.

Theoretical

When a catalytic reaction is studied directly by the gas chromatographic method, the reactant is introduced into a stream of carrier gas as a short pulse. This pulse then passes through a column of catalyst by the normal process of chromatographic elution. Because the products of reaction are formed continuously during the passage of the reactant through the column, they will usually emerge as abnormally broadened bands. This situation is well illustrated in the chromatograms of Fig. 1, which were obtained with a catalyst column having widely different retention characteristics for the reactant and product. The very broad peak of propylene, formed by the catalytic isomerization of cyclopropane, may be compared with the normal peak from propylene introduced at the head of the catalyst column. The catalyst, used for this illustration only, was 4.2 g. of a nickel alumino-silicate prepared from Linde Molecular Sieve 13X by exchanging the sodium cations with nickel. When the catalyst column shows only a slight difference in retentivity for reactant and products, and when very small amounts of catalyst are used, as in the microcatalytic technique, there will usually be more extensive overlapping of the product peaks and the reactant peak than is shown in Fig. 1, as well as the abnormal peak broadening. This was the case in the experiments described below, since the parent Molecular Sieve 13X shows a smaller difference in retentivity for cyclopropane and propylene. In practice it is usually convenient to use a second analytical gas chromatography column to determine the extent of reaction. This is a matter of analytical convenience and is irrelevant to a discussion of the processes occurring in the catalyst column.

The gas chromatographic method permits a simple quantitative study of first-order reactions only. This is because the partial pressure of the reactant varies from point to point through the reactant pulse, and it is only for a first-order reaction that the fractional conversion of reactant to products is independent of pressure. The rate of adsorption must be fast relative to the rate of the surface reaction for the latter to be the rate-controlling step. Under these conditions, apart from the decrease in the total amount of reactant due to reaction, the reactant pulse is eluted in a normal manner. The quantitative treatment also assumes that the adsorption isotherm is linear. This is usually the case for gas chromatographic elution with relatively low sample pressure. Furthermore, the adsorption equilibrium portion of the rate equation is unlikely to contain terms relating to the products. If they are weakly adsorbed, the products will be presented in insufficient amount and will tend to run ahead of the reactant pulse; if strongly adsorbed, they will lag behind the reactant as in Fig. 1.

Consider the situation in a small section of the catalyst column containing δw g. of catalyst at some instant during the passage of the reactant through the reactor. The n moles of reactant contained in this section will be distributed between the gas phase of volume $v_g \delta w$, where v_g is the volume of gas space in a section of the reactor containing 1 g. of catalyst, and the adsorbed phase in which the reaction takes place. If the partial pressure of the reactant in the gas is p_A and the adsorption equilibrium constant is K moles, atm.$^{-1}$, per g. of catalyst, then assuming a linear isotherm

$$n = p_A v_g \delta w / RT + K p_A \delta w$$

The adsorption equilibrium constant K is related to the chromatographic retention volume for 1 g. of catalyst, v_R, measured at column temperature and corrected for column dead space, by the equation[12]

$$K = v_R / RT \qquad (1)$$

Hence

$$n = p_A (v_g + v_R) \delta w / RT$$

If the surface reaction is rate controlling and k sec.$^{-1}$ is the first-order rate constant of the surface reaction, the instantaneous rate of reaction of the adsorbed reactant in the section of catalyst considered is

---

(10) K. Tamaru, *Nature*, **183**, 319 (1959).

(11) R. M. Roberts, This Journal, **63**, 1400 (1959).

(12) H. W. Habgood and J. F. Hanlan, *Can. J. Chem.*, **37**, 843 (1959).

$$-\frac{dn}{dt} = kKp_A\delta w = \frac{kKnRT}{(v_g + v_R)} \qquad (2)$$

The fractional conversion, dn/n, is independent of pressure and equation 2 may be summed over the whole catalytic reactor replacing n by N, the total moles of reactant in the pulse. The integrated form of the equation is

$$\ln\left[\frac{1}{1-x}\right] = \frac{RTkK}{(v_g + v_R)}t$$

where x is the fractional conversion and t the residence time of the pulse. If the flow rate of the carrier gas in the reactor is F ml. sec.$^{-1}$ at column temperature and mean pressure, the residence time of the reactant pulse in the catalyst column is $(v_g + v_R)W/F$ where W is the total weight of catalyst. Substituting for t and for K from equation 1

$$\ln\left[\frac{1}{1-x}\right] = \frac{RTW}{F}kK = \frac{V_R}{F}k \qquad (3)$$

where $V_R = v_RW$ is the chromatographic retention volume of the reactant on the catalyst corrected for column dead space. This result is exactly analogous to the equation giving the conversion in a conventional flow reactor under steady-state conditions, and holds for a catalyst column of any length.

In an experiment, the flow rate is measured at room temperature and corrected to some standard temperature (usually 0°) and mean column pressure giving a value $F^0 = (273/T)F$. The retention volume may also be expressed at the standard temperature and mean pressure as $V^0_R = (273/T)V_R$. Rewriting equation 3 in terms of F^0 gives

$$kK = \frac{F^0}{273RW}\ln\left[\frac{1}{1-x}\right] \qquad (4)$$

The apparent activation energy E may be obtained from the slope of a plot of ln kK vs. $1/T$, and at constant flow rate, F^0, this is equivalent to a plot of $\ln[\ln(1/1 - x)]$ vs. $1/T$. For a first-order reaction at low fractional conversion, the activation energy may also be obtained from a plot of ln x vs. $1/T$ since for x small $\ln(1/1 - x) \approx x$. Even at high fractional conversions a plot of ln x vs. $1/T$ often gives a good straight line, but the value of the activation energy given by the slope differs from the correct value. From a plot of ln K vs. $1/T$ the heat of adsorption L may be obtained.[12] Thus the activation energy of the surface reaction $E_s = E + L$, may be determined.

Experimental

The apparatus used in this study of the catalytic isomerization of cyclopropane was a conventional gas chromatography assembly modified by the introduction of a small catalytic reactor and a product trap[7] between the sample inlet and the analytical column. The reactor, product trap and analytical column each could be by-passed. Samples of reactant were introduced by way of the bore of a two-way stopcock fitted into the shell of a three-way stopcock.[12] The sample volume was approximately 0.20 ml. and the usual pressure was 20 cm. The helium carrier gas was passed through a column of dehydrated Molecular Sieve pellets to remove possible catalyst poisons before entering the system. The detector was a Gow Mac katharometer (Pretzel Model) with a 1 Mv. recorder. The gas flow at the detector exit could be measured to within 1% with a soap bubble flow meter, and the pressure drop between the sample inlet and the atmosphere could be measured with a mercury manometer.

The catalytic reactor consisted of a U-tube of 3 mm. Pyrex tubing containing about 0.1 g. of catalyst held in place by small plugs of Pyrex glass wool. The packed section of the reactor at the bend of the U was about 2 cm. in length. The reactor was heated with a small aluminum block furnace and the temperature could be measured to within 0.5° with a thermocouple adjacent to the packed section of the reactor. The reactor temperature could be held constant within 1° during the elution of a sample by controlling the heater current with a variable transformer. The reactor could be evacuated and the catalyst could be protected from contamination by immersing the connecting tubing in liquid nitrogen. The sample used was 28–48 mesh Linde Molecular Sieve 13X pellets prepared by crushing and sieving the commercial material. The sample was weighed out in the hydrated form after being equilibrated over saturated calcium nitrate solution. It was dehydrated at 420° under vacuum for several hours before any measurements were made.

The product trap consisted of a small U-tube containing about 0.1 g. of crushed Molecular Sieve 13X pellets. The unreacted cyclopropane and reaction products could be collected in the trap for a period following the introduction of a sample of reactant by cooling the trap with Dry Ice. The mixture collected was analyzed by "flashing" it into a carrier gas stream as a sharp band by heating the trap with a furnace at 300°. This procedure caused no significant isomerization of cyclopropane. Using the product trap, the chromatographic peaks obtained were sharp and suitable for quantitative purposes. The analysis of the cyclopropane and reaction products was carried out with a 3-meter by 1/4 inch column of dimethylformamide on firebrick at 0° and with a carrier gas flow rate of 50 ml. per minute. Since van de Craats[13] has shown that the specific peak areas for cyclopropane and propylene are identical, the relative amounts of the two components were determined from the products of peak heights and widths at half height.

The adsorption of cyclopropane on the catalyst sample was studied before and after a series of reaction studies by measuring its chromatographic retention volume. The retention volume was obtained for the catalyst alone by bypassing both the product trap and the analytical column. A small amount of air was admitted with each cyclopropane sample to permit correction for the apparatus dead space. Corrections were made in the usual way for the pressure drop across the column, flow meter temperature and vapor pressure of the flow meter soap solution. As a general procedure, the catalyst sample was heated to 420° before each measurement. While successive replicate measurements of retention volume without intervening heating usually agreed, the over-all reproducibility of the measurements was improved by the heating which probably removed traces of strongly adsorbed poisons. The amount of material driven off the catalyst in this treatment was so small that attempts to collect and analyze it were inconclusive.

In carrying out a reaction, the analytical column was bypassed while the products of a cyclopropane pulse injected into the reactor were collected in the product trap cooled in Dry Ice. Sufficient time was allowed to ensure that all products were collected. During experiments in which the flow rate was varied, the collection time was varied accordingly. At the end of this period, the reactor was bypassed, and the analytical column by-pass shut. The products were then analyzed as described above. Meanwhile the reactor was evacuated and heated to 420° before the admission of the next sample.

Results

The results described were all obtained with a 0.089-g. sample of Linde Molecular Sieve 13X as catalyst. Analysis of the reaction products showed that apart from traces of CO_2 believed due to oxidation by traces of oxygen in the helium, the only reaction was the isomerization of cyclopropane to propylene. No hydrocarbons other than propylene were observed in the reaction products. In a separate experiment with a different catalyst sample,

---

(13) F. van de Craats, "Gas Chromatography," (ed. D. H. Desty) Butterworths Scientific Publications, London, 1958, p. 262.

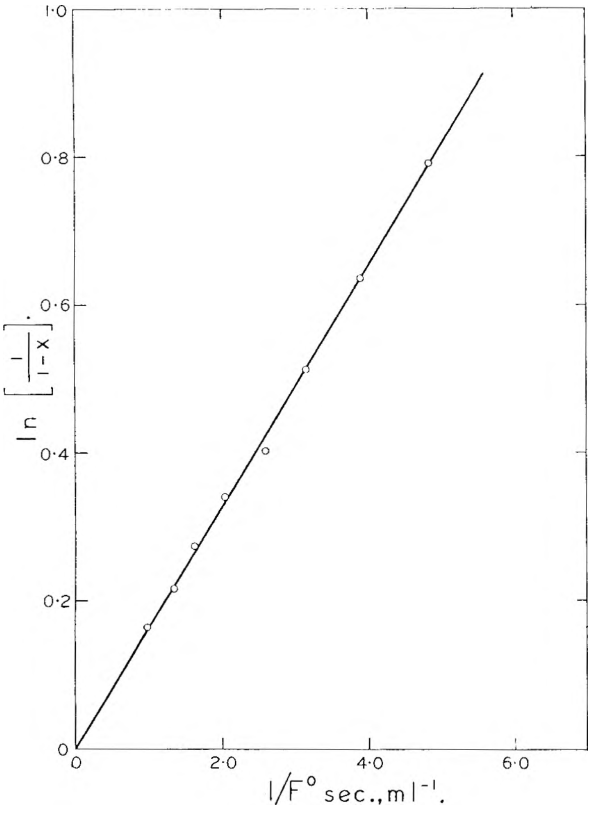

Fig. 2.—Test of first-order rate law for cyclopropane isomerization at 370° on 0.089 g. of Na Zeolite (Linde Molecular Sieve 13X).

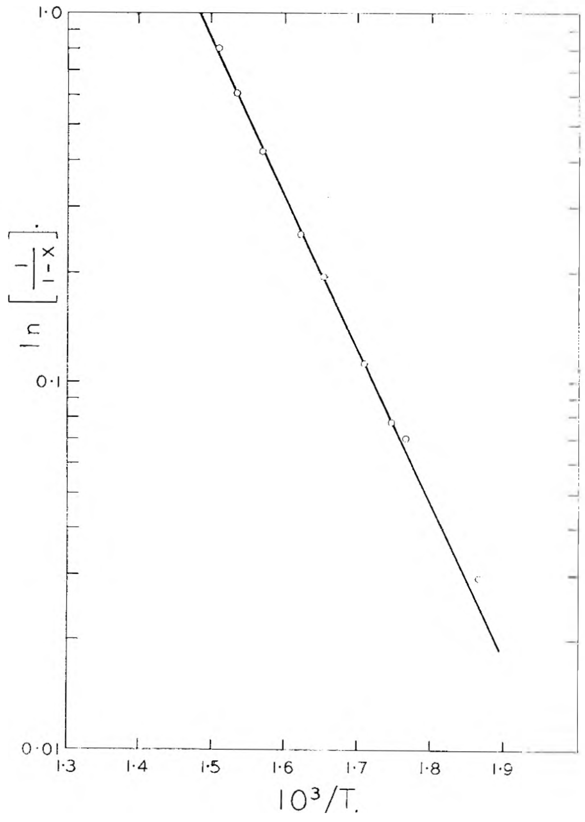

Fig. 3.—Plot of log [ln(1/1 − x)] *vs.* 1/T. The over-all activation energy = 19.0 kcal. mole^{-1}

the reaction products obtained with the catalyst at 350° were collected and analyzed mass spectrometrically. The higher hydrocarbons, which Roberts[11] has reported to form about 1% of the products of reaction at 130° in a steady-state flow system, could not be detected. Under the conditions of higher temperature and lower reactant pressure used in this study, higher hydrocarbons probably formed less than 0.01% of the product.

The retention volume of cyclopropane on the catalyst was measured over the temperature range 102–163°, and the results obtained corresponded to an adsorption equilibrium constant $K = 1.7 \times 10^{-8} \exp(11{,}000/RT)$ mole atm.$^{-1}$ g.$^{-1}$. With the small catalyst sample, measurements of retention volume could not be made at temperatures at which significant reaction was obtained. Measurements made on a larger sample over the temperature range 110–300° gave the usual straight line logarithmic plot against $1/T$ with a heat of adsorption of 10.2 kcal. mole^{-1}. It was therefore assumed that adsorption equilibrium measurements could be extrapolated into the reaction region.

The conversion of cyclopropane to propylene was studied at 370° at a series of flow rates between 1.02 and 0.206 ml. sec.$^{-1}$. Figure 2 shows that over this range equation 4 is obeyed and therefore the reaction is first order. From the slope of this line the value of the product kK at 370° is 0.2×10^{-6} mole atm.$^{-1}$ g.$^{-1}$ sec.$^{-1}$.

Measurements of the extent of reaction were made over the temperature range 263–378.5° at a constant flow rate, F^0, of 0.31 ml. sec.$^{-1}$. The results are shown in Fig. 3. The apparent activation energy of the reaction is 19.0 kcal. mole^{-1}. The value of the product kK at 370° obtained from this set of results is $kK = 7.7 \times 10^{-5}$ mole atm.$^{-1}$ g.$^{-1}$ sec.$^{-1}$.

From the expression given above for K, and the values of kK corresponding to Fig. 3, the rate constant for the surface reaction is $k = 1.3 \times 10^{10} \exp(-30{,}000/RT)$ sec.$^{-1}$. The activation energy, 30 kcal. mole^{-1}, rather than the apparent activation energy should be compared with 65 kcal. mole^{-1} found for the homogeneous gas phase reaction.[14]

Discussion

A number of advantages, particularly those of speed, simplicity and versatility, have been given by Hall and Emmett[4b] for the use of a direct gas chromatographic technique in the study of catalytic reactions. This paper has attempted to show that additional advantages of the method are that it can yield quantitative kinetic measurements; that the extent of adsorption may be determined under reaction conditions; and that, by virtual elimination of interference from adsorbed products, a simplification of the kinetics is obtained which may lead to a deeper understanding of the reaction. Hall, MacIver and Weber[5] have suggested as a serious disadvantage the possibility that equilibrium assumptions are not valid with respect to the adsorption of reactants or the state of the catalyst during elution of a pulse of reactant. However if the adsorption were slow, the chromatographic elution

---

[14] T. S. Chambers and G. B. Kistiakowsky, *J. Am. Chem. Soc.*, **56**, 399 (1934).

peaks for the reactant would be abnormally broadened because the resistance to mass transfer would be high.[15] Separate experiments with 11 inch columns of molecular sieve showed no such effects. Furthermore, adsorption measurements by gas chromatography generally agree closely with measurements by conventional methods.[12,16] Even if adsorption equilibrium is not established with a small proportion of the catalyst surface, such as the innermost pores, the value of the surface rate constant is not necessarily incorrect since it is evaluated from adsorption constants for the surface available under reaction conditions.

The present study of the catalytic isomerization of cyclopropane on a sodium alumino-silicate demonstrates the simplification of reaction kinetics obtained by the use of the gas chromatographic method. In these experiments the reaction was first order, but in the steady-state flow experiments of Roberts[11] the order was not simple and no rate constants were obtained. Using a silica-zirconia-alumina catalyst, Roberts found an apparent activation energy of 19.0 kcal. mole^{-1} in the temperature range 100–135° in agreement with the value found in this study. An apparent first-order rate constant calculated from the results given by Roberts for the 60 min. run at 135° on the silica-zirconia-alumina catalyst is approximately fifty times the rate constant calculated for reaction on the molecular sieve at 135°. It appears therefore that the molecular sieve has a somewhat smaller catalytic activity than conventional cracking catalysts. However, there is some possibility that part of the activity of the molecular sieve is due to the kaolin used as binder in forming the pellets, since experiments with the pure powder showed less reaction. This point is being investigated further.

The activity of alumino-silicate materials as catalysts in hydrocarbon cracking reactions is generally thought to be due to the presence of acidic surface sites, but whether their acidity is protonic under reaction conditions remains undecided. In these experiments the catalyst was normally dehydrated at 420°. Further dehydration at 520° reduced the catalytic activity, but the original activity could be restored by exposing the sample at 400° to water vapor. This suggests that the presence of water or available protons is essential to the formation of a reaction intermediate in the isomerization of cyclopropane, which, as suggested by Roberts,[11] may be a carbonium ion formed by the transfer of an acidic proton from the surface. However, other intermediates, such as the charge transfer complex discussed by Webb,[17] are also possible. Additional experiments are necessary to define more clearly the nature of the surface process.

---

(15) *Cf.* J. J. van Deemter, F. J. Zuiderweg and A. Klinkenberg, *Chem. Eng. Sci.*, **5**, 271 (1956).

(16) R. C. Pitkethly and A. G. Goble, *Am. Chem. Soc. Div. Petrol. Chem. Preprints*, **4**, No. 2, C-103 (1959).

(17) A. N. Webb, *ibid.*, **4**, No. 2, C-171 (1959).

ENERGY SPECTRUM IN A ZERO FORCE FIELD FOR A POLYMER MODEL

By R. G. Langebartel

Department of Mathematics, University of Illinois, Urbana, Illinois

Received December 31, 1959

This paper considers from the wave theoretic point of view the motion of a polymer model with one end anchored at the origin. With the external force field taken as zero there is obtained the energy spectrum for certain difference equation counterparts for the Schrödinger equation in the one, two and three dimensional cases. This problem and the general plan of attack were suggested by Prof. F. T. Wall.

The polymer model is taken as a chain of unit length links free to pivot around the origin, each link pivoting about the terminus of the previous link. The links are weightless with a particle at the terminus of each link, all particles having the same mass. The Schrödinger equation with the time factor removed for such a chain of n links in a zero force field is

$$\sum_{i=1}^{n} \nabla_i^2\psi + \lambda\psi = 0 \qquad (1)$$

where $\nabla_i^2\Psi = \partial^2\psi/\partial x_i^2 + \partial^2\psi/\partial y_i^2 + \partial^2\psi/\partial z_i^2$, (x_i,y_i,z_i) the coördinates of the terminus of the ith link, and $\lambda = 8\pi^2 mE/h^2$ in which m is the mass of a particle, h the Planck constant, and E the energy. This equation is, of course, subject to the restraints imposed by the constant link lengths. By a proper choice of coördinate system these restraints can be absorbed into the form of the Schrödinger equation itself. To this end let $X_k = (x_k, y_k, z_k)$ and $Y_k = (\xi_k, \eta_k, \zeta_k)$ with the relations

$$\begin{cases} Y_k = X_k - X_{k-1}, k = 1,\cdots, n; \; X_0 = 0 \\ X_k = \sum\limits_{i=1}^{k} Y_i \end{cases}$$

Then

$$\sum_{k=1}^{n} \nabla_k^2\psi = \sum_{k=1}^{n} \frac{\partial^2\psi}{\partial X_k^2} = \sum_{k=1}^{n} \left[\frac{\partial^2\psi}{\partial Y_k^2} - 2\frac{\partial^2\psi}{\partial Y_k\partial Y_{k+1}} + \frac{\partial^2\psi}{\partial Y^2_{k+1}}\right] = \sum_{k=1}^{n} \left[\left(\frac{\partial^2\psi}{\partial \xi_k^2} + \frac{\partial^2\psi}{\partial \eta_k^2} + \frac{\partial^2\psi}{\partial \zeta_k^2}\right) - 2\left(\frac{\partial^2\psi}{\partial\xi_k\partial\xi_{k+1}} + \frac{\partial^2\psi}{\partial\eta_k\partial\eta_{k+1}} + \frac{\partial^2\psi}{\partial\zeta_k\partial\zeta_{k+1}}\right) + \left(\frac{\partial^2\psi}{\partial\xi^2_{k+1}} + \frac{\partial^2\psi}{\partial\eta^2_{k+1}} + \frac{\partial^2\psi}{\partial\zeta^2_{k+1}}\right)\right], \frac{\partial\psi}{\partial\xi_{n+1}} = \frac{\partial\psi}{\partial\eta_{n+1}} = \frac{\partial\psi}{\partial\zeta_{n+1}} = 0 \qquad (2)$$

For the two dimensional problem we take

$$Y_k = (\xi_k,\eta_k) = (r_k \cos\theta_k, r_k \sin\theta_k)$$

substitute in (2), assume ψ independent of r_k, and set $r_k = 1$, thereby imposing the restraints of equal length links. This leads to the form

$$\sum_{s=1}^{n} \epsilon_s \frac{\partial^2\psi}{\partial\theta_s^{\,2}} - 2\sum_{s=1}^{n-1} \cos(\theta_s - \theta_{s+1}) \frac{\partial^2\psi}{\partial\theta_s\partial\theta_{s+1}} + \lambda\psi = 0,$$

$$\epsilon_s = \begin{cases} 1, & s = 1, \\ 2, & s = 2, 3, \ldots \end{cases} \qquad (3)$$

for the Schrödinger equation for the two dimensional problem.

A spherical coördinate substitution is indicated

$$Y_k = (\xi_k, \eta_k, \zeta_k) = (\rho_k \sin\omega_k \cos\theta_k,\ \rho_k \sin\omega_k \sin\theta_k,\ \rho_k \cos\omega_k)$$

for the three dimensional problem in which case the Schrödinger equation 1 becomes, after making use of (2) and setting $\rho_k = 1$

$$\sum_{s=1}^{n} \epsilon_s \csc^2\omega_s \frac{\partial^2\psi}{\partial\theta_s^{\,2}} + \sum_{s=1}^{n} \epsilon_s \csc\omega_s \frac{\partial}{\partial\omega_s}\left(\sin\omega_s \frac{\partial\psi}{\partial\omega_s}\right) -$$
$$2\sum_{s=1}^{n-1} [\cos\omega_s \cos\omega_{s+1} \cos(\theta_s - \theta_{s+1}) + \sin\omega_s \sin\omega_{s+1}]$$
$$\frac{\partial^2\psi}{\partial\omega_s\partial\omega_{s+1}} + 2\sum_{s=1}^{n-1} \csc\omega_s \cos\omega_{s+1} \sin(\theta_s - \theta_{s+1}) \frac{\partial^2\psi}{\partial\theta_s\partial\omega_{s+1}} -$$
$$2\sum_{s=1}^{n-1} \cos\omega_s \csc\omega_{s+1} \sin(\theta_s - \theta_{s+1}) \frac{\partial^2\psi}{\partial\omega_s\partial\theta_{s+1}} -$$
$$2\sum_{s=1}^{n-1} \csc\omega_s \csc\omega_{s+1} \cos(\theta_s - \theta_{s+1}) \frac{\partial^2\psi}{\partial\theta_s\partial\theta_{s+1}} + \lambda\psi = 0 \qquad (4)$$

The unwieldly equations 3 and 4 submit to a rather simple analysis for general n when difference equation counterparts are used in their stead. This will amount to a restriction to a discrete set of possible configurations for the chain.

One and Two Dimensional Cases.—With the use of the approximations

$$\frac{\partial^2\psi}{\partial\theta_s^{\,2}} \approx \frac{1}{\kappa^2}[\psi(\theta_1, \ldots, \theta_s + \kappa, \ldots, \theta_n) - 2\psi(\theta_1, \ldots, \theta_n) + \psi(\theta_1, \ldots, \theta_s - \kappa, \ldots, \theta_n)] \qquad (5)$$

$$\frac{\partial^2\psi}{\partial\theta_s\partial\theta_{s+1}} \approx \frac{1}{4\kappa^2}[\psi(\theta_1, \ldots, \theta_s + \kappa, \theta_{s+1} + \kappa, \ldots, \theta_n) - \psi(\theta_1, \ldots, \theta_s - \kappa, \theta_{s+1} + \kappa, \ldots, \theta_n) - \psi(\theta_1, \ldots, \theta_s + \kappa, \theta_{s+1} - \kappa, \ldots, \theta_n) + \psi(\theta_1, \ldots, \theta_s - \kappa, \theta_{s+1} - \kappa, \ldots, \theta_n)]$$

we obtain for the differential equation 3 the difference equation counterpart

$$\sum_{s=1}^{n} \epsilon_s\psi(\theta_1, \ldots, \theta_s + \kappa, \ldots, \theta_n) + \sum_{s=1}^{n} \epsilon_s\psi(\theta_1, \ldots, \theta_s - \kappa, \ldots, \theta_s) - \frac{1}{2}\sum_{s=1}^{n-1} \cos(\theta_s - \theta_{s+1})[\psi(\theta_1, \ldots, \theta_s + \kappa, \theta_{s+1} + \kappa, \ldots, \theta_n) - \psi(\theta_1, \ldots, \theta_s - \kappa, \theta_{s+1} + \kappa, \ldots, \theta_n) - \psi(\theta_1, \ldots, \theta_s + \kappa, \theta_{s+1} - \kappa, \ldots, \theta_n) + \psi(\theta_1, \ldots, \theta_s - \kappa, \theta_{s+1} - \kappa, \ldots, \theta_n)] + [-(4n - 2) + \kappa^2\lambda]\psi(\theta_1, \ldots, \theta_n) = 0 \qquad (6)$$

We seek to solve this characteristic value problem where the boundary condition is periodicity in the θ_s. In order to make best use of this periodicity κ should be chosen to divide 2π an integral number of times. The choice $\kappa = \pi$ gives chains extending along the x-axis, and $\kappa = \pi/2$ corresponds to chains laid on a square grille. The periodicity properties keep this set of equations 6 from being an infinite set if we assume the variables restricted to the values $\theta_i = 0, \kappa, 2\kappa, \ldots, m\kappa = 2\pi$. There are $(2\pi/\kappa)^n$ equations in as many unknowns, the $\psi(\theta_1, \ldots, \theta_n)$.

$\kappa = \pi$.—In this case $\psi(\theta_1, \ldots, \theta_s + \kappa, \ldots, \theta_n) = \psi(\theta_1, \ldots, \theta_s - \kappa, \ldots, \theta_n)$ by periodicity so that the cosine terms, *i.e.*, the terms arising from the mixed derivatives, all vanish. Let the equations be arranged in numerical order of the arguments of the λ term, *i.e.*, for $n = 3$ using merely the coefficients of π the order is 000, 001, 010, 011, 100, 101, 110, 111. Then the secular determinant takes on the form

$$\Delta_n = \begin{vmatrix} A_0 & 2I \\ 2I & A_0 \end{vmatrix}$$

where I is the identity matrix and the matrix A_0 in turn is of the form

$$A_0 = \begin{pmatrix} A_1 & 4I \\ 4I & A_1 \end{pmatrix}$$

This recursion arrangement continues until the final matrix A_{n-1} consisting of but one element, $\mu - 4n + 2$, where $\mu = \pi^2\lambda$, is reached

$$A_r = \begin{pmatrix} A_{r+1} & 4I \\ 4I & A_{r+1} \end{pmatrix}, \quad r = 0, 1, 2, \ldots, n - 2$$
$$A_{n-1} = (\mu - 4n + 2)$$

The values of the respective determinants are

$$\Delta_n = |A_0 + 2I| \cdot |A_0 - 2I|$$
$$|A_s| = |A_{s+1} + 4I| \cdot |A_{s+1} - 4I|, \quad s = 0, 1, 2, \ldots, n - 2$$

By applying these successively we find

$$\begin{aligned} |A_0| &= |A_1 + 4I| \cdot |A_1 - 4I| \\ &= |A_2 + 8I| \cdot |A_2|^2 \cdot |A_2 - 8I| \\ &= |A_3 + 12I| \cdot |A_3 + 4I|^3 \cdot |A_3 - 4I|^3 \cdot |A_3 - 12I| \\ &\cdots\cdots\cdots\cdots\cdots\cdots \\ &= \prod_{k=1}^{n} |A_{n-1} + (4n + 4 - 8k)I|^{\binom{n-1}{k-1}} \end{aligned}$$

where $\binom{n-1}{k-1}$ is the binomial coefficient. Consequently, the secular determinant has the value

$$\Delta_n = \prod_{k=1}^{n} |A_{n-1} + (4n + 6 - 8k)I|^{\binom{n-1}{k-1}} \cdot \prod_{k=1}^{n} |A_{n-1} + (4n + 2 - 8k)I|^{\binom{n-1}{k-1}} =$$
$$\prod_{k=1}^{n} [\mu - 8(k - 1)]^{\binom{n-1}{k-1}} \cdot \prod_{k=1}^{n} [\mu - 8(k - {}^1\!/_2)]^{\binom{n-1}{k-1}}$$

From this result it is apparent that the characteristic values are $\mu = 0, 4, 8, 12, 16, \ldots, 8n - 4$, with the degeneracy distribution function (giving multiplicity of the characteristic values)

$$g_n(\mu) = \begin{cases} \dbinom{n-1}{\frac{\mu}{8}}, & \mu = 0, 8, 16, \ldots, 8(n - 1) \\ \dbinom{n-1}{\frac{\mu-4}{8}}, & \mu = 4, 12, 20, \ldots, 8(n - 1) + 4 \end{cases} \qquad (7)$$

The energy spectrum for the one-dimensional chain is therefore made up of these values of μ multiplied by $h^2/(8\pi^4 m)$. The asymptotic relationship for large n and bounded μ is

$$g_n(\mu) \sim \begin{cases} \dfrac{n^{\frac{\mu}{8}}}{\left(\frac{\mu}{8}\right)!}, & \mu = 0, 8, 16, \ldots, 8M \\[2ex] \dfrac{n^{\frac{\mu-4}{8}}}{\left(\frac{\mu-4}{8}\right)!}, & \mu = 4, 12, 20, \ldots, 8M + 4 \end{cases} \tag{8}$$

For large n and central values of μ, say $\mu = 4n$, the formula becomes

$$g_n(4n) \sim \frac{2^n n^{-1/2}}{\sqrt{2\pi}} = \frac{2^{n-1/2}}{\sqrt{2\pi}} \left(\frac{n}{2}\right)^{-1/2} \tag{9}$$

The determination of the characteristic vectors is achieved by use of the $n \times n$ matrix

$$P_n = \begin{pmatrix} I & I \\ -I & I \end{pmatrix}$$

Post multiplication by P_n and premultiplication by its transpose P_n' reduces the matrix of Δ_n to a "diagonal" matrix whose elements are square matrices of rank $n/2$

$$\begin{pmatrix} 2A_0 - 4I & 0 \\ 0 & 2A_0 + 4I \end{pmatrix}$$

This matrix is then subjected to post and premultiplication by

$$\begin{pmatrix} P_{n/2} & 0 \\ 0 & P_{n/2} \end{pmatrix}$$

(for which we use the notation $P_{n/2} \cdot I_n$) and its transpose, respectively, causing a reduction to a diagonal matrix of square matrices of rank $n/4$. By the successive use in this way of the matrices $P_{n/4} \cdot I_n$, $P_{n/8} \cdot I_n$, ..., $P_2 \cdot I_n$ the full reduction to a "completely" diagonal matrix is effected. Thus the columns of the product matrix

$$P_n(P_{n/2} \cdot I_n)(P_{n/4} \cdot I_n) \ldots (P_2 \cdot I_n) \equiv P$$

represent the components of the characteristic vectors. A representation of P as a single matrix results from the introduction of the matrices Q_n defined by

$$\begin{cases} Q_1 = 1, \\ Q_2 = P_2 = \begin{pmatrix} 1 & 1 \\ -1 & 1 \end{pmatrix} = \begin{pmatrix} Q_1 & Q_1 \\ -Q_1 & Q_1 \end{pmatrix} \\ \cdots\cdots\cdots\cdots\cdots\cdots\cdots\cdots\cdots\cdots \\ Q_n = \begin{pmatrix} Q_{n/2} & Q_{n/2} \\ -Q_{n/2} & Q_{n/2} \end{pmatrix} \end{cases}$$

The key formula

$$P_n(Q_{n/2} \cdot I_n) = \begin{pmatrix} I_{n/2} & I_{n/2} \\ -I_{n/2} & I_{n/2} \end{pmatrix} \begin{pmatrix} Q_{n/2} & 0 \\ 0 & Q_{n/2} \end{pmatrix}$$
$$= \begin{pmatrix} Q_{n/2} & Q_{n/2} \\ -Q_{n/2} & Q_{n/2} \end{pmatrix} = Q_n$$

applied to the continued product for P working from right to left gives the result $P = Q_n$ so that the columns of the matrix Q_n are the characteristic vectors.

$\kappa = \pi/2$.—A study of the secular determinant, Δ_n, for this set of equations (again arranged in numerical order) where now $\mu = \pi^2\lambda/4$ shows that it is of the form

$$\Delta_n = \begin{vmatrix} A_0 & B_0 & 0 & C_0 \\ D_0 & A_0 & E_0 & 0 \\ 0 & B_0 & A_0 & C_0 \\ D_0 & 0 & E_0 & A_0 \end{vmatrix}$$

where 0 is the zero matrix and the matrices B_0, C_0, D_0 and E_0 satisfy $B_0 + C_0 = 2I$, and $D_0 + E_0 = 2I$. For example, if $\theta_1 = 0$ in the fundamental difference equation 6 we get the first row of matrices in Δ_n. In that case it is apparent that there is no term in (6) for which the first argument in ψ is 2 so that the zero matrix is obtained, the third matrix in the first row of matrices. The elements down the main diagonals of B_0 and C_0 are the coefficients of the first two terms in (6) for which $s = 1$. The off-diagonal elements are either zero or else the coefficients in the cosine terms where again $s = 1$. In either case the sum of the corresponding off-diagonal terms in B_0 and C_0 is zero, thereby giving $B_0 + C_0 = 2I$. Precisely similar considerations serve for the remaining three rows of matrices in Δ_n. The elements of A_0 arise from the terms with $s = 2, 3, \ldots, n$. These evidently are going to give rise to the same form for the matrix as that of Δ_n except that $\epsilon_s = 2$ now instead of 1 as before. Thus there is the recursion relationship

$$A_r = \begin{pmatrix} A_{r+1} & B_{r+1} & 0 & C_{r+1} \\ D_{r+1} & A_{r+1} & E_{r+1} & 0 \\ 0 & B_{r+1} & A_{r+1} & C_{r+1} \\ D_{r+1} & 0 & E_{r+1} & A_{r+1} \end{pmatrix}, \quad r = 0, 1, 2, \ldots, n-2$$
$$= (\mu - 4n + 2), \quad r = n - 1$$

in which

$$B_r + C_r = D_r + E_r = 4I, \quad r = 1, 2, \ldots, n - 1$$

The corresponding determinants are easily computed to be

$$\Delta_n = |A_0 + 2I| \cdot |A_0|^2 \cdot |A_0 - 2I|$$
$$|A_s| = |A_{s+1} + 4I| \cdot |A_{s+1}|^2 \cdot |A_{s+1} - 4I|, \quad s = 0, 1, 2, \ldots, n - 2$$

By making use of these relations we find that

$$|A_0| = \prod_{k=1}^{2n-1} |A_{n-1} + 4(n - k)I|^{\binom{2n-2}{k-1}}$$

and

$$\Delta_n = \prod_{k=1}^{2n} |A_{n-1} + (4n - 4k + 2)I|^{\binom{2n-1}{k-1}}.$$
$$\prod_{k=1}^{2n-1} |A_{n-1} + 4(n - k)I|,^{2\binom{2n-2}{k-1}}$$
$$= \prod_{k=1}^{2n} (\mu - 4k + 4)^{\binom{2n-1}{k-1}}.$$
$$\prod_{k=1}^{2n-1} (\mu - 4k + 2)^{2\binom{2n-2}{k-1}}$$

Accordingly, the characteristic values are $\mu = 0, 2, 4, 6, \ldots, 8n-4$ and the degeneracy distribution function is

$$g_n(\mu) = \begin{cases} \dbinom{2n-1}{\frac{\mu}{4}}, & \mu = 0, 4, 8, 12, \ldots 8n - 4 \\[2ex] 2\dbinom{2n-2}{\frac{\mu-2}{4}} & \mu = 2, 6, 10, \ldots, 8n - 6 \end{cases} \tag{10}$$

The energy spectrum for the square lattice is given by $E = h^2\mu/(2\pi^4 m)$. For large n and bounded μ the asymptotic relationship is

$$g_n(\mu) \sim \begin{cases} \dfrac{(2n)^{\frac{\mu}{4}}}{\left(\frac{\mu}{4}\right)!}, & \mu = 0, 4, 8, \ldots, 8M - 4 \\[2ex] \dfrac{2(2n)^{\frac{\mu-2}{4}}}{\left(\frac{\mu - 2}{4}\right)!}, & \mu = 2, 6, 10, \ldots, 8M - 6 \end{cases} \tag{11}$$

For the middle range of μ the asymptotic relationship for large n is

$$g_n(4n) \sim \frac{2^{2n-1/2}}{\sqrt{2\pi}} n^{-1/2} \tag{12}$$

For the characteristic vectors we use as counterpart to P_n the matrix

$$R_n = \begin{pmatrix} I & I & I & I \\ -I & I & -I & I \\ -I & -I & I & I \\ I & -I & -I & I \end{pmatrix}$$

which reduces the secular matrix to a triangular matrix of square matrices of order $n/4$. The complete reduction is then effected by

$$R = R_n(R_{n/4} \cdot I_n)(R_{n/16} \cdot I_n) \ldots (R_4 \cdot I_n)$$

which becomes equal to S_n where the matrix S_n is defined by the recursion relation

$$S_n = \begin{pmatrix} S_{n/4} & S_{n/4} & S_{n/4} & S_{n/4} \\ -S_{n/4} & S_{n/4} & -S_{n/4} & S_{n/4} \\ -S_{n/4} & -S_{n/4} & S_{n/4} & S_{n/4} \\ S_{n/4} & -S_{n/4} & -S_{n/4} & S_{n/4} \end{pmatrix}$$

with $S_1 = 1$. Thus as in the previous case the columns of S_n are the characteristic vectors.

Three-dimensional Case.—In equation 4 there are two sets of independent variables, θ_s and ω_s. In the replacing of the differential equation by a difference equation we represent by κ the difference of successive θ values and by σ the difference of successive ω values. Besides (5) we also need such relationships as

$$\frac{\partial \psi}{\partial \omega_s} \approx \frac{1}{2\sigma} [\psi(\theta_1, \ldots, \theta_n, \omega_1, \ldots, \omega_s + \sigma, \ldots, \omega_n) - \psi(\theta_1, \ldots, \theta_n, \omega_1, \ldots, \omega_s - \sigma, \ldots, \omega_n)] \tag{13}$$

$$\begin{aligned} \frac{\partial^2 \psi}{\partial \theta_s \partial \omega_{s+1}} \approx \frac{1}{4\kappa\sigma} [&\psi(\theta_1, \ldots, \theta_s + \kappa, \ldots, \theta_n, \omega_1, \ldots, \omega_{s+1} + \sigma, \ldots, \omega_n) - \psi(\theta_1, \ldots, \theta_s + \kappa, \ldots, \theta_n, \omega_1, \ldots, \omega_{s+1} - \sigma, \ldots, \omega_n) \\ &- \psi(\theta_1, \ldots, \theta_s - \kappa, \ldots, \theta_n, \omega_1, \ldots, \omega_{s+1} + \sigma, \ldots, \omega_n) + \psi(\theta_1, \ldots, \theta_s - \kappa, \ldots, \theta_n, \omega_1, \ldots, \omega_{s+1} - \sigma, \ldots, \omega_n)] \end{aligned}$$

in order to obtain the difference equation counterpart of (4)

$$\begin{aligned} &\sum_{s=1}^{n} \epsilon_s \left(\frac{1}{\sigma^2} + \frac{1}{2\sigma} \cot \omega_s\right) [\psi(\omega_s + \sigma) - \psi(\omega_s - \sigma)] + \frac{1}{\kappa^2} \sum_{s=1}^{n} \epsilon_s \csc^2 \omega_s [\psi(\theta_s + \kappa) - \psi(\theta_s - \kappa)] \\ &- \frac{1}{2\sigma^2} \sum_{s=1}^{n-1} [\cos \omega_s \cos \omega_{s+1} \cos (\theta_s - \theta_{s+1}) + \sin \omega_s \sin \omega_{s+1}] [\psi(\omega_s + \sigma, \omega_{s+1} + \sigma) - \psi(\omega_s + \sigma, \omega_{s+1} - \sigma) - \psi(\omega_s - \sigma, \omega_{s+1} + \sigma) + \psi(\omega_s - \sigma, \omega_{s+1} - \sigma)] \\ &+ \frac{1}{2\kappa\sigma} \sum_{s=1}^{n-1} \csc \omega_s \cos \omega_{s+1} \sin (\theta_s - \theta_{s+1}) [\psi(\theta_s + \kappa, \omega_{s+1} + \sigma) - \psi(\theta_s + \kappa, \omega_{s+1} - \sigma) - \psi(\theta_s - \kappa, \omega_{s+1} + \sigma) + \psi(\theta_s - \kappa, \omega_{s+1} - \sigma)] \\ &- \frac{1}{2\kappa\sigma} \sum_{s=1}^{n-1} \cos \omega_s \csc \omega_{s+1} \sin (\theta_s - \theta_{s+1}) [\psi(\omega_s + \sigma, \theta_{s+1} + \kappa) - \psi(\omega_s - \sigma, \theta_{s+1} + \kappa) - \psi(\omega_s + \sigma, \theta_{s+1} - \kappa) + \psi(\omega_s - \sigma, \theta_{s+1} - \kappa)] \\ &- \frac{1}{2\kappa^2} \sum_{s=1}^{n-1} \csc \omega_s \csc \omega_{s+1} \cos (\theta_s - \theta_{s+1}) [\psi(\theta_s + \kappa, \theta_{s+1} + \kappa) - \psi(\theta_s - \kappa, \theta_{s+1} + \kappa) - \psi(\theta_s + \kappa, \theta_{s+1} - \kappa) + \psi(\theta_s - \kappa, \theta_{s+1} - \kappa)] \\ &+ \left[-\frac{(4n - 2)}{\sigma^2} - \frac{2}{\kappa^2} \sum_{s=1}^{n} \epsilon_s \csc^2 \omega_s + \lambda \right] \psi = 0 \end{aligned} \tag{14}$$

wherein to save printing only those arguments shifted by σ or κ are explicitly written in ψ. Different types of configurations result from various choices of σ and κ. The one representing the most natural extension of the one- and two-dimensional cases treated above is $\sigma = \kappa = \pi/2$ which gives for each link four equally spaced locations at the "equator" plus the two at the poles. Again the condition of periodicity leads to a characteristic value problem $\Delta_n = 0$ for which the secular determinant now has the form

$$\Delta_n = \begin{vmatrix} A_0 & C_0 & D_0 & E_0 & F_0 & 0 \\ G_0 & A_0 & H_0 & 0 & J_0 & K_0 \\ G_0 & L_0 & A_0 & M_0 & 0 & K_0 \\ G_0 & 0 & H_0 & A_0 & J_0 & K_0 \\ G_0 & L_0 & 0 & M_0 & A_0 & K_0 \\ 0 & C_0 & D_0 & E_0 & F_0 & A_0 \end{vmatrix} \tag{15}$$

with the relations between the square matrices

$$C_0 + E_0 = D_0 + F_0 = H_0 + J_0 = L_0 + M_0 = G_0 + K_0 = 2I$$

which are sufficient to determine Δ_n completely in terms of A_0. The particular arrangement of matrices in (15) is obtained from again setting the equations in numerical order of the arguments of the λ term where the arguments themselves are written in the order $\omega_1, \theta_1, \omega_2, \theta_2, \ldots, \omega_n, \theta_n$. There is a fundamental difficulty in setting up Δ_n due to the inherent singularity in the spherical coördinate system at the poles $\omega = 0, \pi$. This is circumvented by treating the four regular points arising when $\omega = \pi/2$ and then inferring the values taken around the poles from symmetry considerations.

In the same manner as in the previous cases there is a recursion relation on the main diagonal matrices A_r

$$A_r = \begin{pmatrix} A_{r+1} & C_{r+1} & D_{r+1} & E_{r+1} & F_{r+1} & 0 \\ G_{r+1} & A_{r+1} & H_{r+1} & 0 & J_{r+1} & K_{r+1} \\ G_{r+1} & L_{r+1} & A_{r+1} & M_{r+1} & 0 & K_{r+1} \\ G_{r+1} & 0 & H_{r+1} & A_{r+1} & J_{r+1} & K_{r+1} \\ G_{r+1} & L_{r+1} & 0 & M_{r+1} & A_{r+1} & K_{r+1} \\ 0 & C_{r+1} & D_{r+1} & E_{r+1} & F_{r+1} & A_{r+1} \end{pmatrix} \quad r = 0, 1, 2, \ldots, n - 2$$

$$= (\mu - 8n + 4), \qquad r = n - 1$$

where now

$$C_{r+1} + E_{r+1} = D_{r+1} + F_{r+1} = H_{r+1} + J_{r+1} = L_{r+1} + M_{r+1} = G_{r+1} + K_{r+1} = 4I$$

$r = 0,1,2,\ldots, n - 2$ and $\mu = \pi^2\lambda/4$. The determinant (15) easily can be factored into

$$\begin{vmatrix} A_0 & 0 & 0 \\ 0 & A_0 & 0 \\ 0 & 0 & A_0 \end{vmatrix} \cdot \begin{vmatrix} A_0 & 2I & 2I \\ 2I & A_0 & 2I \\ 2I & 2I & A_0 \end{vmatrix}$$

by subtracting the last row of matrices from the first, the fourth from the second, and the fifth from the third, and then adding the first column to the last, the second to the fourth, and the third to the fifth. Thus

$$\Delta_n = |A_0 + 4I| \cdot |A_0|^3 \cdot |A_0 - 2I|^2$$

$$|A_r| = |A_{r+1} + 8I| \cdot |A_{r+1}|^3 \cdot |A_{r+1} - 4I|^2, \qquad r = 0, 1, 2, \ldots, n-2$$

Successive applications of this recurrence formula gives

$$|A_0| = \prod_{k=0}^{3n-3} |A_{n-1} + [8(n-1) - 4k]I|^{\Gamma\binom{3n-3}{k}}$$

where $\Gamma\binom{3p}{k}$ is the coefficient of α^k in the expansion of $(1 + 3\alpha^2 + 2\alpha^3)^p$. The determinant Δ_n then comes out to be

$$\Delta_n = \prod_{k=0}^{3n-3} (\mu - 4k)^{\Gamma\binom{3n-3}{k}} \cdot \prod_{k=0}^{3n-3} (\mu - 4 - 4k)^{3\Gamma\binom{3n-3}{k}} \cdot \prod_{k=0}^{3n-3} (\mu - 6 - 4k),^{2\Gamma\binom{3n-3}{k}}$$

$$= \prod_{k=0}^{3n-2} (\mu - 4k)^{\Gamma\binom{3n-3}{k} + 3\Gamma\binom{3n-3}{k-1}} \cdot \prod_{k=0}^{3n-3} (\mu - 6 - 4k),^{2\Gamma\binom{3n-3}{k}} \qquad (16)$$

in which it is understood that $\Gamma\binom{3p}{k} = 0$ if $k < 0$ or $k > 3p$. The characteristic values are seen from this factorization of Δ_n to be $\mu = 0,4,6,8,10,\ldots,12n - 6$, with the degeneracy distribution function

$$g_n(\mu) = \begin{cases} \Gamma\binom{3n-3}{\frac{\mu}{4}} + 3\Gamma\binom{3n-3}{\frac{\mu}{4} - 1} & \mu = 0, 4, 8, 12, \ldots, 12n - 8 \\ 2\Gamma\binom{3n-3}{\frac{\mu}{4} - \frac{3}{2}}, & \mu = 6, 10, 14, \ldots, 12n - 6 \end{cases} \qquad (17)$$

A representation for the coefficients $\Gamma\binom{3n}{k}$ is obtained from a direct expansion of the polynomial

$$(1 + 3\alpha^2 + 2\alpha^3)^n = [1 + (3\alpha^2 + 2\alpha^3)]^n$$

$$= \sum_{k=0}^{n} \binom{n}{k} (3\alpha^2 + 2\alpha^3)^k$$

$$= \sum_{k=0}^{n} \binom{n}{k} \sum_{p=0}^{k} 3^k \binom{k}{p} \left(\frac{2}{3}\right)^p \alpha^{2k+p}$$

$$= \sum_{k=0}^{n} \sum_{q=2k}^{3k} 3^k \binom{n}{k} \binom{k}{q-2k} \left(\frac{2}{3}\right)^{q-2k} \alpha^q$$

$$= \sum_{q=0}^{3n} \sum_{k=\left[\frac{q+2}{3}\right]}^{[q/2]} \binom{n}{k} \binom{k}{q-2k} \left(\frac{27}{4}\right)^k \left(\frac{2}{3}\right)^q \alpha^q$$

where the symbol $[x]$ stands for the largest integer less than or equal to x. Consequently, it is apparent that

$$\Gamma\binom{3n}{q} = \left(\frac{2}{3}\right)^q \sum_{k=\left[\frac{q+2}{3}\right]}^{[q/2]} \binom{n}{k} \binom{k}{q-2k} \left(\frac{27}{4}\right)^k \qquad (18)$$

This leads to the asymptotic relationships for $g_n(\mu)$ from (17) for large n and bounded μ

$$g_n(\mu) \sim \begin{cases} \dfrac{(3n)^{\frac{\mu}{8}}}{\left(\frac{\mu}{8}\right)!}, & \mu = 0, 8, 16, \ldots, 8M \\ \dfrac{2}{3}\left(\dfrac{\mu}{8} + 4\right) \dfrac{(3n)^{\frac{\mu}{8} - \frac{1}{2}}}{\left(\frac{\mu}{8} - \frac{1}{2}\right)!}, & \mu = 4, 12, 20, \ldots, 8M - 4 \\ \dfrac{2(3n)^{\frac{\mu}{8} - \frac{3}{4}}}{\left(\frac{\mu}{8} - \frac{3}{4}\right)!}, & \mu = 6, 14, 22, \ldots, 8M - 2 \\ \dfrac{4}{3} \dfrac{(3n)^{\frac{\mu}{8} - \frac{5}{4}}}{\left(\frac{\mu}{8} - \frac{9}{4}\right)!}, & \mu = 10, 18, 26, \ldots, 8M - 6 \end{cases}$$

The energy itself for this three-dimensional model is expressed in terms of μ as $E = h^2\mu/(2\pi^4 m)$ with multiplicities given by (17).

The role of P_n and R_n for the determination of the characteristic vectors in the present case is played by the matrix

$$T_n = \begin{pmatrix} 0 & 0 & I & I & I & I \\ 0 & I & 0 & I & -I & I \\ I & 0 & 0 & -2I & 0 & I \\ 0 & -I & 0 & I & -I & I \\ -I & 0 & 0 & -2I & 0 & I \\ 0 & 0 & -I & I & I & I \end{pmatrix}$$

The columns of the matrix U_n are then the characteristic vectors where the defining relation for U_n is

$$U_n = \begin{pmatrix} 0 & 0 & U_{n/6} & U_{n/6} & U_{n/6} & U_{n/6} \\ 0 & U_{n/6} & 0 & U_{n/6} & -U_{n/6} & U_{n/6} \\ U_{n/6} & 0 & 0 & -2U_{n/6} & 0 & U_{n/6} \\ 0 & -U_{n/6} & 0 & U_{n/6} & -U_{n/6} & U_{n/6} \\ -U_{n/6} & 0 & 0 & -2U_{n/6} & 0 & U_{n/6} \\ 0 & 0 & -U_{n/6} & U_{n/6} & U_{n/6} & U_{n/6} \end{pmatrix}$$

with $U_1 = 1$.

Acknowledgment.—This work was made possible by a grant from the National Science Foundation.

EFFECT OF LIGANDS ON RATES OF HYDROGEN EXCHANGE OF SUBSTITUTED METAL AMMINES

By J. W. Palmer and Fred Basolo

Chemistry Department, Northwestern University, Evanston, Illinois

Received December 31, 1959

For octahedral complexes the rates of hydrogen exchange of metal ammines decrease with decrease in cationic charge. Just the opposite is true of square ammines and this behavior is discussed in terms of π-bonding and solvation effects. Two rates of hydrogen exchange are observed for *cis*-$Co(NH_3)_4(NO_2)_2^+$ whereas for the *trans* isomer, all hydrogens are equivalent. Two rates are also found for $Pt(dien)X^+$ complexes where the more labile hydrogen is that opposite X. Likewise, the hydrogen lability increases with an increase in the "*trans*" effect of X.

Hydrogen exchange reactions of N–H bonds are often extremely rapid.[1] However, the base-catalyzed hydrogen exchanges of certain metal ammines in acid buffers are slow and can be studied by conventional techniques.[2] The rate of exchange can be followed by measurements in the near infrared on solutions originally containing hydrogen-1 metal ammines in hydrogen-2 acetate buffer in heavy water.[3] Reported in this paper are the rates of hydrogen exchange of several acidoamminecobalt(III) acidoammineplatinum(II) complexes.

Experimental

Preparation of Compounds.—The cobalt(III) complexes were prepared by methods described in the literature.[4] The compounds were characterized by analysis for at least one element and by a comparison of absorption spectrum with that reported for the known compound. Syntheses and analyses of the platinum(II) and palladium(II) compounds were reported elsewhere.[5]

Rates of Exchange.—The method used to follow the rate of hydrogen exchange in these systems is the same as that described previously.[3] Briefly it involves measurements of optical density at 1.65 μ to determine the increase in OH concentration with time for reaction mixtures originally containing a hydrogen-1 metal ammine in an acetate buffered heavy water solution. The buffer solution was prepared by adding anhydrous sodium acetate and acetic anhydride to 99.5% D_2O to give 0.1 *M* $NaC_2H_3O_2$ and 0.1 *M* $DC_2H_3O_2$. Measurements were made with a Beckman Model DK-2 recording spectrophotometer which was equipped with a cell holder maintained at constant temperature (±0.1°) by circulating water through it from a thermostated waterbath.

The rates of hydrogen exchange were determined by plotting $\log (H_\infty - H_t)$ *vs.* t where H_∞ is the optical density at infinite time and H_t is the optical density at time t. The product of the slopes of these curves and -2.3 gave the pseudo first-order rate constant k_{obsd}, which when divided by $[OD^-]$ gave the reported second-order rate constants, k. The values of k were determined with a precision of 15%. The $[OD^-]$ calculated on the basis of a pK_a of 5.26 for $DC_2H_3O_2$ and a K_i for D_2O[6] of 0.15×10^{-14} was adjusted in each case for the small (never more than 0.2 *p*H unit) variation in *p*H resulting from the addition of the complex to acetate buffered H_2O solutions.[7]

As shown in Fig. 1(A) the plot of $\log (H_\infty - H_t)$ *vs.* t for *cis*-$Co(NH_3)_4(NO_2)_2^+$ is not linear suggesting that the hydrogens may be exchanging at different rates. In this structure there are two types of hydrogens, those on the two ammonias *trans* to each other but *cis* to both nitro groups and those on the two ammonias *trans* to the nitro group. Assuming two different rates of hydrogen exchange, the data were analyzed using methods applicable to linear parallel rates[8] (Fig. 1(B)).

Results and Discussion

Octahedral Complexes.—Data in Table I show that the rates of hydrogen exchange for acidoamminecobalt(III) complexes decrease in the order $Co(NH_3)_6^{3+} > Co(NH_3)_5X^{2+} > Co(NH_3)_4X_2^+$. Such an effect is expected on the basis of electrostatic considerations, the more positive cation containing the more acidic or reactive hydrogens. Infrared studies reported for these complexes show an increase in the N–H stretching frequency with a decrease in cationic charge.[9] These results, interpreted as a greater N–H bond strength, correlate the slower rates of hydrogen exchange. The difference in rate is relatively small for each unit of positive charge on the cation. This is in accord with the observations that the acid strengths of metal ammines do not decrease very much with a decrease in cationic charge, *e.g.*, $pK_a = 7.9$ and 8.1 for $Pt(NH_3)_6^{4+}$ and $Pt(NH_3)_5Cl^{3+}$, respectively.[10] In contrast to this, the charge on the

Table I

Rates of Hydrogen Exchange of Octahedral Metal Ammines in 0.1 *M* $DC_2H_3O_2$–$C_2H_3O_2^-$ Buffer at 25°

Complex	$k \times 10^{-6}$ M^{-1} sec.$^{-1}$	E_a, kcal.	ΔS^*, e.u.
$Co(NH_3)_6^{3+}$	1.6	14 ± 1	14
$Co(NH_3)_5F^{2+}$	0.11		
$Co(NH_3)_5Cl^{2+}$	.15	15 ± 2	11
$Co(NH_3)_5Br^{2+}$	.16		
$Co(NH_3)_5NO_2^{2+}$	.38	12 ± 2	5
$Ir(NH_3)_6^{3+}$	.015	23 ± 2	34
$Ir(NH_3)_5Cl^{2+}$	.002[a]		
$Co(en)_3^{3+}$	2.4		
trans-$Co(NH_3)_4(NO_2)_2^+$	0.15	12 ± 3	3
cis-$Co(NH_3)_4(NO_2)_2^+$	.12(0.45)[b]	11 ± 2[c]	1
trans-$Co(en)_2(NO_2)_2^+$	.068		
cis-$Co(en)_2(NO_2)_2^+$	.072(0.5)[b]		
trans-$Co(en)_2F_2^+$	.001		

[a] Calculated from rate at 48.5° and $E_a = 23$ kcal. [b] Rates in parentheses are presumably for hydrogens *trans* to NO_2^-. See Fig. 1 and text for discussion. [c] E_a and ΔS^* values are for exchange of the less labile hydrogens.

---

(1) A. Berger, A. Loewenstein and S. Meiboom, *J. Am. Chem. Soc.*, **81**, 62 (1959).

(2) J. S. Anderson, H. V. A. Briscoe and N. F. Spoor, *J. Chem. Soc.*, 361, 367 (1943); H. Block and V. Gold, *ibid.*, 966 (1959).

(3) J. W. Palmer, F. Basolo and R. G. Pearson, *J. Am. Chem. Soc.*, **82**, 1073 (1960).

(4) Gmelin, *Handbuch anorg. Chem.*, **58B**, (1930).

(5) F. Basolo, H. B. Gray and R. G. Pearson, *J. Am. Chem. Soc.*, **82**, Aug. (1960).

(6) S. Korman and V. K. LaMer, *ibid.*, **58**, 1403 (1936); R. Kingerley and V. K. LaMer, *ibid.*, **63**, 3260 (1941).

(7) L. H. Cobb and J. S. Anderson, *Trans. Faraday Soc.*, **40**, 145 (1943).

(8) A. A. Frost and R. G. Pearson, "Kinetics and Mechanism," John Wiley and Sons, Inc., New York, N. Y., 1953, p. 150.

(9) G. F. Svatos, C. Curran and J. V. Quagliano, *J. Am. Chem. Soc.*, **77**, 6159 (1955).

(10) A. A. Grinberg and K. I. Gil'dengeishel, *Izvest. Akad. Nauk S.S.S.R.*, 479 (1948).

metal ion has an extremely large effect on the lability of the ammine hydrogens as shown by the observation that $Ir(NH_3)_6^{3+}$ exchanges with a rate constant $k = 1.5 \times 10^6 M^{-1}sec.^{-1}$ at 48.5° whereas the exchange of $Pt(NH_3)_6^{4+}$ is too rapid to determine even in acid solution.

A comparison of the exchange rates for $Co(NH_3)_5X^{2+}$ shows that the rates decrease in the order $NO_2^- > Br^- \sim Cl^- > F^-$. The chloro and bromo compounds have approximately the same rate and are only about 1.5 times faster than the fluoro compound. This result does not correspond to the electronegativity of the halides which would cause the fluoro complex to exchange the fastest. However, the small differences observed between the halides may be due to an opposing crystal (ligand) field effect.[11] There is some evidence that the larger the crystal field stabilization energy (CFSE) of an ammine, the slower its rate of hydrogen exchange.[12] This suggests that the fluoro complex would be the slowest to exchange because the crystal field strengths of the halogens decrease in the order $F^- > Cl^- > Br^-$.

The more rapid rate of $Co(NH_3)_5NO_2^{2+}$ might be due to its ability to vacate a p-orbital on the nitro nitrogen and form pd-π bonds with d-electrons of Co(III). The presence of a π-bonding ligand in the complex would tend to stabilize the transition state of M-NH$_2$—H—OD for hydrogen exchange by enhancing the delocalization of the p-electrons on the amido nitrogen (Fig. 2). This would lower the activation energy for exchange and result in a more rapid rate of hydrogen exchange.

Linear kinetic plots were obtained from the exchange data for complexes of the type *trans*-$Co(NH_3)_4X_2^+$ but for the *cis* isomers these plots show considerable curvature (Fig. 1). For the *cis*-dinitro complexes the curvature was sufficiently large to permit a resolution of the data and an estimate of two rate constants. These differ by a factor of four for the ammine and seven for the ethylenediamine complexes (Table I). That the *trans* isomers show only one rate of hydrogen exchange is readily understandable on the basis of its symmetrical structure which makes all hydrogens equivalent. In contrast to this, the *cis* isomers contain two kinds of hydrogens, those located *cis* to both X groups and those *trans* to X. Because of the orbital geometry, it would appear to be easier to delocalize electrons in the "amido" transition state that are *trans* rather than *cis* to a nitro group (Fig. 2). This assignment of greater lability to the *trans* hydrogens receives some support from the fact that the slower rates are about the same as the rates for the corresponding *trans*-isomers. In both cases, the hydrogens are *cis* to nitro groups and may be expected to have similar rates. Finally the three hydrogens on NH_3 opposite NO_2^- in $Co(NH_3)_5NO_2^{2+}$ are expected to differ from the other twelve hydrogens adjacent to NO_2^-. However any such difference was too small to be detected by our experimental method.

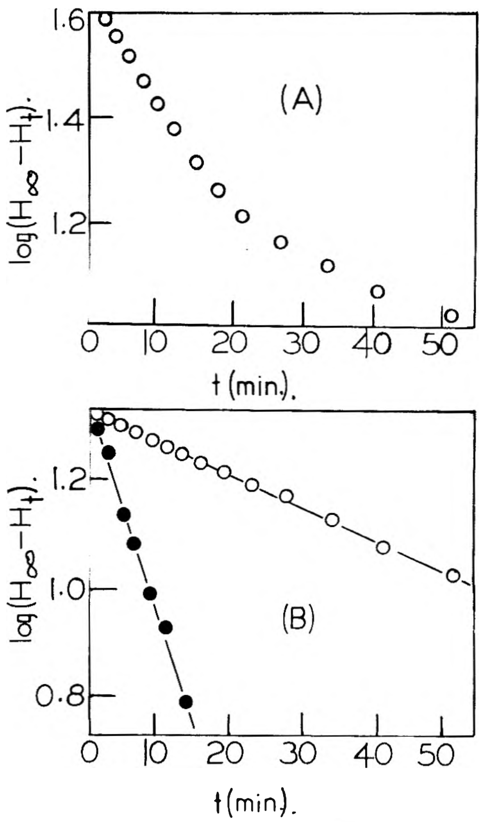

Fig. 1.—Hydrogen exchange of *cis*-$Co(NH_3)_4(NO_2)_2^+$: (A) experimental data; (B) data analyzed for two parallel rates.

Unlike the hexammine results where the exchange rates are $Co(en)_3^{3+} > Co(NH_3)_6^{3+}$, data in Table I show that the relative rates for dinitro complexes are $Co(NH_3)_4(NO_2)_2^+ > Co(en)_2(NO_2)_2^+$. This can be explained in terms of solvation and inductive effects. Because of a cationic charge of one instead of three and because of possible intramolecular hydrogen bonding between ammine hydrogens and adjacent nitro oxygens, the solvation energies are smaller and make a lesser contribution to the hydrogen exchange rates in these systems. The rates of exchange then become more a function of the inductive effect of C_2H_4 and give results consistent with the acidities of NH_4^+ and $H_2NCH_2CH_2NH_3^+$.

Square Complexes.—Except for $X = Cl^-$, data in Table II show that the rates of hydrogen exchange decrease in the order $Pt(dien)X^+ > Pt(en)_2^{2+}$. This rather surprising result differs from those of the cobalt(III) ammines where the rate increases with increase in cationic charge. It is tempting to suggest that the behavior of platinum(II) is a result of its tendency to π-bond with X. Such a sharing of d-electrons of platinum(II) with vacant orbitals of X results in a lower electron density on platinum which may more than compensate for its smaller cationic charge. However palladium(II) is believed[13] to π-bond less than does platinum(II), thus this π-bonding hypothesis cannot be used to explain the much larger difference in rates of hydrogen exchange for palladium(II)

---

(11) F. Basolo and R. G. Pearson, "Mechanisms of Inorganic Reactions," John Wiley and Sons, Inc., New York, N. Y., 1958. Ch. 2.

(12) J. W. Palmer and F. Basolo, *J. Inorg. Nucl. Chem.*, in press.

(13) J. Chatt, L. A. Duncanson and L. M. Venanzi, *J. Chem. Soc.*, 3203 (1958).

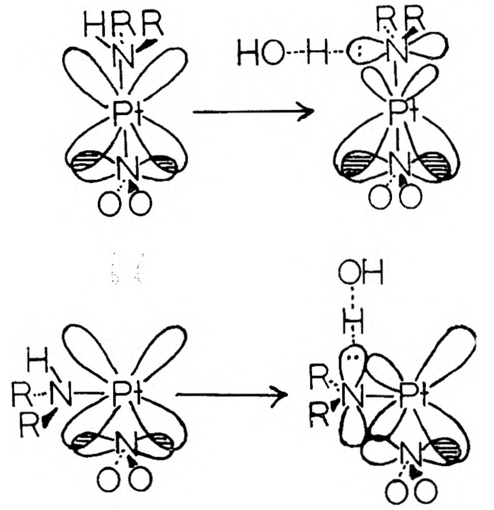

(A) *Trans*-Ammine

(B) *Cis*-Ammine

Fig. 2.—Delocalization of "amido" transition state p-electrons in (A) *trans* and (B) *cis* positions to X(NO_2^-).

complexes, *e.g.*, Pd(dien)$X^+ >$ Pd$(en)_2^{2+}$. One possible interpretation of these results is that solvation energy effects are an important factor in the hydrogen exchange rates of square metal ammines. As mentioned earlier this has the effect of retarding exchange because it stabilizes the ammine ground state with its larger positive charge to a greater extent than its "amido" transition state of smaller positive charge. Thus since the hydration energy of M(dien)X^+ is less than that of M$(en)_2^{2+}$, it follows that the retardation of hydrogen exchange due to solvation effects would be smaller in the univalent complex. Palladium(II) complexes are smaller in size and have a larger hydration energy than do platinum(II) complexes. This means that solvation effects will cause a larger difference in rates of hydrogen exchange of palladium(II) systems than in platinum(II) in agreement with the experimental results. It should also be noted that the exchange rate for univalent cationic cobalt(III) ammines is less than that for analogous divalent cations which indicates that solvation effects are less important in six-coördinated than in four-coördinated systems.

Table II

Rates of Hydrogen Exchange of Square Metal Ammines in 0.1 *M* $DC_2H_3O_2$–$C_2H_3O_2^-$ Buffer at 25°

Complex	$k \times 10^{-6}\ M^{-1}\ sec.^{-1}$	*trans k*/*cis k*
Pt$(en)_2^{2+}$	0.16	
Pt(dien)Cl^+	.15	1
Pt(dien)Br^+	.2 (6)[a]	30
Pt(dien)NO_2^+	1.4 (100)[a]	70
Pt(dien)I^+	2 (200)[a]	100
Pt(dien)SCN^+	3 (600)[a]	200
Pd$(en)_2^{2+}$	1.5	
Pd(dien)Br^+	400	
Pd(dien)NO_2^+	600	

[a] The values in parentheses are presumably for the hydrogen *trans* to X as discussed in the text.

The rates of exchange of Pt(dien)X^+ decrease in the order $SCN^- > I^- > NO_2^- \gg Br^- > Cl^-$ (Table II). This order is essentially the same as the decreasing order of the "*trans*" effect of these X groups.[14] Furthermore, except for X = Cl^-, plots of the hydrogen exchange data show considerable curvature indicating the non-equivalence of hydrogens in these systems. The rapid exchange corresponds to approximately 20% of the N–H hydrogens; in other words, to the H on the nitrogen *trans* to X. That the hydrogens of Pt(dien)Cl^+ all exchange at the same rate may be due to Cl^- and RNH_2 having comparable *trans* effects.

The polarization theory[15] for the *trans* effect requires a weakening of the Pt–A bond *trans* to X with increasing *trans* effect of X. Infrared studies on systems of the type X–Pt–NHR_2 were interpreted in support of this theory because it was found that the Pt–N stretching frequency decreases and the N–H stretching frequency increases with increasing *trans* effect of X.[16] Assuming that the infrared data are a measure of N–H bond strength, then it is seen that this does not correlate the N–H lability. The N–H lability may result from a stabilization of the "amido" transition state due to π-bonding of X with d-electrons of platinum(II). As shown in Fig. 2 this more effectively delocalizes the "amido" electrons on the nitrogen *trans* to X than those *cis*, which agrees with the observation that the *trans* hydrogens are the more labile.

The hydrogen exchange of Pd(dien)X^- is fast and only one rate was obtained for each complex (Table II). Unfortunately it is not known whether the *trans* hydrogens, as in the platinum(II) systems, exchange even more rapidly. On the basis of the π-bonding hypothesis to explain the *trans k*/*cis k* ratio of rates for Pt(dien)X^+ one expects smaller ratios for palladium(II) systems which are believed to π-bond much less. This view receives some support from the observation that the ratio of rates for Pd(dien)Br^+:Pd(dien)NO_2^+ are 1:1.5 compared to 1:7 for Pt(dien)Br^+:Pt(dien)NO_2^+. Presumably the large π-bonding tendency of NO_2^- compared to Br^- is more important in decreasing the electron density on platinum(II) than on palladium(II).

Acknowledgments.—We wish to thank Professor R. G. Pearson for his help with the discussion based on the crystal field theory. This investigation was supported by a National Science Foundation Grant (NSG-G5104).

---

(14) J. V. Quagliano and L. Schubert, *Chem. Revs.*, **50**, 201 (1952).

(15) A. A. Grinberg, *Acta Physicochim. U.R.S.S.*, **3**, 573 (1935).

(16) J. Chatt, L. A. Duncanson and L. M. Venanzi, *J. Chem. Soc.*, 4461 (1955); 2712 (1956); D. B. Powell, *ibid.*, 4495 (1956).

KINETICS OF THE CATALYTIC VAPOR PHASE OXIDATION OF PHTHALIC ANHYDRIDE

BY MACK F. HUGHES AND ROBERT T. ADAMS

California Research Corporation, Richmond, California

Received January 6, 1960

Oxidation of phthalic anhydride over vanadium oxide catalyst was studied between 497 and 575° in a flow system. The rate of oxidation was independent of the oxygen partial pressure above 0.1 atm. but varied with phthalic anhydride partial pressure in a manner similar to a unimolecular surface reaction. A possible reaction mechanism is: adsorption–desorption of phthalic anhydride, desorption of oxidized phthalic anhydride, and oxygen regeneration of the catalyst. Heat and entropy changes involved in some of these steps are given. Phthalic anhydride oxidation increased with decreasing oxygen pressure below 0.1 atm. This anomaly is explained by overreduction of the catalyst.

Introduction

The vapor phase oxidation of naphthalene or *o*-xylene on a vanadium oxide-type catalyst is an important commercial method for producing phthalic anhydride. Fundamental understanding of the reactions involved is of interest not only for optimizing this process, but also for the development of the general theory of heterogeneous oxidation.

It is well established[1–3] in naphthalene oxidation that phthalic anhydride is both a primary and secondary oxidation product, with most of the phthalic anhydride being formed directly from naphthalene. Consequently, the phthalic anhydride yield is dependent both on the catalyst selectivity and the phthalic anhydride stability toward oxidation. The present study of the vanadia-catalyzed oxidation of phthalic anhydride was undertaken to obtain kinetic data which could be used to interpret the reactions which produce the anhydride. The work is the initial phase of a larger program directed toward understanding the kinetics of *o*-xylene oxidation over fused vanadia.

A number of investigators have studied the oxidation of naphthalene[1–11] or *o*-xylene,[12,13] but the overoxidation of phthalic anhydride itself has been to a large degree ignored. Bhattacharyya and Gulati[13] oxidized phthalic anhydride over fused V_2O_5, and Brown and Frazer[4] used 9-molybdo-3-tungstosilicic acid; neither group studied the kinetics. Ioffe and Sherman[2,6] measured the temperature effect on the oxidation of the anhydride over a vanadium–potassium sulfate–silica gel catalyst at a single partial pressure of oxygen and phthalic anhydride. With the assumption of a first-order reaction with respect to phthalic anhydride, they obtained an activation energy of 26 kcal./g. mole in the range from 350 to 480°. D'Allesandro and Farkas[1] made the same first-order assumption and approximated the specific rate constant to fit their naphthalene data.

The role which oxygen plays in the catalytic reaction is strongly affected by catalyst composition and reaction conditions. Bhattacharyya and Gulati[13] found that xylene oxidation at 460° and above was independent of oxygen pressure in the region of 0.2 atm. Both Simard[12] and Cameron[14] and their co-workers demonstrated that the rate of adsorption or desorption of oxygen on vanadium oxide is affected by the presence of impurities. Simard, *et al.*, found that the rate of oxygen uptake by $V_2O_{4.34}$ was independent of oxygen pressure above pressures of 0.01 atm. Hughes and Hill[15] showed that the oxidation of carbon monoxide was independent of oxygen pressure as low as 0.008 atm.

On the other hand, many investigators have concluded[5–7,11] that the rate-controlling step for naphthalene oxidation is the chemisorption of oxygen.

The present work shows that the oxidation of phthalic anhydride can be explained by a unimolecular surface reaction which is independent of oxygen pressure above 0.1 atm. Below 0.1 atm., decreasing the oxygen pressure results in faster rates of oxidation.

Experimental

Apparatus.—The published work on naphthalene and *o*-xylene oxidation consists in the main of studies made either with high temperature gradients in the reactor or with temperature control achieved by operating with very low reactant concentrations. In this work reaction rates were measured under essentially isothermal conditions, yet with reactant concentrations at levels practical for commercial operation.

The kinetic measurements were made in a flow system. The unit consisted of an air metering and preheating section, feed pump, reactor and product scrubbers.

The air flow was measured by an orifice flow meter, calibrated at operating conditions. The air was preheated to 300° before the feed was introduced.

The feed system consisted of a syringe displacement pump, heated feed reservoir, and injection capillary. The pump,

---

(1) A. F. D'Alessandro and A. Farkas, *J. Colloid Sci.*, **11**, 653 (1956).

(2) I. I. Ioffe and Yu. G. Sherman, *Zhur. Fiz. Khim.*, **29**, 692 (1955).

(3) V. P. Ushakova, G. P. Korneichuk and V. A. Roiter, *Ukrain. Khim. Zhur.*, **23**, 310 (1957).

(4) H. T. Brown and J. C. W. Frazer, *J. Am. Chem. Soc.*, **64**, 2917 (1942).

(5) P. H. Calderbank, *J. Applied Chem.*, **2**, 482 (1952).

(6) I. I. Ioffe and Yu. G. Sherman, *Zhur. Fiz. Khim.*, **28**, 2095 (1954).

(7) P. Mars and D. W. van Krevelin, *Special Supplement to Chem. Eng. Sci.*, **3**, 41 (1954).

(8) N. L. Franklin, P. H. Pinchbeck and F. Popper, *Trans. Instn. Chem. Engrs.*, **34**, 280 (1956).

(9) P. H. Pinchbeck, *Chem. Eng. Sci.*, **6**, 105 (1957).

(10) V. P. Ushakova, G. P. Korneichuk and Ya. V. Zhigailo, *Ukrain. Khim. Zhur.*, **23**, 191 (1957).

(11) N. L. Franklin, P. H. Pinchbeck and F. Popper, *Trans. Instn. Chem. Engrs.*, **36**, 259 (1958).

(12) G. L. Simard, J. F. Steger, R. J. Arnott and L. A. Siegel, *Ind. Eng. Chem.*, **47**, 1424 (1955).

(13) S. K. Bhattacharyya and I. B. Gulati, *Ind. Eng. Chem.*, **50**, 1719 (1958).

(14) W. C. Cameron, A. Farkas and L. M. Litz, THIS JOURNAL, **57**, 229 (1953).

(15) M. F. Hughes and G. R. Hill, *ibid.*, **59**, 388 (1955).

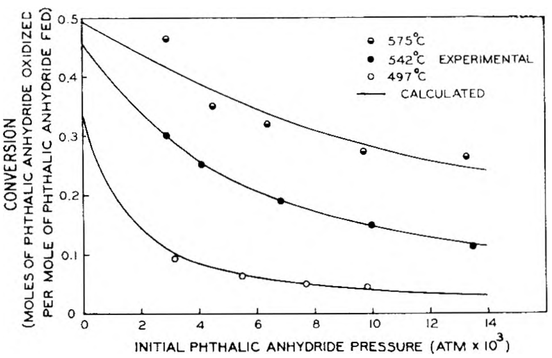

Fig. 1.—Phthalic anhydride oxidation over vanadia catalyst.

a syringe plunger driven by a synchronous motor, had a capacity of 0.005–0.150 ml./min. Mercury was pumped from the syringe to the feed reservoir. Molten phthalic anhydride, displaced by the mercury, was forced through the injection capillary into the hot air stream and vaporized. The feed system was jacketed and heated with circulating oil maintained at constant temperature ± 0.05°.

The reactor consisted of a preheating coil and a reaction chamber. The preheating coil was 7 mm. Pyrex tubing, 55 cm. long; this was sufficient to heat the reactants from 300° to the reaction temperature. The reaction chamber was a Pyrex rectangular parallelepiped (0.7 cm. × 1.5 cm. × 7 cm.) with a thickness of twice the diameter of the catalyst pellets. At the base of the chamber was a fritted glass plate which supported the catalyst and evenly dispersed the reactants. Temperature was measured by a chromel–alumel thermocouple suspended in the catalyst bed.

The entire reactor was heated by a bath of molten alloy, American Smelting and Refining Company No. 158–194. The bath temperature was controlled to ± 1°.

Isothermal conditions were not completely attained in the catalyst bed with this reactor design, but temperature gradients were small. In the runs at the lower temperatures no difference was observed between the bed temperature and the bath. In the most severe case (575° and 13.3×10^{-3} atm. phthalic anhydride partial pressure) the maximum temperature variation observed in the catalyst bed was 10°. The average temperature of the bed was taken as the reaction temperature.

Reactants.—Phthalic anhydride supplied by the Oronite Chemical Company was used as feed without further treatment. Its melting point was 130.9°. Air was the source of oxygen, and it was cleaned by passing it over Drierite and Ascarite. The flow rate was adjusted to give about 0.1 second contact time based on the catalyst void volume and the flow rate of the reactant mixture corrected to the temperature and pressure of the reaction chamber. In those runs where oxygen pressure was varied, air and nitrogen were blended in the desired proportions.

Catalyst.—The catalyst, fused vanadia on silicon carbide, contained 14% V_2O_5 and was sized between 6- and 10-mesh sieves. Vanadium pentoxide was prepared by roasting technical grade (99+%) ammonium metavanadate supplied by Vanadium Corporation of America. The catalyst, a low area type, had a surface area less than 1 m.^{2}/g. In all runs a 6.5-g. catalyst charge was used, with a 2.4 ml. void volume.

Analysis.—The product stream was analyzed for phthalic anhydride, maleic anhydride, CO_2, CO, O_2 and inert gas. Phthalic and maleic anhydrides were removed from the product gases by scrubbing with water, and the scrubber liquor was analyzed polarographically.[16] In general, the polarographic analysis consisted of electroreducing phthalic and maleic acids against a standard calomel electrode in a solution buffered to *p*H 1.0 with sulfate and bisulfate. Under the specified conditions, the increase in current between −1.06 and −1.22 volts was proportional to the phthalic anhydride concentration. Similarly, maleic anhydride concentration was proportional to the increase in current in the region of the maleic acid half-wave potential (−0.61 volt). The accuracy of this method of analysis was within 1% at the 90% confidence level. Carbon dioxide, carbon monoxide, oxygen and nitrogen in the scrubbed gases were determined with a Fischer Precision Gas Analysis Unit. The total nitrogen in the product gases was used as a basis for calculating the oxygen consumed. The phthalic anhydride fed was calculated from the density and volume of phthalic anhydride displaced from the calibrated feed reservoir. In all runs the carbon balance was 93% or better.

Procedure.—For 30 minutes preceding a run, air and feed were passed over the catalyst at the desired rate and temperature for the experiment. This was found to be sufficient to bring the system to a steady-state condition before any rate measurements were made. A run was started by connecting the water scrubber into the system and terminated by disconnecting it. Throughout the run a fraction of the exit gases was collected in a gas sampling bulb.

Results

A simulated run was made at 575° without any catalyst to determine if oxidation other than that catalyzed by the vanadia occurred. In this run 98% of the phthalic anhydride was recovered unchanged; and no measurable amounts of the other products, maleic anhydride, CO_2 and CO were detected. In a similar experiment with a steel reactor of the same design, more than 15% of the phthalic anhydride was oxidized. It was for this reason that the reactor was made of Pyrex instead of a better thermal conductor such as steel.

To determine the effect of phthalic anhydride partial pressure on the catalytic oxidation of phthalic anhydride, a series of conversion isotherms was made at three different temperatures. Results of these studies are presented in Fig. 1. The conversions at 575° correspond to a contact time of 0.098 second, the 542° conversions to 0.102 second, and the 497° conversions to 0.108 second.

The plots of phthalic anhydride partial pressure *versus* conversion are typical of surface reactions where the rate-determining step involves one molecule of a single reactant, *i.e.*, the differential rate equation is

$$-\frac{dp}{dt} = \frac{Ap}{1 + Bp} \qquad (1)$$

Integration of eq. 1 and substituting conversion (x) for $(p_0 - p_t)/p_0$ gives conversion in terms of the initial phthalic anhydride partial pressure (p_0), time (t), and the rate constants A and B.

$$2.303 \log (1 - x) - Bp_0x = -At \qquad (2)$$

Values for A and B at 575, 542 and 497° were calculated from the experimental points by the method of least squares. These values are listed in Table I. The solid lines in Fig. 1, which agree with the experimental results, were calculated with equation 2 and the times and rate constants listed in Table I.

Table I

Experimental Rate Constants for the Oxidation of Phthalic Anhydride on a Vanadia Catalyst

Temp. (°C.)	Contact time (sec.)	A (sec.$^{-1}$)	B (atm.$^{-1}$)	A/B (atm. sec.$^{-1}$ $\times 10^3$)
575	0.098	6.9	120	58
542	.102	6.0	300	20
497	.108	3.8	900	4.2

The scatter of points at 575° is due probably to the temperature gradient which existed in these

---

[16] M. F. Hughes and R. P. Buck, unpublished work, "Polarographic Analysis of Phthalic and Maleic Anhydrides."

runs, thus making it difficult to define the reaction temperature as well as in the low conversion runs.

Figure 2 shows how maleic anhydride yield was affected by initial phthalic anhydride partial pressure and temperature. The yield increase observed with greater phthalic anhydride pressure probably is due to the larger number of phthalic anhydride molecules competing with maleic anhydride for the catalyst sites. The decrease in yield with increasing temperature indicates either maleic anhydride oxidation is more temperature dependent than phthalic anhydride or the selectivity shifts to favor maleic anhydride formation at the lower temperature.

Oxygen dependence at constant temperature, flow rate and initial phthalic anhydride partial pressure is given in Table II. The oxygen concentration was varied by changing the air–nitrogen ratio in the reactant mixture. The degree of accuracy in these runs was less than in the other work because of the inconsistency of the feed system.

TABLE II

PRODUCT DISTRIBUTION FROM PHTHALIC ANHYDRIDE OXIDATION AT 550°, 0.1 SEC., AND VARIOUS OXYGEN PRESSURES

Initial O_2 pressure, atm.	0.211	.0101	.0044	0.034
Phthalic anhydride oxidized, mole %	20	22	37	62
Phthalic anhydride converted to				
CO_2, mole %	49	47	57	78
CO, mole %	35	38	30	17
Maleic anhydride, mole %	10	12	10	4

Normally, one would expect the rate of oxidation to decrease[5–7,11] or at least remain constant as the oxygen pressure is reduced. In oxygen lean mixtures, however, vanadium is reduced to a lower oxide, thus producing a different catalyst.[12] This new catalyst greatly enhances phthalic anhydride oxidation and changes the product distribution, probably due to a change of mechanism.[10] The catalyst reduction was reversible to a high degree. Operating for 8 hours at 0.21 atm. of oxygen regenerated the catalyst almost to its original state of activity.

This phenomenon is similar to that found by Ushakova, *et al.*,[10] who observed that the selectivity of vanadium oxide in oxidizing naphthalene to phthalic anhydride was dependent upon the ratio of V_2O_4 to V_2O_5 in the catalyst. A 79% V_2O_4 and 21% V_2O_5 catalyst was very active for oxidizing naphthalene but the yield of phthalic anhydride was low because the catalyst had a high activity for oxidizing phthalic anhydride.

Discussion

A mechanism that accounts for the observed kinetic law, eq. 1, is

$$\text{PA} + (\text{VO}) \underset{k_{-1}}{\overset{k_1}{\rightleftarrows}} (\text{VOPA}) \qquad \text{(I)}$$

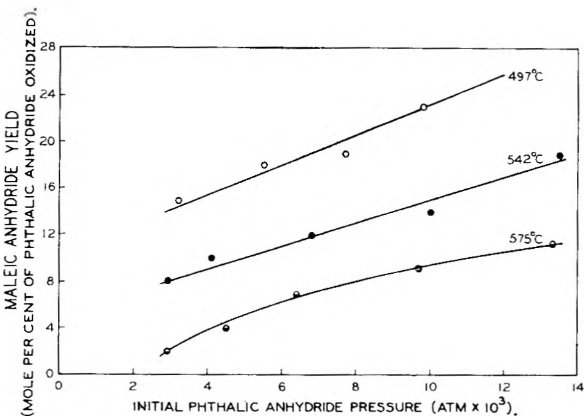

Fig. 2.—Maleic anhydride produced from phthalic anhydride oxidation.

$$(\text{VOPA}) \xrightarrow{k_2} (\text{V}) + \text{O-PA} \qquad \text{(II)}$$

$$(\text{V}) + O_2 \xrightarrow{\text{fast}} (\text{VO}) \qquad \text{(III)}$$

In these reactions the parentheses indicate surface species. VOPA is produced by the adsorption of phthalic anhydride on a potentially active surface site, VO. V is a surface site deficient in oxygen due to the desorption of oxidized phthalic anhydride, O-PA. The constants, k_1, k_{-1} and k_2, are specific reaction rate constants for adsorption and desorption of phthalic anhydride and desorption of oxidized phthalic anhydride, respectively.

According to this mechanism, the rate of phthalic anhydride oxidation is proportional to the concentration of the VOPA species. Hence

$$-\frac{dp}{dt} = k_2k'\theta \qquad (3)$$

where θ is the fraction of the surface occupied by VOPA species and k' is a conversion factor for changing the fraction of the surface covered to the true surface concentration.

In order to obtain an expression for θ which can be determined experimentally, the steady-state treatment was used. Assuming that Reaction III is very fast, the steady-state expression for θ becomes

$$\frac{d\theta}{dt} = k_1(1 - \theta)p - k_{-1}\theta - k_2\theta = 0 \qquad (4)$$

where $(1 - \theta)$ is the fraction of the potentially active surface covered by VO species. Rearranging eq. 4 and making one further assumption—that the rate constants are independent of θ—the expression for θ becomes

$$\theta = \frac{k_1p}{k_{-1} + k_2 + k_1p} \qquad (5)$$

Therefore, the rate law for the oxidation of phthalic anhydride is

$$-\frac{dp}{dt} = \frac{\dfrac{k_1k_2k'}{k_{-1} + k_2}p}{1 + \dfrac{k_1p}{k_{-1} + k_2}} \qquad (6)$$

which is of the same form as eq. 1, with A equal to $k_1k_2k'/k_{-1}+k_2$, B equal to $k_1/k_{-1}+k_2$, and A/B equal to k_2k'.

The logarithms of A, B and A/B are linear functions of $1/T$. From the change of A/B with temperature, ΔH_2^*, the heat of activation for the desorption of oxidized phthalic anhydride, was found to be 44 kcal./g. mole.

To interpret the thermodynamic significance of the variation of A and B with temperature, it is of interest to consider two limiting cases, *viz.*, when $k_{-1} = 0$ and when $k_{-1} >> k_2$. When k_{-1} is zero, reaction I is irreversible, and eq. 6 reduces to

$$-\frac{dp}{dt} = \frac{k_1k'p}{1 + \left(\frac{k_1}{k_2}\right)p} \qquad (7)$$

The second limiting case ($k_{-1} >> k_2$) requires that reaction I be an equilibrium adsorption. The rate law reduces to

$$-\frac{dp}{dt} = \frac{k_2k'Kp}{1 + Kp} \qquad (8)$$

where $K = k_1/k_{-1}$. It is evident that for this case the experimental rate constant B is equal to K, the adsorption equilibrium constant for reaction I. The temperature coefficient of K is a measure of the heat of adsorption. From the thermodynamic relationship between K, ΔF, ΔH and ΔS for equilibrium processes, the entropy change for the reversible adsorption can be calculated.

The thermodynamic quantities derived from the experimental rate constants are summarized in Table III. No choice can be made at this time between the postulates of irreversible adsorption of phthalic anhydride or an equilibrium adsorption; the thermodynamic values are quite reasonable for either process. Even if the adsorption is reversible but not at equilibrium, it is likely that the heat of activation (ΔH_1^*) and the heat of adsorption (ΔH_1) for phthalic anhydride adsorption are not far different from the values calculated in the limiting cases.

As a consequence of the proposed mechanism, the identity, $A/B \equiv k_2k'$, is independent of the precise nature of the adsorption step. It is of interest to estimate the magnitude of k' by substituting for k_2 in eq. 3 an expression derived from the absolute reaction rate theory[17]

$$\text{rate} = \kappa \frac{kT}{h} k'\theta e^{-\Delta H_2^{\ddagger}/RT} e^{\Delta S_2^{\ddagger}/R} \qquad (9)$$

where κ is the transmission coefficient, and k and h are Boltzmann's and Planck's constants, respectively. The value for the entropy of activation (ΔS_2^*) for the desorption of oxidized phthalic anhydride should be quite small, because it represents the entropy change in going from an adsorbed molecule to an activated complex on the surface. For the purpose of this semi-quantitative analysis, it will be assumed that ΔS_2^* is zero.

TABLE III

THERMODYNAMIC QUANTITIES DERIVED FROM THE EXPERIMENTAL RATE CONSTANTS A AND B

Irreversible adsorptn. of phthalic anhydride followed by desorptn. of oxidn. products	Equilibrium adsorptn. of phthalic anhydride followed by slow desorptn. of oxidn. products
$A = k_1k'$ $A/B = k_2k'$	$B = K = k_1/k_{-1}$
$\Delta H_1^* = 11$ kcal./g. mole	$A/B = k_2k'$
$\Delta H_2^* = 44$ kcal./g. mole	$\Delta H_1 = -33$ kcal./g. mole
	$\Delta S_1 = -29$ cal./(g. mole) (°C.)
	$\Delta H_2^{\ddagger} = 44$ kcal./g. mole

At $T = 815$°K. (542°), when θ was 0.5 the rate was 1.5×10^{-3} atm./(g)(sec.) [5.4×10^{-8} g. mole/(g)(sec.)]. Assuming that κ had a value of unity, k' was found to be 10^{15} molecules per gram of catalyst. The catalyst had an area of about 1 square meter per gram, so that k' was about 10^{11} molecules per square cm. Aebi[18] found that the O–O distance was essentially the same in V_2O_5 and $V_2O_{4.34}$ and that the O–O distance along the octahedron edges of $V_2O_{4.34}$ was 2.7 to 3.3 Å. Assuming all the oxygen atoms on the surface to be this distance apart, the surface would have approximately 10^{15} oxygen sites per square cm. This would suggest that 1/10,000 of the surface oxygens were covered, a result which is reasonable in magnitude.

Tests of other kinetic models were made in an effort to fit the experimental results. If the regeneration of the catalyst (reaction III) were a slow step, the rate law would show a dependence on oxygen pressure. Experimentally, the rate was independent of oxygen pressure in the region where the kinetic data were measured.

Acknowledgment.—The authors wish to acknowledge the help of Mr. T. B. Robertson who did much of the experimental work.

---

[17] S. Glasstone, K. J. Laidler and H. Eyring, "The Theory of Rate Processes," McGraw-Hill Book Co., Inc. New York, N. Y., 1941, p. 196.

[18] F. Aebi *Helv. Chim. Acta*, **31**, 8 (1948).

THE REACTION OF HOT HYDROGEN ATOMS WITH CARBOXYLIC ACIDS[1]

BY ALI M. ELATRASH,[2] RUSSELL H. JOHNSEN AND RICHARD WOLFGANG

Chemistry Department, Florida State University, Tallahassee, Florida

Received January 11, 1960

The reaction of hot hydrogen atoms with a number of liquid carboxylic acids has been studied. Recoil tritium from the nuclear reaction $Li^6(n,\alpha)H^3$ was used as the source of the hot hydrogen. Labeled hydrogen (HT), tritium labeled parent acid, CH_3T and other labeled degradation products which may be formed by the replacement of an atom or group by a tritium atom account for nearly the entire yield. These products are, with the exception of HT, insensitive to the presence of I_2 as a radical scavenger. This suggests that the primary reaction of hot atoms in the gas phase—a high-energy fast displacement mechanism—is also operative in the liquid phase. The distribution of products reveals that a hot displacement reaction may take place at any type of bond and that its probability is proportional to the number of bonds of that type. Several trends among these competitive modes of displacement attack emerge clearly: *e.g.*, attack on C–H is more likely than on C–C; attack on C–H yields more HT than labeled acid, especially with secondary C–H bonds; etc. The stability of a labeled species toward dissociation due to excitation introduced by the displacement reaction, has a detectable effect on the yield pattern. Comparison with data on hot hydrogen reactions with gaseous hydrocarbons suggests that the same simple mechanistic model of the hot displacement process is applicable to both phases.

Introduction

Recoil tritium from the nuclear reactions $Li^6(n,\alpha)H^3$ and $He^3(n, p)H^3$ has been used as a source of high kinetic energy hydrogen atoms to study the properties of that species. The kinetics of its reaction in the gas phase have been determined.[3-5] The chief mechanism of the reaction of such hot hydrogen atoms with gaseous hydrocarbons appears to be a direct displacement reaction. In systems such as $T + CH_4$ it was found that a large fraction (about 70%) of the tritium atoms participate in a displacement reaction by virtue of their high kinetic energy to form HT, CH_3T and CH_2T. The remainder lose their excess energy by collision and then undergo thermal reactions.

The reactions of "hot" tritium atoms have also been investigated in condensed phases such as solid glucose,[6,7] liquid methyl alcohol, ethyl alcohol and acetone.[8] The results of these studies also suggest a mechanism in which a hot hydrogen atom displaces an atom or a group in a one-step reaction to produce the labeled parent compound.

In the present work we have extended the investigation of hot hydrogen atom reactions to a homologous series of carboxylic acids, including the following: acetic, propionic, *n*-butyric, isobutyric, *n*-valeric, isovaleric, *t*-valeric(pivalic), *n*-hexoic, and isohexoic. The nuclear reaction $Li^6(n,\alpha)H^3$ was used as the source of the hot tritium atoms. The immediate purpose of the work was: (1) to survey reactions in the liquid phase and compare them with those in the gas phase; (2) to determine the validity of a fast, localized direct displacement mechanism *vs.* other possible mechanisms in which an intermediate well-defined transition complex, with an equilibrium distribution of energy in its various degrees of freedom, decays in a statistically determined manner to give the various products; (3) to study the mechanism of the various competitive modes of the direct displacement process.

Experimental

Materials.—All the acids used in this work were pure reagent grade and were further purified by fractional distillation (except pivalic acid) in a 60 cm. column packed with $^3/_{16}''$ Pyrex helices. Center cuts having a boiling range of less than 0.2° were used. Pivalic acid was prepared by a standard method,[9] and was purified by fractional crystallization.

Sample Preparation and Irradiation.—Solutions of anhydrous lithium chloride in the various acids were prepared in a dry box[10] having at room temperature a relative humidity not greater than 5%. The concentration of these solutions ranged from 4% by weight for acetic and propionic acids, 2% for butyric acids to 1% for valeric and hexoic acids.

To prepare iodine containing solutions, ten milliliter fractions of the acid–lithium chloride solutions were transferred to a volumetric flask and the amount of iodine required to make the necessary concentration was added. Solutions of different iodine concentrations were prepared for acetic acid, ranging from 2.4×10^{-4} *M* to 1.4×10^{-2} *M*. For the remaining acids solutions 5×10^{-3} *M* in iodine were prepared.

Quartz ampoules of about 10 mm. o.d. and 10 cm. long with a breakoff seal were used for irradiation. All samples were thoroughly degassed by repeated freezing, pumping and thawing. They were then irradiated in the Brookhaven Laboratory graphite reactor using the water-cooled facility. In order to produce the same number of tritons, solutions of different concentrations in LiCl were irradiated for varying lengths of time. The 4% solutions were irradiated for one hour, the 2% for two hours and the 1% for four hours. Some of the samples were irradiated at a flux of $\sim 1.7 \times 10^{12}$ n/cm.^{2}/sec., while others at a flux of $\sim 3.9 \times 10^{12}$ n/cm.^{2}/sec. In order to determine the flux to which each group of samples was subjected, a solution of LiCl in water was irradiated with each group and the activity of the water sample was used as a monitor for the neutron flux.

Tritium Assay: Gaseous Products.—After irradiation, samples were opened in a vacuum system and cooled with an ordinary ice trap. Thus only those contituents which have a reasonably high vapor pressure at 0° were determined. The radioassay of the gaseous activity was made by a gas chromatographic method described by Wolfgang and Rowland.[11] An aliquot of the sample was injected into a stream of helium passing through a chromatograph column. After separation the gas stream passed through a thermal conductivity cell which detected and recorded any macroscopic amounts of material. The helium was then converted into a counter gas by continuous injection of methane and flowed through an internal flow proportional counter. The

---

[1] This work was supported in part by the U. S. Atomic Energy Commission under Contract AT-(40-1)-2001 and in part by the FSU Research Council.

[2] Abstracted from a thesis submitted by A. M. Elatrash in partial fulfillment of the requirements for the degree of Doctor of Philosophy.

[3] P. J. Estrup and R. Wolfgang, *J. Am. Chem. Soc.*, **82**, 2661 (1960).

[4] M. Amr ElSayed and R. Wolfgang, *ibid.*, **79**, 3286 (1957).

[5] M. Amr ElSayed and R. Wolfgang, THIS JOURNAL, **62**, 1356 (1958).

[6] F. S. Rowland, C. P. Turton and R. Wolfgang, *J. Am. Chem. Soc.*, **78**, 2354 (1956).

[7] H. Keller and F. S. Rowland, THIS JOURNAL, **62**, 1373 (1958).

[8] W. J. Hoff, Jr., and F. S. Rowland, *J. Am. Chem. Soc.*, **79**, 4867 (1957).

[9] H. Gilman and A. H. Blatt, "Organic Syntheses," Vol. 1, Second Ed., John Wiley and Sons, Inc., New York, N. Y., 1948, pp. 144, 521.

[10] R. E. Johnson, *J. Chem. Educ.*, **34**, 80 (1957).

[11] R. Wolfgang and F. S. Rowland, *Anal. Chem.*, **30**, 903 (1958).

TABLE I

EFFECT OF SOME EXPERIMENTAL PARAMETERS ON INCORPORATION OF HOT HYDROGEN IN ACETIC ACID

Run no.	Irrad. conditions	Flux × 10^{-12} (n/cm.^{2}/sec.)	LiCl concn., %	Time of irrad., hr.	% Tot. T in liq.	C-T Act. in parent acid (c.p.m./mg.) × 10^{-3}	% Tot. T as C-T in parent acid
8	No air present	1.7	4	1	53	4.0	18
1	Air pres.	1.7	4	1	54	4.0	18
22	No air pres.	3.9	2	2	58	10.5	19
19	Air pres.	3.9	2	2	58	10.6	19
4	11% H_2O added	1.7	4	1	61	3.3	17
16	5×10^{-3} M I_2	1.7	4	1	53	4.0	18

radioactivity detected was fed into an integrating scaler and a recording rate-meter. An 11-foot silica-gel column was used to separate the hydrocarbons. The column was operated at temperatures ranging from 25 to 110° in order to elute such higher hydrocarbons as the pentanes. Relative retention volumes of the various fractions were determined at the various operating temperatures by injecting small amounts of the unlabeled gases.

Tritium Assay: Liquid and Solid Compounds.—Samples were converted to gas by the method of Wilzbach, Kaplan and Brown.[12] A standard aliquot of the resulting methane–hydrogen mixture was introduced into a silver-walled gas proportional counter with an active volume of 85 cc. The counter filling was completed with 90% argon–10% methane mixture to about atmospheric pressure. The measurements were reproducible to approximately 1%. The over-all accuracy of the assay is about 5%.

Tritium Assay: Water Samples.—Ampoules containing irradiated water were opened in a vacuum system and cooled with liquid air. The gas (HT) was transferred to the glass proportional counter and counted to give the total gaseous activity. The activity in the liquid water was assayed by the reduction method described earlier.

Preparation of the Acid Derivatives.—In order to purify and separate the parent acid from other decomposition products, a solid derivative (the *p*-toluidide) which is readily purified by crystallization, was prepared. This procedure obviously limits assay of the tritium activity to the nonlabile positions only.

The acid chloride was prepared in each case using benzoyl chloride except for C_6-acids where thionyl chloride was used. The acid chloride in anhydrous ethyl ether was then added to a solution of *p*-toluidine in the same solvent. After washing the ether solution with dilute HCl, saturated $NaHCO_3$ solution and water, it was dried over anhydrous Na_2SO_4. The ether was evaporated and the derivative recrystallized from benzene and petroleum ether. Recrystallization was repeated to a constant melting point and then to a constant specific activity.

Errors were incurred mainly in the separation and counting procedures. The probable error in the determinations of the major products is estimated to be about 5% of the activity, and that of the minor ones correspondingly larger. Values obtained by subtraction as in Table V will of course have correspondingly higher deviations.

Results

Table I shows the effect of several variables on the per cent. entry of recoil tritium in liquid acetic acid. It is observed that the flux, the presence of oxygen or iodine, both of which act as radical scavengers, and also the presence of small amounts of water have no effect on the yield of the parent acid. Similar results were observed for the other acids investigated.

The distribution of activity among the various types of labeled products formed in the absence of I_2 is shown in Table II. The percentages listed are those of the total calculated activity using water as a monitor for the neutron flux. Column 2 lists the activity of the gross liquid before the separation of the parent acid as the *p*-toluidide. Column 4, which is the difference between column 2 and column 3, represents the activity in the form of –O–T and in other liquid decomposition products. The per cent. total activity in the gas was computed by subtracting the per cent. total activity found in the liquid (column 2) from the total produced as determined using the water monitors.

TABLE II

CHEMICAL STATE OF RECOIL T PRODUCED IN LIQUID CARBOXYLIC ACIDS (I_2 ABSENT)

	% Total calculated activity in:							
Acid irradiated	Liquid	Parent acid	Labile and[a] other liq. products	Gas[b]	HT	CH_3T	H.C.A.[c]	Other gaseous product
Acetic	53	18	35	47	33	13	CH_3T	1.0
Propionic	46	22	24	54	43	2.1	7.5	2.4
n-Butyric	43	27	16	57	49	2.6	3.7	1.7
i-Butyric	44	26	18	56	47	4.7	3.3	1.0
n-Valeric	28	20	8	72	65	2.0	2.2	2.8
i-Valeric	44	33	11	56	48	4.5	2.1	1.4
t-Valeric	40	20	20	60	43	9.6	6.8	0.6
n-Hexoic	50	27	23	50	46	1.3	0.9	1.8
i-Hexoic	61	33	28	39	34	2.8	0.8	1.4

[a] Values in this column obtained by subtracting values of column 3 from those in column 2. [b] Per cent. gas is obtained by subtracting per cent. liquid from 100. [c] (H.C.-A.) stands for "The Hydrocarbon of the Parent Acid," *i.e.*, CH_4 from acetic, C_2H_5 from propionic, etc.

The effect of variation in iodine concentration for the case of acetic acid is shown in Table III. It is noted that at iodine concentrations below 10^{-4} M, no effect on the distribution of activity among the different gaseous products was observed. However, at higher concentrations of iodine, the yields of hydrocarbons higher than CH_4 are reduced but not completely eliminated. Even at concentrations as high as 10^{-2} M in iodine, where iodine was still in excess after irradiation, a considerable amount of labeled ethane was observed. The yield of the labeled parent acid is not affected by iodine.

Table IV shows the radioactive gaseous products produced by the interaction of recoil tritium with other pure carboxylic acids. The percentages listed are calculated by normalizing the sum of the activities of all the gases to 100. In Table V are shown the products obtained in the presence of iodine. In cases where iodine was added, the percentage yields are not based on the total observed activity as is the case in the iodine-free run. Instead, these yields were computed on the basis of the total activity observed in identical control runs in which no iodine was present. This was done because in the presence of iodine labeled iodides, es-

---

[12] K. Wilzbach, L. Kaplan and W. G. Brown, *Science*, **118**, 522 (1953).

TABLE III

EFFECT OF I_2 CONCENTRATION ON THE YIELDS OF PRODUCTS FROM ACETIC ACID

Run no.	I_2 concn., M	Measd. activity in an aliquot of gas, counts	% of Measured activity in[a]: H_2	CH_4	C_2H_6	C_2H_4	C_2H_2	C_3H_8	% Tot. T[b] as C-T in parent acid
8	0	156,600	70.3	27.5	1.4	0.40	0.22	0.16	18
10	1.3×10^{-4}	[c]	[c]	[c]	1.4	.42	.20	.21	17
13	1.3×10^{-3}	173,000	75.0	33.0	1.3	.30	.24	.19	19
16	5×10^{-3}	164,500	72.0	31.6	0.96	.15	.22	.08	18
17	1.4×10^{-2}		72.0	27.8	1.1	[c]	[c]	[c]	18

[a] Per cent. listed in I_2 runs are computed on the basis of the total measured gaseous activity in runs where iodine was absent (*i.e.*, run No. 8). [b] Per cent. listed is that of the total calculated activity. [c] Not determined.

TABLE IV

ACTIVE GASEOUS PRODUCTS FROM REACTION OF RECOIL T WITH LIQUID ALIPHATIC ACIDS (I_2 ABSENT)

Tritiated product	Acid irradiated, %[a]: Acetic	Propionic	Butyric *n*	Butyric *i*	Valeric *n*	Valeric *i*	Valeric *t*	Hexoic *n*	Hexoic *i*
Hydrogen	70.3	78	85.6	83.6	91.0	86.0	71.0	92.0	88.0
Methane	27.5	3.9	4.5	8.4	2.7	7.9	16.0	2.6	7.3
Ethane	1.4	13.6	2.1	0.2	1.4	0.8	0.2	1.3	0.3
Ethylene	0.4	1.5	0.6	.3	0.4	.2	.1	0.2	.2
Acetylene	.22	1.5	0.2	.2	.1	.1	.2	.1	.1
Propane	.16	0.4	6.5	5.9	.9	.9	.1	.9	.9
Propylene	...	..	0.6	1.4	.2	.5	.4	.07	.3
i-Butane	...	..	..	0.2	..	2.4	11.0	..	.9
n-Butane	...	1.1	0.1	..	3.0	1.4	0.1	.6	.1
Butylene	...	..	..	..	..	..	0.3	..	..
i-Pentane	...	..	..	..	..	0.3	..	..	1.9
n-Pentane	...	0.1	..	..	0.2	..	..	1.7	..

[a] % listed is % of observed gaseous activity; .. undetectable amounts.

TABLE V

ACTIVE GASEOUS PRODUCTS FROM REACTION OF RECOIL T WITH LIQUID ALIPHATIC ACIDS (I_2 PRESENT, 5×10^{-3} M)

Tritiated product	Acid irradiated %[a]: Acetic	Propionic[b]	Butyric *n*	Butyric *i*	Valeric *n*	Valeric *i*	Valeric *t*	Hexoic *n*	Hexoic *i*
Hydrogen	72.0	73	78.9	71.9	83	78	68	86	79
Methane	31.6	3.8	4.4	8.4	2.8	7.7	16	2.55	7.4
Ethane	0.96	13.5	1.9	0.2	1.3	0.7	0.19	1.3	0.3
Ethylene	0.15	1.3	0.6	.3	0.4	.2	.1	0.2	.2
Acetylene	0.22	1.5	0.2	.2	0.1	.1	.2	0.1	.1
Propane	0.08	0.1	6.6	6.0	1.0	.8	.1	1.0	.8
Propylene	...	..	0.6	1.4	0.2	.4	.4	0.06	.3
i-Butane	...	..	...	0.07	...	2.4	11.2	...	1.0
n-Butane	...	0.4	0.04	...	3.1	1.5	0.1	0.6	0.08
Butylene	...	..	...	...	...	...	0.3	...	...
i-Pentane	...	..	...	...	...	0.15	...	...	2.1
n-Pentane	...	..	...	...	0.08	...	...	1.7	...

[a] % listed is computed from the observed activity in identical control runs where I_2 is absent. [b] The iodine concentration is 0.1 M. .. Undetectable amounts.

pecially TI, which would not be detected by the analytical method used, would be expected.

It is observed that in both cases a large percentage of the gaseous activity is in the form of HT and is relatively higher for the normal acid than for the corresponding iso-acid. It is also to be noted that the activity in CH_3T is about two to three times as great for the branched chain acid as for the normal acid with the same molecular weight.

In addition to hydrogen, methane and the hydrocarbon formed by decarboxylation of the parent acid (H.C.A.) are among the main gaseous products.

In the presence of iodine as a radical scavenger the production of labeled hydrocarbons higher than that of the parent acid, *i.e.*, "synthesis" products, is reduced but not completely eliminated. This is clearly demonstrated with propionic acid where I_2 concentrations were as high as 0.1 M. The hydrogen yield is slightly decreased. However, the yield of the labeled hydrocarbon of the parent acid (*e.g.*, methane from acetic, ethane from propionic, etc.) as well as the yield of other degradation products is unaffected within the experimental error.

Discussion

1. Hot *vs.* Thermal Reactions.—There are three experimental criteria for establishing that a reaction is caused by hot atoms. (1) Diminution of the yield of hot product by the addition of a large excess of moderator, *i.e.*, chemically inert substances such as helium which remove the excess kinetic energy from the hot atom. (2) Insensitivity of yield to temperature (since the hot atom provides essentially all the required activation energy). (3) Insensitivity of yield to small amounts of scavengers which react avidly with thermalized species. Most thermal reactions will be inhibited by such scavengers since the species causing them usually undergo many collisions before reacting and thus are liable to encounter and be trapped by the scavenger. Hot species are not sensitive to small amounts of scavenger since they must react in a few collisions, before losing their excess energy.

The hot displacement reaction mechanism of recoil tritium with gaseous substances has been established by all of these criteria.[4,5] In the liquid phase, however, the use of only the scavenger technique has been practical to this time. Thus the finding of Hoff and Rowland[8] that the products of reaction of recoil tritium with acetone and alcohol were insensitive to the presence of diphenylpicrylhydrazyl may be taken as evidence that the reactions proceeding were due to a hot mechanism. Similarly in this work, we find (Tables III, IV, and V) that the presence of 5×10^{-3} M I_2 eliminates only of the order of 10% of the gaseous products. (This 10% presumably forms T-labeled iodides which are not detected). Formation of the labeled form of the acid irradiated is apparently completely independent of the presence of either I_2 or O_2 as scavengers (Tables I and III).

Conversely, those (rather minor) products which are affected most by the presence of I_2 are all "synthesis" products which, since they contain more atoms than the original acid, cannot have been formed by direct hot reaction. These products, for instance C_2H_5T and C_3H_7T formed in the reaction with acetic acid (Table III) presumably were formed by interaction of thermal tritium with radiation produced species. Again, this is in complete analogy with gas phase systems.[4,5] However, in contrast to the gas phase situation these synthesis products are not entirely eliminated by scavenger—even I_2 at a concentration of 0.1 M (Table V). This residual yield—which corresponds to less than 1% of the recoil tritium—presumably is due to the combination of tritium just thermalized with a radical held in the same solvent cage. Such tritium will react before it can be reached by the scavenger.

The yield of HT is also somewhat affected by the presence of I_2. It appears that most of the tritium reaching thermal energies abstracts a hydrogen atom from a molecule of acid. This is the expected reaction for thermal hydrogen.[13]

2. Nature of the Hot Reaction.—For the hot reaction of hydrogen with saturated compounds in the gas phase a simple displacement mechanism in which the entering hydrogen replaces an atom or group has been postulated. This general mechanism also appears dominant for liquid acids since nearly all the observed products (99%) can be made by breaking a single bond and replacing the atom or group removed with tritium. The low yield of rearrangement or isomerization products (*e.g.*, see pentanes and butanes from hexoic acids and butanes from valeric acid) already has been remarked on and seems difficult to explain by any other mechanism. In particular, any mechanism involving an activated complex or transition state in which an equilibrium distribution of energy in the degrees of freedom is approached must be excluded.

3. Competitive Hot Displacement Reactions.—In a relatively complex molecule the hot displacement reaction can occur competitively at several different types of bonds, and the hot atom may combine with either of the entities on the two sides of the bond. We will examine here the relative importance of the various modes of hot displacement reaction.

To a first approximation the amount of a given product depends on the fraction of the total bonds, which on being broken in a hot displacement reaction can give that product. This is illustrated by Fig. 1 which shows that the ratio of HT to CH_3T is approximately proportional to the relative number of C–H and C–CH_3 bonds. The approximate constancy of the yields of the labeled form of the parent acid and of HT, particularly when corrected for the fraction of C–H bonds in the molecule also supports this generalization.

The observations just cited suggest that the concept of an approximately equal probability of attacking every bond in the molecule may have some limited validity. Obviously factors involving the structure and stability of the entities involved will cause deviations from this overly simple model. To determine the nature of such deviations it is instructive to compare actual experimental results with results calculated with the "equal probability" hypothesis of the hot displacement mechanism. In Table VI this is illustrated for n-hexoic acid. The first column has been calculated assuming equal probability of attack on each bond and that there is an equal chance that the tritium will join with the entity on each side of the bond.

The good qualitative agreement in Table VI strengthens the previous conclusion that nearly all products can be formed by simple replacement without rearrangement. In similar calculations for the other acids the qualitative experimental distributions follow equally well. However, the quantitative disagreement clearly shows deviations from the "equal probability" hypothesis. These deviations are summarized below with comments on their probable origin.

(a) In every case except one, the yield of HT is higher than that calculated by random attack, even when the thermal contribution is allowed for. (The exception, isohexoic acid, may be due to experimental error since the absolute values of gaseous activity are not accurate, being obtained by difference between liquid activity and total calculated activity.) Further, in most cases activity found in labile form and in liquid products other than the labeled parent acid is low. This indicates that attack on a C–H bond is relatively more probable than attack on any other. A similar conclusion may be drawn from results on reaction with gaseous ethane[4] and other hydrocarbons. Since the C–H bond is a relatively strong one its higher susceptibility must be ascribed to its greater ex-

---

[13] E. W. R. Steacie, "Atomic and Free Radical Reactions," 2nd ed., Reinhold Publ. Corp., New York, N. Y. 1954, p. 551.

posure to attack and to a greater ability to absorb the energy of and stop the hot hydrogen atom.

TABLE VI

RESULTS OF ATTACK OF HOT TRITIUM ON NORMAL HEXOIC ACID

Product	% total activity Calcd. on "equal probability" hypothesis	Exptl.
HT	32.6	46.0
CH_3T	2.6	1.3
C_2H_5T	2.6	0.6
C_3H_7T	2.6	.4
n-C_4H_9T	2.6	.3
i-C_4H_9T	0.0	.0
n-$C_5H_{11}T$	2.6	.9
i-$C_5H_{11}T$	0.0	.0
t-$C_5H_{11}T$	0.0	.0
Labeled parent acid	29.0	27.0
Labile T and other liquid products	26.0	23.0
Other products	0.0	0.2

(b) Attack on a C–H bond is more likely to yield HT than the labeled acid. Further, the yield of HT as a "hot" product is consistently higher with normal than with branched acids. Thus with *n*-valeric acid HT accounts for 65% of the total gas yield, while with isovaleric acid it represents 48% and with *t*-valeric acid 43%. Evidently HT is more likely to be formed with secondary than with primary C–H bonds. As a corollary to this, a higher yield of labeled parent compound would be expected when interaction is with primary C–H bonds. This was observed by Hoff and Rowland,[8] studying C_2H_5OH, who found that the specific activity per H atom was higher in the CH_3 moiety than in the CH_2. With the acids we would therefore expect a higher yield for the branched compounds and this is actually observed for isohexoic and isovaleric acid. However, the yield of labeled isobutyric acid is about the same as that of *n*-butyric acid and that of *t*-valeric acid as that of *n*-valeric acid (see below).

This variation in the ratio of HT to labeled parent was also observed in studies of hot hydrogen attack on gaseous hydrocarbons.[14] In the hydrocarbon study this trend was quantitatively predictable, on the basis that HT production followed attack along the axis of the C–H bond, while displacement of H to form the labeled parent followed attack by the T toward the carbon atom. Varying, but predictable, steric obstruction in different systems toward the latter type of attack, causes a variation in the yield ratio of HT to labeled parent which correlates approximately with the ratio of secondary to primary C–H bonds. The fact that the ratio of HT to labeled carboxylic acid follows a similar trend indicates that this model of the displacement process, in which the point and direction of impact of the hot atom primarily determines the course of the reaction, is applicable in liquid as well as gas phase.

The lower than expected yields of *t*-valeric and isobutyric acids may be explained in terms of an excitation mechanism. A hot displacement reaction by an incident hydrogen atom is likely to leave a certain residual excitation energy in the molecule. In *t*-valeric and isobutyric acids the carboxyl groups are attached to the carbon atom where branching occurs. Decarboxylation should therefore proceed more readily than with the other acids since the relatively stable tertiary and secondary radicals, respectively, are formed. Independent evidence for this view derives from the finding[15] that the G-value for the production of CO_2 from isobutyric acid irradiated with Co^{60} γ-rays is much greater than that for isovaleric, isohexoic and *n*-butyric acids irradiated under the same conditions.

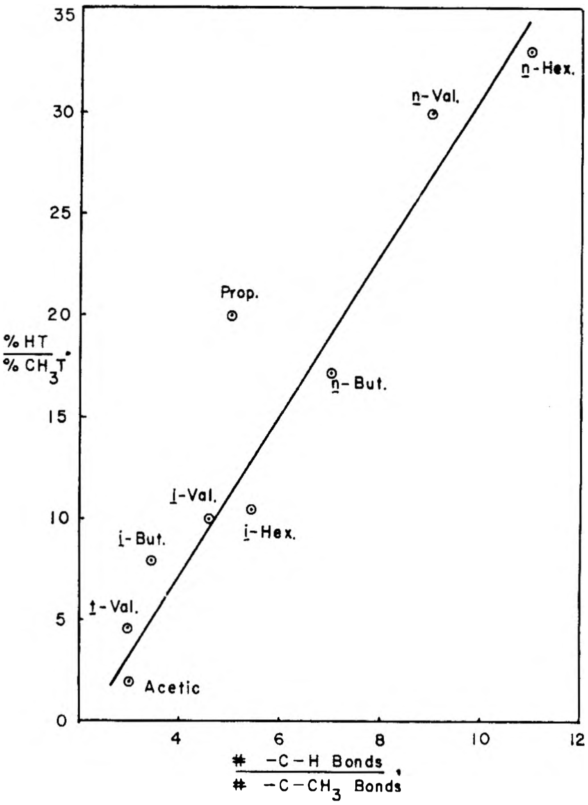

Fig. 1.—Relation between labeled products and the relative number of bonds which on rupture give rise to these products.

(c) Rupture of a C–C bond to form a gaseous hydrocarbon becomes progressively more likely as the end of the molecule away from the COOH group is approached. This conclusion is substantiated by the facts summarized in Table VII. (Products formed by the rupture of the C–COOH have not been included here.) This means that the probability that T attacks the 1st, 2nd, 3rd and 4th C–C bond from the CH_3-terminal of the chain to form labeled alkane is approximately 4:2:1.3:1.

Work on the reaction of hot tritium with a number of gaseous hydrocarbons[14] has shown that the position of the C–C bond does not greatly affect the probability of attack there. However, the same simple steric model that justifies this fact also predicts that the hot hydrogen is more likely to attack toward the sterically less obstructed side of the C–C bond. Thus, of the two possible products the smaller and less complicated is formed in greater

---

(14) D. Urch and R. Wolfgang, *J. Am. Chem. Soc.*, in press.

(15) R. H. Johnsen, THIS JOURNAL, **63**, 2041 (1959).

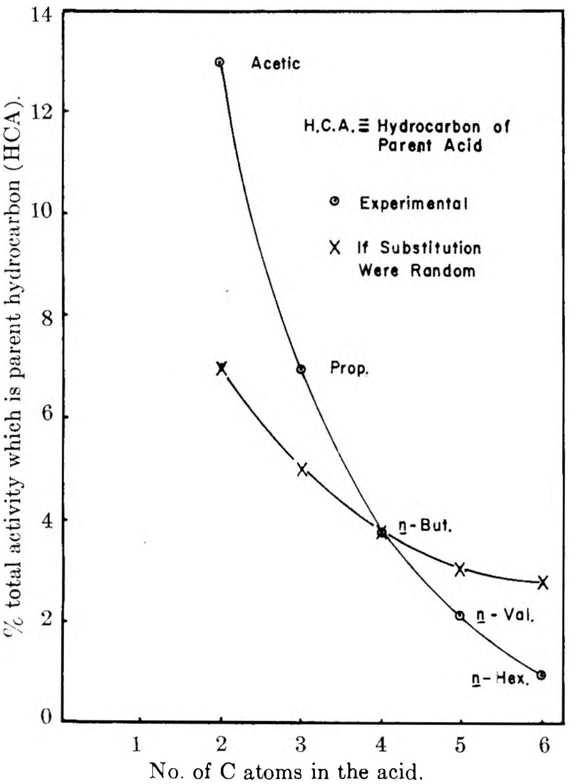

Fig. 2.—Yield of tritiated decarboxylation product from normal acids.

Table VII

Ratio of Terminal to Other C–C Bond Cleavage

Product ratio	*n*-Butyric	*n*-Valeric	*n*-Hexoic
$\frac{CH_3T}{C_2H_5T}$ =	$\frac{4.4}{2}$	$\frac{2.8}{1.4}$	$\frac{2.6}{1.3} \approx 2$
$\frac{CH_3T}{C_3H_7T}$ =	..	$\frac{2.8}{0.9}$	$\frac{2.6}{0.9} \approx 3$
$\frac{CH_3T}{n\text{-}C_4H_9T}$ =	..	..	$\frac{2.6}{0.6} \approx 4$

yield (*e.g.*, attack on the C–C bond in neopentane yields eight times as much CH_3T as isobutane-T.)

The present data on the higher yields of small hydrocarbons from carboxylic acids may be similarly interpreted. This provides another indication that the basic hot hydrogen reaction mechanisms operating in the gas phase also apply in liquids.

(d) The yield of labeled hydrocarbons resulting from decarboxylation is relatively high, especially in the lower acids (Fig. 2). One explanation of this might be that the C–COOH bond is especially vulnerable to displacement by hot T atoms, although it is not a particularly weak bond. This does not appear to be the case since in the higher acid these yields become lower than predicted by the "equal probability" hypothesis. A more likely explanation is the one already used to account for the low yields of labeled *t*-valeric and isobutyric acids: namely that displacement reaction elsewhere in the molecule results in sufficient excitation energy to cause decarboxylation. As the size of the molecule increases, the excess energy will be dissipated through a large number of degrees of freedom. Thus insufficient energy will be localized at any particular bond to cause its rupture. Such an effect of chain length upon decomposition of an excited molecule is demonstrated by the decreasing yield of CO_2 with increasing chain length in higher fatty acids irradiated with α-particles and deuterons,[16] as well as in the γ-ray case.[15]

The hypothesis that decomposition of acid molecules excited during tritium displacement of H atoms, as well as direct displacement of the COOH group, contributes significantly to the yield of labeled hydrocarbon seems especially plausible since, as discussed previously, it also accounts for the irregularities in the yield of labeled acid. This explanation also accounts for the pattern of butane production from the three valeric acids. The ready decarboxylation of *t*-valeric acid to a relatively stable tertiary radical intermediate is in accordance with the threefold higher production of butane from this isomer. A similar excess of labeled propane production from isobutyric acid *vs.* *n*-butyric acid would also be expected, but was not observed.

(e) Small amounts (~1%) of unsaturated products are formed. These are probably an indirect result of displacement of two H atoms or groups (such as has been observed with methane[4,5] and other hydrocarbons[14]) to form labeled radicals. In gaseous hydrocarbons such tritiated radicals undergo decomposition without rearrangement to form a smaller radical and a labeled alkene.[14,17] A similar process is to be expected for carboxylic acids.

Only a very tiny fraction of the yield, the saturated isomerization products and acetylene, amounting to a few tenths of a per cent., cannot be accounted for by the simple displacement mechanism. (These products may be partially due to a small residue of unscavenged thermal T atoms reacting with radiation produced radicals in the same solvent cage (see section 1 of this discussion). There may be also occasional displacement processes in which sufficient energy is deposited in the molecule to cause further decomposition and rearrangement.)

Summary

(1) Hot hydrogen atoms react with liquid carboxylic acids by the same general mechanism found for gaseous alkanes, *i.e.*, by a high-energy local displacement of some atom or radical. This displacement process can assume a number of modes. As in the gas phase, the point and direction of impact of the hot atom on the acid molecule appear to be the primary factors in determining these modes and the products formed. This essentially steric or impact model is consistent with the findings summarized below.

(2) The probability of reaction of a given type of bond is proportional to the number of bonds of that type.

(3) Attack on a C–H bond is more probable than on a C–C bond.

(4) Attack on a C–H bond is more likely to yield

---

[16] W. P. Whitehead, C. Goodman and I. A. Berger, *J. chim. phys.*, **48**, 184 (1951).

[17] D. S. Urch and R. Wolfgang, *J. Am. Chem. Soc.*, **81**, 2025 (1959).

HT than labeled acid. This bias is most pronounced in acids containing a large proportion of primary H atoms.

(5) Attack on a C–C bond to form a labeled hydrocarbon is much more probable at the more exposed terminal C–C bonds.

(6) Excitation energy introduced during the displacement may cause decomposition of a labeled acid. This is particularly noticeable with acids which tend to decarboxylate readily.

THE EQUILIBRIUM $^{2}/_{3}\mathrm{Bi(l)} + {}^{1}/_{3}\mathrm{BiCl_3(g)} = \mathrm{BiCl(g)}$ AND THE THERMODYNAMIC PROPERTIES OF BiCl GAS[1]

By DANIEL CUBICCIOTTI

Stanford Research Institute, Menlo Park, California

Received January 12, 1960

The reaction $^{2}/_{3}\mathrm{Bi(l)} + {}^{1}/_{3}\mathrm{BiCl_3(g)} = \mathrm{BiCl(g)}$ was investigated by a transpiration technique in the range 600 to 700°. The stoichiometry of the reaction was checked both by varying the activity of the gaseous reactants and by comparing the measured entropy (18 e.u.) with a calculated value. The enthalpy change for the reaction was found to be 24 kcal., which led to a value of 7 kcal. per mole for the enthalpy of formation of BiCl, gas, at 25°.

Introduction

In the vapor over liquid Bi–$\mathrm{BiCl_3}$ mixtures there is evidence that some Bi species exists of lower valence than three. For example, one can observe the transport of Bi through a vapor phase containing $\mathrm{BiCl_3}$ under conditions in which the vapor pressure of Bi itself is much too small to be considered. Also, the existence of the gaseous diatomic molecule BiCl under certain conditions is known from spectroscopic observation.

The present paper is a report of work performed to determine the molecular species to be found in the vapor over Bi–$\mathrm{BiCl_3}$ mixtures and the equilibrium pressures of such species.

Experimental

The reaction of $\mathrm{BiCl_3}$ vapor with liquid Bi was studied in a type of transpiration experiment. $\mathrm{BiCl_3}$, carried in a $\mathrm{N_2}$ stream, was equilibrated with liquid Bi and the amount and over-all composition of the condensed vapor was determined. To obtain the greatest fraction of lower-valent Bi species in the vapor, the equilibrium between liquid Bi and relatively low pressures of $\mathrm{BiCl_3}$ was studied.

A stream of high purity $\mathrm{N_2}$ was dried by passage over silica gel at solid $\mathrm{CO_2}$ temperatures and deoxidized over Cu and Fe filings at 400°. It was then divided into two streams, whose relative flow rates could be controlled; one stream was passed over liquid $\mathrm{BiCl_3}$ at about 240° while the other bypassed the $\mathrm{BiCl_3}$ to rejoin the first $\mathrm{N_2}$ downstream. In that way a stream of $\mathrm{N_2}$ with a controllable pressure of $\mathrm{BiCl_3}$ was produced. This stream was bubbled successively through three small Vycor bubblers, each containing 3 to 4 g. of Bi at 600 to 700°. The stream was then passed out of the furnace through a collector tube in which the various Bi–Cl species condensed while the $\mathrm{N_2}$ was collected and determined in a constant pressure eudiometer. The condensed Bi–Cl sample was weighed and the Cl determined gravimetrically.

To determine whether equilibrium had been established the flow rate was more than doubled in several experiments and the resultant equilibrium constant checked for agreement. This may be seen in Table I by comparing the following pairs of experiments: at 601–602°, the 3rd and 4th, the 5th and 6th, the 7th and 8th; at 659°, the 5th and 6th.

In this type of flow experiment condensable material is carried out of the hot zone by diffusion as well as by the $\mathrm{N_2}$ stream. In order to calculate the pressures of condensable species correctly, the amount of material that reached the cold zone by diffusion must be subtracted from the total amount deposited. Therefore an auxiliary study of the rate of diffusion of the Bi–Cl species in the $\mathrm{N_2}$ stream was made by simply bypassing the Bi–Cl laden $\mathrm{N_2}$ stream around the mouth of a collector. In that way, material was deposited in the collector only by diffusion. Diffusion measurements were made over the entire range of temperatures of these experiments under varying pressures of Bi–Cl species. The results allowed a correction to be made for each transpiration experiment. In this correction it was assumed that the composition of the diffused material was the same as the equilibrium mixture.

Transpiration experiments were made at Bi temperatures from 600 to 700°. Below 600° the proportion of lower-valent Bi species was too small for convenient determination. The experimental $\mathrm{BiCl_3}$ pressure at each of the several temperatures was varied over a tenfold or greater range so that the stoichiometry of the equilibrium could be determined.

It should be noted that vapor pressure[2] of Bi in the temperature range studied was too small to influence the results. At 700° its vapor pressure is about 10^{-2} mm. and that of the lower-valent Bi species a few mm. At 600° the Bi pressure is about 10^{-3} mm. and that of the lower-valent species about one mm.

The $\mathrm{BiCl_3}$ used was dried by vigorous boiling and doubly distilled in an $\mathrm{N_2}$ stream. The Bi used was Johnson–Matthey's "specpure" grade.

Results

Equilibrium Constants.—The measured quantities, pertinent to the equilibrium under study, were the moles of $\mathrm{N_2}$ passed, the weight of Bi–Cl species condensed, the weight of AgCl formed from the Bi–Cl sample, and a diffusion correction. From these one can calculate the partial pressures of the Bi–Cl species in the equilibrium gas, provided he has independent information of their molecular weights. It will be shown that there is no substantial contribution from species with more than one chlorine per molecule, thus excluding species with Bi oxidation number two. The presence of species with low oxidation numberr is also demonstrated by average oxidation numbers of the Bi in the transported gas of less than two. It is not possible to eliminate species such as $\mathrm{Bi_xCl}$ (*i.e.*, $\mathrm{Bi_2Cl}$, $\mathrm{Bi_3Cl}$) *a priori;* however, as will be seen, the agreement of the enthalpy and entropy of reaction observed in these experiments with those calculated from spectroscopic data for BiCl indicate that the contribution from such species must have been small.

---

[1] This work was made possible by the financial support of the Research Division of the United States Atomic Energy Commission.

[2] L. Brewer, "The Chemistry and Metallurgy of Miscellaneous Materials," NNES, IV-19B, McGraw-Hill Book Co., Inc., New York, N. Y., 1950, p. 31.

TABLE I

EXPERIMENTAL RESULTS AND EQUILIBRIUM CONSTANTS

Bi temp., °C.	Duration of expt., min.	Moles N_2 passed	Sample wt., g.	AgCl wt., g.	Amount[a] diffused, g.	p_{BiCl_3}, mm.	p_{BiCl}, mm.	K_1, mm.$^{2/3}$	K_2, mm.$^{1/3}$
602	1207	0.414	0.1349	0.1162	0.0034	0.273	0.638	0.98	0.75
602	986	.155	.0811	.0771	.0044	.57	.82	.99	.59
602	1093	.193	.1099	.1076	.0053	.66	.84	.96	.55
602	425	.145	.0858	.0843	.0020	.71	.89	1.00	.57
602	412	.130	.0868	.0857	.0022	.81	.98	1.05	.56
602	1145	.169	.1129	.1143	.0062	.85	.91	0.96	.51
602	980	.147	.1177	.1213	.0065	1.05	1.00	.98	.49
601	382	.125	.1022	.1065	.0025	1.13	1.03	.99	.48
602	317	.105	.0972	.1032	.0024	1.33	1.09	.99	.45
601	971	.143	.1527	.1672	.0085	1.60	1.10	.94	.40
601	328	.108	.1311	.1490	.0032	2.04	1.10	.87	.34
602	384	.0632	.0850	.0975	.0040	2.22	1.12	.86	.33
602	360	.0544	.0870	.1001	.0045	2.67	1.32	.95	.34
628	998	.364	.1337	.1006	.0034	0.185	0.89	1.49	1.36
628	348	.120	.0862	.0786	.0022	0.72	1.27	1.42	0.80
628	268	.106	.1068	.1000	.0023	1.07	1.70	1.67	.81
628	395	.0586	.0749	.0731	.0043	1.46	1.87	1.65	.73
659	995	.401	.1844	.1233	.0044	0.115	1.25	2.58	2.66
659	1096	.214	.1266	.0865	.0063	.170	1.53	2.77	2.51
659	1148	.168	.1120	.0775	.0055	.207	1.70	2.88	2.42
659	1186	.211	.1297	.0912	.0072	.208	1.53	2.58	2.20
659	1077	.162	.1802	.1493	.0011	.78	2.24	2.43	1.32
659	390	.115	.1328	.1118	.0041	.88	2.35	2.45	1.28
659	326	.105	.1274	.1128	.0037	1.10	2.27	2.20	1.22
659	1071	.155	.3008	.2887	.0189	2.12	3.01	2.35	0.92
698	1149	.412	.2991	.1985	.0089	0.170	1.98	3.58	3.22
697	1084	.268	.2906	.2015	.0133	.344	2.96	4.23	3.02
698	307	.0742	.0963	.0721	.0042	.629	3.07	3.59	2.10
698	335	.0662	.1444	.1186	.0073	1.51	4.50	3.93	1.71

[a] The values in this column were calculated from the results of several diffusion experiments at each temperature.

A general equation for the reaction studied can therefore be written

$$\tfrac{2}{3}x\,\mathrm{Bi(l)} + \tfrac{1}{3}x\,\mathrm{BiCl_3(g)} = \mathrm{Bi}_x\mathrm{Cl}_x\mathrm{(g)}$$

To evaluate the quantity x, the method of Brewer and Lofgren[3] was used. That is, the slope of the logarithm of the pressure of $BiCl_3$ *vs.* the logarithm of the pressure of the Bi_xCl_x will give the quantity $3/x$. Since the pressure of Bi_xCl_x is proportional to the pressure of BiCl, it is only necessary to observe the slope of the log–log plot for the species $BiCl_3$ and BiCl to determine x.

The experimental results are listed in Table I. Also given in the table are values of the equilibrium pressures of BiCl and $BiCl_3$ calculated from the data. From those pressures it is a relatively simple matter to calculate the pressures to be assigned to any other arbitrary pair of species.

The log–log plot required to evaluate x is shown in Fig. 1. It may be seen from the figure that the experimental points fell close to a straight line at each temperature. Thus over the pressure range studied there was only one important subhalide species. If another species had become important enough to influence the equilibrium, the experimental points would have deviated systematically from a straight line. The value of x derived from the data, then, is unity over the range of temperature and pressure studied. Thus the subhalide species was BiCl and the equilibrium studied was

$$\tfrac{2}{3}\mathrm{Bi(l)} + \tfrac{1}{3}\mathrm{BiCl_3(g)} = \mathrm{BiCl(g)} \qquad (1)$$

The equilibrium constant

$$K_1 = \frac{p_{\mathrm{BiCl}}}{(p_{\mathrm{BiCl_3}})^{1/3}(a_{\mathrm{Bi}})^{2/3}}$$

was calculated for each experiment and the results are given in Table I. In that calculation the activity of liquid bismuth was taken as unity because very little $BiCl_3$ would dissolve in the Bi at the low pressures used.

Thermodynamic Data.—The values of the thermodynamic functions for reaction 1 can be derived from the equilibrium constant K_1 and its change with temperature. In Fig. 2 the logarithm of the equilibrium constant is plotted against $1/T$. From the slope of the line, an enthalpy change of 24 ± 2 kcal. per mole for reaction 1 is calculated in the temperature range studied (600–700°). The standard free energy change for the reaction (the standard states being 1 atm. for the gases, and pure liquid for the Bi) is calculated from the equilibrium constants to be 7.8 ± 0.15 kcal. at 600° and 6.0 ± 0.15 kcal. at 700°. From these the standard entropy change is 18 ± 3 e.u. over the temperature range studied.

Comparison with Literature Data

Entropy.—There is sufficient spectroscopic and molecular-constant data available to calculate the entropies of the gaseous species of reaction 1 by statistical methods. There are also measured heat

(3) L. Brewer and N. Lofgren, *J. Am. Chem. Soc.*, **72**, 3038 (1950).

capacities for Bi in the condensed phases so that the calculated entropy can be compared with the entropy change observed in the present measurements.

For BiCl, gas, the fundamental vibration frequency is given by Herzberg[4] as 308 cm.$^{-1}$; an estimate of the internuclear distance was given by Stevenson[5] as 2.3 Å.; the symmetry number is one; and the molecular weight is 244. Using the statistical formula for the entropy, such as that given by Kelley,[6] the standard entropy of BiCl, gas, is 70.4 ± 0.5 e.u. at 600° and 71.3 ± 0.5 e.u. at 700°.

For $BiCl_3$, gas, the vibration frequencies come from measurements on the liquid. These and the other molecular constants are reported by Kelley.[7] They lead to a standard entropy of 106.3 ± 1.0 e.u. at 600° and 108.4 ± 1.0 e.u. at 700°.

The heat capacities of liquid and solid Bi, its heat of fusion and entropy at 298°K. are all reported by Kubaschewski and Evans.[8] They lead to values for the standard entropy of liquid Bi of 26.0 ± 1.0 e.u. and 26.8 ± 1.0 e.u. at 600 and 700°, respectively.

Thus the value for the entropy change for reaction 1 calculated from molecular constant data is 17.7 ± 1.4 e.u. at 600° and 17.4 ± 1.4 at 700°. This agrees very well with the entropy derived from the transpiration experiments and gives support that reaction 1 was indeed the equilibrium observed in those experiments.

To show how valid a confirmation this entropy comparison is for reaction 1, the data were calculated as though the subhalide species was Bi_2Cl_2. The equilibrium for that case becomes

$$^4/_3\mathrm{Bi(l)} + {}^2/_3\mathrm{BiCl_3(g)} = \mathrm{Bi_2Cl_2(g)} \qquad (2)$$

Equilibrium "constants" were calculated from the data on the basis of reaction 2: these values are shown as K_2 in Table I. The K_2's were averaged for each temperature and an entropy derived from the temperature coefficient of their logarithms. The entropy change for reaction 2 so derived from the transpiration data was 25 e.u. To calculate the entropy Bi_2Cl_2 gas from molecular-constant data the molecule was assumed to be a square with a Bi–Cl distance 1.06 times that of BiCl. (These assumptions are based on results obtained for the alkali halide dimers.[9]) For the vibrational entropy the assumptions of Rice and Klemperer[10] were made. The resultant entropy so estimated for Bi_2Cl_2 gas at 600° was 102 e.u. From this value one calculates an entropy for reaction 2 of −2 e.u., that is 27 e.u. less than the value derived by calculating the transpiration data on the basis of that reaction. The entropy comparison therefore provides evidence in favor of the monomer as opposed to dimer or higher polymers since the disagreement between experimental and calculated entropies will become greater for larger polymers. It may be that some of the BiCl was in a dimerized form; however, the concordance of the calculated and observed entropy values for reaction 1 would seem to indicate that only a small percentage of the BiCl was polymerized.

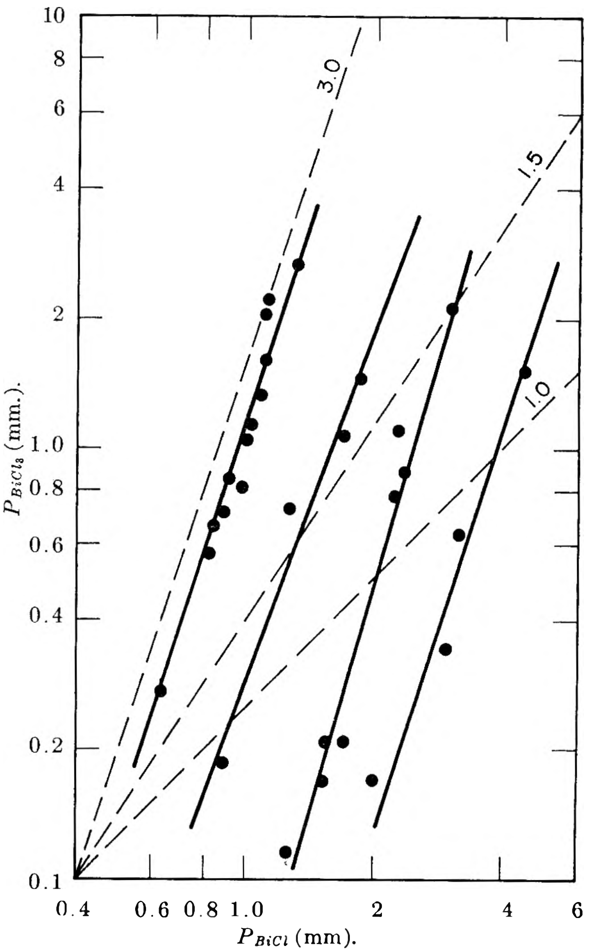

Fig. 1.—Plot of log p_{BiCl} vs. log. p_{BiCl_3}. The full lines and associated points, reading from left to right, are for 602, 628, 659 and 698°. The slopes of the lines were found to be 3.1, 2.7, 3.5 and 3.1, respectively. The dotted lines show slopes expected for BiCl (slope 3.0), Bi_2Cl_2 (slope 1.5) and Bi_3Cl_3 (slope 1.0).

Enthalpy.—The enthalpy change for reaction 1 was found to be 24 ± 2 kcal. from 600 to 700°. This can be converted to 25° as follows. The differences of the enthalpies of gaseous BiCl and $BiCl_3$ from 25 to 650° can be calculated from the molecular-constant data, and that for Bi, solid at 25 and liquid at 650°, can be determined from its heat capacities and heat of fusion. Making this correction one obtains 27 ± 2 kcal. at 25° for the enthalpy change of the reaction

$$^1/_3\mathrm{BiCl_3(g)} + {}^2/_3\mathrm{Bi(s)} = \mathrm{BiCl(g)}$$

The enthalpy of sublimation of $BiCl_3$, gas, has been given by Darnell and Yosim[11] at 420°K. as 28.4 kcal. Using the heat content values of Kelley[6] for $BiCl_3$, gas, and estimating the heat capacity of the liquid as 25 cal. per mole degree,

---

[4] G. Herzberg, "Molecular Spectra and Molecular Structure," Vol. I, 2nd Ed., D. Van Nostrand Co., New York, N. Y., 1950, p. 510.

[5] D. P. Stevenson, *J. Chem. Phys.*, **8**, 898 (1940). Note: His entropy for BiCl is wrong.

[6] K. K. Kelley, United States Bureau of Mines Bull. 477, 15 (1950).

[7] Ref. 4, p. 27.

[8] O. Kubaschewski and E. L. Evans, "Metallurgical Thermochemistry," 2nd Ed., John Wiley and Sons, Inc., New York, N. Y., 1956.

[9] T. A. Milne and D. Cubicciotti, *J. Chem. Phys.*, **29**, 846 (1958).

[10] S. A. Rice and W. Klemperer, *ibid.*, **27**, 643 (1957).

[11] A. J. Darnell and S. J. Yosim, THIS JOURNAL, **63**, 1813 (1959).

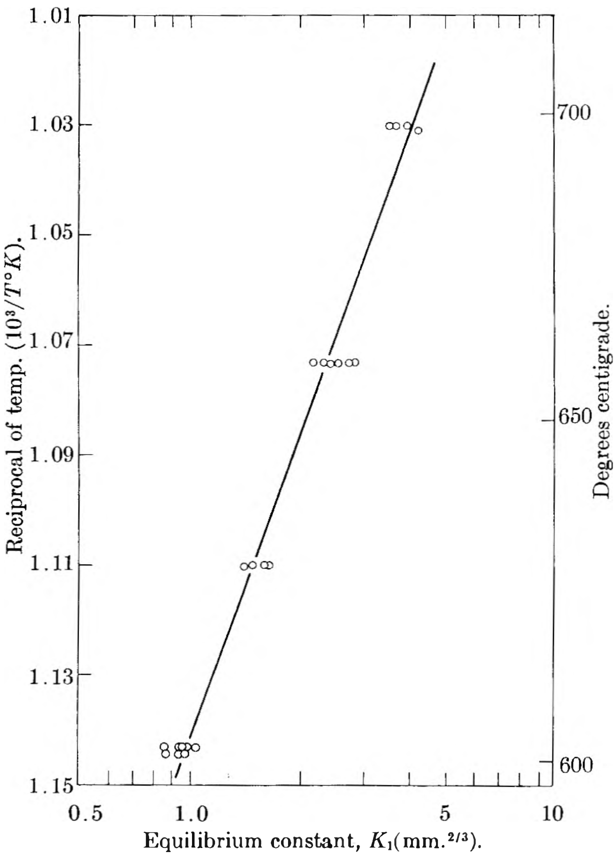

Fig. 2.—The logarithm of the equilibrium constant for reaction 1 *versus* reciprocal of absolute temperature.

one calculates the enthalpy of sublimation at 25° to be 29.1 kcal. Therefore the enthalpy change at 25° is 37 ± 2 kcal. for the reaction

$$^1/_3\text{BiCl}_3(\text{s}) + {}^2/_3\text{Bi}(\text{s}) = \text{BiCl}(\text{g})$$

The enthalpy of formation[12] of solid $BiCl_3$ is −90.6 kcal. at 25°. Therefore, the enthalpy of formation of BiCl, gas, at 25° is 7 ± 2 kcal. per mole. This value is felt to be more reliable than the one derived from spectroscopic data,[12,13] namely, 10.7 ± 4 kcal., because a long extrapolation is required to obtain the spectroscopic value.

Discussion

The reaction studied, namely reaction 1, is interesting because although it is quite endothermic ($\Delta H_{650°} = 24$ kcal.), conditions could be found at which there was a measurable concentration of products. The reason, of course, is that the entropy change was sufficiently large to counterbalance most of the unfavorable enthalpy change; thus the resultant free energy was small, though positive, in the temperature range studied.

This situation is reminiscent of the reactions

$$aM(\text{solid or liquid}) + b/2\ \text{X}_2(\text{gas}) = M_aX_b(\text{gas})$$

discussed by Brewer,[14] in which an "unfavorable" enthalpy change of a reaction can be overridden by a favorable entropy change at sufficiently high temperatures. In such reactions for b less than three the entropy change is positive and increasing temperature favors the formation of the compound. In that type of reaction the entropy change is not strongly dependent on the value of a so that information about it is not, in general, obtained from the entropy change. The reason is that the entropy per mole of M (solid or liquid), which mainly is vibrational, is approximately equal to the increase in absolute entropy per mole of $M_{a+1}X_b$ over that of M_aX_b, which increase is again chiefly vibrational.

In the type of reaction considered in the present work the entropy change is sensitive to the degree of polymerization of the product. This may be understood by considering reactions 1 and 2 above. The increase in absolute entropy of Bi_2Cl_2 over BiCl is mainly in the vibrational degrees of freedom; whereas the entropy of the reactants has an appreciable contribution from translational degrees of freedom, which give appreciably larger entropies than the vibrational. The entropy change of reaction 2 is therefore smaller than that of reaction 1. Thus the entropy change of this type of reaction can give information concerning the degree of polymerization of the products.

In our earlier study of the pressure of $BiCl_3$ over liquid Bi–$BiCl_3$ mixtures[15] some Bi was transported through the vapor phase, presumably as a lower-valent species. Analysis of the material transported in those experiments indicated that less than 0.1 mole % of the Bi–Cl vapor was the lower-valent species. It is interesting to extrapolate the data of the present study to estimate the per cent. BiCl to be expected in the vapor over the liquid Bi–$BiCl_3$ mixtures.

From an estimated heat capacity change of −2 cal. per mole degree for reaction 1 and the values of ΔH and ΔS^0 at 650°, the equilibrium constant for that reaction was estimated to be 2×10^{-6} and 6×10^{-5} at 300 and 400°, respectively. From these and the pressures of $BiCl_3$ over the saturated solutions from reference 15 one calculates that the ratio of BiCl to $BiCl_3$ in the vapor over the two-phase liquids was about 2×10^{-4} and 10^{-4} at 300 and 400°. Thus the fraction of lower-valent Bi in the experiments of reference 15 was indeed negligible.

Acknowledgments.—The laboratory work was performed by Mr. William E. Robbins and the research was influenced by many fruitful discussions with Drs. T. A. Milne, F. J. Keneshea, Jr., and C. M. Kelley. The author is grateful to Professor Leo Brewer for constructive criticism of the manuscript.

---

(12) F. D. Rossini, D. D. Wagman, W. H. Evans, L. Levine and I. Jaffe, National Bureau of Standards Circular 500, 1952.

(13) T. L. Cottrell, "The Strengths of Chemical Bonds," 2nd Ed., Butterworths, London, 1958, p. 228.

(14) L. Brewer, *Experientia* (Suppl. VII, XVI Internat. Cong. Pure and Appl. Chem. Paris, 232 (1957).

(15) D. Cubicciotti, F. J. Keneshea, Jr., and C. M. Kelley, THIS JOURNAL, **62**, 463 (1958).

INFRARED SPECTRA OF 2-METHYL-2-HYDROXYPROPANE (*t*-BUTANOL) AND 2-METHYL-2-DEUTERIOXYPROPANE (*t*-BUTANOL-*d*)

BY J. G. PRITCHARD AND H. M. NELSON

Mellon Institute, Pittsburgh, Pa.

Received January 15, 1960

Infrared spectra have been recorded for *t*-butanol (2-methyl-2-hydroxypropane) and *t*-butanol-*d* (2-methyl-2-deuterioxypropane) as pure liquids, as dilute solutions in non-polar solvents and as solids. The spectra for the solid alcohols are only slightly modified compared to those for the pure liquids. A complete assignment has been made for the observed vibrational bands for this type of structure. The effect of dilution in non-polar solvent is to displace the bands associated with the vibrations of the OH and OD groups in the pure alcohols toward the frequencies observed for these groups in the vapor phase spectra. The effect of deuterium substitution on the ν_{OH} (stretching) and τ_{OH} (torsional) bands is a shift to lower frequencies by usual factors: $\nu_{OH}/\nu_{OD} = 1.35$, $\tau_{OH}/\tau_{OD} = 1.31$. The isotope effect for the degree of freedom associated with the in-plane bending motion of the COH group is split between two frequencies the primary assignments of which for pure *t*-butanol are δ_{COH} (bending) at 1380 cm.$^{-1}$ and ρ_{CH_3} (symmetric methyl rocking) at 1189 cm.$^{-1}$: $\delta_{COH}\rho^{H}{}_{CH_3}/\delta_{COD}\rho^{D}{}_{CH_3} = 1.35$. The coupling of these motions is discussed. The CO stretching vibration in the alcohols occurs at 1208 cm.$^{-1}$ and is almost unchanged in the spectra of the solid complexes *t*-BuOK·*t*-BuOH and *t*-BuOK·*t*-BuOD. The bands associated with the OH and OD vibrations are considerably modified in the complexes. The discussion of these results aids in explaining current uncertainties in the assignment of bands within the 900 to 1500 cm.$^{-1}$ region in the spectra of alcohols.

Introduction

Difficulties with the assignment of vibrational frequencies for the in-plane OH bending motion of the COH group in aliphatic alcohols (δ_{COH}) arise from four main causes. (1) Frequencies associated with the OH group are different for the liquid and vapor states as a result of hydrogen-bonding in the liquid. (2) The spectra of alcohols in the 900 to 1500 cm.$^{-1}$ region almost invariably contain superimposed bands which are not readily resolvable. (3) Most alcohols show changes in at least two bands in the 900 to 1500 cm.$^{-1}$ region on replacing the *ol*-hydrogen by deuterium or on dilution of the liquid in non-polar solvents. (4) For a large group of alcohols, the position of an intense "alcohol-band" for primary alcohols at *ca.* 1050 cm.$^{-1}$ is shifted in secondary and tertiary alcohols to *ca.* 1100 and 1150 cm.$^{-1}$, respectively. (There are many exceptions to this rule.)

The early discussions of the spectra of methanol and methanol-*d* show, for example,[1,2] that it is not possible to determine whether a strong band at 1340 cm.$^{-1}$ or a possible masked band at about 1030 cm.$^{-1}$ or both may be due to the COH bending motion. Within the last decade, this problem has been investigated for many alcohols but the observed phenomena do not appear to be well understood. A good survey of the subject is to be found in the recent text by Bellamy,[3] who emphasizes that in almost all cases two bands in the 1000–1400 cm.$^{-1}$ region appear to be associated with δ_{COH} for simple aliphatic alcohols (and also for phenols and sterols). Some of the more important work is cited below. Supporting an original suggestion by Davies,[2] it is reported that for a series of seven alcohols in the liquid state (ranging from butanol to decanol) a strong band in the range 1030–1060 cm.$^{-1}$ is closely overlapped by an apparent δ_{COH} band in the 1010–1035 cm.$^{-1}$ region.[4] The two bands are resolved only for the alcohols of higher molecular weight for which the stronger band is at 1060 cm.$^{-1}$. Two more recent studies show particularly that at least two bands in the 1000 to 1400 cm.$^{-1}$ range may be connected with δ_{COH} in alcohols.[5,6] For example, in the case of ethanol vapor two bands at 1243 and 1030 cm.$^{-1}$ are clearly replaced by two bands at 890 and 790 cm.$^{-1}$ in ethanol-*d* vapor[5]; however, it is claimed for liquid ethanol[6] that three bands at 1419, 1330, 1092 cm.$^{-1}$ appear to be replaced by only one band at 956 cm.$^{-1}$ for liquid ethanol-*d*. The duality of frequencies associated with the COH bending vibration in alcohols has been attributed variously to rotational isomerism,[5] combination tones[7] and coupling effects involving the CO stretching or CH bending vibrations.[8–10]

The overlapping of important bands occurs for branched alcohols in the 1100 to 1150 cm.$^{-1}$ region.[9,11,12] Several studies on *t*-butanol and *t*-butanol-*d* have been reported and are referred to later. However, since *t*-butanol and *t*-butanol-*d* molecules are of effectively high symmetry for which the complication of rotational isomerism cannot enter, we have considered it worthwhile to make a new and complete study of their infrared spectra giving particular attention to the resolution of the types of difficulties discussed above. A detailed assignment for every observed spectral band is attempted. The frequencies due to the *t*-butoxide skeleton are checked by comparison with the spectra of potassium *t*-butoxide complexes made from both light and heavy alcohols. It is hoped that this study may form a model showing the distinct effects which should be searched for generally in the spectra of other

---

(1) G. Herzberg, "Infrared and Raman Spectra of Polyatomic Molecules," D. Van Nostrand Co., Inc., New York, N. Y., 1945, pp. 334 and 335, and refs. therein cited.

(2) M. Davies, *J. Chem. Phys.*, **16**, 267 (1948).

(3) L. Bellamy, "Infrared Spectra of Complex Molecules," 2nd Ed., John Wiley and Sons, New York, N. Y., 1958, pp. 108–110, and refs. therein cited.

(4) J. R. Quinan and S. E. Wiberley, *Anal. Chem.*, **26**, 1762 (1954).

(5) P. Tarte and R. Deponthiere, *J. Chem. Phys.*, **26**, 962 (1957); *Bull. soc. chim. Belges*, **66**, 525 (1957).

(6) M. Maclou and L. Henry, *Compt. rend. acad. sci. Paris*, **244**, 1494 (1957).

(7) F. A. Smith and E. C. Creitz, *J. Research Natl. Bur. Standards*, **46**, 145 (1951).

(8) S. Krimm, C. Liang and G. B. B. M. Sutherland, *J. Chem. Phys.*, **25**, 778 (1956).

(9) A. V. Stuart and G. B. B. M. Sutherland, *ibid.*, **24**, 559 (1956).

(10) C. G. Swain, A. D. Ketley and R. F. W. Bader, *J. Am. Chem. Soc.*, **81**, 2353 (1959).

(11) W. Weniger, *Phys. Rev.*, **31**, 388 (1910).

(12) H. H. Zeiss and M. Tsutui, *J. Am. Chem. Soc.*, **75**, 897 (1953).

TABLE I

FREQUENCIES (CM.$^{-1}$) OF INFRARED BANDS[a] OBSERVED FOR LIQUID *t*-BUTANOL AND *t*-BUTANOL-*a*

t-BuOH (pure liquid)	*t*-BuOH (0.05 *M*)	*t*-BuOD (pure liquid)	*t*-BuOD (0.05*M*)	Assignment
	3616w			ν_{OH} (mono.)
3362s,b ↗				ν_{OH} (assoc.)
2970s	2970s	2970s	2970s	ν'_{CH}
			2655w	ν_{OD} (mono.)
		2485s,b ↗		ν_{OD} (assoc.)
1472m	1472m	1472m	1472m	δ'_{CH_3}
(1389vw)	1389vw	1389w	1389w	δ_{CH_3}
1380m ↘				δ_{COH} and ρ_{CH_3} (assoc.)
1364s	1364s	1364s	1364s	δ_{CH_3}
	1329m			δ_{COH} and ρ_{CH_3} (mono.)
		1276m ↘		ρ_{CH_3} and δ_{COD} (assoc.)
1239m	1239w	1239m	1239w	ν'_{CC}
1208s	1208s	1208s	1208s	ν_{C-OH}
(1189m) ↘				ρ_{CH_3} and δ_{COH} (assoc.)
	1141s			ρ_{CH_3} and δ_{COH} (mono.)
1027w	1016w	1053m	1053w	ρ'_{CH_3}
		952s,b ↘		δ_{COD} and ρ_{CH_3} (assoc.)
914s	912s	919s	912s	ρ'_{CH_3}
			882w	δ_{COD} and ρ_{CH_3} (mono.)
747m	747m	747m	747m	ν_{CC}
640s,vb	. . .			τ_{OH}
		490s,vb	. . .	τ_{OD}
465w	462w	467w	455w	δ'_{CCC}
424w	. . .	422w	. . .	δ_{CCC}
346w	348w	350w	345w	ρ'_{C-OH}

[a] s = strong, m = medium, w = weak, b = broad, v = very, sh = shoulder.

alcohols and which indeed have been found at least piecemeal for many.

Experimental

_t_-Butanol.—A commercial sample of at least 99% purity[13] was distilled from *ca.* a one tenth molecular proportion of sodium. A middle cut had m.p. 25.5° and was stored in a tightly stoppered vessel in a desiccator.

_t_-Butanol-_d_.—Forty g. of lithium aluminum hydride was dissolved in 2500 ml. of dry ether and 300 ml. of pure *t*-butanol added gradually with stirring under an efficient reflux condenser. The mixture was refluxed for 1 hour to complete the reaction. The gray precipitate of lithium tris-(*t*-butoxy) aluminum hydride was filtered off and washed thoroughly with dry ether, residual ether being removed from the product (193 g.) under vacuum in a desiccator. To this material, 35 ml. of deuterium oxide (> 99.5%) was added and the mixture was refluxed for 36 hours. The fluid was distilled off and then redistilled repeatedly from quantities of sodium and lastly potassium until a product (*ca.* 50 g.) melting at 25 to 25.5° was obtained. Pains were taken to protect the materials from moist air throughout.

"Potassium _t_-Butoxide."—*Ca.* 0.5 g. of metallic potassium (weighed under pentane) was dissolved in *ca.* 15 ml. of *t*-butanol. The resulting solution was cooled until it solidified and then the excess *t*-butanol was removed by pumping, finally at *ca.* 50° (1 mm.). The product was a fine, white powder, only slightly hygroscopic, having an equivalent weight of *ca.* 186 against standard acid, corresponding to a composition *t* BuOK·*t*-BuOH. The experiment was repeated with *t*-butanol-*d* with a similar result: *t*-BuOK·*t*-BuOD.

Spectroscopy.—All spectra were run on a Beckman IR-4 instrument with sodium chloride and cesium bromide optics. The instrument was calibrated using the ammonia and water vapor spectra. Accuracy is estimated at ± 10 cm.$^{-1}$ for the 4000 to 2000 cm.$^{-1}$ region and ±2 cm.$^{-1}$ for the lower frequencies. Spectra for the pure alcohols were obtained using capillary films between sodium chloride and cesium bromide plates for the respective regions: 4000 to 660 and 660 to 300 cm.$^{-1}$. The non-polar solvents used for dilution of the alcohols were as indicated in Fig. 1. The 0.05 *M* solutions were run without compensation in 1 mm. cells. The 0.5 *M* solutions were run using matched cells with solvent in the reference beam. The spectra for the solid alcohols were run in the conventional type of low temperature cell using solid CO_2–$CHCl_3$–CCl_4 as coolant.

The potassium *t*-butoxide complexes were run as mulls in Halocarbon Oil for the 4000 to 1300 cm.$^{-1}$ region and in Nujol for the 1300 to 300 cm.$^{-1}$ region. The mulls were prepared in a dry-box by pressing samples of the complexes and oil between sodium chloride and cesium bromide plates. The reproducibility of the spectra from different mulls was frequently poor, especially in the 300 to 900 cm.$^{-1}$ region, due to scattering effects. Exposure of the mulls to a humid atmosphere for a few seconds resulted in the slight decomposition of the complexes, as shown by the appearance of weak bands corresponding to ν_{OH} and ν_{OD} (mono.) in the spectra.

Results and Discussion

The Spectra of _t_-Butanol and _t_-Butanol-_d_.—Table I gives the observed spectral bands for the liquid alcohols and for their dilute solutions in non-polar solvent. The spectra obtained for moderately concentrated solutions of *t*-butanol and *t*-butanol-*d* in the non-polar solvent include bands due to both the associated alcohols and their monomeric forms and are reproduced for the 600 to 4000 cm.$^{-1}$ region in Fig. 1. The bands for the pure alcohols in the 300 to 600 cm.$^{-1}$ region are also included in Fig. 1. Most of the observed bands were quite distinct in all spectra taken and the general complexion of the *t*-butanol spectra agree well with those previously published.[14–16]

The two bands in parentheses for pure *t*-butanol (Table I) are overlapped by adjacent bands and their presence could be affirmed only by careful

---

[13] K. and K. Laboratories, Long Island, New York.

[14] R. B. Barnes, V. Liddel and V. Z. Williams, *Anal. Chem.*, **15**, 683 (1943).

[15] O. D. Shreve and M. R. Heether, *ibid.*, **23**, 283 (1951).

[16] L. B. Cannell and R. W. Taft, Jr., *J. Am. Chem. Soc.*, **78**, 5815 (1956).

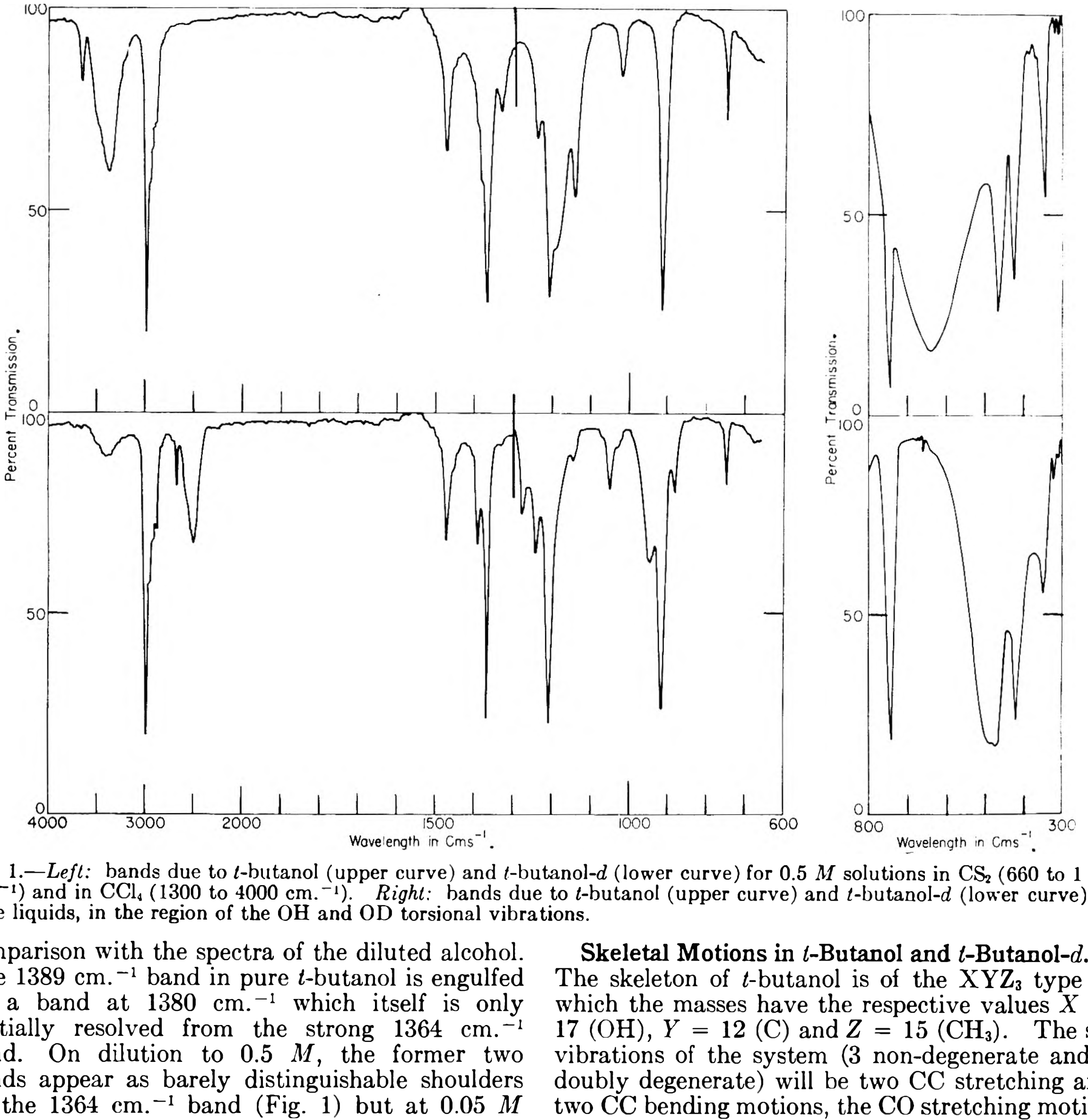

Fig. 1.—*Left:* bands due to *t*-butanol (upper curve) and *t*-butanol-*d* (lower curve) for 0.5 *M* solutions in CS_2 (660 to 1 00 cm.$^{-1}$) and in CCl_4 (1300 to 4000 cm.$^{-1}$). *Right:* bands due to *t*-butanol (upper curve) and *t*-butanol-*d* (lower curve) as pure liquids, in the region of the OH and OD torsional vibrations.

comparison with the spectra of the diluted alcohol. The 1389 cm.$^{-1}$ band in pure *t*-butanol is engulfed by a band at 1380 cm.$^{-1}$ which itself is only partially resolved from the strong 1364 cm.$^{-1}$ band. On dilution to 0.5 *M*, the former two bands appear as barely distinguishable shoulders on the 1364 cm.$^{-1}$ band (Fig. 1) but at 0.05 *M* dilution the 1380 cm.$^{-1}$ band has disappeared entirely leaving the other two sharply resolved. The 1189 cm.$^{-1}$ band in pure *t*-butanol has the effect of broadening the 1208 cm.$^{-1}$ band toward lower frequencies, but at 0.5 *M* dilution it is resolved as a distinct shoulder, *cf.* Fig. 1. Two bands in this region, at *ca.* 1210 and 1190 cm.$^{-1}$, are also indicated from the Raman spectrum of *t*-butanol.[17]

The bands which are different for the light and heavy alcohols are printed in heavy type; the same are also affected markedly by degree of dilution (arrows), so corroborating the assignments. From the observation of the disappearance of these bands for the pure alcohols it is evident that below 0.05 *M* dilution the alcohols exist completely in the monomeric form. On the assumption that the 1276 and 952 cm.$^{-1}$ association bands for *t*-butanol-*d* behave similarly, it is likely that the former moves to about 1200 cm.$^{-1}$ on dilution although this cannot be discerned.

Skeletal Motions in *t*-Butanol and *t*-Butanol-*d*.—The skeleton of *t*-butanol is of the XYZ_3 type in which the masses have the respective values X = 17 (OH), Y = 12 (C) and Z = 15 (CH_3). The six vibrations of the system (3 non-degenerate and 3 doubly degenerate) will be two CC stretching and two CC bending motions, the CO stretching motion (ν_{C-OH}) and the OH group rocking motion (ρ'_{C-OH} or δ'_{CCO}).

Simpson and Sutherland[18] have calculated a set of normal vibrational frequencies for the XYZ_3 case in which the groups Z = methyl and X = alkyl are bound to the central carbon atom Y = C through bonds of equal strength. From their results, choosing a hypothetical Z = 17, we estimate that the three parallel vibrational modes ν_{CX}, ν_{CC} and δ_{CCC} have frequencies of approximately 1270, 720 and 430 cm.$^{-1}$, respectively, and the three doubly degenerate, perpendicular modes ν'_{CC}, δ'_{CCC} and δ'_{CCX} have frequencies of approximately 1280, 440 and 310 cm.$^{-1}$. These frequencies should be a good guide to assignments for *t*-butanol assuming that the force constant for the CO bond is not very different from those for the CC bonds. In fact, a set of six frequencies corresponding to those above can be found easily in our *t*-butanol spectra. Accordingly, ν'_{CC} and ν_{C-OH} are assigned as the two close bands at 1239 and 1208

---

[17] W. G. Braun, D. F. Spooner and M. R. Fenske, *Anal. Chem.*, **22**, 1105 (1950).

[18] D. M. Simpson and G. B. B. M. Sutherland, *Proc. Roy. Soc.* (*London*), **A199**, 169 (1949).

cm.$^{-1}$ with ν_{CC} at 747 cm.$^{-1}$. The three bands in the cesium bromide region, 465, 422 and 350 cm.$^{-1}$ are assigned to δ'_{CCC}, δ_{CCC} and ρ'_{C-OH} (or δ'_{CCO}), respectively.

Motions of the OH and OD groups.—The OH and OD stretching vibrations for the single molecules give rise to the weak, narrow bands at 3616 and 2655 cm.$^{-1}$. The association band for pure *t*-butanol is very broad (3600 to 3100 cm.$^{-1}$), a well known general phenomenon in alcohols. Thus, using a high resolution instrument, Kuhn[19] has shown that separate broad bands due to dimeric *t*-butanol and polymeric forms may be resolved at 3495 and 3340 cm.$^{-1}$. The ν_{OD} association band is almost equally broad (2650 to 2400 cm.$^{-1}$).

The OH bending frequency (δ_{COH}) is assigned as 1380 cm.$^{-1}$ since the force constant for bending of the HOC bond is unlikely to be very different from that for the HCC bond, for which frequencies in the 1350 to 1500 cm.$^{-1}$ range are observed. Such assignment has fair precedent[1,3,9] and the characteristic behavior of our 1380 cm.$^{-1}$ band on deuteration and dilution establishes the connection between this type of band and the OH bending motion, an apparently corresponding δ_{COD} band[20] being at 1276 cm.$^{-1}$. The coupling of these vibrations with a methyl-rocking vibration is discussed later.

The torsional motion of the OH group (τ_{OH}) is thought to be a combination of oscillation in some molecules and restricted rotation in others of the same species in liquid alcohols[21] and gives rise to the very broad band extending from *ca.* 500 to 800 cm.$^{-1}$, *cf.* Fig. 1. The corresponding band for OD appears sharper from 400 to 600 cm.$^{-1}$. These broad bands disappear on dilution to 0.05 *M* in non-polar solvent. Presumably, the fairly free rotation of the OH group in the unassociated molecules does not give rise to bands of observable intensity in this region.

Motions of the Methyl Groups.—If each methyl group attached to the central carbon atom in *t*-butanol is considered as an isolated XCH_3 unit, the system should give rise to six distinct vibrations (3 non-degenerate and 3 doubly degenerate). Four of these are the principal bending and stretching motions of the methyl hydrogen atoms, a fifth is the rocking motion of the methyl group as a whole and the sixth, which has already been considered in the section on skeletal motions, is the XC stretching vibration. The asymmetric CH stretching band occurs familiarly at 2970 cm.$^{-1}$. The unresolved shoulders on the low frequency side of this band (Fig. 1) are due partly to the symmetric CH stretching vibration (which may be split due to mixing of the methyl vibrations through the central carbon atom) and partly to overtones or combination tones from the CH bending modes at 1472 and 1364 cm.$^{-1}$. The latter, symmetric band is split[22] due to mixing effects giving the additional weak band at 1389 cm.$^{-1}$.

The rocking motions of the three methyl groups may likewise mix to give rise to three distinct frequencies, one symmetric and two asymmetric. In pure *t*-butanol the two asymmetric ρ'_{CH_3} modes (doubly degenerate) and the symmetric ρ_{CH_3} mode (non-degenerate) are assigned to the bands at *ca.* 1020, *ca.* 915 and 1190 cm.$^{-1}$, respectively, in general agreement with a previous discussion primarily devoted to *t*-butyl fluoride,[23] and by analogy with the assignments made in this region for methyl-rocking modes in propylene, propane and dimethylacetylene.[24] The ρ'_{CH_3} bands show small apparent shifts in going from *t*-butanol to *t*-butanol-*d* but these are probably due to intensity changes in the individuals of split rocking bands, as detailed in later sections. The ρ_{CH_3} band shifts markedly on dilution of the alcohol. The band in the spectrum of pure *t*-butanol-*d* in this region, at 952 cm.$^{-1}$, shows the same behavior.

The effect of dilution in non-polar solvent on both the δ_{COH} and the ρ_{CH_3} bands is a displacement to lower frequencies by about 4%. Our bands at 1329 and 1141 cm.$^{-1}$ are almost identical with the position of similar bands quoted by Tarte and Deponthiere for *t*-butanol *vapor*.[5] These workers also reported a band for *t*-butanol-*d vapor* corresponding to our ρ_{CH_3} band at 882 cm.$^{-1}$, but they too failed to find a corresponding δ_{COD} band. This band may be weak or be masked by the strong ν_{C-OH} band at 1208 cm.$^{-1}$, *cf.* Table I. Details of the coupling between the δ_{COH} and δ_{CH_3} motions are considered later.

Table II

Frequencies (cm.$^{-1}$) of Certain Infrared Bands for Solid *t*-Butanol and *t*-Butanol-*d* at *ca.* −40°

t-BuOH (solid)		*t*-BuOD (solid)		Assignment
3285s,b				ν_{OH}
		2445s,b		ν_{OD}
(*ca.* 1380)				δ_{COH} and ρ_{CH_3}
		1281m		ρ_{CH_3} and δ_{COD}
1214s		1210s		ν_{C-OH}
1198w				ρ_{CH_3} and δ_{COH}
		963m,b		δ_{COD} and ρ_{CH_3}
1027w	....	1056m	1032w	ρ'_{CH_3}
927s	919sh	923s	908w	ρ'_{CH_3}

Comparison with Spectra of Solid *t*-Butanol and *t*-Butanol-*d*.—The ν_{CH}, δ_{CH_3} and ν_{CC} frequencies in the region 660 to 4000 cm.$^{-1}$ are almost identical for both solid and liquid phases of the two alcohols. The δ_{COH} band is again unresolved but its coupled partner, ρ_{CH_3} in *t*-butanol, is readily observable in the solid as a weak band at *ca.* 1198 cm.$^{-1}$ on the side of the strong ν_{C-OH} band at 1214 cm.$^{-1}$.

---

[19] L. P. Kuhn, *J. Am. Chem. Soc.*, **74**, 2492 (1952).

[20] Maclou and Henry (ref. 6) apparently failed to observe this band. They reported the bands associated with the OH bending motion in liquid *t*-butanol as follows: 1382, 1200 (assoc.); 1330, 1145 (mono.) and for liquid *t*-butanol-*d* as: 956 (assoc.); 879 cm.$^{-1}$ (mono.). These values are in good agreement witn those observed by us.

[21] *Cf.* Ta-You Wu, "Vibrational Spectra and Structure of Polyatomic Molecules," J. W. Edwards, Ann Arbor, Michigan, 1946, pp. 282–284.

[22] *Cf.* ref. 3, p. 24.

[23] D. E. Mann, N. Acquista and D. R. Lide, Jr., *J. Mol. Spectroscopy*, **2**, 575 (1958). These authors quote spectral bands for *t*-butanol taken from a compilation in K. W. F. Kohlrausch's "Ramanspektren," Becker and Erler, Leipzig, 1943, p. 242 (in U.S.A.: J. W. Edwards, Ann Arbor, Michigan, 1945). This set of frequencies is not complete and in the 900 to 1500 cm.$^{-1}$ region is somewhat different from our observations.

[24] *Cf.* ref. 1, pp. 355, 357 and 361.

TABLE III

FUNDAMENTAL ASSIGNMENTS FOR *t*-BUTANOL AND POTASSIUM *t*-BUTOXIDE COMPLEXES

Symmetry species		Vibrational type	Band Assignments		
group C_{3v}	group C_s		Pure *t*-BuOH	*t*-BuOK·*t*-BuOH	*t*-BuOK·*t*-BuOD
A_1	A′	ν_{CH}	(*ca.* 2920sh)	(*ca.* 2920sh)	(*ca.* 2920sh)
A_1	A′	ν_{CH}	(*ca.* 2920sh)	(*ca.* 2920sh)	(*ca.* 2920sh)
A_1	A′	δ_{CH_3}	1389w	1375m	1374m
A_1	A′	δ_{CH_3}	1364s	1351s	1351s
A_1	A′	ν_{C-OH}	1208s	1213s	1214s
A_1	A′	ρ_{CH_3}	1189sh,b	...	...
A_1	A′	ν_{CC}	747m	735w	723w
A_1	A′	δ_{CCC}	424m	416m	400m
E	A′ and A″	ν'_{CH}	2970s	2955s	2955s
E	A′ and A″	ν'_{CH}	2970s	2955s	2955s
E	A′ and A″	ν'_{CH}	2970s	2955s	2955s
E	A′ and A″	δ'_{CH_3}	1472m	1473m	1472w
E	A′ and A″	δ'_{CH_3}	1472m	1473m	1472w
E	A′ and A″	δ'_{CH_3}	1472m	1473m	1472w
E	A′ and A″	ρ'_{C-OH}	346m	352m	344m
E	A′ and A″	ρ'_{CH_3}	1027w	1027w	1026w,b
E	A′ and A″	ρ'_{CH_3}	914s	942s	947s
E	A′ and A″	ν'_{CC}	1239w	1266w,b	1270vw,b
E	A′ and A″	δ'_{CCC}	465m	477w	452m
E	A′ and A″	τ'_{CH_3}	...	...	...
A_2	A″	ν''_{CH}	not observed	2855w?	2855w?
A_2	A″	ν''_{CH}	not observed	2855w?	2855w?
A_2	A″	ρ''_{CH_3}	not observed	885w?	889vw?
A_2	A″	τ''_{CH_3}	not observed	...	...
A_1	A′	ν_{OH}	3362s	...	...
A_1	A′	δ_{COH}	1380m	...	...
A_2	A″	τ_{OH}	640s,b	...	...

In the solid, the ρ'_{CH_3} bands show the presence of splitting much more clearly than in the liquid alcohols. Thus the only bands shifted on solidification of the alcohols are the OH frequencies involved in hydrogen-bonding and the methyl-rocking motions, which are probably modified through specific orientation of the molecules in the crystalline solid, *cf.* Table II.

Symmetry Considerations.—The presence of the hydroxyl proton would be expected to perturb the $(CH_3)_3CO$ group (symmetry C_{3v}) only slightly. The *t*-butanol molecule (symmetry C_S) may therefore be treated as giving rise to 24 fundamental frequencies, based on C_{3v} symmetry, plus three frequencies corresponding to the three degrees of freedom of the hydroxyl proton. Table III shows a complete assignment. For the group of 12 frequencies which transform from E (doubly degenerate) to A′ and A″ (non-degenerate) on going from C_{3v} to C_S, we do not observe any systematic splitting in the assigned bands as would be expected on the C_S group assignment. Hence the approximation to C_{3v} seems to be fair. However, our piecemeal observation of splitting for the ρ'_{CH_3} motions for liquid and solid *t*-butanol and *t*-butanol-*d* (Tables I and II) we interpret as intensity changes in two close A′ and A″ bands in each case. The inactive A_2 modes in class C_{3v} which transform into active A″ modes in C_S are almost certainly of unobservably low intensity in *t*-butanol. The methyl torsional motions (τ_{CH_3}) probably have frequencies below 300 cm.$^{-1}$.

The frequency assignments for the alcohols are confirmed through a comparison with the spectra of the solid ionic complexes *t*-BuOK·*t*-BuOH and *t*-BuOK·*t*-BuOD, included in Table III. The striking point about these spectra is the apparent absence of bands due to the motions of the OH and OD groups and those coupled with them. Notably, the broad shoulder associated with ρ_{CH_3} at *ca.* 1189 cm.$^{-1}$ in pure *t*-butanol is absent in the complexes, leaving the strong ν_{C-OH} band clear and symmetrical at 1213 cm.$^{-1}$. Most of the *t*-butoxyl bands are within 20 cm.$^{-1}$ of the corresponding bands in *t*-butanol and for ν_{CC}, ν'_{CC}, δ_{CCC} and ρ'_{CH_3} this difference lies between 20 and 30 cm.$^{-1}$. In the complexes, two additional weak bands at 2855 and at *ca.* 887 cm.$^{-1}$ may be due to additional A″ modes. The general complexion of the bands in Table III indicates that an approximation of C_{3v} symmetry for the *t*-butoxyl group is as valid for the complexes as for the pure alcohols.

The empirical formulas of the complexes strongly suggest that the form of *t*-butoxide ion is a hydrogen-bonded structure similar to that shown below (A). In such structures, the OH or OD bands are expected *a priori* to be shifted to lower frequencies (compared to the alcohols) and broadened considerably as a result of hydrogen bonding.[25]

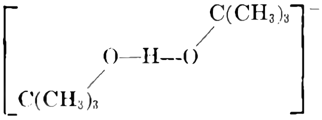

A

Thus, in *A*, the motions of the hydrogen atom of the OH group (or D of OD) may be influenced

---

(25) *Cf.* N. Albert and R. M. Badger, *J. Chem. Phys.*, **29**, 1193 (1958).

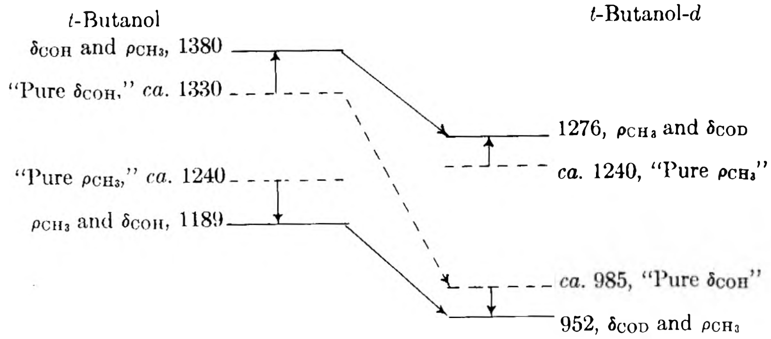

Fig. 2—Isotopic shifts in *t*-butanol and *t*-butanol-*d* (cm^{-1}).

strongly by both neighboring oxygen atoms. If this is the case, there will be two absorptions associated with OH stretching in the O–H---O system; and the former δ_{COH} and τ_{OH} motions in free *t*-butanol would tend to become equivalent in *A*, especially if the two CO bonds should be perpendicular. It is also likely that the solid complexes contain more than one structure similar to *A*, in which, for example, the angle between the two CO bonds and the degree of hydrogen-bonding are different. Hence, the bands due to the OH and OD motions in the complexes may be so broadened as to escape detection.

Isotope Effects.—Table IV summarizes the observed ratios of frequencies which are shifted by significant amounts for deuterium substitution in *t*-butanol. The theoretical value of the ratio of the products of the frequencies for the light and heavy alcohols may be calculated from the Redlich product formula, for anharmonic vibrations in the lowest quantum states. In our case the formula may be factorized into two separate terms corresponding to the two symmetry types A′ and A″

$$\mathrm{A}': \pi_i\omega_i^{\mathrm{H}}/\omega_i^{\mathrm{D}} = (m^{\mathrm{D}}/m^{\mathrm{H}})(M^{\mathrm{H}}/M^{\mathrm{D}})(I_z^{\mathrm{H}}/I_z^{\mathrm{D}})^{1/2}$$

$$\mathrm{A}'': \pi_i\omega_i^{\mathrm{H}}/\omega_i^{\mathrm{D}} = (m^{\mathrm{D}}/m^{\mathrm{H}})^{1/2}(M^{\mathrm{H}}/M^{\mathrm{D}})^{1/2}(I_x^{\mathrm{H}}I_y^{\mathrm{H}}/I_x^{\mathrm{D}}I_y^{\mathrm{D}})^{1/2}$$

The individual ratios have the following values $m^D/m^H = 2.00$ (mass), $M^H/M^D = 0.987$ (molecular weight), $I_x^H/I_x^D = 0.99$, $I_y^H/I_y^D = 0.94$ and $I_z^H/I_z^D = 0.96$. The moments of inertia (*I*) about the principal axes of the *t*-butanol and *t*-butanol-*d* molecules were calculated in good approximation assuming the *x*-axis along the CO bond with the others perpendicular to the *x*-axis and passing through the central carbon atom, which is very close to the center of mass of the system (COH group in the *xy*-plane). The calculated and observed values of $\pi_i\omega_i^H/\omega_i^D$ are as follows for the associated form of the alcohols: for A′, 1.93 (calcd.) 1.82 (obsd.); for A″, 1.35 (calcd.) 1.31 (obsd.). The differences are equivalent to *ca.* 3% per degree of freedom of the hydroxyl proton and may be attributed to anharmonicity effects.

The observed value of 1.35 for the isotope effect on ν_{OH} is sufficiently high to represent the total effect for the one degree of freedom for this mode. Therefore the remaining degree of freedom in the A′ class is shared entirely by the δ_{COH} and ρ_{CH_3} vibrations, which must be coupled.[26] All the normal vibrations of a complex molecule are coupled through the bonds connecting the vibrating atoms. However, the type of coupling observed for the δ_{COH} and ρ_{CH_3} vibrations in *t*-butanol probably requires a more specific effect. A simple scale model shows that the hydroxyl-hydrogen atom is always close to hydrogen atoms of the methyl groups. It therefore seems plausible that a high-amplitude methyl-rocking motion of the required A′ symmetry could be coupled with the COH bending motion through non-bonding forces between the hydrogen atoms of the different groups.

Table IV

Frequency Ratios (ω^H/ω^D) for *t*-Butanol and *t*-Butanol-*d*

Mode	Symmetry	ω^H/ω^D (assoc.)	ω^H/ω^D (mono.)
ν_{OH}	A′	1.35	1.36
δ_{COH} and ρ_{CH_3}	A′	1.08	*ca.* 1.04
ρ_{CH_3} and δ_{COH}	A′	1.25	1.29
τ_{OH}	A″	1.31	

It should be emphasized that because of the coupling between them the assigned δ_{COH} and ρ_{CH_3} vibrations in Tables I to IV cannot be regarded strictly as individual assignments. The primary assignments (written *first* in Tables I, II and IV) are derived from the probable detailed relationship between the coupled bands shown in Fig. 2. Our observed coupled bands in pure *t*-butanol occur at 1380 and 1189 cm.$^{-1}$. The hypothetically pure δ_{COH} and ρ_{CH_3} motions in *t*-butanol therefore most probably have frequencies *ca.* 1330 and *ca.* 1240 cm.$^{-1}$, respectively. The isotope effect for "pure ρ_{CH_3}" on going to *t*-butanol-*d* would be zero; the effect on "pure δ_{COH}" should give a "pure δ_{COD}" shifted, by a factor of *ca.* 1/1.35, to *ca.* 985 cm.$^{-1}$. Coupling of the latter vibration with "pure ρ_{CH_3}" then would give rise to our observed bands at 1276 and 952 cm.$^{-1}$ for *t*-butanol-*d*.

Other Alcohols.—It appears to be almost universal in alcohols for the δ_{COH} band, in the range *ca.* 1250 to *ca.* 1400 cm.$^{-1}$, to be coupled with one of two overlapping bands in the range *ca.* 1000 to *ca.* 1200 cm.$^{-1}$, one of which is the ν_{C-OH} band.[5] In our interpretation of the *t*-butanol and "potassium *t*-butoxide" spectra, ν_{C-OH} is most plausibly assigned as the consistently strong band at *ca.* 1210 cm.$^{-1}$. Also, it does not appear likely that non-bonding forces, between the C and H atoms of the COH group involved, would be sufficiently strong to produce special coupling of the δ_{COH} and ν_{C-OH} motions. We therefore tentatively suppose

---

(26) R. C. Lord and F. A. Miller, *Applied Spectroscopy*, **10**, 115 (1956).

that coupling of the δ_{COH} motion in alcohols involves only CH bending motions.[27] Thus, it may be concluded from the extensive work of Stuart and Sutherland[9] that δ_{COH} is coupled with CH motions having frequencies in the 1400 to 1450 cm.$^{-1}$ region in the case of most primary and secondary alcohols, and bands in this region almost certainly cannot be confounded with ν_{C-OH} or any other skeletal motion. This in itself strongly suggests that δ_{COH} should be able to couple with CH bending motions of lower frequency in the 900 to 1200 cm.$^{-1}$ region. In the case of pure ethanol,[6,9] for example, we would assign δ_{COH} at 1330 cm.$^{-1}$ and ρ_{CH_3} at 1092 cm.$^{-1}$ by analogy with *t*-butanol. The additional band at 1419 cm.$^{-1}$ associated with the COH bending motion in pure ethanol, we would assign to the wagging motion of the CH_2 group. The situation of three coupled bands probably arises through rotational isomerism in the associated liquid, as indicated by the structures *B* and *C*.

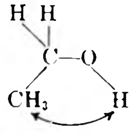

B

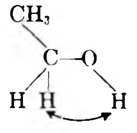

C

The coupling of the CH_2-wagging motion seems to disappear in monomeric ethanol.[5,6] Thus structure *C* may not be important in the monomeric alcohol as a result of free rotation of the COH group. (This effect has been pointed out previously in the case of polyvinyl alcohol, which is very similar to ethanol.[8]) The δ_{C-OD} band for pure ethanol-*d* occurs distinctly at 956 cm.$^{-1}$ but the positions of the corresponding coupled CH bands have not been discovered[6,9,28] (*cf.* Fig. 2).

---

[27] This is almost certainly the case for methanol; *cf.* C. Tanaka, K. Kuratani and S. Mizushima, *Spectrochimica Acta*, **9**, 265 (1957).

[28] D. Hadzi and D. Jeramic, *Spectrochimica Acta*, **9**, 263 (1957).

THE EMULSION POLYMERIZATION OF VINYL ACETATE. PART I[1]

BY R. PATSIGA, M. LITT AND V. STANNETT

Department of Chemistry, State University College of Forestry at Syracuse University Syracuse 10, New York

Received January 16, 1960

The emulsion polymerization of vinyl acetate and styrene at 60° has been studied using a polyvinyl acetate seed. A rate constant for the polymerization of styrene of 153 l./mole/sec. was found in good agreement with other work. It was shown that much, and possibly most, of the vinyl acetate emulsion polymerization occurred in the water phase. When vinyl acetate is polymerized using an anionic surfactant, the polymer is stabilized in the water phase by adsorption of the soap. Eventually it is swept up by a polymer particle and continues growing there, but chain transfer to monomer produces a small radical which diffuses out of the particle and grows in the water phase as before. Evidence is given to support this view.

Introduction

The kinetics of emulsion polymerization of non-water-soluble monomers such as styrene, butadiene or isoprene, stabilized with a soap or ionic detergent has been studied by Harkins,[2a] and Smith and Ewart,[2b] and Smith[3] and the salient characteristics elucidated. Recently all information pertaining to emulsion systems has been collected.[4]

The standard Smith–Ewart picture[2b] is as follows: Radicals are generated in the water phase when a water-soluble initiator is used, *e.g.*, $K_2S_2O_8$, diffuse into a micelle where there is a high concentration of monomer and initiate polymerization to produce soap stabilized particles. These continue to form until the soap has been exhausted. The number of particles formed is proportional to the soap concentration to the $^3/_5$ power, and to the initial rate of free radical production to the $^2/_5$ power. After the soap is used up and while a separate monomer phase exists, up to 50–60% conversion with styrene, the rate of polymerization is independent of conversion and persulfate concentration. When the monomer phase disappears, the rate of polymerization starts to decrease.

Very little has been published on the emulsion polymerization of vinyl acetate using a soap or ionic emulsifier. Most of the investigators have used non-ionic detergents[5,6] which do not form micelles. The present work was undertaken to elucidate the mechanism of the micellar emulsion polymerization of vinyl acetate.

The method of approach was to study the polymerization of styrene and vinyl acetate monomers using a polyvinyl acetate seed. Rates of polymerization were determined and the resultant particle sizes of the lattices were measured. A comparison of styrene, which polymerizes only in the particles, with vinyl acetate, enabled us to study the basic differences between the two systems. It was found that the Smith–Ewart[2b] kinetics were inapplicable to the vinyl acetate system.

Experimental

Materials.—Commercial grade vinyl acetate and styrene were purified by distillation under nitrogen before use. Sodium lauryl sulfate and analytical grade $K_2S_2O_8$ were used as received.

Apparatus and Procedures.—**Preparation of Seed.**—The seed emulsion was made by preparing 900 ml. of an aqueous solution containing sodium lauryl sulfate 6.6 g. and $K_2S_2O_8$ ($8 \times 10^{-4}M$), adding 110 g. of vinyl acetate,

---

[1] This paper was presented at the Division of Polymer Chemistry at the American Chemical Society Meeting in April, 1960.

[2] (a) W. D. Harkins, *J. Chem. Phys.*, **13**, 381 (1945); **14**, 47 (1946); *J. Am. Chem. Soc.*, **69**, 1428 (1947). (b) W. V. Smith and R. H. Ewart, *J. Chem. Phys.*, **16**, 592 (1948).

[3] W. V. Smith, *J. Am. Chem. Soc.*, **70**, 3695 (1948); **71**, 4077 (1949).

[4] F. A. Bovey, I. M. Kolthoff, A. I. Medalia and E. J. Meehan, "Emulsion Polymerization," Interscience Publ. New York, N. Y., 1955.

[5] J. T. O'Donnell, R. B. Mesrobian and A. E. Woodward, *J. Polymer Sci.*, **28**, 171 (1958).

[6] D. M. French, *ibid.*, **32**, 395 (1958).

and stirring under N_2 for two hours at 60° to polymerize all the monomer. The persulfate in the seed latex was determined by a colorimetric method.[7]

Seed Polymerization.—The seed was used as prepared above, or the water phase was diluted three- or ten-fold. Potassium persulfate was added to bring its concentration in the water phase to 8×10^{-4} *M*. Enough monomer was then added so that the emulsion contained 25% solids by weight after polymerization. The rate of polymerization at 60° was then determined dilatometrically[7] while stirring under N_2.

Electron micrographs of the polymer were made by Dr. W. Coté of the College of Forestry. The polymer was first iodinated by adding iodine crystals and a trace of KI to the diluted emulsion. There was no coagulation if the salt concentration was kept low. Photomicrographs were then taken of the unshadowed polymer. The photographic negatives were projected and particle diameters measured on the projection with a millimeter scale.

The turbidities of the polyvinyl acetate latices at scattering angles of 0, 45, 90 and 135° were measured by the standard procedure[8] using a Brice–Phoenix Light Scattering Photometer. The refractive index change with concentration was assumed to vary linearly as the volume fraction of polymer thus

$$\frac{dn}{dc} = \frac{1.467 - 1.333}{1.13} = 0.118$$

Measurements were taken at wave lengths of 436 and 546 mμ.

Results and Discussion

Average Particle Sizes.—Diameters of 150 to 350 particles were measured from the electron photomicrographs for each latex, and number and weight average volumes calculated.

$$\bar{V}_n = \frac{\pi/6\Sigma N_iD_i^3}{\Sigma N_i} \tag{1}$$

$$\bar{V}_w = \frac{\pi/6\Sigma N_iD_i^6}{\Sigma N_iD_i^3} \tag{2}$$

The weight average volumes then could be compared with the volumes determined from turbidity measurements in the case of the polyvinyl acetate latices (see Table I). It would have been possible to obtain average volumes for the polyvinyl acetate–polystyrene latices by extrapolating to zero angle. This was not carried out, however, as the turbidity measurements were used only to check the electron photomicrograph values and the correlation for polyvinyl acetate emulsion was considered satisfactory.

Table I

Variation of Rate of Polymerization and Particle Size with Seed Concentration

Expt. no.	Water phase vol. seed / final vol.	Monomer polymerized	Particle volume ($cm.^3 \times 10^{16}$)			Rate of polymn. moles/min./180 cc. H_2O
			Electron microscope		Turbidity	
			$\bar{V}_n$	$\bar{V}_w$	$\bar{V}_w$	
51	Seed	VAc	(0.95)[b]	(1.02)[b]	0.23–0.35[c]	....
53	1/1	VAc	1.73	3.76	....	0.0120
60	1/3	VAc	3.95	6.08	4.92	.0102
57	1/3	VAc	3.51	4.94	4.85	00805
61[a]	1/10	VAc	5.08	9.12	8.15	0096
54	1/1	Styrene	1.83			.0137
59	1/3	Styrene	2.72			0076
62	1/10	Styrene	4.60			.0043$_2$
64	1/10	Styrene	4.56			.0045$_7$

[a] Concentration of $K_2S_2O_8$ was 5.0×10^{-4}. [b] Measured volume much too high. See Discussion. [c] Six determinations over a tenfold concentration range gave these values. If one extrapolates to zero concentration, $\bar{V}_w = 0.35 \times 10^{-16}$ cm.³. Hc/τ did not vary with concentration for the other emulsions.

Since the particles were not shadowed for the electron photomicrographs the edges were not sharply defined, which caused measurement errors. These were, of course, more important in the measurement of smaller particles, and no particles smaller than 0.03 to 0.04 μ were visible because they were transparent to the electron beam. Depending on the size of the particles, the maximum error in measurement of the average diameter was estimated as 3 to 7%. The volume error is therefore 10–20% which is greater than the difference in $\bar{V}_w$'s for the two methods except for the seed.

The agreement in volume measurements by the two different methods in expt. 60, 57 and 61 indicates that both methods are accurate for large particles. The electron photomicrograph for expt. 51, the seed, had no particles with a diameter larger than 0.07 μ. Particles slightly smaller than this were already difficult to measure due to lack of contrast.

The light-scattering volume, $\bar{V}_w = 0.35 \times 10^{-16}$ cm.³, is the real one, and shows that most of the seed polymer particles are too small to be measured by electron microscope using a direct viewing technique. Our turbidimetric value compares well with W. J. Priest's electron microscope value of $\bar{V}_n = 0.2 \times 10^{-16}$ cm.³, using a similar recipe.[9] He used a gold shadowing technique which enabled him to measure much smaller particles.

If we estimate $\bar{V}_n$ for the seed at about 0.15×10^{-16} cm.³, one-half $\bar{V}_w$, the average ratio for the final latices, then the number average molecular weight per particle is 10,000,000. (We will show later that $\bar{V}_n$ cannot be larger than this estimate.) Since there are larger particles, there also must be smaller particles present. However, much smaller particles will probably be in true solution rather than emulsion. It has been shown that polyvinyl acetate of the order of 0.3 g./l. and less can be dissolved in dilute soap or alkyl sulfonate solutions[10–12] to give clear or opalescent solutions. By turbidity[11,12] or viscosity[10] measurements, the polymer was found to be dissolved molecularly, with adsorbed soap molecules causing it to act as a polyelectrolyte. In our case, since much of the polymerization is in the water phase (see later discussion), the same phenomenon will occur during the formation of polymer, producing stabilized polymer molecules or small aggregates, as well as larger particles.

Recent qualitative experiments at this Laboratory tend to confirm the above conclusion. The seed latex was precipitated by adding an equal volume of 10% NaCl or $MgSO_4$ solution and filtered through a medium sintered glass filter. The filtered supernatant liquid was slightly opalescent. Saponification analysis showed it contained 0.4 g. of polyvinyl acetate per 100 cc. of original seed latex. When the coagulum was washed with water the ex-

---

(7) R. Patsiga, M. Litt and V. Stannett, to be published.

(8) Operation Manual OM-1000 Phoenix Precision Instrument Co., 1955.

(9) W. J. Priest, This Journal, **56**, 1077 (1952).

(10) N. Sata and S. Saito, *Kolloid Z.*, **128**, 154 (1952).

(11) W. Prins and J. J. Hermans, *Proc. Kon. Ned. Akad. Van Wetensch., Amsterdam*, **B59**, 298 (1956).

(12) T. Isemura and A. Imanishi, *J. Polymer Sci.*, **33**, 337 (1958).

tractable polymer rose to 1.2 g. per 100 ml. seed. In this case, though, the extract was definitely turbid. Since the initial solids concentration was 10 g. per 100 cc., at least 4% of the seed was in the form of individual polymer molecules or very small aggregates which could not be precipitated by the ordinary techniques.

A test for the presence of polymer in the plasma is its reaction with iodine. When polymer is present, the solution turns deep red-violet from an amount of iodine that would barely color water. It is very likely that soluble polymer was the cause of trouble in persulfate determinations which liberated iodine. When this test was used on plasmas from expt. 54 and 60, no polymer whatever was found, indicating that all microparticles and free polymer molecules had disappeared with further polymerization.

One can calculate the number of particles in each latex, and from this estimate the number of particles produced from each ml. of seed latex. If one assumes $\bar{V}_n = 0.15 \times 10^{-16}$ cm.^{3} for seed particles, the apparent efficiency of particle survival can be estimated.

If all the particles in the final latex are produced from the seed, Table II shows that the average seed particle size can be no larger than 0.15×10^{-16} cm.^{3}, and may be smaller. The closer correspondence between the fraction of particles retained for a given dilution for both the styrene and vinyl acetate cases indicates that no new particles are formed, since it is well known that this is true for the case of styrene.[3,4] In a similar system, French[6] found that the number of polyvinyl acetate particles was constant after 20% conversion. At high concentrations most of the seed nuclei agglomerate, but with dilution the particles have a better chance to grow independently. At the highest dilution investigated, most of the seed nuclei survive as separate particles.

TABLE II

RETENTION OF PARTICLES WITH DILUTION

Expt. no.	Added monomer	Seed diln. factor initial/final vol. H_2O	No. of particles per cc. H_2O $\times 10^{-15}$	No. of particles retained $\times 10^{-15}$ per cc. H_2O of initial seed	Fraction of original particles retained
51	....	Seed	6.6	6.6	..
53	Vinyl acetate	1/1	1.7	1.7	0.26
60	Vinyl acetate	1/3	0.75	2.25	.34
57	Vinyl acetate	1/3	.84	2.52	.38
61	Vinyl acetate	1/10	.58	5.80	.88
54	Styrene	1/1	1.60	1.60	.24
59	Styrene	1/3	1.08	3.24	.49
62	Styrene	1/10	0.641	6.41	.97
64	Styrene	1/10	0.646	6.46	.98

[a] $\bar{V}_n$ assumed 0.15×10^{-16} cm.^{3}.

Finally, what is the dependence of polymerization rate on particle concentration? Since all the latices had the same solids concentration, and all except one the same persulfate concentration, they are directly comparable. The data are presented in Table III and Fig. 1.

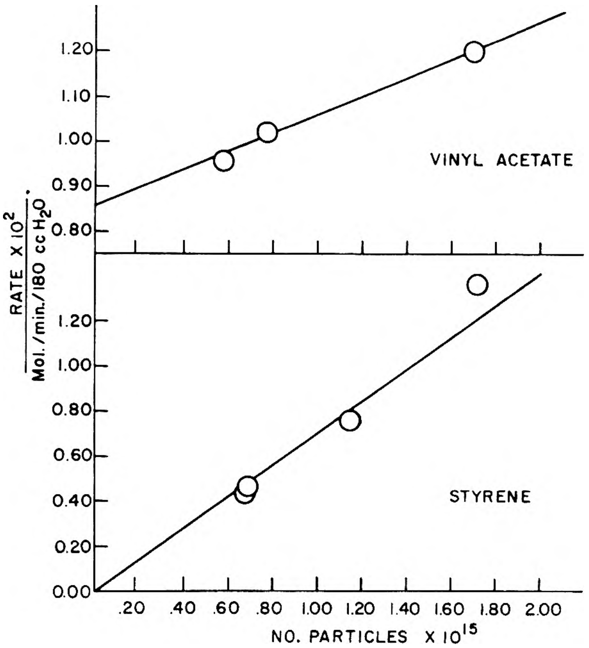

Fig. 1.—Rate of polymerization of styrene and vinyl acetate *vs.* number of particles using a vinyl acetate seed.

TABLE III

VARIATION OF POLYMERIZATION RATE WITH PARTICLE CONCENTRATION

Expt. no.	Monomer polymerized	No. particles per cc. H_2O $\times 10^{-15}$	Rate of polymn. moles/min. 180 cc. H_2O
53	Vinyl acetate	1.70	0.0120
60	Vinyl acetate	0.75	.0102
57	Vinyl acetate	0.84	.00805
61[a]	Vinyl acetate	0.58	.0096
54	Styrene	1.72	.0137
59	Styrene	1.15	.0076
62	Styrene	0.68	.00432
64	Styrene	0.69	.00457

[a] Concn. of $K_2S_2O_8$ was 5.0×10^{-4} *M*.

Styrene.—The styrene data plotted in Fig. 1 show that the rate of polymerization is zero when the particle concentration is zero, as it should be if all polymerization occurs in the particles. Making the standard assumptions, that half the particles are polymerizing at any one time and the equilibrium concentration of styrene in the particles is 5.2 mole/l.[13] in the region of 30 to 60% conversion, the absolute rate constant of polymerization was found to be 153 l./mole/sec. at 60°. This compares well with the data of other investigators who have found 176,[14] 120[15] and 204[13] when calculated for 60°.

Vinyl Acetate.—The data for vinyl acetate in Table III and Fig. 1 are extremely interesting. If we assume all polymerization is in the particles, then a log-log plot shows that the rate of polymerization is proportional to the 0.2 power of the number of particles. If the usual assumption is made, that the polymerization rate in the particles is proportional to the number of particles, then one must conclude that polymerization within the par-

---

(13) M. Morton, P. P. Salatiello and H. Landfield, *J. Polymer Sci.*, **8**, 279 (1952).

(14) M. S. Matheson, E. E. Auer, E. B. Bevilacqua and B. J. Hart, *J. Am. Chem. Soc.*, **73**, 1700 (1951).

(15) A. M. Burnett, *Trans. Faraday Soc.*, **46**, 772 (1950).

ticles is relatively unimportant and that most of the polymerization is taking place in the water phase!

There is much evidence to support the second conclusion: 1. Other work in this Laboratory[7] has shown the rate of polymerization to be independent of soap concentration over a very wide range, and thus presumably independent of particle concentration. 2. We have also found[7] that the rate of conversion in an ordinary emulsion polymerization is proportional to the persulfate concentration to the first power. 3. After the initiation period, the rate of polymerization remains constant until 80–85% conversion, although the separate monomer phase disappears at or before 35% conversion. Data from other investigators show the same phenomenon,[5,6] and were presented without comment. A constant rate will be found when the reaction medium has a constant composition, and the only such medium in this system is the water phase. Since the activity of monomer dissolved in polymer is almost unity, the latex particles will act as a monomer reservoir, keeping the water saturated with vinyl acetate. After 80–85% conversion, there is not enough monomer left to saturate the water phase.

Although we do not have enough data to present a quantitative picture of vinyl acetate emulsion polymerization, we feel that the following picture is accurate in its main outlines and different enough from other emulsion polymerizations to be worth presenting in its present incomplete state.

The discussion given will consider a system of 25% solids after reaction. Other solids concentrations will alter the conversions quoted, but will not change the picture.

During the initial phase of polymerization, soluble polymer molecules are produced which are stabilized in that form by the soap; these probably function as nuclei for further polymerization and thus become monomer swollen polymer particles. When the surface area of the particles exceeds the covering power of the soap, the remaining polymer molecules and micro-particles are partly destabilized and can be swept up by the larger particles.

During the main portion of the reaction, after the separate monomer phase has vanished, from about 20 to 80% conversion, the number and size of the particles have become constant and the course of polymerization is envisioned as follows: Initiation and much, or most, of the polymerization is in the water phase. The growing polymer in the water phase is partly stabilized by soap molecules which delays its absorption by a large particle. There probably is chain transfer to monomer and polymer in the water phase, but this does not appear in the kinetic picture. Eventually, the polymer molecule is absorbed by a particle, and polymerization then proceeds in the particle until chain transfer to monomer occurs. The monomer free radical diffuses out of the particle and polymerization continues in the water phase until the new polymer molecule is again swept up. It can be shown that the low molecular weight free radical produced by chain transfer will diffuse without reaction from a particle of 0.1 μ diameter at least 99 times out of 100.[16]

When we consider the concentration of monomer in the water and polymer phases,[17] it can be seen that, for example, with the same amount of polymerization per radical in each phase, the radical will spend only 4 to 20% of its time in the polymer phase. The exact proportion will depend on the monomer concentration in the particles since the rate of chain transfer to monomer depends on this. It will be 4% initially and rise slowly as the monomer is depleted until it amounts to 20% of the total time at 80% conversion. Since the time of residence in the water phase remains constant (because the water phase is invariant), the rate of polymerization, with this hypothesis, will decrease 15% in the interval of 20 to 80% conversion, a factor which is too small to pick up by the usual kinetic methods. When the concentration of monomer falls below 0.5 M over-all, there is not enough left in the polymer particles to replenish the water phase, and the rate of polymerization starts to drop rapidly to zero.

The termination step may be some obscure zero-order reaction, or the standard emulsion termination when two radicals enter the same particle. There is also a possibility of radical–radical termination in the water phase. As yet there is not enough information to decide whether any of these is correct.

We wish to thank the National Starch and Chemical Corporation for their generous support of this work, and Drs. A. I. Goldberg and A. Loebel for helpful suggestions and discussions.

[16] A similar view with respect to oil soluble catalysts was expressed recently by H. Edelhauser and J. W. Breitenbach, *J. Polymer Sci.*, **35**, 423 (1959).

[17] At 60°, the solubility of vinyl acetate in water is 0.33 mole/l.[7] If there is no separate monomer phase the concentration in the polymer is about 8 M at 20% conversion and 1.4 at 80% conversion.

A RATE EQUATION FOR THE FISCHER-TROPSCH SYNTHESIS ON IRON CATALYSTS

By ROBERT B. ANDERSON[1] AND FRED S. KARN[1]

Branch of Coal-to-Oil Research, Division of Solid Fuels Tech., Bureau of Mines, Region V, Pittsburgh, Penna.

Received January 18, 1960

The kinetics of the Fischer–Tropsch synthesis on iron catalysts has been investigated as a part of Bureau of Mines' studies on coal-to-oil processes. A rate equation, $r = a'p_{H_2}^{0.6}p_{CO}^{0.4} - f'r^{0.5}p_{H_2O}^{0.5}$, where r is the differential reaction rate, p_{H_2}, p_{CO} and p_{H_2O} are the partial pressures of H_2, CO and water vapor, and a' and f' are rate constants, was shown to be reasonably accurate. The equation is based on current concepts of the reaction mechanism: A complex C_1 of the type 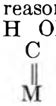 $\overset{\text{H}\ \ \text{OH}}{\underset{\underset{\text{M}}{\|}}{\text{C}}}$ is formed from adsorbed reactants. This C_1 complex may react with C_1 and complexes of higher carbon number to produce hydrocarbons, or it may be removed by reaction with water vapor.

The earlier kinetic data for the Fischer–Tropsch synthesis on iron catalysts reviewed by Anderson[2] and Tramm[3] and Uchida, *et al.*,[4] have proposed kinetic equations. Hall, Kokes and Emmett[5] have interpreted a semi-empirical equation of Anderson[2] in terms of more recent information on the mechanism of the synthesis. Recently, Frye, Pickering and Eckstrom[6] described the kinetics of the Fischer–Tropsch synthesis on iron catalysts at substantially higher temperatures (300–340°) than had been used in most previous studies. In this temperature range, time-dependent changes of rate occurred after variations in operating conditions. Powers has proposed rate equations that approximate both steady-state and transient conditions.[7]

The previous analyses of kinetic data from our laboratory have shown that the initial reaction rate r_0 in terms of $H_2 + CO$ consumed[8] can be approximated by

$$r_0 = k_1 p_{H_2}^{n} p_{CO}^{1-n}$$

where k_1 is a constant with an activation energy of about 20 kcal./mole, p_{H_2} and p_{CO} are, respectively, the partial pressures of hydrogen and carbon monoxide, and n is about 0.66.[9] In general the rate may be approximated by $r = f(x)g(P)h(T)$, where $f(x) \sim (1 - x)^{0.5 \text{ to } 1.0}$, $g(P) \sim P$, and $h(T) \sim \exp(-20 \text{ kcal. mole}^{-1}/RT)$; in these expressions x is the fraction of $H_2 + CO$ reacted and P the operating pressure. The function $f(x)$ may be approximated by $n_g/(1 + bn_{H_2O})$ or by $n_g(1 - cn_{H_2O})$ where n_g and n_{H_2O} are the mole fractions of $H_2 + CO$ and water vapor, respectively, and b and c are constants.[10] The equations of Tramm[3] have as their principal terms $p_{H_2}^{n}/p_{CO}$, where n is 1 or 2. This expression does not fit the data from Bureau of Mines experiments with fused iron catalysts. The equations of Uchida[4] fail to express the variation of rate with operating pressure.[10]

Experiments in which water vapor, CO_2 and CH_4 were added to the feed indicate that water vapor and CO_2 are, respectively, strong and weak inhibitors or temporary poisons and that CH_4 is only a diluent.[11]

In the present paper a rate equation is developed in terms of fractional coverages of the surface by reactants and products. These surface coverages are then approximated by Freundlich isotherms, that is the coverage by component i is proportional to the partial pressure of i to a positive exponent less than one. This approximation has been shown to be valid in a number of systems.[12–13] Exponents of the partial pressure terms were adjusted to make the equation consistent with observations cited in the foregoing, and the equation was tested in a differential form.

A Semi-fundamental Rate Equation.—The present development follows a simplified version of the scheme of chain growth postulated by Storch, Golumbic and Anderson.[14] An intermediate C_1 of the type 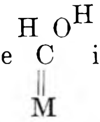 $\overset{\text{H}\ \ \text{O}^{\text{H}}}{\underset{\underset{\text{M}}{\|}}{\text{C}}}$ is formed on the catalyst surface by the reaction of adsorbed H and CO. Intermediate C_1 reacts with other intermediates C_1, C_2, ... C_n to form the next higher intermediate or is removed by reaction with water vapor, according to

---

[1] Physical Chemist, Bureau of Mines, Region V, U. S. Department of the Interior, Pittsburgh, Pa.

[2] R. B. Anderson, in "Catalysis," Vol. 4, Chap. 3, edited by P. H. Emmett, Reinhold Publ. Corp., New York, N. Y., 1956, pp. 257–372.

[3] H. Tramm, *Brennstoff-Chem.*, **33**, 21 (1952).

[4] H. Uchida, M. Kuraishi, H. Ichinokawa and K. Ogawa, *Bull. Chem. Soc., Japan*, **29**, 181 (1956).

[5] W. K. Hall, R. J. Kokes and P. H. Emmett, *J. Am. Chem. Soc.*, **82**, 1027 (1960).

[6] C. G. Frye, H. L. Pickering and H. C. Eckstrom, THIS JOURNAL, **62**, 1508 (1958).

[7] J. E. Powers, *ibid.*, **63**, 1219 (1959).

[8] In this paper unless specifically mentioned the differential reaction rate is defined as volumes (S.T.P.) of $H_2 + CO$ reacted per volume of catalyst space per hour, as given by $r = dx/d(1/S)$, where x is the fraction of $H_2 + CO$ reacted and S is the hourly space velocity expressed as volumes (S.T.P.) of $H_2 + CO$ fed to the reactor per unit volume of catalyst space per hour. The subscript zero denotes an extrapolated differential reaction rate at $x = 0$. In a later part of the paper a differential reaction rate in terms of volumes of CO reacted per unit volume of catalyst per hour is also used.

[9] F. S. Karn, B. Seligman, J. F. Shultz and R. B. Anderson, *ibid.*, **62** 1039 (1958).

[10] F. S. Karn, J. F. Shultz and R. B. Anderson, *ibid.*, **64**, 446 (1960).

[11] F. S. Karn, J. F. Shultz and R. B. Anderson, submitted to International Congress on Catalysis, Paris, July, 1960.

[12] (a) S. Weller, *A.I.Ch.E. J.*, **2**, 59 (1956); (b) M. Boudart, *ibid.*, **2**, 62 (1956).

[13] O. Stelling and O. V. Krusenstierna, *Acta Chem. Scand.*, **12**, 1095 (1958).

[14] H. H. Storch, N. Golumbic and R. B. Anderson, "The Fischer-Tropsch and Related Syntheses," John Wiley and Sons, New York, N. Y., 1951, pp. 582–593.

$$2H_{ads} + CO_{ads} \longrightarrow C_1 \qquad (1)$$

$$C_1 + \left\{\begin{array}{l} C_1 \\ C_2 \\ \vdots \\ C_n \\ \vdots \end{array}\right. \longrightarrow \left\{\begin{array}{l} C_2 \\ C_3 \\ \vdots \\ C_{n+1} \\ \vdots \end{array}\right. + H_2O \qquad (2)$$

$$C_1 + H_2O_{ads} \longrightarrow 2H_2 + CO_2 \qquad (3)$$

Intermediates C_i desorb from the surface at a rate proportional to their concentration to form product of carbon number i. According to previous chain growth postulates[15] $C_n \cong C_1\alpha^{n-1}$, where α is a constant, $0 < \alpha < 1$, and $\sum_1^\infty C_i = C_1/(1 - \alpha) = C_1g$, where $g = 1/(1 - \alpha)$.

Reactions 1, 2 and 3 are postulated to control the rate of synthesis. The rate of formation of C_1 is given as

$$r_1 = a\theta_H{}^2\theta_{CO} \qquad (4)$$

and the rate of removal of C_1 by equations 2 and 3

$$\begin{aligned} r_{2,3} &= b\theta_1\left(\sum_1^\infty \theta_i\right) + c\theta_1\theta_{H_2O} \\ &= b\theta_1{}^2g + c\theta_1\theta_{H_2O} \qquad (5) \end{aligned}$$

where a, b and c are rate constants, and θ_H, θ_{CO}, θ_{H_2O}, θ_1 and θ_i are, respectively, the fractional coverage of the surface by hydrogen atoms, CO, H_2O and C_1 and C_i intermediates. For steady-state conditions, $r_1 = r_{2,3}$ and

$$a\theta_H{}^2\theta_{CO} = bg\theta_1{}^2 + c\theta_1\theta_{H_2O} \qquad (6)$$

The rate of synthesis measured in terms of H_2 + CO consumed (or hydrocarbon produced) may be given as

$$r = bg\theta_1{}^2 \qquad (7)$$

and from 6

$$\begin{aligned} r &= a\theta_H{}^2\theta_{CO} - c\theta_1\theta_{H_2O} \\ &= a\theta_H{}^2\theta_{CO} - (c/\sqrt{bg})r^{1/2}\theta_{H_2O} \qquad (8) \end{aligned}$$

It is now assumed that surface coverages may be approximated by $\theta_j = m_jp_j{}^{n_j}$, where m_j and n_j are constants ($0 < n_j < 1$) and p_j is the partial pressure of component j. The exponents of these Freundlich isotherms are adjusted to provide the observed dependence of rate on total pressure and on gas compositions, leading to a final equation

$$r = a'p_{H_2}{}^{0.6}p_{CO}{}^{0.4} - f'r^{0.5}p_{H_2O}{}^{0.5} \qquad (9)$$

where $a' = am^2{}_Hm_{CO}$ and $f' = cm_{H_2O}/\sqrt{bg}$. The exponents of p_{H_2} and p_{CO} differ slightly from those of the previous paper[9] and were chosen by trial and error to provide better agreement with available experimental data.

The integration of rate equation 9 is virtually impossible, especially because the usage ratio, H_2/CO, is not constant. Therefore, the rate data were differentiated to yield the differential reaction rate. The rate equation was then tested in the linear form

$$p_{H_2}{}^{0.6}p_{CO}{}^{0.4}/r = (1/a') + (f'/a')p_{H_2O}{}^{0.5}/r^{0.5} \qquad (10)$$

Differentiation of Rate Data and Test of Equation.—Differential reaction rates were obtained by numerical or graphical differentiation of data reported previously for synthesis on 6- to 8-mesh nitrided iron catalysts D3001 with feed gas ratios of H_2/CO of 2, 1, 0.7 and 0.25 at 21.4 atm. and 225 and 240°.[9] Smooth curves were passed through plots of conversion of H_2+CO, x, as a function of reciprocal hourly inlet space velocity, S^{-1}, for each set of experimental data, and values of x were read from the curves at small equal intervals of S^{-1}.

Two methods of differentiation were used. In the first, at each point a four-constant polynomial was fitted to the reference point and three equal intervals immediately above and below it by a central difference equation involving least squares methods.[16] The differential reaction rate, $r = dx/dS^{-1}$ at the reference point, is then given by the coefficient of the second term of the polynomial. The second method used log–log plots as described previously.[17] The results by the two methods were essentially the same, except for conversions greater than 0.6, where the log–log method became difficult to apply. Derivatives obtained for known curves usually deviated from actual values by less than 3%. Values of r at zero conversion were averages obtained from $^1/_2$- and 1st-order empirical equations.[8] The numerical differentiation resulted in smooth plots of the derivatives as a function of conversion as shown in Fig. 1. Plots of equation 10 were made from these values of r and partial pressures of H_2, CO and H_2O, as shown in Fig. 2, where the positions of the lines were determined by least squares. As the values of rate and partial pressure of water vapor have uncertainties of about ±5%, the equation is considered to be a satisfactory representation of the data. Also plotted on Fig. 2 are three points for initial reaction rates obtained from water addition experiments at 240°.[11] These values obtained with a different charge of the same catalyst agree reasonably well with data from experiments in which no water was added. Values of constants of equation 9 and activation energies are given in Table I. The activation energy of constant a' is similar to that obtained by empirical methods.[9] At low to moderate conversions the rate is determined principally by the first term of equation 9.

TABLE I

CONSTANTS OF EQUATION 9 FOR SYNTHESIS ON NITRIDED, FUSED IRON CATALYST D3001 AT 21.4 ATM.[9]

	Temp., °C.		Activation energy, kcal./mole.
	225	240	
a' (atm.$^{-1}$ hr.$^{-1}$)	15.2	27.6	20.2
f' (atm.$^{-1/2}$ hr.$^{-1/2}$)	1.67	2.87	18.5

As a test of the accuracy of equation 9, values of r were computed for each of the points in Fig. 1 using constants in Table I, and the relative error, $(r_c - r_{obsd})/r_{obsd}$ where r_c and r_{obs} are, respectively,

---

(15) R. A. Friedel and R. B. Anderson, *J. Am. Chem. Soc.*, **72**, 1212 (1950).

(16) A six-constant equation could be fitted exactly to the seven points; however, this equation would accentuate fluctuations of the data, and would represent the trend of the curve less satisfactorily.

(17) R. B. Anderson, *Ind. Eng. Chem.*, **52**, 89 (1960).

the calculated and observed values of the differential reaction rate, was computed. Five of the 49 calculated values, all at relatively high conversions, deviated from the observed by more than 20%. For the remainder, the average of absolute values of relative error was 5.5%. In addition systematic deviations were noted. For feed gases containing $2H_2 + 1CO$ and $0.25H_2 + 1CO$, calculated rates were smaller than observed, and for $0.7H_2 + 1CO$ they were larger. Changing the exponents of the first term of equation 9 from $p_{H_2}{}^{0.6}p_{CO}{}^{0.4}$ to $p_{H_2}{}^{0.66}p_{CO}{}^{0.34}$ improved the plots somewhat for all feed gases except $0.25H_2+1CO$, but for this feed gas deviations from the best line were much larger. The exponents used in equation 9 seem to be the best choice.

In developing equation 9 the production of all of the CO_2 was not ascribed to reaction 3. In equation 9 the first term is a measure of the total CO consumed and the second term is the CO converted to CO_2. Our results indicate that processes other than reaction 3 must also produce CO_2. First, the second term in equation 9 is too small to cause the observed production of CO_2. Second, if all CO_2 were produced by equation 3, the quantity $r_{CO}/p_{H_2}{}^{0.6}p_{CO}{}^{0.4}$ should be constant for a given temperature. The quantity $r_{CO} = dx_{CO}/d(1/S_{CO})$, where x_{CO} is the fractional conversion of CO and S_{CO} the volumes of CO (S.T.P.) fed to the reactor per volume of catalyst space per hour, was determined by numerical differentiation. The values of $r_{CO}/p_{H_2}{}^{0.6}p_{CO}{}^{0.4}$ were not constant.

For a given feed gas, CO_2 production compared at constant conversions is essentially independent of temperature and pressure. Thus, the processes producing CO_2 have about the same dependence on temperature and pressure as the primary synthesis reaction. Kul'kova and Temkin[18] presented a rate equation for the water-gas shift on iron oxide catalysts that at least qualitatively describes the production of CO_2 in the Fischer-Tropsch synthesis in terms of gas composition and has the same dependence on operating pressure as the synthesis.[10] The activation energy of the principal constant of this equation was 16.5 kcal./mole in the temperature range 400 to 500°.

In synthesis experiments with iron catalysts in which $C^{14}O_2$ was added to $1H_2 + 1CO$ feed, Hall, Kokes and Emmett[19] reported that C^{14} was not found in sizable quantities in either the carbon monoxide remaining or hydrocarbons produced. This result could arise from the situations: (a) All the CO_2 is produced by a series of steps, of which at least one is irreversible, coupled with the primary synthesis reaction, or (b) the water-gas shift occurs, but the reverse reaction is slow compared with the forward reaction. The present rate equation requires the production of most of the CO_2 by processes other than the postulated primary synthesis reactions. For the Kul'kova-Temkin equation with concentrations typical of the synthesis, the rate of the reverse shift is only about 2% of the forward reaction. Thus, the reverse shift may be sufficiently slow to explain the results of Hall, Kokes and Emmett.[19]

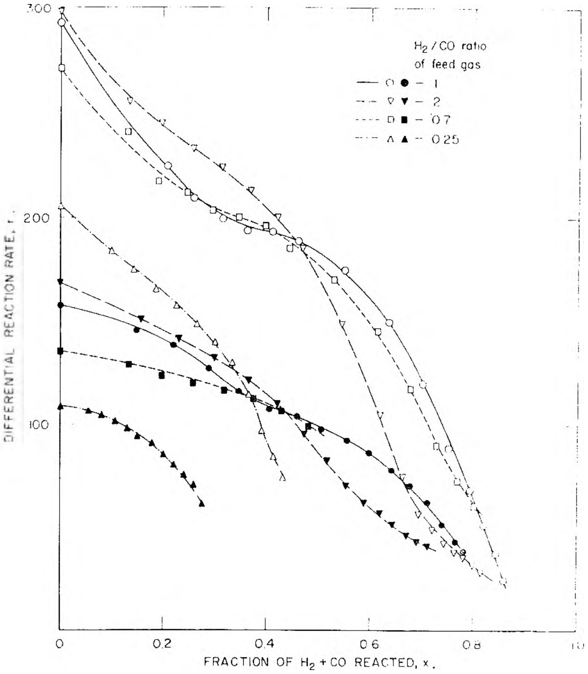

Fig. 1.—Differential reaction rates obtained by numerical differentiation. Open symbols denote 240° and solid 225°.

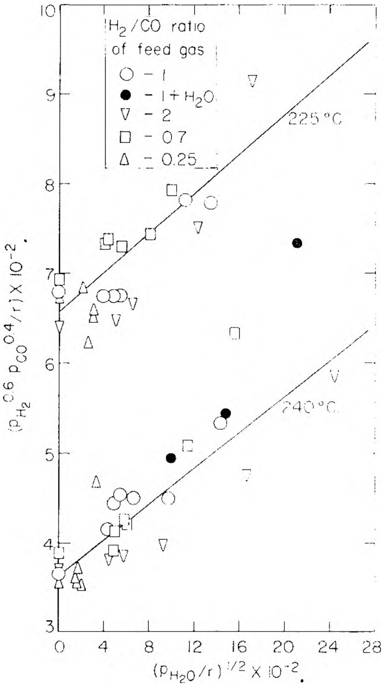

Fig. 2.—Plots of equation 9 for nitrided fused iron catalyst D-3001 at 21.4 atm.

Although the kinetic equation presented here was derived from a simple model based on available concepts of the reaction mechanism, it must be regarded as a semifundamental rate expression for the reasons: (1) Surface coverages are approximated by Freundlich isotherms with the exponents adjusted to provide the observed dependence of rate on gas composition and total pressure; (2)

---

(18) N. W. Kul'kova and M. I. Temkin, *Zhur. Fiz. Khim.*, **23**, 695 (1949).

(19) W. K. Hall, R. J. Kokes and P. H. Emmett, *J. Am. Chem. Soc.*, **79**, 2983 (1957).

Diffusion of reactants and products in oil-filled catalyst pores coupled with the reaction at the surface is important in the present system.[20,21] The assumption is made that the effects of diffusion will change only the values of exponents, but not the nature of the rate equation. For very simple hypothetical reactions this assumption is valid; (3) Methane production (as well as reactions producing carbon which are unimportant for the present system) has been ignored. In addition the present equation does not account for the small inhibiting effect of CO_2 on rate.[10]

ADDED IN PROOF.—Blyholder and Emmett[22] investigated the incorporation of tagged ketene in the Fischer–Tropsch synthesis on iron catalysts. Ketene apparently dissociates to methylene and carbon monoxide on the catalyst. The methylene radical initiates the formation of higher hydrocarbons in the same way as ethanol added to the feed, but the carbon monoxide from ketene acts the same as gaseous carbon monoxide. These results suggest, but do not necessarily prove, that the C_1 complex in the synthesis is methylene. The present kinetic scheme can be modified, at least superficially, to accommodate this type of C_1 complex. The postulate of methylene as the C_1 complex requires an extensive reconsideration of current concepts of the synthesis mechanism, especially the formation of oxygenated molecules.

---

[20] J. F. Shultz, M. Abelson, K. C. Stein and R. B. Anderson, THIS JOURNAL, **63**, 496 (1959).

[21] R. B. Anderson and L. J. E. Hofer, *J. Chem. Eng. Data*, in press.

[22] G. Blyholder and P. H. Emmett, THIS JOURNAL, **63**, 962 (1959); **64**, 470 (1960).

STRUCTURE OF MOLTEN MERCURIC HALIDES. IV. MERCURIC BROMIDE–ALKALI METAL BROMIDE MIXTURES[1]

BY GEORGE J. JANZ AND JEROME GOODKIN

Department of Chemistry, Rensselaer Polytechnic Institute, Troy, N. Y.

Received January 21, 1960

An investigation of the cryoscopy of molten $HgBr_2$ having Li, Na, K, Rb and Cs/Br as solutes is reported. The solvent exhibits only small deviations from the thermodynamically ideal behavior predicted for $\nu = 1$ in each mixture. These results, together with the earlier data on electrical conductance and viscosity for the mixtures are in accord with strong solvent–solute interactions and a highly ionic nature for the mixtures. An explanation of the cryoscopic properties is seen in the interaction of the solute with the molecular solvent with the probable formation of the species M^+ and $(MHgBr)_4^-$ in these mixtures.

Based on physico-chemical measurements and Raman spectra a liquid state structure for molten mercuric bromide has been advanced[2,3] in which the predominant entities are the tri-atomic linear molecular species, HgX_2. The present communication reports the results for the cryoscopic behavior of molten $HgBr_2$ containing the alkali metal bromides, MBr (M = Li, Na, K, Rb and Cs) and some discussion of the structure of these molten salt mixtures.

Experimental

Chemicals.—The purification of $HgBr_2$ by vacuum drying and sublimation has been described elsewhere[2] in detail. The melting point of the $HgBr_2$ used in this investigation was 238.1 ± 0.1°. The alkali metal bromides, reagent grade purity, were vacuum dried at a maximum temperature of 450° using the inert gas purge-temperature increment procedure[4] and used without further purification.

Cryoscopic Apparatus.—The high vapor pressures of $HgBr_2$ (m.p. 238°, b.p. 318°) make the use of a sealed type cryoscopic tube with some external device for stirring almost imperative. A shaking type assembly designed for the present measurements consisted of an indented Pyrex glass tube with a thermocouple well sealed after the cryoscopic mixture by weight has been introduced. Samples were prepared in sets of 6, with solute added to all but one tube in each set. All weighings and salt transfers were made in a dry inert gas atmosphere. The freezing point depressions were thus obtained relative to the freezing point of the pure solvent in each series. The indentations of the tube aided turbulence on shaking. The sample tube was held in place by 3 discs mounted on two $^1/_8$ in. steel rods and 2 springs. The length of the reciprocating rod on the eccentric wheel was adjusted to maintain the sample for the entire shaking stroke in the uniform temperature zone of the furnace. Temperatures were measured with Pt–Pt, Rh thermocouples and the recording differential potentiometer.[5]

Data and Results.—The results for the five solutes Li, Na, K, Rb and Cs/Br in $HgBr_2$ are summarized in Table I and illustrated in Fig. 1. The measurements were restricted to the region of dilute solutions since the interest was to observe the value of cryoscopic slope as $m \to 0$. The entries in Table I are based on not less than three determinations for each, the accuracy being within the limits ± 0.05° for the freezing point measurements.

The dashed line in Fig. 1 is the cryoscopic slope predicted from the integrated van't Hoff isochore

$$\ln a_1 = -\frac{\Delta H}{R}\left(\frac{1}{T} - \frac{1}{T_0}\right)$$

for ideal behavior (*i.e.*, $a_1 = N_1$) with the recently determined[6] value, 4280 cal./mole, for the heat of fusion of $HgBr_2$. For each solute, the function $(\Delta T_f/K_f m_2)$ *vs.* m_2 was graphed to determine[7] the number of particles formed by dissociation of the solute and foreign to the solvent as $m_2 \to 0$. The value of K_f based on the above heat of fusion is 43.8 deg. mole^{-1} 1000 g.$^{-1}$. The number of foreign particles, ν, at infinite dilution for each solute in molten $HgBr_2$ is thus

---

[1] Abstracted in part from a thesis submitted by J. Goodkin in partial fulfillment of the requirements for the Ph.D. degree. Parts I–III in this series see, respectively, THIS JOURNAL, **63**, 1975 (1959); *Ann. N. Y. Acad. Sci.*, **79**, 790 (1960); *Spectrochim. Acta*, submitted (1960).

[2] G. J. Janz and J. D. E. McIntyre, *Ann. N. Y. Acad. Sci.*, **79**, 790 (1960).

[3] G. J. Janz, Y. Mikawa and J. D. E. McIntyre, *Spectrochimica Acta*, submitted (1960).

[4] G. J. Janz, H. J. Gardner and C. T. Brown, THIS JOURNAL, **60**, 1458 (1956).

[5] C. Solomons and G. J. Janz, *Anal. Chem.*, **31**, 623 (1959).

[6] C. J. Janz and J. Goodkin, THIS JOURNAL, **63**, 1975 (1959).

[7] For a review of theoretical aspects of cryoscopy in molten salts refer: G. J. Janz, C. Solomons and H. J. Gardner, *Chem. Revs.*, **58**, 461 (1958).

TABLE I

ALKALI METAL BROMIDES IN MERCURIC BROMIDE

m_{MBr}	N_{HgBr_2}	$-R \ln N \times 10^{-3}$	T_f	$\frac{1}{T_f} \times 10^3$
		LiBr		
0.0000	1.0000	0.00	511.36	1.9556
.0058	0.9979	4.12	511.11	1.9565
.0195	.9930	14.2	510.92	1.9573
.0371	.9868	26.5	510.53	1.9587
.0567	.9800	40.3	510.31	1.9586
.0907	.9683	64.04	510.11	1.9604
		NaBr		
0.0000	1.0000	0.00	511.36	1.9556
.0070	0.9975	5.03	511.14	1.9564
.0157	.9945	11.0	510.82	1.9576
.0250	.9911	17.84	510.44	1.9591
.0448	.9841	32.02	509.76	1.9617
.0768	.9731	54.4	509.15	1.9641
.0876	.9694	61.8	508.54	1.9664
.1028	.9643	72.3	508.22	1.9677
.1220	.9579	85.1	508.06	1.9683
		KBr		
0.0000	1.0000	0.00	511.36	1.9556
.0109	0.9961	7.78	510.85	1.9575
.0216	.9923	15.4	510.32	1.9596
.0343	.9878	24.4	510.09	1.9604
.0586	.9793	41.5	509.50	1.9627
.0947	.9670	66.7	508.01	1.9685
.1022	.9645	71.8	507.90	1.9689
		RbBr		
0.0000	1.0000	0.00	511.36	1.9556
.0092	0.9967	6.59	510.83	1.9576
.0145	.9948	10.3	510.41	1.9592
.0286	.9898	20.4	509.79	1.9616
.0590	.9792	41.8	508.77	1.9655
.0925	.9677	65.1	507.81	1.9693
		CsBr		
0.0000	1.0000	0.00	511.36	1.9556
.0121	.9956	8.69	510.69	1.9581
.0271	.9903	19.2	509.98	1.9612
.0555	.9804	39.3	509.29	1.9635
.0717	.9748	50.8	507.91	1.9689
.1134	.9607	79.1	506.27	1.9752

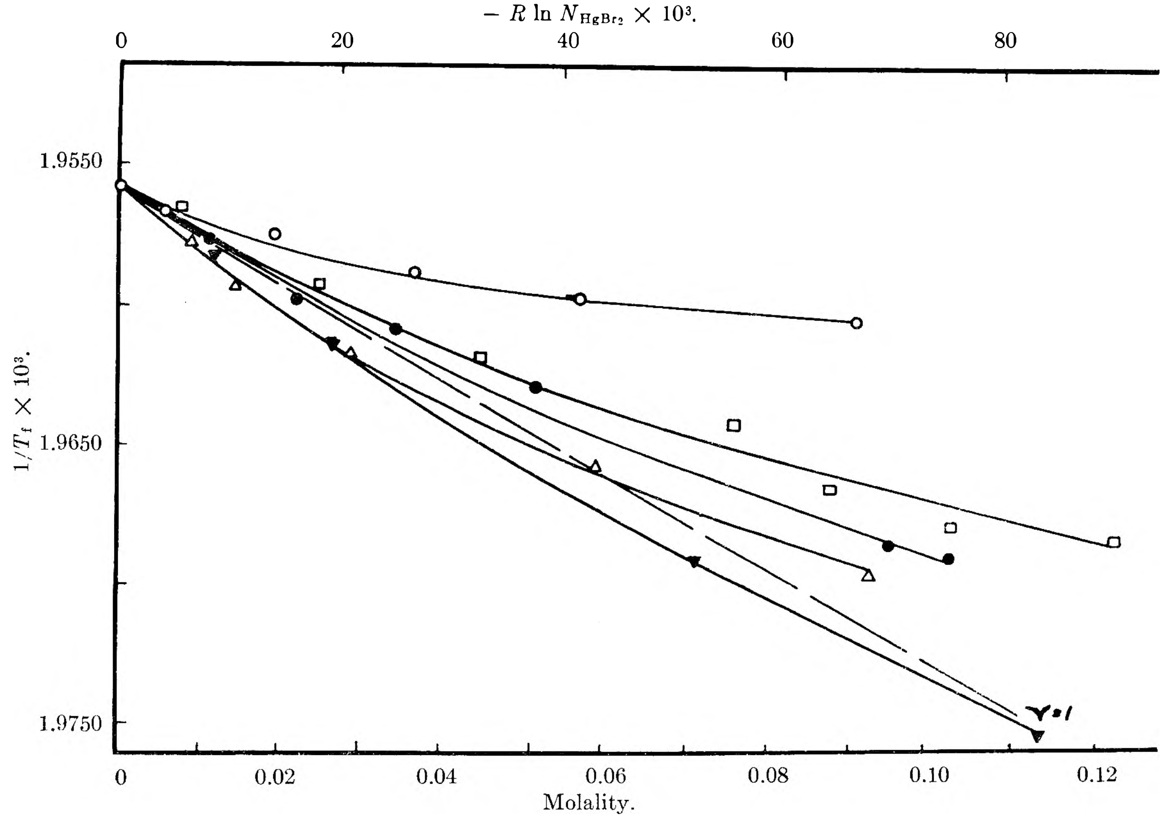

Fig. 1.—Comparison of the freezing points of $HgBr_2$ containing alkali metal bromides with the theoretical limiting slope predicted from the van't Hoff equation. Experimental points. LiBr, ○; NaBr, □; KBr, ●; RbBr, △; and CsBr, ▼. Theoretical slope for one (ν = 1) foreign particle, — —.

Solute	LiBr	NaBr	KBr	RbBr	CsBr
ν	1.0	1.0	1.1	1.4	1.4

The behavior of the NaBr and KBr in $HgBr_2$ melts based on a value for cryoscopic constant of 37.5 for the solvent has been investigated previously by Jander and Broderson.[8] A comparison of the present results with the recal-

---

(8) G. Jander and N. K. Broderson, *Z. anorg. allgem. Chem.*, **264**, 57 (1951).

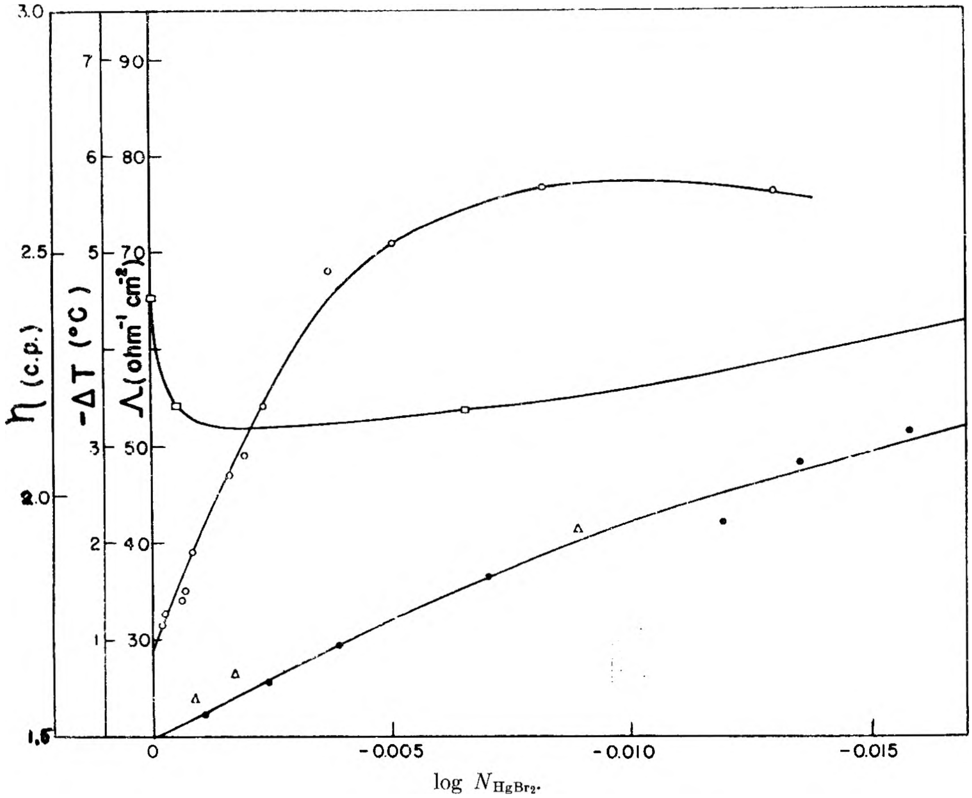

Fig. 2.—Comparison of change in electrical conductance, viscosity and freezing point depression of molten $HgBr_2$ containing increasing amounts of NaBr. Experimental points: $-\Delta T$ (freezing point depression), ●, this work; Δ, Jander and Broderson[8]; Λ (conductance, ○) and η (viscosity, □) Jander and Broderson.[8]

culated values of the earlier study, together with some results for the viscosity[8] and equivalent conductances[8] of the $NaBr-HgBr_2$ mixtures is illustrated in Fig. 2. The freezing point results of Jander and Brodersen were gained by visual observation using a mercury-in-glass thermometer. The two sets of cryoscopic behavior are essentially in agreement; the differences may be attributed undoubtedly in large part to the problems of corrections inherent in the use of glass thermometers and visual observation techniques at elevated temperatures. Analyses of the earlier cryoscopic data for KBr in $HgBr_2$ of Guinchant[9] similarly in light of the above cryoscopic constant for this solvent shows that in the dilute solution region the ν factor clearly approaches 1, *i.e.*, the results are in accord with the present observations.

The results of Beckmann[10] for the cryoscopy of KCl, RbCl and CsCl in molten $HgCl_2$ were similarly recalculated for comparison. The ν factors for these chloride mixtures were quite similar to those found above for the corresponding alkali bromides in $HgBr_2$.

Discussion

Comparison of the cryoscopy of aqueous solutions and molten mercuric solutions of the alkali metal bromides is of interest. In aqueous solutions, as is well known, the freezing point depressions are in accord with a ν factor of 2 at infinite dilution, *i.e.*, two foreign entities added to the solution per molecule of solute, as predicted for complete ionization. Mercuric bromide has been shown[2,3] to form a melt in which the predominant species are simple $HgBr_2$ molecules and, indeed, in which the degree of ionization (to kinetically free ions) is estimated[2] to be approximately 10^{-4} in the liquid state (*cf.* H_2O, 10^{-7}). By analogy with aqueous solutions, a value of $\nu = 2$ would be predicted for the alkali bromides if the role of the solvent was comparable and complete ionization of the solute occurred. Alternately a value of $\nu = 1$ may be predicted for the solution of non-electrolyte species in molten mercuric bromide (*i.e.*, solutes dissolve in molecular form). The latter seems most improbable and the former is clearly in contradiction to the observed properties for these molten salt mixtures. The greatly enhanced conductivity and the correspondingly large changes in viscosity (refer Fig. 2) on addition of trace amounts of the alkali bromides speak for a highly ionic nature of these solutions and strong solute–solvent interactions.

An explanation of the properties of these melts is apparent if it is assumed that ionization of the solute is promoted by interaction with the molecular solvent in accord with the processes in which (iii)

$$2MBr + HgBr_2 = [M_2HgBr_4] \qquad (i)$$

$$[M_2HgBr_4] = M^+ + (MHgBr_4)^- \qquad (ii)$$

$$2MBr + HgBr_2 = M^+ + (MHgBr_4)^- \qquad (iii)$$

corresponds to the over-all process assuming the solute–solvent molecular type complex (i) ionizes completely (ii) in the process of solution.

This scheme corresponds closely with that first proposed by Foote and Martin[11] for mercuric chloride alkali chloride[10] mixtures. A cryoscopic value of $\nu = 1$ per mole of MBr, the enhanced electrical conductance, and the changes in viscosity are understood in the light of the above. Species such as $MHgBr_3$ seem less probable in this

---

(9) M. Guinchant, *Comp. rend.*, **149**, 479 (1909).

(10) E. Beckmann, *Z. anorg. Chem.*, **55**, 175 (1909).

(11) H. W. Foote and N. A. Martin, *Amer. Chem. J.*, **41**, 451 (1909).

concentration range where the excess solvent would favor solvent rich complexes since the process corresponds to a cryoscopic activity of 2

$$\mathrm{MBr} + \mathrm{HgBr_2} = [\mathrm{MHgBr_3}] = \mathrm{M^+} + \mathrm{HgBr_3^-} \quad \text{(iv)}$$

per mole of solute present. The possibility that species M_2HgBr_4, $MHgBr_4^-$, M^+, Br^- and $HgBr_3^-$, are present in simultaneous equilibria near infinite dilution with a net cryoscopic activity averaging to $\nu = 1$ as observed is not ruled out. The pronounced tendency to form molecular complexes may be attributed to the low shielding efficiency[11] (Hg^{+2}, 0.67 *cf.* K^+, 1.0) and high anion affinity[12] ($Hg^{++}/Sr^{++} = 1.70$) for the mercuric ion in the mercuric halides. With increasing concentrations[8] additional interactions undoubtedly contribute to the properties of freezing point depression, electrical conductance, and viscosity of these mixtures.

Interpretation of the deviations from the theoretical slope ($\nu = 1$) in Fig. 2 is possible in thermodynamic activity concepts. Calculation of the activity coefficients for $HgBr_2$ in the conventional manner show that at the upper limit of the concentration range investigated ($m_2 = 0.10$) the activity coefficients for $HgBr_2$ are 1.022, 1.012, 1.008, 1.005 and 0.999, in the mixtures containing LiBr, NaBr, KBr, RbBr and CsBr, respectively. The solvent exhibits only small deviations from the thermodynamically ideal cryoscopic behavior.

An explanation for the higher ν values for RbBr and CsBr is seen in the possibility of solid solution formation occurring in the mixtures, assuming that the ionic processes are the same for these solutes as for the three other bromides. The data are insufficient to resolve this point.

Acknowledgments.—The authors wish to thank Dr. Cyril Solomons for helpful suggestions and continued interest during the course of this investigation. Support of this work by the Monsanto Chemical Company and the U. S. Air Force, Office of Scientific Research, is gratefully acknowledged.

---

[11] L. H. Ahrens, *Nature*, **174**, 664 (1954).

[12] L. H. Ahrens, *Geochim. Cosmochim. Acta*, **3**, 1 (1953).

THE SORPTION OF H_2O AND D_2O VAPORS BY LYOPHILIZED β-LACTOGLOBULIN AND THE DEUTERIUM-EXCHANGE EFFECT[1]

By Lloyd H. Reyerson and Wasyl S. Hnojewyj[2]

The School of Chemistry, University of Minnesota, Minneapolis 14, Minnesota

Received January 22, 1960

Data are reported for the sorption of H_2O and D_2O vapors by dry, lyophilized β-lactoglobulin at 17 and 27°. The amounts adsorbed and the calculated differential heats of sorption for D_2O turn out to be higher than for H_2O under the same conditions. A definite exchange effect was observed which indicated that the labile hydrogens of the dry protein were readily replaced by deuterium atoms during the sorption of D_2O molecules. This exchange reverses itself when H_2O is sorbed on the protein-containing "labile deuterium" atoms.

In the previous study, reported from this Laboratory,[3] it was shown that more D_2O vapor was sorbed at the same temperatures and pressures by lysozyme than was the case for H_2O. Furthermore, during the D_2O sorptions, this protein showed a permanent gain in weight following a complete adsorption–desorption isotherm. This gain in weight was due to the exchange process which took place between the labile hydrogens of the protein and the deuterium of the sorbed D_2O. The maximum exchange reported was 1.37% of the weight of the dry protein and was found at the end of three complete adsorption–desorption. This amount of exchange is less than the total number of labile hydrogens in the protein. Additional adsorption–desorptions on this same protein sample, lysozyme, showed that this maximum exchange of the labile hydrogens is all that is possible and that afterward many complete adsorption–desorptions of H_2O molecules are required to replace the deuterium in the deuterated protein. These results will be published in the near future.

In the present investigation, similar studies were carried out using β-lactoglobulin as the lyophilized dry protein. Sorption data were obtained at 17 and 27° and it became evident that once again more D_2O than H_2O was adsorbed at the same temperature and pressure. In this case the differential heats of adsorption were greater for D_2O than for H_2O at lower vapor pressures, in contrast to the values obtained for lysozyme at low vapor pressures. It should be noted that at the end of the first complete adsorption–desorption of D_2O molecules, the final weight of the sample had an added weight equal to 0.832% of the original weight of the protein. This added weight due to deuterium exchange increased in the succeeding isotherm determinations but the exchange was found to be essentially complete at the end of the third run.

Experimental

The quartz helix-spring, used in these determinations, had a sensitivity of 24.7 mg./cm. and a cathetometer, having an accuracy of ±0.02 mm., permitted a precise measurement of spring extension during sorption. The Carlsberg Laboratories in Copenhagen provided the lyophilized β-lactoglobulin. This protein was part of a larger batch that had been used in numerous earlier experiments at Carlsberg. Since the unused material had been stored for some time as wet crystals, the protein to be used in this study was twice recrystallized from 0.1 *M* NaCl followed by dialysis against water. A slurry of the crystals so ob-

---

[1] This work was supported by a Research Grant from the National Institutes of Health.

[2] Research Associate, University of Minnesota.

[3] W. S. Hnojewyj and L. H. Reyerson, This Journal, **63**, 1653 (1959).

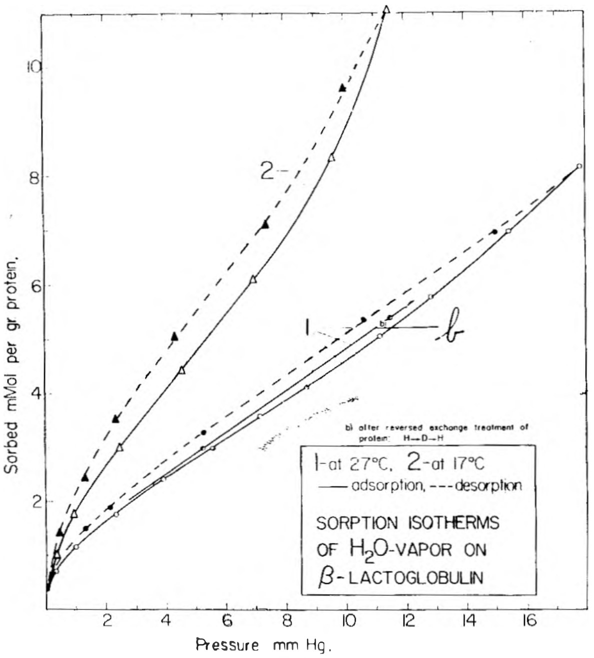

Fig. 1.—(b) after reversed exchange treatment of protein: H → D → H.

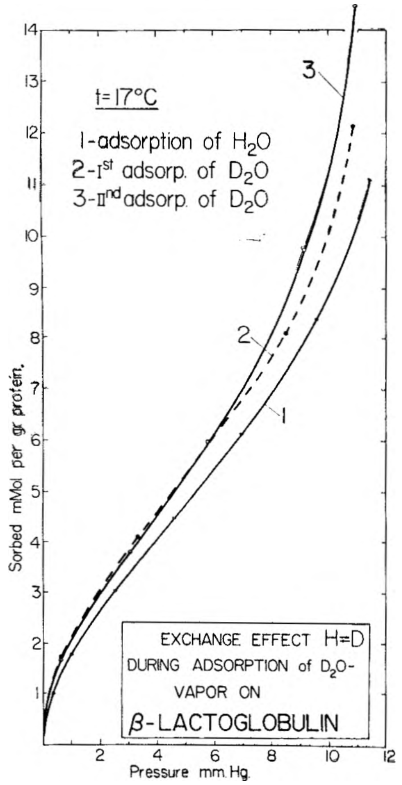

Fig. 2.

tained was then carefully lyophilized. Five hundred and sixty-four mg. of this protein was weighed into a light glass bucket which was then suspended from a hook at the lower end of the spring balance. Equilibrium vapor pressures, in the sorption system, were measured by a mercury manometer, using a traveling microscope accurate to ±0.005 mm. All pressures were corrected by converting the densities of mercury to 0°.

The sections of the sorption system containing the bucket and the upper part containing the quartz spring were each water-jacketed. The water, circulating through the upper jacket, was maintained at a slightly higher temperature than that of the bucket in order to prevent vapor condensation on the spring as saturation was reached. The jacket surrounding the sample maintained it at the reported temperature. The protein was outgassed at 27° until a constant weight had been maintained for a long time at 10^{-6} mm. pressure. Adsorption–desorption isotherms were then determined at 27 and 17° as previously described.[4] Prior to these runs the purified H_2O and D_2O (99.5%) had been outgassed during a series of freezings and thawings while pumping down to a pressure of 10^{-6} mm. The isotherms for H_2O were first run at 27 and then at 17°. These were first followed by sorption of D_2O at 17 and then at 27°. At the end of each desorption, at a given temperature, the system was pumped down to a constant weight at a pressure of 10^{-6} mm.

Results and Discussion

Figures 1, 2 and 3 give the isotherms for the amounts of H_2O and D_2O sorbed by dry, lyophilized β-lactoglobulin, as plotted against equilibrium vapor pressures at 17 and 27°. The first isotherm, Fig. 1, for H_2O was determined at 27°, and the adsorption points were obtained up to a vapor pressure of 17.86 mm. At this point the protein sorbed 8.15 mmoles of H_2O per gram (14.67% by weight of the dry protein). After complete desorption at 27 the isotherm at 17° was run. At the completion of each desorption, the weight of the dry protein was found to be identical with the initial weight at the start of each run.

The early, non-linear, rapid rise in the isotherms changes after the protein has adsorbed 2 millimoles per gram, and becomes essentially a straight line over a considerable range of vapor pressure. An interesting observation may be made at this point. If the straight lines for both isotherms are extrapolated back to the zero vapor pressure ordinate, they meet on this ordinate. This suggests a definite relationship to total area coverage at the two temperatures. If the straight-line sections of both isotherms are extrapolated forward, until they cross the ordinates for saturated vapor pressures of H_2O at each temperature (14.53 mm. at 17° and 26.74 mm. at 27°), then the intersections show identically the same amounts adsorbed for each temperature. As will be proved by later experiments, these hypothetical amounts, adsorbed at the two saturated vapor pressures, just equal in moles the amount of D_2O required to account for the D for H exchange which the experiments prove takes place when D_2O is sorbed by the protein. This seems to be very strong evidence that mono-layer coverage of all of the adsorption sites of the protein for water has not been exceeded until the amounts adsorbed are greater than the values given by the forward extrapolations of the straight-line portions of the isotherms. It may be suggested that the first rapid rise in the isotherms represents adsorption on the most easily accessible sites of the solid protein. The rates of attainment of adsorption equilibrium during the first part of the isotherms are about double that found for the straight lines as well as for the following portions of the curves. Following adsorption on the more easily accessible sites, the amounts adsorbed increase regularly with vapor pressure. It should be noted that the rate of desorption was most

---

[4] J. G. Foss and L. H. Reyerson, *ibid.*, **62**, 1214 (1958).

rapid at the beginning of this process, becoming very slow as the last vapor was removed. The data for one complete isotherm usually could be obtained in two weeks, an average of 8 hours being required for each equilibrium point. The white, powdery protein showed no observable swelling during adsorption but a slight definite contraction was observed on desorption. These slight volume changes had no effect on the sorption surface area since several points were rechecked on the straight-line sections of the isotherms and the amounts sorbed checked the earlier values, indicating complete reversibility in the ranges checked.

Using the same sample, upon which the H_2O isotherms had been completed, D_2O vapor was adsorbed up to a vapor pressure of 10.86 mm. at 17°. It was immediately apparent that the protein adsorbed more D_2O than H_2O at the same vapor pressure. Curve 2 in Fig. 2 gives the data for the adsorption branch of the first D_2O isotherms. Curve 1 shows the H_2O isotherm under the same conditions. The D_2O isotherm lies above that for H_2O throughout its whole course, indicating that more D_2O molecules were adsorbed by the protein under like conditions. For example, the protein adsorbed more than 12 mmoles of D_2O at a vapor pressure of less than 11 mm. compared to an adsorption of 10 mmoles of H_2O.

Upon the complete desorption of D_2O in the same manner as for H_2O, it was found that the protein had gained 0.832% of its original weight. Curve 3 in Fig. 2 is the adsorption branch of the second complete isotherm for D_2O, using the increased weight of the protein as the zero-weight point at the beginning of the second run. Upon completion of the second adsorption–desorption isotherm, the protein showed a second but smaller increase in weight. The total weight gained at this time amounted to 1.007% of the original weight. A third complete isotherm showed a further slight gain in weight. The total measured gain in weight amounted to 1.094%. Further sorptions proved that this gain in weight due to the deuterium exchange was the maximum to be found. Complete isotherms for the sorption of D_2O on the deuterated protein were then run at 17 and 27°. The results appear in Fig. 3. The adsorption branch of isotherm 2 in Fig. 3 was so nearly identical with 3 of Fig. 2 that one further concludes that the maximum deuterium exchange had been reached at the end of the third complete sorption of D_2O.

Following the final desorption of D_2O at 27°, isotherm 1 of Fig. 3, an adsorption of H_2O was carried out at relatively high vapor pressure and this was followed by a complete desorption. At this point the protein showed a definite loss in weight, indicating that hydrogen was now replacing deuterium in the protein. However, six successive adsorption–desorptions of H_2O were required to complete the exchange of hydrogen for the deuterium. The protein then weighed exactly the same as it did at the initiation of the very first adsorption of H_2O. Water vapor was again adsorbed by this protein at several vapor pressures. Curve b in Fig. 1 shows the first of these results. Since the isotherm lies slightly above the adsorption branch of curve 1 of Fig. 1, three additional adsorption–desorptions of H_2O were carried out with no change in the amounts adsorbed nor in the final weights at the end of each desorption. The fact that the points lie slightly above the original adsorption curve suggests the possibility that the deuterium–hydrogen and hydrogen–deuterium exchanges may have slightly increased the capacity of the protein to adsorb H_2O. This might mean small structural changes in the dry protein, resulting in the making of additional sorption sites available to H_2O.

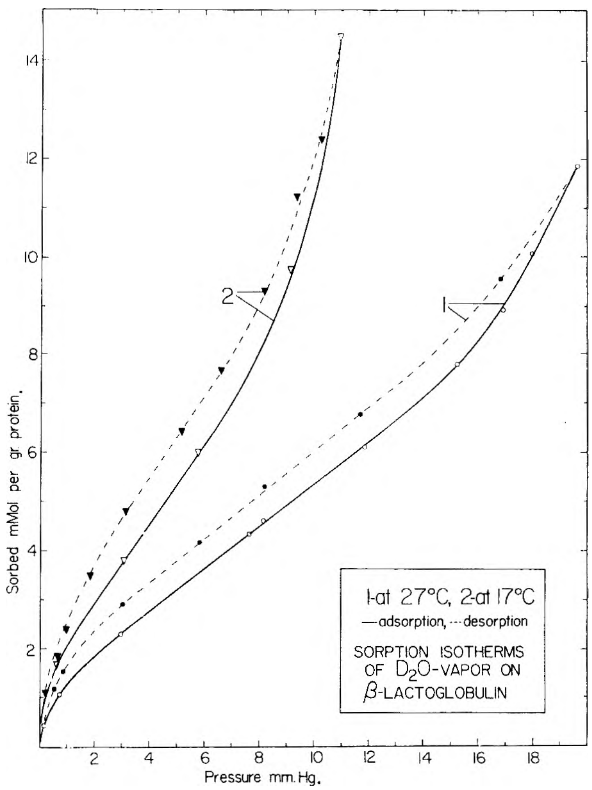

Fig. 3.

These results clearly show that β-lactoglobulin sorbs more D_2O than H_2O at a given vapor pressure. The sorbed D_2O, prior to or at the time of its desorption, exchanges D for labile hydrogens in the solid protein. Desorption isotherms show large hysteresis loops but the adsorbed vapors are reversibly desorbed except that a gain in weight has occurred due to the exchange. Since the maximum exchange increased the weight of the protein by an amount equal to 1.094% of the original weight, the total number of deuterium atoms exchanged for hydrogen are easily determined. Since the exchange of one mole of deuterium for hydrogen increases the molecular weight of the protein by 1.0066 g., it is necessary to use an accepted molecular weight for β-lactoglobulin. In a recent publication, E. Waldschmidt-Leitz[5] gives the molecular weight of β-lactoglobulin as 35,400, while Linderstrøm-Lang[6] uses 37,300 in his discussion of deuterium exchange on the

---

[5] E. Waldschmidt-Leitz, "Chemie der Eiweisskoerper," Verlag von Ferdinand Enke, Stuttgart, 1957.

[6] K. Linderstrøm-Lang, Souvenir, *J. Soc. Biol. Chemists, India*, 191 (1955).

TABLE I

NUMBER AND DISTRIBUTION OF EXCHANGEABLE (LABILE) HYDROGENS IN THE β-LACTOGLOBULIN MOLECULE

Possible participating units in the protein	Moles	Number and kind of groups containing labile hydrogen							
		$-NH_2$	$-NH$	$=NH$	$-SH$	$-OH$	$-\overset{O}{\overset{\|}{C}}-\overset{H}{\overset{\|}{N}}-$ (peptide)	COOH	Σ
A. Total in the protein backbone (having 3 chains): 300 (= 320 − 17 (proline))									
B. Side chains:									
End groups of the chains	3	3	..	..	..	..	..	3	
Tyrosine	8	..	..	..	..	8	..	..	
Tryptophan	3	..	3	..	..	..	..	..	
Serine	14	..	..	..	..	14	..	..	
Threonine	16	..	..	..	..	16	..	..	
Cysteine	3	..	..	..	3	..	..	..	
Arginine	6	6	6	6	..	..	..	..	
Histidine	4	..	..	4	..	..	..	..	
Lysine	29	29	..	..	..	..	..	..	
Aspartic acid	32	..	..	..	..	..	..	32	
Glutamic acid	48	..	..	..	..	..	..	48	
Ammonia	28	28	..	..	..	..	..	−28	Used by amide
Total no. of hydrogens in B		66 × 2	9	10	3	38	..	55	247

protein in solution. Both of these writers use practically the same analytical data for the kinds of amino acids and numbers of their residues which make up the composition of the protein. Furthermore, Linderstrøm-Lang considers this protein to be made up of three chains of residues, giving the protein three terminal amino groups and three carboxyl groups. The total possible numbers of exchangeable hydrogens in the protein as given by Linderstrøm-Lang[6] are shown in Table I, where, instead of merely giving the number of hydrogens for the amino acid side chains, the labile hydrogen-containing groups are shown.

From this table it is readily seen that in addition to 300 hydrogens in the backbone of the protein there are 247 possible labile hydrogens in the terminal groups and in the various side chains of the known amino acid residues. Lang[6] finds that theoretically, 547 hydrogens do exchange in solution at higher temperatures and at high *p*H values, but at ordinary room temperatures and at *p*H of the isoelectric point of 5.2[5] only about 450 of these hydrogens exchange with deuterium. In the present study on the dry lyophilized protein, the maximum weight increase is due to an exchange of 406 hydrogens per mole of protein having a molecular weight of 37,300. It is thus obvious that about 141 supposedly labile hydrogens do not exchange under the conditions of these experiments. Failure to reach true equilibrium is not the answer because several of the isotherms took more than a week for completion and in some instances additional time was allowed to determine whether further exchange took place. These results showed that equilibrium had been reached. One must therefore assume that the structure of the dry protein molecule is such that D_2O cannot be adsorbed throughout the solid on sites close enough to all of the labile hydrogens to permit exchange. It is conceivable that during the process of lyophilization and drying the unreacted side-chain carboxyls of aspartic and glutamic acid did react with the NH_2 or NH groups liberating water. This would reduce the number of labile available hydrogens by 110 leaving 31 to be accounted for, and these might well be strongly hydrogen bonded or buried in the structure. Certainly the availability of labile hydrogens for exchange in the solid protein differs markedly from the protein in solution at higher temperatures and higher *p*H values where the polar water molecules must relax the molecule. However the observed exchange of 406 hydrogens is a reasonable check with the 450 found by Lang at similar temperatures at about the isoelectric point of the protein in solution. Adsorption–desorptions carried up to saturated vapor pressures of D_2O will be done in an attempt to prove whether further exchange occurs as the protein begins to solvate.

Using the sorption data at 17 and 27°, as shown in Fig. 1 and 3, differential heats of adsorption and desorption for H_2O and D_2O were calculated by the Clausius–Clapeyron method. These heat values were then plotted against the amounts of sorbed H_2O and D_2O, expressed in millimoles per gram of protein. The resulting curves appear in Fig. 4A. The dashed sections of the curves indicate possible lack of precision due to slight inaccuracies in the sorption values at very low vapor pressures. It should be pointed out that a number of extra points actually were determined for each isotherm at low relative pressures. These were plotted on a large-scale graph. The best average values were used in the calculations of the points on the dashed section of the curves. The rise and fall in the heat values for the first sorptions of H_2O are quite similar to those reported earlier from this laboratory for ribonuclease.[4] The solid lines are considered to be reasonably good values. From a higher initial value of 14.46 kcal./mole at an adsorption of 0.56 mM/g. of H_2O ($\sim$20.9 moles of H_2O per mole of protein), the ΔH value falls to 11.64 kcal./mole at an adsorption of 0.86 mM/g. ΔH then increases to a maximum of 15.42 kcal./mole at a value of 1.67 mM/g. Following this, calculations show a steady but slow decline in ΔH until a value of 11 kcal. is reached at an adsorption

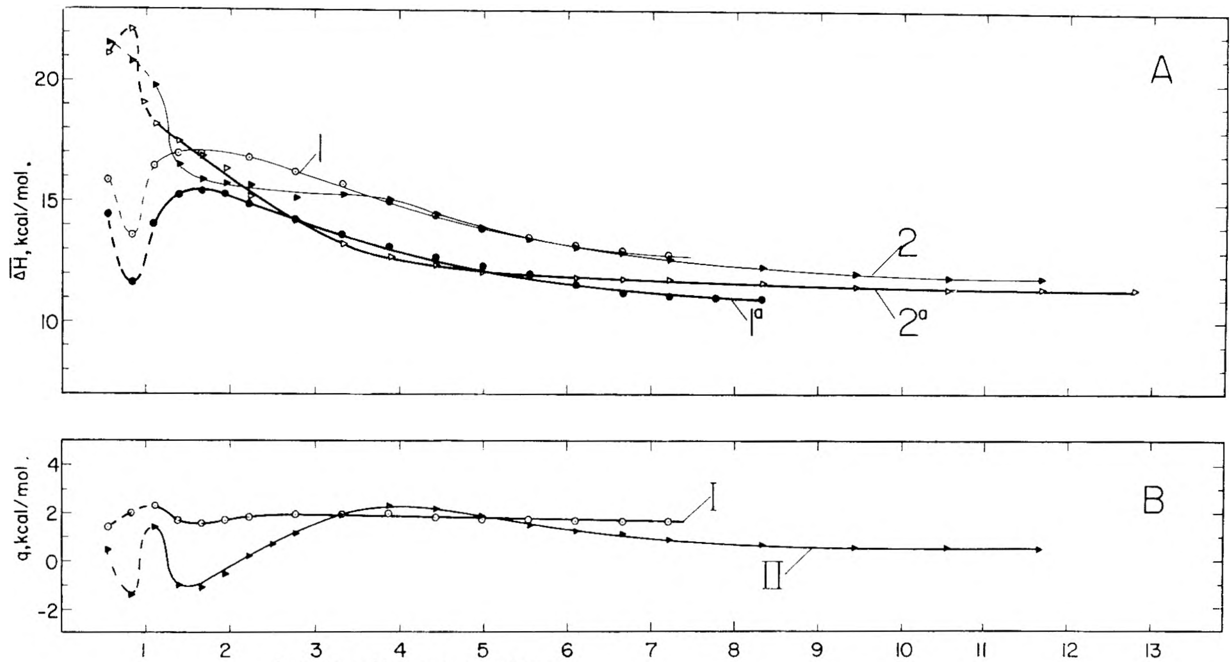

Fig. 4—Heats of vapor sorption on β-lactoglobulin: (A) adsorption: 1^a, H_2O; 2^a, D_2O; desorption: 1, —··—; 2, —··—. (B) ΔH_{desorp}-ΔH_{ads} = q: I, H_2O; II, D_2O.

of 8.33 mM/g., a value approaching the heat of condensation of H_2O.

The calculated differential heats of H_2O desorption give a curve quite parallel to the heats of adsorption but, as shown in Fig. 4B, curve I (where $q = \Delta H_{des} - \Delta H_{ads}$ *vs.* the amount sorbed), the values are about 2 kcal./mole higher for the whole range of sorption. This value approximates the activation energy for the vaporization of H_2O. (The sharp fall and rise of the ΔH values in the early stage of the isotherm is similar to that observed in this Laboratory for the sorption of H_2O by ribonuclease.[4])

The ΔH values for the adsorption of D_2O are quite different from those of H_2O. At the same initial amount adsorbed as for H_2O, the ΔH value turned out to be more than 21 kcal./mole. Instead of dropping to a minimum and then rising, as was found for H_2O, the calculated values rise to a maximum at 22.2 kcal./mole and first fall rapidly and then more slowly until they cross the curve for H_2O at an adsorption of slightly less than 3 mM/g. From this point up to an adsorption of about 5 mM/g., the values lie slightly below those for H_2O. At higher adsorption values, as is shown in Fig. 4A, the ΔH values again rise slightly above those for H_2O but they remain almost constant at slightly above 11 kcal./mole to the end of the adsorption measurements, approaching the heat of condensation. The ΔH values calculated for the desorption isotherm of D_2O do not parallel those of adsorption as they do for H_2O. As desorption begins they lie slightly above the values for adsorption but they rise slightly and soon are identical with the values for the desorption of H_2O. However, below a sorption of 4 mM/g., the desorption ΔH values, as plotted in Fig. 4A, fluctuate as much as ±1.5 kcal./mole about those for adsorption. Since these calculations were made from the isotherms of fully deuterated protein, exchange effects cannot be the cause of the variations. There seems to be no simple explanation for this nor for the variation in the ΔH desorption $- \Delta H$ adsorption, shown in curve II, Fig. 4B. It is hoped that direct calorimetric measurements may provide a clue to a correct interpretation of these results.

Conclusions

The results presented here show that D_2O is more strongly sorbed by dry lyophilized deuterated β-lactoglobulin than is H_2O by the undeuterated protein. The calculated ΔH values are higher than for H_2O in the early and late ranges of adsorption.

Deuterium of the D_2O sorbed by the lyophilized β-lactoglobulin exchanges with labile hydrogen while sorbed or during the process of desorption. The exchange reaches a maximum at an exchange of 406 hydrogens per mole of protein. Since D_2O molecules must be sorbed on sites adjacent to labile hydrogens, the solid protein has a very extensive surface available for such sorption. The number of moles of D_2O needed for this maximum exchange just equals the amount of H_2O theoretically adsorbed at the point where the extrapolation of the straight-line portions of the isotherms of H_2O meet the saturation vapor pressure ordinates for each temperature. Thus no more than a mono-layer coverage of the adsorption sites available to H_2O or D_2O molecules exists until a relatively large amount of these vapors has been sorbed. Use of BET theory for the determination of mono-layer coverage for solid proteins sorbing H_2O no longer seems feasible, and earlier results indicating multilayers of sorbed H_2O should be re-examined.

THE SOLUBILITY OF SILVER SULFATE IN ELECTROLYTE SOLUTIONS. PART 7. SOLUBILITY IN URANYL SULFATE SOLUTIONS[1]

By M. H. Lietzke and R. W. Stoughton

Contribution from the Chemistry Division, Oak Ridge National Laboratory, Oak Ridge, Tennessee

Received January 23, 1960

The solubility of Ag_2SO_4 has been measured in 0.100 to 1.348 *m* UO_2SO_4 solutions as a function of temperature to about 200°. The agreement between calculated and observed solubilities was good when hydrolytic and complexing reactions of the uranyl ion were taken into account. The calculated concentrations of all assumed species are presented as functions of UO_2SO_4 concentration and temperature, and it is concluded that the relative stability of the neutral species UO_2SO_4 compared to UO_2^{++} and $UO_2(SO_4)_2^{--}$ increases with temperature. Both the enthalpy and entropy for the association of UO_2^{++} and SO_4^{--} into the neutral species appear to attain large positive values at elevated temperatures, indicating that a large degradation of solution structure occurs as the ions associate.

Previous papers in this series have described the solubility of Ag_2SO_4 in KNO_3, K_2SO_4, H_2SO_4, HNO_3 and $MgSO_4$ solutions.[2] It was shown in these papers that single parameter expressions of the Debye–Hückel type could be used to describe the variation of the Ag_2SO_4 activity coefficient over a wide range of temperature and ionic strength. In each of these cases complete dissociation was assumed except for the species HSO_4^- and HNO_3. The equations for the variation of the acid constants K_i^0 of these species with temperature were obtained from Young,[3] while the variation of the acid quotients K_i with ionic strength I at any temperature were also assumed to be given by single parameter Debye–Hückel expressions

$$\ln K_i = \ln K_i^0 + \mathcal{S}_T\sqrt{I}/(1 + A_i\sqrt{I}) \qquad (1)$$

where $\mathcal{S}_T$ is the appropriate Debye–Hückel limiting slope at any temprature, A_i is the single parameter, and K_i^0 represents the thermodynamic constant (at $I = 0$). In all cases best agreement between observed and calculated solubilities was obtained when each single A_i parameter was assumed to be temperature independent and to be either ionic strength independent or to decrease slowly with increasing ionic strength.

The present paper deals with the solubility of Ag_2SO_4 in aqueous UO_2SO_4 solutions, the study having been undertaken in order to compare this medium with $MgSO_4$ solutions. Since the assumption of complete dissociation in the case of $MgSO_4$ gave good agreement between observed and calculated solubilities and since UO_2SO_4 is known[4] not to be completely dissociated at moderate concentrations, a comparison was thought to be of interest. The following independent assumptions were made in attempting to explain the data: (1) complete dissociation of UO_2SO_4, (2) complexing of UO_2^{++} with SO_4^{--}, (3) hydrolysis of UO_2^{++}, and (4) both complexing and hydrolysis of UO_2^{++}.

Experimental

The solubility measurements were carried out with the same technique described previously.[5] The measurements were extended at each concentration of UO_2SO_4 to as high a temperature as possible, the limit depending on the temperature of appearance of a red hydrolysis product of uranium containing silver. The values at 1.348 *m* (molality of) UO_2SO_4 below 174° were taken from previous work.[6]

Results and Discussion

In Fig. 1 the open circles represent the experimentally observed solubilities of Ag_2SO_4 in H_2O and in 0.100, 0.409, 0.622, 1.060 and 1.348 *m* UO_2SO_4 solutions. The results in H_2O to 100° were obtained from the work of Barre,[7] while the values at higher temperatures were reported in the first paper in this series.[2] The data in Fig. 1 show that uranyl sulfate causes a large enhancement of the solubility of Ag_2SO_4, particularly at the higher temperatures; this enhancement is appreciably greater than that shown by $MgSO_4$.[2] For example, the observed solubilities at 150° are about 0.11 and 0.40 molal in 1 *m* $MgSO_4$ and UO_2SO_4, respectively. (The solid heavy lines show the solubilities calculated when taking into account complexing and hydrolysis; see section 1b below).

1. Solubility Calculations (a). Assuming Complete Dissociation.—If both UO_2SO_4 and Ag_2SO_4 are assumed to be completely dissociated the only equilibrium which need be considered is

$$\underline{Ag_2SO_4} = 2Ag^+ + SO_4^{--} \qquad (2)$$

The variation of the (molality) solubility product $S = m_{Ag^+}{}^2 m_{SO_4^{--}}$ where I from the value in pure water $S_0 = 4s_0^3$ (where s_0 is the molal solubility in pure water) is given by the equation

$$\ln S = \ln S_0 + 6\mathcal{S}_1\left[\frac{\sqrt{I}}{1 + A_s\sqrt{I}} - \frac{\sqrt{3s_0}}{1 + A_s\sqrt{3s_0}}\right] \qquad (3)$$

$\mathcal{S}_1$ is the Debye–Hückel limiting slope for an ion of unit charge, and A_s is the single parameter.

The value of the A_s parameter in eq. 3 which gave the best fit with the data is lower than any of those for the other electrolytes studies in this series; *e.g.*, it is about 0.4 compared to about 0.75 for $MgSO_4$ solutions and 0.65 to 1.1 for the others. If the A_s parameter is optimized at each UO_2SO_4 concentration it shows an increase with the latter from

---

[1] This paper is based upon work performed for the United States Atomic Energy Commission at the Oak Ridge National Laboratory operated by Union Carbide Corporation.

[2] M. H. Lietzke and R. W. Stoughton, This Journal, **63**, 1183, 1186, 1188, 1190, 1984 (1959).

[3] T. F. Young, private communication; also T. F. Young, L. F. Maranville and H. M. Smith, Chapter 4, "The Structure of Electrolytic Solutions," edited by W. J. Hamer, John Wiley and Sons, Inc., New York, N. Y., 1959, pp. 35–62.

[4] K. A. Kraus and F. Nelson, Chap. 23, "The Structure of Electrolytic Solutions," Edited by W. J. Hamer, John Wiley and Sons, Inc., New York, N. Y., 1959, p. 349.

[5] M. H. Lietzke and R. W. Stoughton, *J. Am. Chem. Soc.*, **78**, 3023 (1956).

[6] Ernest V. Jones, M. H. Lietzke and William K. Marshall, *ibid.*, **79**, 267 (1957).

[7] M. Barre, *Ann. chim. phys.*, [8] **24**, 211 (1911).

0.23 at 0.1 m to 0.43 at 1.348 m. In all of the other media studied the optimized value of A_s showed a decrease or no change with increasing supporting electrolyte concentration. The assumption of a temperature-independent, concentration-dependent A_s showed poorer agreeement between observed and calculated solubilities in the case of UO_2SO_4 than in the other cases.

The (activity) solubility product of silver sulfate K_s^0 was evaluated at each 25° interval to 125° by extrapolating to zero ionic strength as described previously[8] and compared with the average value obtained in the other media. While the maximum deviations of the log K_s^0 values in K_2SO_4, H_2SO_4, HNO_3 and $MgSO_4$ media from the average varied only from 0.006 of a log unit at 25° to 0.026 at 125°, the values of log K_s^0 computed here for UO_2SO_4 media varied by 0.3 to 0.45 of a log unit from the previous average.[8]

Thus the assumption of complete dissociation of UO_2SO_4 does not allow good agreement between observed and calculated solubilities nor does it allow the evaluation of a thermodynamic solubility product consistent with those obtained in other media. This situation is as expected in view of the fact that both hydrolysis[9] and complexing[4] are known to occur in UO_2SO_4 solutions at 25°.

2. (b) **Assuming Hydrolysis and Complexing Reactions.**—Calculations were carried out taking hydrolysis and complexing of U(VI) into account. The 25° value of Ahrland, Hietanen and Sillen[9] of about 1.0×10^{-6} was used for the hydrolysis quotient K_h for the reaction

$$2UO_2^{++} + H_2O = U_2O_5^{++} + 2H^+ \quad K_h \qquad (4)$$

at an ionic strength of about unity in $NaClO_4$ media. Values of $K_{01}^0 = 5.3 \times 10^2$ and $K_{12}^0 = 30$ of Kraus and Nelson[4] were used for the formation constants (zero ionic strength) for the homogeneous reactions

$$UO_2^{++} + SO_4^{--} = UO_2SO_4 \quad K_{01} \qquad (5)$$

$$UO_2SO_4 + SO_4^{--} = UO_2(SO_4)_2^{--} \quad K_{12} \qquad (6)$$

Since hydrolysis of UO_2SO_4 would produce HSO_4^- ions, the HSO_4^- dissociation also had to be considered.

$$HSO_4^- = H^+ + SO_4^{--} \quad K_2 \qquad (7)$$

As before, Young's[3] relation (in terms of the absolute temperature T)

$$\log K_2^0 = -\frac{775.3835}{T} + 6.947210 - 0.0212472T \qquad (8)$$

was taken for the variation of the acid constant K_2^0 with temperature, while eq. 3 was used for the variation of the molality solubility product of Ag_2SO_4 with ionic strength.

The relation between K_h and K_h (I = 1) and ionic strength at 25° was assumed to be given by an equation similar to 3, with the second term in brackets being $1/(1 + A_h)$. The equilibrium quotients K_2 and K_{01} were assumed to vary with ionic strength according to single parameter Debye–Hückel expressions (eq. 1). The limiting slope S_T is zero for eq. 6 and hence it was assumed that $K_{12} = K_{12}^0$ at any temperature. For equilibria 4 and 5 the slope is negative. The value A_2 = 0.4 was used for ln K_2 (eq. 7) since this value was found to hold over a wide range of ionic strength for pure H_2SO_4 media by Baes[10] using Young's data,[3] and since it was also found to hold in H_2SO_4 media in previous work.[2]

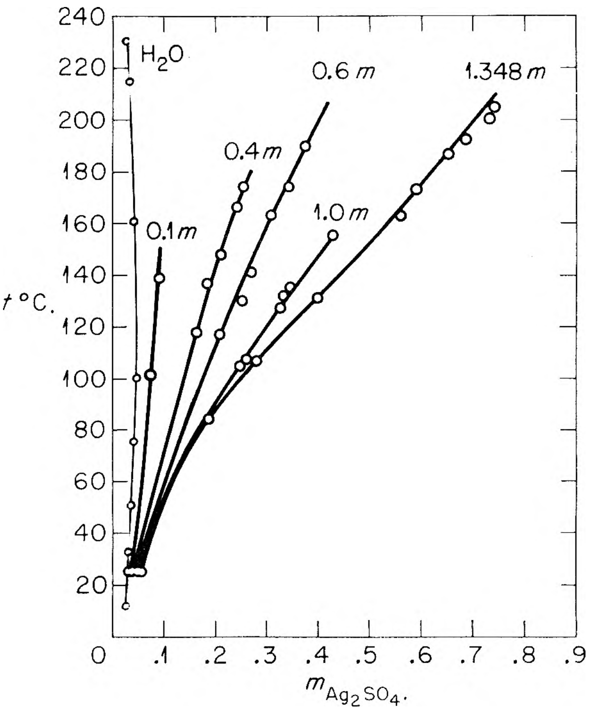

Fig. 1.—Solubility of Ag_2SO_4 in UO_2SO_4 solutions. (The circles are observed solubilities; the solid heavy lines show solubilities calculated on taking hydrolysis and complexing into account.)

TABLE I

TEMPERATURE AND IONIC STRENGTH PARAMETERS FOR EQUILIBRIUM CONSTANTS AND QUOTIENTS SHOWN IN EQUATIONS 1 THROUGH 9

Equilibrium quotient	$K^0(25°)$	a	b	A
K_2	[a]	[a]	[a]	0.4
K_h	3.2×10^{-6}	4.808×10^{-2}	-1.404×10^{-4}	1.0
K_{01}	5.3×10^2	2.939×10^{-2}	3.230×10^{-4}	0.9
K_{12}	30	5.388×10^{-3}	-9.392×10^{-7}	[b]
S	[c]	[c]	[c]	0.7

[a] See equation 7. [b] K_{12} was assumed to be independent of ionic strength. [c] See equation 3, where $S_0(t) = 4s_0^3$ and $s_0 = 1.7260 \times 10^{-2} + 4.3344 \times 10^{-4}t - 1.6898 \times 10^{-6}t^2$.

The A values for equilibria 4 and 5 were determined such that best agreement between observed and calculated solubilities was obtained at 25° by using the above values of the various constants (see Table I) and taking into account equilibria 2, 4, 5, 6 and 7. It was found that the (concentration independent) A_{01} could be determined with relatively little uncertainty; *i.e.*, it was by no means possible to fix A_{01} and then find a value for A_h such that agreement was good (or even such that a solution was obtainable in many cases). The ionic strength (based on the concentrations of all ions) and all concentrations of species were obtained by successive iterations using an IBM-704 computer.

---

(8) R. W. Stoughton and M. H. Lietzke, THIS JOURNAL, **64**, 133 (1960).

(9) S. Ahrland, S. Hietanen and L. G. Sillen, *Acta Chem. Scand.*, **8**, 1907 (1954).

(10) C. F. Baes, private communication.

TABLE II

MOLAL CONCENTRATIONS OF SPECIES IN UO_2SO_4 SOLUTIONS SATURATED WITH RESPECT TO Ag_2SO_4

t(°C.)	s_{obsd}[a]	s_{calcd}	$F_{UO_2^{++}}$	$F_{UO_2SO_4}$	$F_{UO_2(SO_4)_2^{--}}$	$F_{U_2O_5^{++}}$	100 $m_{SO_4^{--}}$	1000 $m_{HSO_4^-}$	1000 m_{H^+}
A. 0.100 m UO_2SO_4									
25	0.0341	0.0346	0.357	0.286	0.332	0.026	3.88	0.88	1.67
50	.050	.0504	.224	.346	.403	.027	3.40	1.30	1.43
75	.065	.0648	.097	.408	.465	.029	2.91	1.80	1.13
100	.075	.0757	.026	.435	.520	.020	2.68	1.47	0.49
125	.086	.0824	.0042	.420	.565	.0098	2.64	0.84	.141
150[b]		.0858	.00048	.398	.599	.0032	2.60	0.29	.025
B. 0.409 m UO_2SO_4									
25	0.0456	0.0454	0.450	0.159	0.378	0.0132	7.91	1.28	4.10
50	.0741	.0726	.367	.204	.412	.0163	5.88	2.05	4.61
75	.108	.107	.254	.293	.435	.0178	3.79	2.73	4.54
100	.146	.147	.123	.421	.437	.0185	2.32	3.42	4.13
150	.208	.205	.0047	.522	.469	.0035	1.55	0.98	0.46
175[b]		.223	.00047	.491	.508	.00035	1.57	.110	0.031
C. 0.6218 m UO_2SO_4									
25	0.0513	0.0498	0.472	0.127	0.393	0.0082	10.3	1.00	4.07
50	.080	.0812	.401	.163	.421	.0151	7.56	2.37	7.03
75	.125	.124	.306	.237	.441	.0168	4.75	3.14	7.34
100	.180	.181	.181	.366	.438	.0146	2.68	3.13	5.92
125	.230	.237	.0605	.508	.421	.0104	1.63	2.74	3.74
150	.281	.278	.0101	.549	.437	.0037	1.37	1.35	1.17
175	.339	.312	.0011	.518	.480	.00075	1.40	0.30	0.168
200[b]		.344	.00009	.470	.529	.00043	1.50	0.19	0.076
D. 1.060 m UO_2SO_4									
25	0.0568	0.0559	0.488	0.0943	0.410	0.0073	14.5	1.14	6.59
50	.093	.0934	.435	.119	.433	.0123	10.6	2.39	10.6
75	.150	.148	.362	.174	.450	.0132	6.60	2.93	11.1
100	.230	.229	.257	.281	.449	.0126	3.58	3.02	10.4
125	.320	.330	.120	.448	.422	.0101	1.85	2.74	8.01
150	.410	.413	.0262	.561	.408	.0051	1.25	1.76	3.68
200[c]		.559	.00028	.485	.515	.00030	1.42	0.14	0.17
E. 1.348 m UO_2SO_4									
25	0.0583	0.0588	0.493	0.0823	0.418	0.0074	16.9	1.26	8.72
50	.099	.0994	.448	.104	.439	.0101	12.3	2.12	11.5
75	.160	.160	.383	.150	.454	.0121	7.71	2.84	13.5
100	.254	.253	.288	.244	.455	.0125	4.17	3.04	13.8
125	.370	.379	.155	.407	.429	.0090	2.07	2.34	9.84
150	.495	.495	.0395	.553	.401	.0056	1.25	1.81	5.78
175	.597	.591	.0052	.557	.436	.0017	1.19	0.67	1.61
200	.725	.698	.00048	.490	.508	.0009	1.39	0.40	0.82

[a] These are smoothed values determined from the actual data. [b] A red precipitate formed below this temperature; hence these concentrations may be considered as extrapolated values. [c] The concentrations at 200° are extrapolated values.

The A parameters (Table I) were assumed both temperature and concentration independent, as found previously for the multi-electrolyte systems.[2] By repeating the process of optimizing agreement between observed and calculated solubilities, K_{01}^0, K_{12}^0 and K_h^0 were evaluated at 100 and 150°. Here again it was not possible to change one of the complex constants arbitrarily and then evaluate the other such that observed and calculated solubilities showed good agreement. The values computed for the hydrolysis constant K_h^0 on the other hand are known with less certainty since the solubilities were not greatly affected by a relatively large change in this parameter. About all that can be said with certainty is that the hydrolysis quotient is not larger than that calculated by about an order of magnitude.

The K^0 values at 25, 100 and 150° for reactions 4, 5 and 6 were fitted to quadratic functions of the centigrade temperature t

$$\ln K_i^0(t) = \ln K_i^0(25°) + a_i(t - 25) + b_i(t - 25)^2 \quad (9)$$

and the parameters a_i and b_i evaluated. The computed values of these parameters are also given in Table I. By using the parameters shown in Table I solubilities and concentrations of the various species in solution were calculated. These are shown in Table II along with graphically smoothed experimental solubilities. The uranium concentrations are expressed as fractions F_i of total uranium in the form of each species i; the solubility on the assumptions made is equal to one-half the Ag^+ concentration.

As an additional check on the consistency of the current treatment, values of the log of the (activity) solubility product K_s^0 were determined at 25° intervals to 150° by extrapolation, using eq. 3 and $A_s = 0.7$. At all temperatures the value obtained was within 0.03 of a log unit of the average value obtained in the other systems.[8]

1. (c) Other Assumptions Regarding Species.—For completeness in the over-all treatment of the data calculations were carried out in which complexing without hydrolysis and hydrolysis without complexing were assumed. In each case the parameters were optimized.

The closest agreement between calculated and observed solubilities was obtained assuming both hydrolysis and complexing; assuming only complexing showed nearly as good results (*e.g.*, a 1.5 *vs.* a 1.0% deviation in a typical case); while assuming only hydrolysis was definitely poorer. Since the assumption of both hydrolysis and complexing involves more arbitrary parameters than the others better agreement in itself does not constitute a very strong point in its favor. However, this assumption is also most consistent with current knowledge of species present in uranyl sulfate solutions at 25° and hence is preferred.

2. Behavior of UO_2SO_4 Solutions.—It was pointed out some time ago by Kraus[11] that there is reason to believe that K_{01} increases rapidly with temperature and more rapidly than K_{12}. Since multicharged metallic ions in general have a considerable tendency to hydrolyze and precipitate (as a hydrolysis product) the higher the temperature (*e.g.*, $ZnSO_4$ and $MgSO_4$), one would expect U(VI) in sulfate media to precipitate at moderate concentrations at elevated temperatures. Such precipitation would be expected if K_h increased and if K_{01} and K_{12} increased by about the same factor, since then the UO_2^{++} ion concentration would be nearly temperature independent while its tendency to hydrolyze would be greater the higher the temperature. Since this does not occur to as large an extent as exhibited by some other polyvalent metallic ions, Kraus suggested that K_{01} must increase appreciably more rapidly with temperature than K_{12}.

This is indeed what the current calculations show and it is evidenced by the calculated concentrations shown in Table II. Moreover, the values in this table show that in going to 150° (a) the H^+ and UO_2^{++} concentrations decrease less the larger the value of *m* (except perhaps for the lowest *m*) and (b) at any *m* the fractional decrease in UO_2^{++} ion concentration is about an order of magnitude greater than that of H^+. Thus, in spite of the fact that the hydrogen ion concentration decreases and the hydrolysis quotient K_h increases with temperature, the tendency of U(VI) to precipitate as a hydrous oxide[12] does not substantially increase because the UO_2^{++} concentration decreases rapidly with increasing temperature. The fraction as neutral UO_2SO_4 and as $UO_2(SO_4)_2^{--}$ show a small increase with temperature in the mixed electrolyte solutions (at least to about 150°).

3. Standard Enthalpy and Entropy Changes for Complexing Reactions.—Standard enthalpy and entropy changes were calculated for equilibria 4, 5 and 6 using eq. 9. Differentiation of these equations with respect to temperature gives $\Delta\bar{H}^0/RT^2$ values, while the entropy changes were calculated using eq. 10

$$\Delta\bar{F}^0 = -RT\ln K^0 \text{ and } T\Delta\bar{S}^0 = \Delta\bar{H}^0 - \Delta\bar{F}^0 \quad (10)$$

In addition, the K^0 values for 25, 100 and 150° were expressed by eq. of the form

$$\ln K^0(T) = \ln K^0(298.16°\text{K.}) + \alpha\ln(T/298.16) + \beta(1 - 298.16/T) \quad (11)$$

as used by Kraus.[11] The values of the coefficients obtained were

Equilib. const.	α	β
K^0_{01}	137.95	−133.99
K^0_{12}	3.5663	− 1.9969
K^0_h	−15.841	31.694

In this case $\Delta\bar{H}^0$ becomes

$$\Delta\bar{H}^0 = R(\alpha T + 298.16\beta) \quad (12)$$

Using eq. 12 and 10 a second set of enthalpy and entropy changes were evaluated. The resulting $\Delta\bar{H}^0$ and $\Delta\bar{S}^0$ values for the complex formation reactions are shown in Table III. As required by the method of fit the results of the two calculations (Table III) show approximately the same values at intermediate temperatures but deviate more at the extremes. Since the values for the hydrolysis reaction are relatively uncertain they are not shown; however the values that were obtained indicate that $\Delta\bar{H}_h^0$ and $\Delta\bar{S}_h^0$ for equilibrium 4 appear to vary from about 9 to 1 kcal. and from about 1 to −12 e.u., respectively, in going from 25 to 200°.

TABLE III

ENTHALPIES AND ENTROPIES FOR HYDROLYSIS AND COMPLEX FORMATION REACTIONS

($\Delta\bar{H}$ values are in kcal.; $\Delta\bar{S}$ values are in e. u.)

	Equilibrium 5				Equilibrium 6			
	Eq. 9		Eq. 11		Eq. 9		Eq. 11	
t °C.	$\Delta\bar{H}_{01}^0$	$\Delta\bar{S}_{01}^0$	$\Delta\bar{H}_{01}^0$	$\Delta\bar{S}_{01}^0$	$\Delta\bar{H}_{12}^0$	$\Delta\bar{S}_{12}^0$	$\Delta\bar{H}_{12}^0$	$\Delta\bar{S}_{12}^0$
25	5.19	29.9	2.35	20.4	0.95	10.0	0.93	9.9
50	9.45	43.6	9.20	43.7	1.13	10.5	1.11	10.4
100	21.5	78.2	22.9	81.8	1.53	11.6	1.46	11.5
150	39.2	122.3	36.6	116.3	2.00	12.8	1.82	12.4
200	63.3	176.2	50.3	147.0	2.54	14.0	2.17	13.2

Equation 11 is equivalent to assuming a constant $\Delta\bar{C}_p^0$; eq. 9 is equivalent to assuming $\Delta\bar{C}_p^0$ is expressible as the sum of a linear plus a quadratic term in temperature (without a constant term). Since $\Delta\bar{C}_p^0$ values in general are expressible more accurately by a constant plus a linear term than by either of the assumptions made here and since probably a constant term is better than a linear plus a quadratic term, the "best" values of $\Delta\bar{H}^0$ and $\Delta\bar{S}^0$ probably lie between those obtained from the two methods of calculation and are perhaps closer to those evaluated using eq. 11 and 12.

In any case, both the $\Delta\bar{H}^0$ and $\Delta\bar{S}^0$ values for the equilibrium

$$UO_2^{++} + SO_4^{--} = UO_2SO_4$$

appear to get very large at elevated temperatures. This indicates that considerable degradation of solute–solvent (or solvent–solvent) "structure" occurs when UO_2^{++} and SO_4^{--} ions form the neutral species at elevated temperatures. As shown in pre-

---

[11] K. A. Kraus, private communication; also see K. A. Kraus and R. J. Raridon, "Anion Exchange Studies XXXI. Adsorption of Zn(II) and Ga(III) from HCl Solutions in the Temperature Range 25 to 150°," unpublished work.

[12] C. H. Secoy, *J. Am. Chem. Soc.*, **70**, 3450 (1948).

vious work both $\Delta\bar{H}^0$ and $\Delta\bar{S}^0$ for dissolution of Ag_2SO_4 have large negative values at elevated temperatures, indicating a large enhancement of "structure" in a solution containing Ag_2SO_4 compared to that existing in the pure solvent. If this is generally true when a sulfate salt dissolves (into a very dilute solution) then the results in Table III indicate that such enhancement in structure is lost when the ions associate into neutral species.

By comparison the reaction for formation of $UO_2(SO_4)_2^{--}$ from neutral UO_2SO_4 and SO_4^{--} (eq. 6) shows far less dramatic effects: the K^0, $\Delta\bar{H}^0$ and $\Delta\bar{S}^0$ of the latter reaction show very little change with temperature.

Acknowledgment.—The authors wish to express their appreciation to Laura Cain Meers for performing the experimental solubility determinations at UO_2SO_4 concentrations to 1.060 *m;* to Raymond Jensen for performing the measurements above 170° at 1.348 *m* UO_2SO_4; and to Dr. Kurt A. Kraus for interesting discussions concerning these studies.

MASS ACCOMMODATION COEFFICIENTS AT A LIQUID-VAPOR BOUNDARY

BY TED A. ERIKSON

Chemistry Research Division, Armour Research Foundation of Illinois Institute of Technology, Technology Center, Chicago 16 Illinois

Received January 25, 1960

The data of Alty[1,2] are used to calculate mass accommodation coefficients at a liquid–vapor boundary on the basis that these coefficients should exhibit a univalued dependence on the surface temperature (for a pure liquid) as suggested by Schrage.[3]

Introduction

In the course of a study of the forced vaporization process as it may be described by a new language of steady-state thermodynamics,[4,5] a digression resulted into a description of the kinetics of interphase mass transfer. This paper reports the results of this digression, particularly with regard to the expressions that can be used to define a term which has the "feel" of a mass accommodation coefficient for gas–liquid collisions in a one-component system.

Forced vaporization is a simple steady-state process in which steady mass flow is effected across a liquid–vapor boundary by a pressure gradient, which is maintained, for example, by controlled pumping on a pure liquid. Alty[1] performed experiments which involved the measurement of the mass flow that resulted when a fixed pressure was maintained above a tube of water immersed in a constant temperature bath. Water was pumped on through six selected orifices to establish a steady rate of vaporization at each of three thermostat temperatures, and the corresponding pressure was measured. In later work,[2] Alty performed improved experiments on water and carbon tetrachloride at one intermediate temperature, and he extrapolated his data to zero pressure (above the liquid) so that an accommodation coefficient could be calculated from the equation

$$\alpha^0 = \frac{\dot{n}^0(2\pi RMT_s^0)^{1/2}}{P_s^0} \qquad (1)$$

where α is the mass accommodation coefficient, $\dot{n}$ is the steady mass flow, R is the gas constant, M is the molecular weight, T_s is the measured surface temperature, P_s is the saturated equilibrium vapor pressure at T_s, and the superscript ^{0} refers to the extrapolated value at zero pressure above the liquid.

Equation 1 is derived from a theory concerning the kinetics at the interface. As suggested in Schrage's book,[3] an accommodation coefficient should be calculated from the complete equation derived therein, which in equivalent form is

$$\alpha^{\Gamma} = \frac{\dot{n}(2\pi RMT_0)^{1/2}}{P_0[(T_0/T_s)^{1/2}(\tilde{P}_s/P_0) - \Gamma]} \qquad (2)$$

The tilde superscript is used to denote the actual pressure that exists at the liquid–vapor interface and the subscript 0 denotes experimental conditions. The symbol Γ stands for a distribution correction factor calculated from the approximate value of another function, ϕ, defined as

$$\phi \cong \frac{\dot{n}(2\pi RMT_s)^{1/2}}{2\pi^{1/2}\tilde{P}_s} \qquad (3)$$

Paired values of ϕ, $\Gamma + \phi$, and $\Gamma - \phi$ are tabulated in Appendix B of Schrage's book.[3] Actually, in practice $\tilde{P}_s$ is believed to differ only slightly from P_s, and the correction factor, Γ, is assumed to be unity by most investigators. Thus, one may write

$$\alpha_s = \frac{\dot{n}(2\pi RMT_0)^{1/2}}{P_0[(T_0/T_s)^{1/2}(P_s/P_0) - 1]} \qquad (4)$$

Of course, when $P_0 = 0$, eq. 4 reduces to eq. 1.

In reconsidering this experiment, the author has wondered whether the steady pressure that can be maintained above the liquid is simply fixed by the surface temperature, *i.e.*, T_s^* is the temperature at which the maintained steady pressure *is* the equilibrium saturated vapor pressure. This results in an approximate equality between P_s and P_0, and one obtains

$$\alpha^* = \frac{\dot{n}(2\pi RMT_0)^{1/2}}{P_0[(T_0/T_s^*)^{1/2} - 1]} \qquad (5)$$

---

[1] T. Alty, *Proc. Roy. Soc. (London)*, **A131**, 554 (1931).

[2] T. Alty and F. H. Nicoll, *Can. J. Res.*, **4**, 547 (1931).

[3] R. W. Schrage, "A Theoretical Study of Interphase Mass Transfer," Columbia University Press, New York, N. Y., 1953.

[4] T. A. Erikson, Masters Thesis at I.I.T., "Thermodynamics of the Steady State," 1959.

[5] R. J. Tykodi and T. A. Erikson, *J. Chem. Phys.*, **31**, 1521 (1959).

Another definition can be based on the proposed thermodynamic model[4,5] for a monothermal steady-state process. This model supposes that the forced vaporization process can be divided (arbitrarily) into three regions: state 1, the liquid at equilibrium vapor pressure, P_0^{Eq}, and T; state 2, the alleged uniform gas at P_0 and T; and a part on-the-line region where potential gradients occur. Further, the part on-the-line is assumed to be steady with respect to time, and therefore might be adequately represented by constant "averaged" state properties, P_{g}, T_{g} and n_{g}. A steady mass flow may be predicted from the collision frequencies which are calculated from the steady properties that exist in states 1 and 2.

Since the model assumes there is no net gain of mass for the part on-the-line with respect to time, then

$$\dot{n} = \alpha_{\mathrm{g}}\dot{n}_1 - \alpha_{\mathrm{g}}\dot{n}_2 \qquad (6)$$

where α_{g} is an "averaged" accommodation coefficient with such a gradient region, and $\dot{n}_1$ and $\dot{n}_2$ are the collision frequencies calculated from properties of states 1 and 2, respectively. Thus, the usual expression for collision frequency is introduced, and eq. 6 becomes

$$\alpha_{\mathrm{g}} = \frac{\dot{n}(2\pi RMT_0)^{1/2}}{P_0[(P_0^{\mathrm{Eq}}/P_0) - 1]} \qquad (7)$$

The state 2 (gas) properties are identified by the subscript 0 for consistency with previous equations. It is assumed that state 1 (liquid) pressure can be identified by the equilibrium vapor pressure, P_0^{Eq}, at the same temperature.

Results and Discussion

Table I summarizes the pertinent points for the five relations that have been presented for the calculation of a mass accommodation coefficient from data such as those reported by Alty. Such calculations were performed for the data he obtained with water at 60, 40, 30 and 18° thermostat temperatures and with carbon tetrachloride at a 1.6° thermostat temperature.

TABLE I

SUMMARY OF RELATIONS FOR A MASS ACCOMMODATION COEFFICIENT AT A PURE LIQUID–VAPOR BOUNDARY

Equation[a]	Derived from	Surface condition
1	Extrapolated limit of T_s and $\dot{n}$ as P_0 approaches zero	T_s^0 (Extrapolated)
2	Exptl. data for T_s, P_0 and $\dot{n}$, where P_s is the satd. vapor pressure at surface temp. T_s; Schrage's Γ distribution correction	T_s (Measured)
4	As α^{Γ} without Γ correction, *i.e.*, Γ = 1	T_s (Measured)
5	Assumes steady pressure, P_0, is satd. vapor pressure for actual surface temp. T_s^*; causes T_s^* to be somewhat lower than T_s measd.)	T_s^* (Derived)
7	Assumes that gradient region can be selected so as to define an "averaged" surface condition	T_s (Measured)

[a] Numbers refer to equations in text.

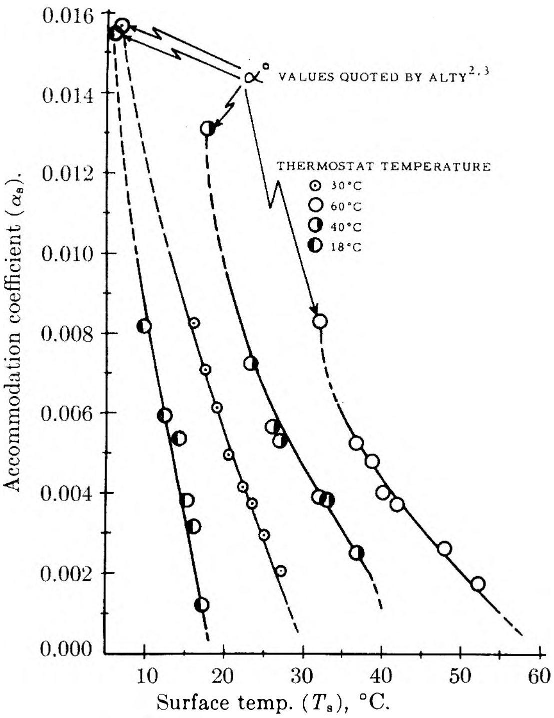

Fig. 1.—Plot of α_s (eq. 4) as a function of measured surface temperature for Alty's experiments with water.

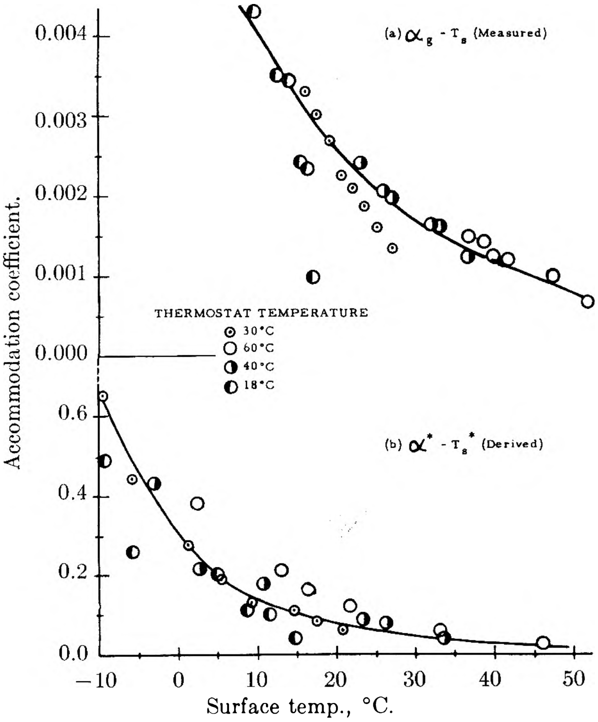

Fig. 2.—Plots of: (a) α_g as a function of T_s (eq. 7), and (b) α^* as a function of T_s^* (eq. 5) for Alty's experiments with water.

It was found that the Γ correction suggested by Schrage resulted in less than a 0.2% variation between α^{Γ} and α_s, α^{Γ} being slightly smaller than α_s. The results for α_s, α^* and α_g are presented in Fig. 1, 2 and 3.

The α_s *vs.* T_s dependency for the water experiments is shown in Fig. 1, with the values of α^0 quoted by Alty also indicated. Figure 2 shows the

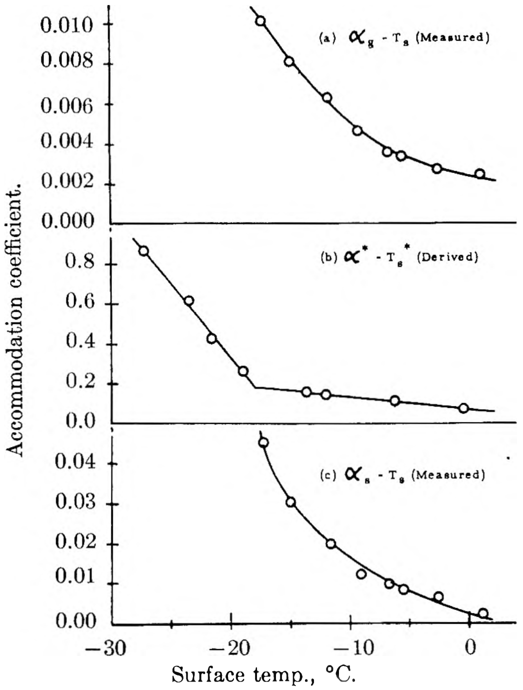

Fig. 3.—Plots of: (a) α_g as a function of T_s (eq. 7), (b) α^* as a function of T_s^* (eq. 5), and (c) α_s as a function of T_s (eq. 4) for Alty's experiments with carbon tetrachloride at 1.6°.

α_g *vs.* T_s and the α^* *vs.* T_s^* dependencies for the water experiments. The carbon tetrachloride results are presented in Fig. 3. (α^0 for carbon tetrachloride = 1, as quoted by Alty, not shown.)

One would expect that an accommodation coefficient should be solely a function of the surface condition. For a pure liquid-vapor system, the surface temperature is presumed to describe adequately the surface condition. On such a basis, the accommodation coefficient as derived from usual theory, eq. 2 or 4, appears to be inadequate in the intermediate regions. Note in Fig. 1 that at identical measured surface temperatures the calculated accommodation coefficients in the intermediate regions are progressively lower as the *bath* temperature is decreased. In other words, by this equation α_s is apparently dependent upon the thermostat temperature, a condition which is not considered likely.

The same data shown in Fig. 2 indicate some unique functionality of the pairs α^*–T_s^* and α_g–T_s. It seems important that these relations result in an accommodation coefficient that is relatively independent of the temperature of the thermostat in which the experiment is performed. A very pronounced change in slope for the carbon tetrachloride α^*–T_s^* dependency is shown in Fig. 3 which is not apparent in the corresponding α_g–T_s and α_s–T_s plots in the same figure. The change in slope occurs at a derived surface temperature near −17°, close to the freezing point of carbon tetrachloride. However, it is also suspected from previous analysis[4,5] that nucleate boiling is beginning at this region. If true, the calculated α^* would be reduced as a result of the increased surface area.

In conclusion, the results reported herein indicate that the problem of a mass accommodation (or condensation[3]) coefficient at a pure liquid-vapor boundary warrants further clarification before its features can be used implicitly.

NOTE ADDED IN PROOF.—Recently, the work of Littlewood and Rideal[6] has been brought to the author's attention. Their results show that the surface temperature of benzophenone was lowered 2.8° *in vacuo* (10^{-4} mm.) at 20°, as measured with thermocouples that were 25 microns in diameter; whereas their calculations indicate that the temperature drop should be approximately 6°. They estimated the heat flux for Alty's experiments to be 5 × 10^3 times greater in comparison, which indicates that the temperatures reported by Alty are higher than the temperatures which actually exist at the liquid surface. Littlewood and Rideal conclude that "evaporation coefficients" are unity, but the limitations of the heat supply causes a difference between the actual and the measured surface temperatures. Fig. 2b of the present article is based on the lowest surface temperature which must exist.

Acknowledgment.—The author wishes to acknowledge stimulating discussions with Dr. R. J. Tykodi, Assistant Professor at the Illinois Institute of Technology, and staff associates at the Armour Research Foundation.

(6) R. Littlewood and R. Rideal, *Trans. Faraday Soc.*, **52**, 1598 (1956).

NOTES

THE RELATIONSHIP BETWEEN O–H STRETCHING FREQUENCY AND ELECTRONEGATIVITY IN HYDROXIDES OF VARIOUS ELEMENTS[1]

BY ROBERT WEST AND RONALD H. BANEY

University of Wisconsin, Madison, Wisconsin

Received December 19, 1959

The influence of inductive effects of substituent groups on infrared frequencies has been studied in a number of different systems.[2] Among compounds of several types, linear relationships have been found between the electronegativities of substituents and certain vibrational frequencies.[3] The O–H stretching frequencies of alcohols[4] and phenols[5]

---

(1) This research was supported by the United States Air Force through the Air Force Office of Scientific Research of the Air Research and Development Command, under Contract No. AF 49(638)-285. Reproduction in whole or in part is permitted for any purpose of the United States Government.

(2) L. J. Bellamy, "The Infrared Spectra of Complex Molecules," Second Edition, Methuen, London, 1958, p. 389–394.

(3) L. J. Bellamy, *J. Chem. Soc.*, 4221 (1955); J. V. Bell, J. Heisler, H. Tannenbaum and J. Goldenson, *J. Am. Chem. Soc.*, **76**, 5185 (1954); R. E. Kagarise, *ibid.*, **77**, 1377 (1955).

(4) M. I. Batuev, A. P. Meshcheryakov and A. D. Matveeva, *Zhur. Eksptl. Teoret. Fiz.*, **20**, 318 (1950); *C.A.*, **44**, 6276 (1950).

(5) L. L. Ingraham, J. Corse, G. F. Bailey and F. Stitt, *J. Am. Chem. Soc.*, **74**, 2297 (1952).

are decreased by electronegative substituent groups, in accord with theoretical prediction.[2] However, alcohols are abnormal in that the O–H frequencies fall going from primary to secondary to tertiary alcohols.[6] Since the opposite would be expected from the known inductive effects of these groups,[7] the observed trend suggests that a hyperconjugative effect is also operating.

This article reports the study of the O–H stretching band frequency in a series of hydroxyl compounds in which the OH group is bonded to different elements. The five triphenyl-hydroxy compounds of the group IVB elements were investigated, having the general formula $(C_6H_5)_3MOH$, where M = C, Si, Ge, Sn and Pb. Four other hydroxyl compounds, diphenylsilanediol, phenyldihydroxyborane, N-phenylhydroxylamine and *t*-butyl hydroperoxide, also were studied. The O–H frequencies are compared with the electronegativities of the elements to which the hydroxyl group is bonded. The electronegativities of the elements of periodic group IVB recently have been studied carefully by Allred and Rochow, and are now known with exceptional accuracy.[8]

Experimental

Compounds.—The preparation and properties of the triphenylhydroxy compounds of the group IVB elements, and of diphenylsilanediol, will be described elsewhere.[9] Phenyldihydroxyborane and N-phenylhydroxylamine were obtained from K and K Laboratories, Inc., and *t*-butyl hydroperoxide was purchased from Matheson, Coleman and Bell. These compounds were of reagent grade and were used without further purification. Merck carbon tetrachloride from freshly-opened bottles was used as a solvent.

Spectra.—The infrared spectra of the compounds in the OH region were determined using a Perkin–Elmer Model 112 spectrometer with a lithium fluoride prism, calibrated against water vapor and ammonia. The compounds were examined as approximately 0.01 *M* solutions in carbon tetrachloride at a path length of 0.3 cm. At this concentration O–H bands due to self-associated species were negligibly weak. Triphenyllead hydroxide was soluble in carbon tetrachloride only to the extent of about 0.001 *M* and was studied as a saturated solution. Band positions were reproducible to ± 1 cm.$^{-1}$ and are believed accurate to ± 2 cm.$^{-1}$.

Discussion

The free O–H frequencies for all of the compounds are listed in Table I. For compounds in which the hydroxyl group is bonded to carbon, tin, lead, nitrogen and oxygen, a remarkably good linear relationship is found between the electronegativities of these atoms and the O–H frequency. The relationship is in the direction predicted from inductive effects[2]; as the electronegativity of the element bonded to oxygen decreases, inductive release of electrons is facilitated, and the OH bond is strengthened and its force constant is increased. A least-mean-squares treatment of the data for the C, N, Sn and Pb compounds gave the equation $\nu_{OH} = 3750.6 - 54.1\chi$, where χ is the electronegativity of the element bonded to the hydroxyl group. Band positions for the four hydroxy compounds of these elements did not deviate from this linear relationship by more than the experimental error of ±1 cm.$^{-1}$ (Table I). The OH frequency for the oxygen compound *t*-butyl hydroperoxide was within 3 cm.$^{-1}$ of that predicted from the formula.

TABLE I

O–H STRETCHING FREQUENCIES AND ELECTRONEGATIVITIES, χ^{10}

Compound	χ	Ref.	γ_{OH}, cm.$^{-1}$	Deviation, cm.$^{-1a}$
Ph_3COH	2.60	8	3609	−1
Ph_3SiOH	1.90	8	3677	+29
$Ph_2Si(OH)_2$	1.90	8	3682	+33
Ph_3GeOH	2.00	8	3651	+9
Ph_3SnOH	1.93	8	3647	+1
Ph_3PbOH	2.45	8	3618	0
$PhB(OH)_2$	2.01	11	3666 (3632)	+28
PhNHOH	3.07	11	3585 (3480) (3398) (3320)	0
Me_3COOH	3.50	11	3558	−3

[a] Deviation from the equation $\nu_{OH} = 3750.6 - 54.1\chi$.

The O–H frequencies for triphenylsilanol, diphenylsilanediol, triphenylgermanol and phenyldihydroxyborane, however, deviate significantly from the linear relationship discussed above. In all of these compounds the O–H absorption occurs at higher frequency than expected (Table I). Considerable evidence for extensive dative π-bonding from oxygen to a vacant 3d orbital on silicon[14] in silanols has been presented by the authors in a series of recent papers.[13,15] The 2p orbital on boron can also accept partial double bonding from oxygen.[16] The authors suggest that dative π-bonding takes place in all four of the compounds mentioned above, increasing the s character of the O–H sigma bond, and thereby increasing the O–H bond force constant and frequency. This O–H frequency shift parallels the well known frequency increase for C–H absorptions with increasing s character in the bond hybridization at carbon.[17]

The fact that the frequency enhancement is greater for triphenylsilanol than for triphenylger-

---

(6) F. A. L. Anet and P. M. G. Bavin, *Can. J. Chem.*, **34**, 1756 (1956); M. I. Batuev and A. D. Matveeva, *Izvest. Akad. Nauk S.S.S.R., Otdel. Khim. Nauk*, 448 (1951); A. R. H. Cole and P. R. Jefferies, *J. Chem. Soc.*, 4391 (1956).

(7) R. W. Taft, Jr., *J. Am. Chem. Soc.*, **74**, 3126 (1952).

(8) A. L. Allred and E. G. Rochow, *J. Inorg. Nucl. Chem.*, **5**, 269 (1958).

(9) R. West and R. H. Baney, *J. Am. Chem. Soc.*, in press.

(10) The Allred–Rochow "best values" of electronegativities for the group IVB elements[8] were used. For other elements, values given by the same authors based on electrostatic calculations have been taken.[11] The conclusions of this study are not dependent on these choices. A similar straight line, differing only in minor respects, is obtained using other sets of electronegativity values recently calculated.[11,12]

The effective electronegativities of the substituent atoms should depend somewhat on the nature of the other groups bonded to them. For this reason we have used phenyl substituted compounds in this study whenever possible; however, we have shown elsewhere that the influence of this secondary inductive effect on the O–H frequency is slight.[13]

(11) A. L. Allred and E. G. Rochow, *J. Inorg. Nucl. Chem.*, **5**, 264 (1958).

(12) M. A. Fineman and R. Daignault, *ibid.*, **10**, 205 (1959); *cf.* H. O. Pritchard and H. A. Skinner, *Chem. Revs.*, **55**, 745 (1955); R. T. Sanderson, *J. Am. Chem. Soc.*, **74**, 4792 (1952).

(13) R. West and R. H. Baney, *J. Am. Chem. Soc.*, **81**, 6145 (1959).

(14) F. G. A. Stone and D. Seyferth, *J. Inorg. Nucl. Chem.*, **1**, 112 (1955).

(15) R. West and R. H. Baney, *ibid.*, **7**, 297 (1958); *cf.* L. H. Allred, E. G. Rochow and F. G. A. Stone, *ibid.*, **2**, 416 (1956); R. H. Baney, K. J. Lake, R. West and L. S. Whatley, *Chemistry & Industry*, 1121 (1959).

(16) E. W. Abel, W. Gerrard, M. F. Lappert and R. Shafferman, *J. Chem. Soc.*, 2895 (1958).

(17) L. J. Bellamy, ref. 3, p. 387–389.

manol,[18] and that no enhancement is found for the tin, lead and carbon compounds, is consistent with recent studies of the acidity and basicity of these triphenylhydroxy compounds, which indicate that oxygen-to-metal π-bonding is strongest in the silicon compound, weaker for germanium, and negligible in the tin, lead and carbon compounds.[9,19]

The O–H absorption of phenyldihydroxyborane is abnormal in that a second somewhat broader band appears at 3632 cm.$^{-1}$, 34 cm.$^{-1}$ below the free O–H frequency. Both bands are found even at low concentrations. Two hydroxyl frequencies might be expected for this compound, since the two hydroxyl groups in phenyldihydroxyborane may not be equivalent. However, both the magnitude of the splitting and the appearance of the lower-frequency band suggest that this band may denote a hydrogen bonded hydroxyl group. Intramolecular hydrogen bonding between hydroxyl groups may take place in phenyldihydroxyborane, or possibly a hydrogen-bonded cylic dimer may be present in dilute solutions of the compound. It is interesting that the structurally similar compound diphenylsilanediol shows only a single sharp band at 3682 cm.$^{-1}$.

The near infrared spectrum of N-phenylhydroxylamine is also complex. In addition to the free O-H band at 3585 cm.$^{-1}$, weak bands are found at 3480, 3398 and 3320 cm.$^{-1}$, which may be attributed to the N–H and O-H groups. *t*-Butyl hydroperoxide shows only a single free O–H band at 3558 cm.$^{-1}$ in dilute solution. It is noteworthy that this absorption frequency, while quite low for a non-hydrogen bonded hydroxyl group, is more than 100 cm.$^{-1}$ higher than that reported for hydroperoxides by Russian workers.[20]

---

[18] Similar results are obtained if other recently-calculated electronegativity values are used.[11,12]

[19] R. West and R. H. Baney, paper presented at the 15th Southwest Regional Meeting, American Chemical Society, Baton Rouge, Louisiana, December, 1959.

[20] A. V. Karyakin and V. A. Nikitin, *Izvest. Akad. Nauk S.S.S.R., Ser. Fiz.*, **17**, 636 (1953).

PHASE RELATIONS IN THE SYSTEMS CsF–LiF, CsF–NaF AND CaF_2–LiF

By Daniel L. Deadmore and James S. Machin

Illinois State Geological Survey, Urbana, Illinois

Received January 11, 1960

In the course of a rather broad investigation of the stability of certain inorganic fluorine-bearing compounds, attention was directed to binary mixtures of some alkali and alkaline earth fluorides. The LiF–CaF_2 system was included because it may be considered to be a weakened model of the important MgO–ThO_2 system[1] and because of this may give some clues to relations in this very refractory system.

Experimental Procedures.—The liquidus and solidus data reported here were obtained from cooling curves. A ten-gram batch was melted to a clear liquid in an 8-ml. platinum crucible and cooled at rates of 3 to 10°/min. The temperature was followed with a bare Pt–Pt + 10% Rh thermocouple immersed in the melt. The thermocouple was calibrated at the melting points of NaCl and NaF and was found to agree with the reported melting points to ± 5°. In most runs the time temperature relation was recorded on a Speedomax strip chart recorder. In other runs the temperature was measured manually at one-minute intervals with a Leeds and Northrup type K potentiometer. In every case where both methods were used on samples having the same composition excellent agreement of the arrest points was observed. In many runs using the recorder the melt was observed during cooling, and the temperature at which the first crystals appeared in the liquid was recorded. In all cases this temperature was approximately 5° higher than the recorded arrest point; these points are reported. The liquidus temperatures are considered to be accurate to ±10° and the solidus temperatures to ±5°.

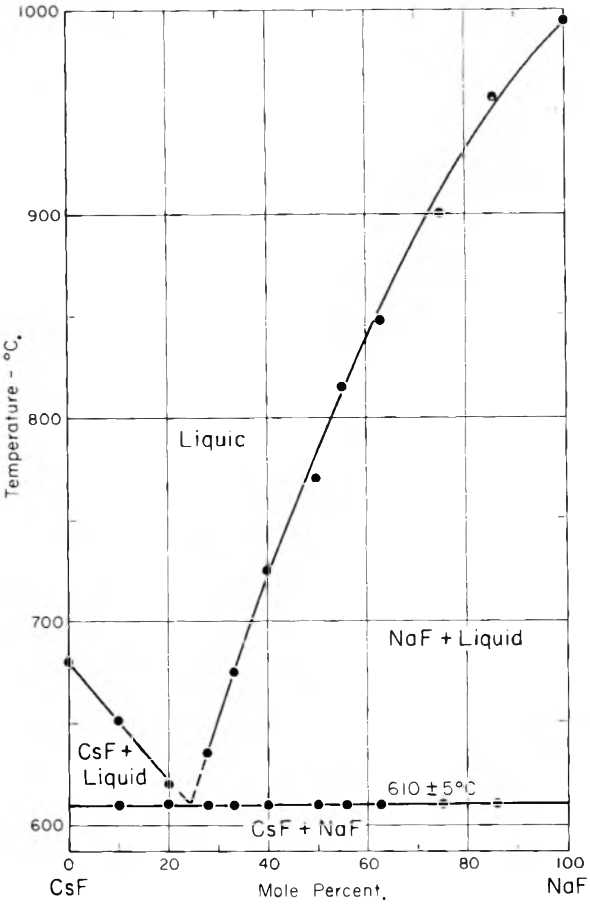

Fig. 1.—The system CsF–NaF.

Twenty-five, fifty and seventy-five mole % compositions in each system were heated in a quench furnace to temperatures above the liquidus temperature and after 2 to 4 hours were dropped into mercury. X-Ray powder diffraction patterns of these quenched compositions were made on a General Electric Co. XRD-3 diffractometer using nickel filtered Cu radiation. Samples containing CsF were mixed with petrolatum to reduce moisture pickup.

Starting Materials.—Lithium fluoride was obtained from the DeRewal International Rare Metals Co. Its melting point was found to be 860 ± 5°. Roy, Roy and Osborn[1] report 870°, and Bergman and Dergunov[2] report 844° for the melting point of LiF. Sodium fluoride of reagent grade was used. Its melting point was found to be 995 ± 5°. Sense, Alexander, Bowman, Stone and Filbert[3] report the melting point of NaF as 996°, whereas Bergman and Dergunov[2] report 990°. Cesium fluoride was obtained from the American Potash and Chemical Corporation. Its chemical composition was claimed to be CsF 96.8%, RbF 1.8%, KF 0.12

---

[1] D. M. Roy, R. Roy and E. F. Osborn, *J. Am. Cer. Soc.*, **33**, 85 1950).

[2] G. Bergman and E. P. Dergunov, *Compt. rend. acad. sci., U.S.S.R.*, **31**, 753 (1941).

[3] K. A. Sense, C. A. Alexander, R. E. Bowman, R. W. Stone and R. B. Filbert, Jr., This Journal, **61**, 384 (1957).

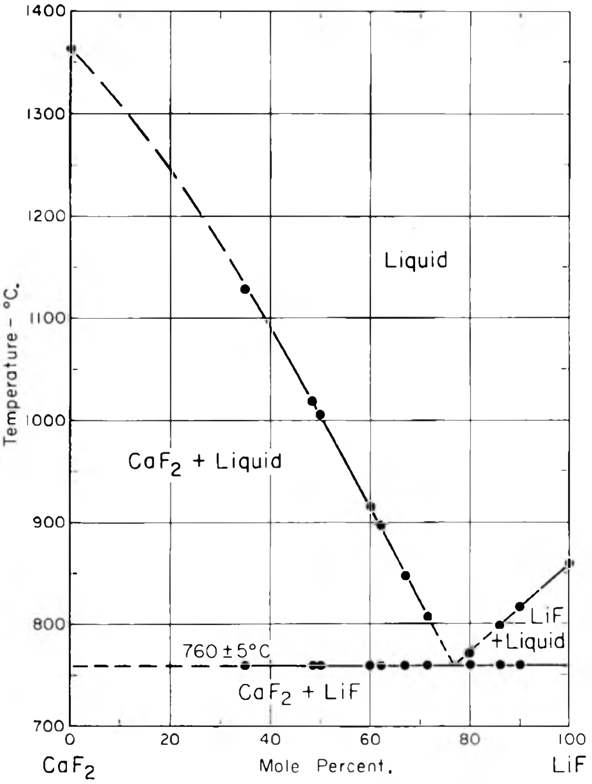

Fig. 2.—The system CaF_2–LiF.

%, NaF 0.04%, Na_2CO_3 0.48% and water 0.0004%. The melting point of this material was found to be 680 ± 5°. Schmitz-Dumont and Weeg[4] report the melting point of CsF to be 705°, whereas Thoma[5] reports 680°. Calcium fluoride was reagent grade material. The melting point was not determined by us. The value of 1361° reported by Pascal[6] was used.

Discussion

Figures 1 and 2 show the phase relations for the CsF–NaF and CaF_2–LiF systems. No diagram for the CsF–LiF system is given here because our data agree very well with those listed by Thoma.[7] He reports a peritectic at 55 mole % CsF with an invariant temperature of 495 ± 5°. Our data indicate a peritectic composition of 54 mole % CsF with an invariant temperature of 488 ± 5°. The eutectic composition given by Thoma is at 63 mole % CsF with an invariant temperature of 475 ± 5°. Ours falls at 64 mole % with an invariant temperature of 470 ± 5°. This is considered essential agreement.

X-Ray examination of the quenched samples from all three systems showed crystals to be present. It is evidently not possible, by the method used, to cool rapidly enough to prevent crystallization. In the CsF-NaF and CaF_2–LiF systems the crystals were those of the primary phases with no detectable solid solution. In the CsF–LiF system another phase was detected, which is presumed to be the compound CsF·LiF (see Thoma[7]).

In every system the eutectic compositions were located by extrapolation of the liquidus curves. This was necessary because it proved impossible to detect on the cooling curves an arrest point that corresponded to the liquidus temperature as the eutectic composition was approached closely.

In the CaF_2–LiF system, the region up to 35 mole % LiF was not investigated, therefore the liquidus and solidus curves are shown as dashed lines.

Roy, Roy and Osborn[1] have pointed out that certain fluoride systems are weakened models of oxide systems. They define a model structure as one in which the radius of each ion in one structure is nearly the same as that of each corresponding ion in the second, but the charges on the ions in the two structures are not the same. The structure having the lower charges is the weakened model of the other. Since the fluoride ion has a radius nearly identical to that of the oxygen ion but has one-half the charge, some fluorides are weakened models of corresponding oxides, and the fluorides have lower melting temperatures. The phase relations in weakened model systems, with their lower melting points, are commonly more easily studied and may give important suggestions from which inferences may be drawn concerning relations in much more refractory oxide systems.

Lithium fluoride, with an ionic radius of 0.78 for lithium and 1.33 for the fluoride ion, is a weakened model of magnesium oxide, where the magnesium ion has a radius of 0.78 and the oxygen ion is 1.32. By the same argument, calcium fluoride can be considered a weakened model of ThO_2. Therefore, a knowledge of the phase relations given in Fig. 2 for the LiF–CaF_2 system may be of some aid in the eventual study of the very refractory MgO–ThO_2 system. The weakened model system indicates that the oxide system may have a simple binary eutectic phase relation with a eutectic composition in the vicinity of 75 mole % MgO. This agrees roughly with a eutectic composition arrived at by calculation, using a relation due to Epstein and Howland,[8] which has been found[9] to give eutectic compositions in surprisingly good agreement with experiment for some simple binary systems.

---

(4) O. Schmitz-Dumont and A. Weeg, *Z. anorg. Chem.*, **265**, 152 (1951).

(5) R. E. Thoma, ed., Oak Ridge National Laboratory, ORNL-2548, 92 (1959).

(6) Von P. Pascal, *Z. Elektrochem.*, **19**, 611 (1913).

(7) R. E. Thoma, ed., Oak Ridge National Laboratory, ORNL-2548, 17 (1959).

(8) L. F. Epstein and H. W. Howland, *J. Am. Ceram. Soc.*, **36**, 334 (1953).

(9) S. M. Lang, F. P. Knudsen, C. L. Fillmore and R. S. Roth, National Bureau of Standards Circ. No. 568, p. 6 (Feb. 20, 1956).

THE ENRICHMENT OF WATER IN H_2O^{18} BY LIQUID THERMAL DIFFUSION

BY GILBERT S. PANSON AND PATRI SULLIVAN

The Newark Colleges of Rut University, Newark, N. J.

Received January 12, 1960

It has been shown previously by a number of investigators[1–3] that H_2O–D_2O mixtures can be fractionated by thermal diffusion in the liquid phase. In each case the D_2O concentrated at the bottom of the diffusion column. The system H_2O^{16}–H_2O^{18}

---

(1) H. Korsching and K. Wirtz, *Naturwiss.*, **27**, 367 (1939).

(2) K. Hirota and O. Kimura, *Bull. Chem. Soc. Japan*, **17**, 42 (1942).

(3) I. Prigogine, L. De Brouckere and R. Buess, *Physica*, **18**, 915 (1952).

represents an isotopic mixture of the same relative mass difference as H_2O–D_2O. Moreover the mechanism of transport should be similar in the two cases. Water of normal isotopic composition contains approximately 1 part in 500 of H_2O^{18}. The authors have studied the thermal diffusion behavior of such "normal" water. The isotopic fractionation by thermal diffusion of water initially containing 1.6 atom % H_2O^{18} also was studied.

Experimental

The apparatus used for these studies was a flat, parallel-plate column constructed of brass and similar to that used by Korsching and Wirtz[1] except for dimensions. The column height was 25 cm. The upper and lower reservoirs were of equal volume with a total working volume of 4.16 ml. The separation of the walls was 0.25 mm. The temperature difference between the walls was maintained at 55 ±2° with the cold wall at 20° and the hot wall at 75° giving a thermal gradient of approximately 2000°/cm.

The column was filled with water of normal isotopic composition and allowed to run for lengths of time varying in different experiments between 2 and 7 days. At the end of each run, the contents of the upper and lower reservoirs were removed. Aliquots of 0.4 ml. were then equilibrated with 10 ml. of CO_2 (measured at 1 atmosphere) for 24 hours. The CO_2 then was analyzed for the ratio of mass 46 to mass 44 by a Consolidated-Nier isotope ratio mass spectrometer. The 46/44 ratio of tank CO_2 was determined before and after each series of analyses to ensure that no variation in operating parameters had occurred. Four independent determinations of the initial isotopic composition were made by a similar method. The values listed in Table I represent the mean value of these determinations. The average deviation from the mean for these measurements was 1 part in 1000. A series of runs using water initially containing 1.6 atom % H_2O^{18} was similarly made.

Results and Discussion

Table I lists the results of the thermal diffusion experiments starting with water of normal isotopic composition. Table II lists the results of similar determinations starting with water enriched in H_2O^{18}. The mass 46/44 ratios reported are for CO_2 equilibrated with the indicated sample as described in the Experimental section. The R values refer to the ratios of mass 46/44 for the indicated sample to the mass 46/44 for the initial material.

TABLE I

Time, hr.	Top Mass 46/44 × 10^3	Bottom Mass 46/44 × 10^3	R_{Top}	R_{Bottom}
0	4.203	4.203	1.0000	1.0000
48	4.148	4.260	0.9869	1.0136
96	4.127	4.279	.9819	1.0181
168	4.065	4.341	.9672	1.0328

TABLE II

Time, hr.	Top Mass 46/44 × 10^3	Bottom Mass 46/44 × 10^3	R_{Top}	R_{Bottom}
0	23.774	23.774	1.0000	1.0000
48	23.495	24.057	0.9882	1.0118
90	23.465	24.078	.9871	1.0129
168	23.462	24.079	.9869	1.0128

In every case there was enrichment of H_2O^{18} at the bottom of the column with a corresponding depletion at the top. The magnitude of the separation is too small to justify the employment of liquid thermal diffusion as a large scale method of separation. However, the results are of some theoretical interest. Prigogine, de Brouckere and Buess[3] accounted for the magnitude of the observed fractionation of H_2O–D_2O mixtures on the basis of a model of the diffusion system as a quasi-crystalline lattice with the diffusing species treated as harmonic oscillators. Isotopic effects in thermal diffusion would then result from differences in the zero point vibrational energies of the isotopic species. The Soret coefficient, on the basis of this treatment, is a function of $\Delta m/m$, the relative mass difference, of the isotopic species and the intermolecular vibrational frequency of water. The relative mass difference for the system H_2O^{16}–H_2O^{18} is identical with that for H_2O–D_2O, so that separations of comparable magnitude should be expected. This was found to be the case. Prigogine, *et al.*,[3] found that the magnitude of the separation for H_2O–D_2O mixtures decreased with increasing initial D_2O concentration. A comparison of Tables I and II shows a similar result for the system H_2O^{16}–H_2O^{18}.

THE DISSOCIATION PRESSURE OF CdSb

By V. J. SILVESTRI

Research Laboratory, International Business Machines Corporation, Poughkeepsie, New York

Received January 15, 1960

The compound semiconductor CdSb[1] is of considerable interest as a potential thermoelectric power material,[2] as a light filter with high infrared transmission[3] and most recently as a compound exhibiting cyclotron resonance.[4]

A knowledge of the dissociation pressure of thermally unstable compounds is necessary for the preparation of homogeneous single crystals.

The dissociation pressure of CdSb has been measured in the temperature range 287 to 448° employing a dew point technique. This method is applicable to binary compounds such as CdSb wherein the dissociation products are elements which have several orders of magnitude difference in their vapor pressures. Thus, the dissociation pressure can be reasonably approximated by measuring the dew point of the more volatile dissociation product.

CdSb has been found to dissociate thermally according to the reaction

$$\mathrm{CdSb(s)} \rightleftarrows \mathrm{Cd(g)} + \mathrm{Sb(s)} \qquad (1)$$

This reaction was determined by separate experiments in the following manner. CdSb was placed at one end of a quartz tube which was evacuated and sealed. The tube was placed in a Hoskins furnace such that the CdSb could be heated while the opposite end of the tube, which protruded from the furnace, acted as a condensation point for the volatile dissociation products. The compound then was heated at 400°, for three days, during which time material condensed on the reaction tube walls outside of the furnace. X-Ray diffraction powder patterns of the condensate revealed only

---

(1) E. Justi and G. Lautz, *Z. Naturforsch.*, **7A**, 191 (1952); **7A**, 602 (1952).

(2) I. M. Pilat, *Phys. Metals and Metallography USSR*, **4**, #2, 31 (1957).

(3) W. J. Turner, A. S. Fischler and W. E. Reese, *J. Electrochem. Soc.*, **106**, 206C (1959), Abstract No. 101.

(4) M. J. Stevenson, *Bull. Am. Phys. Soc.*, Ser. II, **4**, 453 (1959).

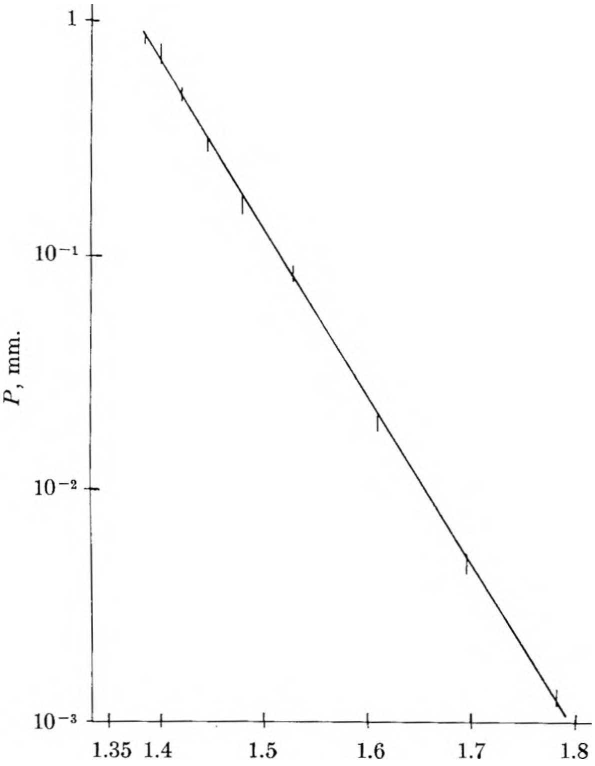

Fig. 1.—Dissociation pressure of CdSb.

the presence of cadmium. A trace of antimony (0.05%) was detected only through a spectrographic examination of the condensate. From these results it was seen that a reasonably good determination of the compound dissociation pressure could be made by measuring the cadmium pressure in equilibrium with solid CdSb.

The dissociation pressures were measured employing the techniques and apparatus used previously for the compounds $ZnAs_2$[5] and $CdAs_2$.[6] Dissociation of the compound in order to provide a cadmium atmosphere for the measurements will result in the formation of a layer of antimony on the sample surface. In order to minimize the thickness of the antimony layer a large sample surface area to reaction tube volume ratio is necessary. Pulled monocrystalline CdSb[7] (10 g.) which contained no spectrographically detectable impurities was broken into small pieces (1-2 mm. in diameter) and sealed in an evacuated quartz reaction tube whose volume was 50 cc. Thermocouple wells were located in each end of the tube. The furnace consisted of two contiguous windings of nichrome ribbon on a quartz tube which was then enclosed in a second quartz tube such that the entire reaction tube was visible. The CdSb, located at one end of the tube, then was heated to the temperatures indicated in Table I and allowed to equilibrate for a period of from 0.5-2 hours. The corresponding cadmium dew points then were observed at the opposite end of the tube in a manner previously described.[5-6] Measurements were made with both increasing and decreasing CdSb temperatures.[8]

Figure 1 is a plot of the experimental data. In the temperature range covered by the measurements the data may be represented as a straight line which fits the equation

$$\log P = -\frac{7200}{T} + 10 \qquad (2)$$

where P is pressure in millimeters of mercury and T is absolute temperature. The equilibrium constant for the dissociation represented by equation 1 when only monomeric[9] Cd is considered is

$$K_p' = P_{Cd} \qquad (3)$$

From equation 2 the calculated heat of reaction for (1) is 33 kcal./mole of solid CdSb.

TABLE I

CdSb DEW POINT MEASUREMENTS

CdSb temp., °C.	Cd condensation temp., °C.	Cd pressure,[a] mm.
287.8	224.0-228.7	0.0012-0.0015
316.9	249.4-253.4	.0044- .0054
348.3	279.4-284.8	.018 - .021
381.0	315.4-320.0	.078 - .092
402.8	332.8-339.1	.15 - .18
418.4	351.0-354.6	.28 - .32
430.1	365.6-368.0	.46 - .52
440.5	376.5-381.8	.66 - .80
448.9	381.9-386.0	.80 - .88

[a] Cadmium pressures were obtained from R. E. Honig, *R. C. A. Rev.*, **18**, 195 (1957).

The author wishes to express his thanks to Mr. V. J. Lyons for preparation of the crystals used in the experiments and for his helpful discussions and comments.

---

(5) V. J. Lyons, THIS JOURNAL, **63**, 1142 (1959).

(6) V. J. Lyons and V. J. Silvestri, THIS JOURNAL, **64**, 266 (1960).

(7) V. J. Lyons, V. J. Silvestri and G. A. Silvey, *J. Electrochem. Soc.*, **106**, 206C (1959), Abstract No. 100.

(8) Temperatures were measured with Pt, Pt-10% Rh thermocouples calibrated with a NBS standardized Pt, Pt-10% Rh thermocouple. Thermocouple voltages were read on a Leeds and Northrup Potentiometer, Model #8662.

(9) D. R. Stull and G. C. Sinke, "Thermodynamic Properties of the Elements," Advances in Chemistry Series, No. 8, 1956.

THE VAPOR PRESSURES OF LIQUID $Bi-BiCl_3$ SOLUTIONS[1]

BY F. J. KENESHEA, JR., W. WILSON AND DANIEL CUBICCIOTTI

Stanford Research Institute, Menlo Park, California

Received January 21, 1960

In previous studies[2-4] we have reported on the vapor pressure of bismuth trihalide over $Bi-BiCl_3$, $Bi-BiBr_3$ and $Bi-BiI_3$ solutions measured by means of a transpiration technique. In this method independent information about the molecular weight of the gaseous species is required to convert the measured mass transferred into pressure. Analysis of the condensate in the transpiration experiments and comparison of the vapor pressure of pure $BiCl_3$ and $BiBr_3$ with data obtained by a boiling point method[5]

---

(1) This work was made possible by the financial support of the Research Division of the United States Atomic Energy Commission.

(2) D. Cubicciotti, F. Keneshea and C. Kelley, THIS JOURNAL, **62**, 463 (1958).

(3) D. Cubicciotti and F. Keneshea, *ibid.*, **62**, 999 (1958).

(4) D. Cubicciotti and F. Keneshea, *ibid.*, **63**, 295 (1959).

indicated that the vapor over the pure salt and over the metal–salt solutions was essentially pure monomeric trihalide. Prior to this knowledge, however, it was thought that more than one gaseous species might exist in equilibrium with the metal–salt solutions and that an additional measurement of the total (absolute) pressure would be required to establish the partial pressures of such species. With this in mind, two other methods of measuring the vapor pressure of $BiCl_3$ were investigated. The results obtained in these measurements are reported in this paper.

Experimental

Quasi-static Method.—One type of vapor pressure measurement investigated was a quasi-static method developed by Rodebush and Dixon[6] and used by Fiock and Rodebush[7] to measure the vapor pressure of some alkali halides. This method proved fairly satisfactory for pure $BiCl_3$, but because of the rather large hold-up of material in the condensing tubes of the apparatus the composition of a solution would not be accurately known. Therefore, as it seemed that the method would not be suitable for the Bi–$BiCl_3$ solutions, no measurements were attempted with the mixtures.

A Pyrex vapor pressure cell was used which was essentially the same as that described by Rodebush and Dixon.[6] In use, the system was heated to a fixed temperature with dry air present in both legs of the cell at a pressure greater than the vapor pressure of the salt. The pressure in one leg was then reduced by small decrements until there was a permanent difference in pressure between the two legs, as measured by a differential manometer connected between them. At this point the inert gas pressure in the high pressure leg of the cell, as measured with a Hg manometer, was equal to the vapor pressure of the sample.

The $BiCl_3$ used was first dehydrated under HCl gas and distilled into the cell. The Hg levels in the measuring manometer were determined with the aid of a cathetometer. Liquid temperatures were measured with a chromel–alumel thermocouple which was standardized against NBS samples of Sn, Pb and Zn.

Spiral Gauge Method.—The other method utilized a completely closed system in which the pressure was measured by means of a spiral gauge similar to that described by Yorke.[8] A hollow Vycor spiral was attached vertically to a Pyrex bulb containing the sample and was surrounded by a Pyrex envelope. Any change of pressure inside the spiral caused a twisting movement which was observed by means of a light beam reflected from a mirror attached to the spiral. The gauge was used as a null instrument by changing the pressure outside the spiral to return it to its original position.

In making a measurement, $BiCl_3$ was distilled into the bulb under reduced pressure and the bulb evacuated and sealed off. A weighed quantity of bismuth was added to the bulb before distilling in the $BiCl_3$. Before and during the distillation the spiral section of the gauge was enclosed in a furnace and heated to 400° to remove adsorbed water. The sealed gauge was immersed in a stirred molten nitrate heating bath and pressure readings made at various temperatures. The pressure was measured with a Hg manometer using a cathetometer for reading the Hg levels. Temperatures were measured with a calibrated Pt–Pt:10% Rh thermocouple placed next to the bulb containing the liquid being measured.

The gauge was calibrated before use by heating it with both sides of the spiral evacuated and measuring the zero shift with temperature and the sensitivity. During use the spiral often showed a zero shift with time (usually of the order of 1–3 mm.) and corrections for this shift had to be applied to the readings. It was assumed that the shift was linear with time. Because of the zero shift and the inability to read pressures better than ±1 mm. it was estimated that the error in the spiral gauge pressures was ±2 mm.

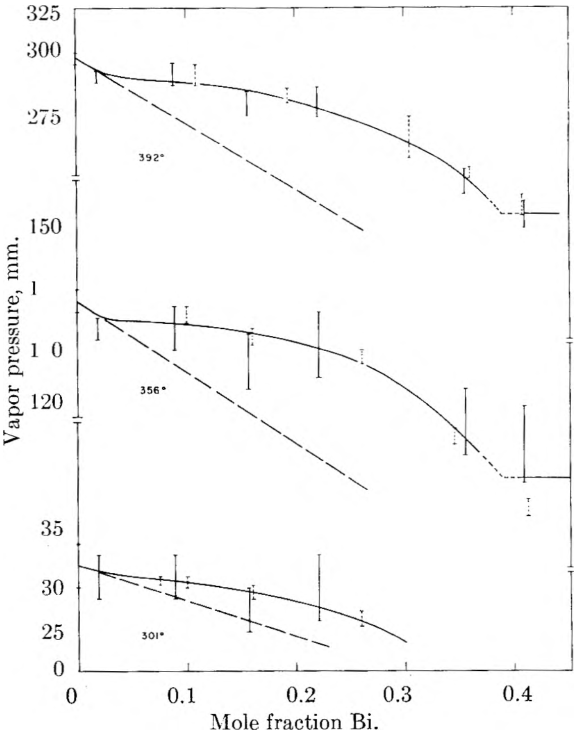

Fig. 1.—Vapor pressure of Bi–$BiCl_3$ as a function of composition at 301, 356 and 392°: I, spiral gauge; I, transpiration (ref. 2a) The dashed curve represents Raoult's law.

The spiral gauge was tested by measuring the vapor pressure of triply distilled mercury. The observed vapor pressures agreed with literature data[9] within ±2mm. over the pressure range of 10 to 700 mm.

Results and Discussion

Pure $BiCl_3$.—The quasi-static results agreed with the transpiration data[2] within 3% in the temperature range of 275 to 365° (pressures about 15 to 200 mm.); at higher temperatures they were as much as 7% lower while at lower temperatures they were as much as 9% higher than the transpiration results. The lower values at higher temperatures may be due to failure of this method in the pressure range about 300 mm., at least for this salt. The reason is not known but it may be associated with the higher rate of reflux which occurs at higher temperatures—possibly the liquid was superheated at the larger rates of boiling required. It should also be mentioned that in the experiments the permanent difference in the differential manometer at the higher temperatures could not be maintained for much longer than a few minutes, which indicated improper behavior of the system.

The spiral gauge results agreed within 3% of the transpiration results from 300° to the highest temperature measured, 425° (*i.e.*, pressures in the range of 30 to 600 mm.). In this temperature range the spiral gauge data fitted a straight line having the equation, $\log p_{\mathrm{mm}} = 8.547 - 4032/T$. The heat of vaporization, determined from the slope, was 18.5 ± 0.2 kcal. per mole. This value compares with

---

(5) E. V. Evnevich and V. A. Sukhodskii, *J. Russ. Phys. Chem. Soc.*, **61**, 1503 (1929).

(6) W. H. Rodebush and A. L. Dixon, *Phys. Rev.*, **26**, 851 (1925).

(7) E. F. Fiock and W. H. Rodebush, *J. Am. Chem. Soc.*, **48**, 2522 (1926).

(8) S. J. Yorke, *J. Sci. Instr.*, **22**, 196 (1945).

(9) D. R. Stull and G. C. Sinke, "Thermodynamic Properties of the Elements," Am. Chem. Soc. Washington, D. C., 1956, p. 129.

18.9 ± 0.2 kcal. per mole found by the transpiration method over the same temperature range.[2]

The agreement between the spiral gauge data and the transpiration data lends further support to the conclusion previously made that only monomeric $BiCl_3$ exists in the vapor above liquid $BiCl_3$.

Bi–$BiCl_3$ Mixtures.—The vapor pressures of several Bi–$BiCl_3$ mixtures (obtained with the spiral gauge) are shown in Fig. 1 for three temperatures, where they are compared with vapor pressures determined by the transpiration method. The rather large error limits are due to corrections that had to be made in these measurements for a permanent gas impurity which presumably was released by the Bi, or by reaction of impurities in the Bi with the $BiCl_3$. It was found that this gas impurity could be avoided by maintaining the molten Bi–$BiCl_3$ solution under vacuum for several minutes before sealing off the gauge.

Comparison of the spiral gauge data with the transpiration results in Fig. 1 indicates that they are in agreement within experimental error. In addition to the results shown in Fig. 1 the pressures over a solution containing 0.95 mole fraction of Bi were measured and found to be 103 ± 7 mm. at 356° and 232 ± 7 mm. at 392°. These are the same pressures that are found at 0.41 mole fraction, and thus indicates that the measurements at 0.41 and 0.94 were made in the two-phase region of the system, as would be predicted from phase diagram information.[10]

The values for the activities and the derived thermodynamic properties of $BiCl_3$ can be found in a previous report.[2] The activity of the $BiCl_3$ in these solutions, as is evident from the vapor pressure curves (Fig. 1), obeys Raoult's law at low Bi concentrations but shows marked positive deviations at higher concentrations.

Acknowledgment.—The authors are indebted to Dr. C. M. Kelley for helpful discussions.

---

(10) S. J. Yosim, A. J. Darnell, W. G. Gehman and S. W. Mayer, THIS JOURNAL, **63**, 230 (1959).

PYROLYSIS OF TRIPHENYLMETHANE

By GEORGE J. JANZ AND MICHAEL A. DECRESCENTE

Rensselaer Polytechnic Institute, Department of Chemistry, Troy, N. Y.

Received January 19, 1960

The present note reports some experimental results for the pyrolysis of triphenylmethane at fast flow rates in the temperature range of 700°.

Experimental

Triphenylmethane (Eastman Kodak Co.) was brought to constant weight by continuous high vacuum pumping (10^{-6} mm.) and used without further purification (m.p. obsd, 93.2°(u); lit.,[1] 92.6°).

Apparatus and Procedure.—A study of the kinetics of hydrogen evolution using gas flow techniques as in the thermal method for the measurement of bond dissociation energies[2,3] was selected for the present work. The flow control was achieved by heating the triphenylmethane in a Woods metal thermostat to temperatures giving the vapor pressures necessary for the desired flow rates through the capillary orifice in the neck of the flask. A Hoke packless vacuum value, maintained at 200°, was used to admit the flask to the hot zone for the duration of the pyrolysis experiment. The reaction zone was a 67.41 cc. quartz tube maintained at pre-selected temperatures, ±0.5° by a suitably wound electric furnace. Pressures were measured by a novel type thermostated null manometer described elsewhere.[4] At the exit, the vapors passed through a trap at 25° and two traps at −80°. The remaining volatiles, after further possible condensables were taken off at −196°, were transferred by auxiliary mercury diffusion and Toepler pumps to calibrated storage volumes for analyses by PVT measurements.

Products.—Efforts were made to determne the hexaphenylethane collected in the first receiver (25°) by benzoyl peroxide titration.[5] Quantitative results could not be obtained owing to the large amounts of triphenylmethane present in this mixture. The non-condensable gas at −196° was confirmed to be hydrogen both by its emission spectrum and by mass spectrometry. The latter established that the gas was 100% hydrogen within the limits of analyses; no traces of methane were found in this gaseous fraction. The fraction collected at −196° but not condensable at −80° contained the C_2 hydrocarbons evolved in the pyrolyses. This was found to be relatively small, a maximum of about 3% only being observed at the highest temperature (743°) and was not investigated further. The absence of significant amounts of C_2 hydrocarbons indicated that complete decomposition of triphenylmethane was not occurring in the temperature range studied. The fraction collected at −80° and not condensable at 25° at these low pressures was confirmed to be principally benzene (>90%) by mass spectrometry. Quantitative determinations established that the ratio of benzene/hydrogen in the pyrolyses was 7.5/1.0 at 680°.

Results

A summary of the data and kinetic results for the reaction velocity studies is given in Table I. The temperature range, 645–745°, pressure range, 2–12 mm., and contact time range, 0.15–2.1 sec. were investigated. The kinetic analysis was based on the rate of hydrogen evolution owing to the difficulty of quantitative estimates of the small amounts of hexaphenylethane in the product mixtures. A plot of the first-order rate constants (Table I) *vs.* reciprocal temperatures (°K.) gave a straight line Arrhenius type graph from which the equation

$$k = 2.8 \times 10^{16} e^{-83{,}000/RT} \text{ sec.}^{-1}$$

was determined for the reaction kinetics over the temperature range studied. The rate constant for the first-order pyrolysis of triphenylmethane at 664°, from a series of seven experiments in which pressure and contact time were both varied, was found to be 6.8 ± 0.5 × 10^{-3} sec.$^{-1}$.

Discussion

An interest of the present investigation was in the possible use of triphenylmethane as a carrier gas[2,6] in the kinetic technique for bond dissociation energy measurements. Whereas the rate of pyrolysis judged by hydrogen evolution conforms to a first-order rate analysis, the high ratio of C_6H_6 to H_2 indicates that in addition to the possible primary steps

---

(1) G. Egloff, "Physical Constants of Hydrocarbons," Reinhold Publ. Corp., New York, N. Y., 1946.

(2) M. Szwarc, *J. Chem. Phys.*, **16**, 128 (1948); *Chem. Revs.*, **47**, 75 (1950).

(3) H. Blades, A. T. Blades and E. W. R. Steacie, *Can. J. Chem.*, **32**, 298 (1954).

(4) M. A. DeCrescente and G. J. Janz, *Rev. Sci. Instr.*, **19**, 502 (1958).

(5) G. S. Hammond, A. Raave and F. J. Modic, *Anal. Chem.*, **24**, 1373 (1952).

(6) T. L. Cottrell, "The Strengths of Chemical Bonds," Butterworths Sci. Publ. Co., London, 1954.

TABLE I

DATA AND RESULTS FOR TRIPHENYLMETHANE PYROLYSIS

Temp., °C.	Contact time, sec.	Press., mm.	Mole of gas, × 10^4	$k_1 \times 10^3$, sec.$^{-1}$
645	0.730	2.9	0.182	9.89
655	.595	5.5	.323	35.8
661	.437	4.5	.535	5.80
663	2.06	11.5	1.16	6.38
663	0.571	4.2	0.383	6.49
664	.770	3.3	.367	6.29
664	.307	2.1	.342	6.61
664	.323	4.7	.330	7.02
667	.168	8.0	1.22	9.25
680	.191	2.1	0.515	25.1
704	.498	3.4	1.47	35.8
729	.156	7.7	5.24	109
735	.193	1.6	3.35	203
738	.159	3.0	8.73	250
743	.328	11.3	13.4	141

$$(C_6H_5)_3CH \begin{cases} \longrightarrow (C_6H_5)_3C + H & (1) \\ \longrightarrow (C_6H_5)_2CH + C_6H_5 & (2) \end{cases}$$

such processes as

$$(C_6H_5)_3CH + C_6H_5 \longrightarrow (C_6H_5)_2CH(C_6H_4) + C_6H_6 \quad (3)$$

$$(C_6H_5)_3CH + H \begin{cases} \longrightarrow (C_6H_5)_2CH + C_6H_6 & (4) \\ \longrightarrow (C_6H_5)_2CH(C_6H_4) + H_2 & (5) \end{cases}$$

undoubtedly contribute to the pyrolysis mechanism. Thus for the toluene pyrolysis a reaction comparable to step 4 in the above scheme has been postulated by Szwarc[2] and was confirmed by Blades and Steacie.[3] It is apparent that the actual amount of hydrogen formed may be considerably greater than that observed. These considerations, and the fact that the *A* parameter is approximately 10^3 greater than that for related 1st order processes (*cf.* toluene) preclude a simple interpretation of the temperature dependence of the hydrogen evolution rate in the pyrolyses of $(C_6H_5)_3CH$ as a bond dissociation energy. The results of present limited study also show clearly that triphenylmethane is less satisfactory than toluene as a carrier gas in the the kinetic method for bond energy determinations.

Acknowledgments.—Support of this research, in part, by grants-in-aid from Union Carbide Chemicals Co., and Monsanto Chemical Co. is gratefully acknowledged. The authors wish to thank Sidney W. Benson, Alec Sehon and Michael Szwarc for stimulating comments in the course of this work.

RADIOLYSIS OF TRINITROMETHANE IN AQUEOUS SOLUTIONS BY Co-60 γ-RADIATION

By A. HENGLEIN[1] AND J. LANGHOFF[2]

Institute for Physical Chemistry, University of Cologne, Germany

Received January 26, 1960

Tetranitromethane has previously been shown to be an effective scavenger of many free radicals produced in aqueous solutions under the influence of ionizing radiations.[3,4] The reaction product is the deeply colored anion of aci-trinitromethane. Hydrogen atoms, for instance, react according to

$$H\cdot + C(NO_2)_4 \longrightarrow H^+ + [C(NO_2)_3]^- + NO_2\cdot \quad (1)$$

Nitrous and nitric acid are by-products of the reaction. The anion of trinitromethane formed is sensitive to radiation too. This becomes perceptible in the irradiation of tetranitromethane at higher doses when trinitromethane is more and more accumulated in the solution.[3] In order to understand more thoroughly the action of tetranitromethane as a scavenger, the radiolysis of its reaction product trinitromethane in aqueous solutions has been studied. Although it is not possible to present a very detailed mechanism of this radiolysis, publication of some of our experiences may be helpful since tetranitromethane seems at present to be used as a scavenger in radiation chemical and other free radical studies by various laboratories.

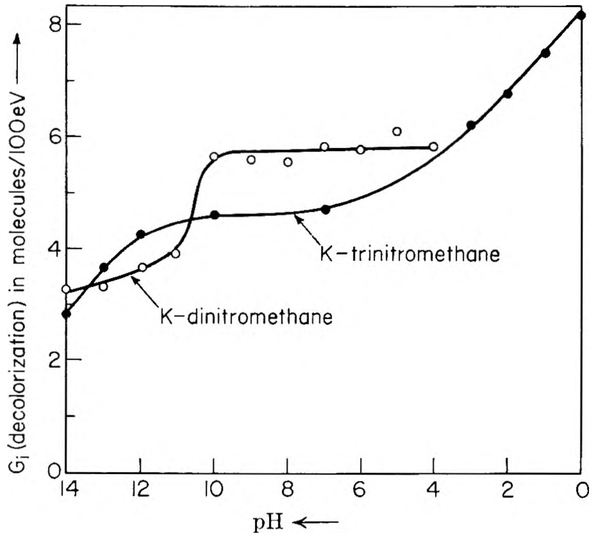

Fig. 1.—Decolorization of trinitromethane and dinitromethane in 2 × 10^{-3} *M* air-free aqueous solutions of different *p*H. (The compounds were dissolved in the form of their potassium salts. Potassium hydroxide and sulfuric acid, respectively, were added to prepare solutions of various acidity.)

The decomposition of trinitromethane in solution has been measured by the decrease in the optical density at 350 mμ (extinction coefficient, 1.50 × 10^4 moles^{-1} liter cm.$^{-1}$). The initial yield of this decolorization in molecules/100 e.v. is shown as a function of the *p*H in Fig. 1. *G*(decolorization), however, is only equal to $G(-[C(NO_2)_3]^-)$ if no colored reaction product is formed. In strongly alkaline solutions the decolorization occurs with a yield of 2.8 molecules/100 e.v. which approximately corresponds to *G*(OH). It increases with increasing hydrogen ion concentration up to the value of 8.2 at *p*H 0. This high radiation sensitivity of trinitromethane in acid solutions may be responsible for the low yields of trinitromethane in acid solutions of tetranitromethane.[3]

In alkaline solutions the absorption maximum of the $[C(NO_2)_3]^-$ ion at 350 mμ not only becomes less intense but also is shifted to longer wave lengths. This indicates the formation of dinitromethane

---

[1] Hahn-Meitner-Institut fur Kernforschung, Berlin-Wannsee, Germany.

[2] Max Planck Institut fur Chemie, Mainz, Germany.

[3] A. Henglein and J. Jaspert, *Z. physik. Chem.*, *Neue Folge*, **12**, 324 (1957).

[4] A. Henglein, J. Langhoff and G. Schmidt, THIS JOURNAL, **63**, 980 (1959).

which absorbs at slightly longer wave lengths (maximum at 363 mμ, extinction coefficient, 2.18×10^4 moles^{-1} liter cm^{-1}). Dinitromethane may be formed from trinitromethane by dissociative electron transfer from a hydrogen atom as trinitromethane is formed from tetranitromethane according to eq. 1

$$\mathrm{H}\cdot + [\mathrm{C(NO_2)_3}]^- \longrightarrow \mathrm{H}^+ + [\mathrm{C(NO_2)_2}^{--} + \mathrm{NO_2}\cdot \quad (2)$$

$$[\mathrm{C(NO_2)_2}]^{--} + \mathrm{H_2O} \longrightarrow [\mathrm{CH(NO_2)_2}]^- + \mathrm{OH}^- \quad (3)$$

If dinitromethane is the only radiolysis product of trinitromethane, no essential decrease in the optical density at 350 mμ should be observed since the anions of both compounds have nearly the same specific extinction at this wave length. The observed decolorization in Fig. 1 must therefore be due to an additional decomposition reaction of trinitromethane which leads to an uncolored product. This reaction is perhaps caused by the OH radicals from the radiolysis of the solvent

$$[\mathrm{C(NO_2)_3}]^- + \mathrm{OH}\cdot \longrightarrow \text{uncolored products} \quad (4)$$

In the presence of small amounts of alcohols the decolorization as well as the shifting of the 350 mμ absorption band are strongly retarded. Apparently the RCHOH radicals, which are formed in these solutions by hydrogen abstraction reactions of the H and OH radicals, react only slowly with trinitromethane. This protection effect has already been found in the radiolysis of aqueous tetranitromethane solutions.[3] Trinitromethane can be accumulated in these solutions in much higher concentrations without any essential decomposition when small amounts of alcohol are present. This is important for the use of tetranitromethane solutions as chemical dosimeter.

No dinitromethane has been found in irradiated neutral and acid trinitromethane solutions. However, another reaction product has been observed, the absorption maximum of which occurred at 315 mμ. This compound also has been found in the radiolysis of tetranitromethane in water[3] and in cyclohexane.[4] The formula of dinitroformaldoxime has been assigned to it.[4,5] It seems therefore that hydrogen atoms reduce a $\mathrm{NO_2}$ group in trinitromethane in neutral and acid solutions without breaking the C–N bond as in alkaline solutions (eq. 2). An alternative explanation of the formation of dinitroformaldoxime and the absence of dinitromethane is the occurrence of reactions 2 and 3 immediately followed by a thermal reaction between the dinitromethane and nitrous acid formed

$$\mathrm{CH_2(NO_2)_2} + \mathrm{HNO_2} \longrightarrow \mathrm{C(NO_2)_2NOH} + \mathrm{H_2O} \quad (5)$$

According to reactions 2–5 decolorization of trinitromethane solutions is caused by OH radicals only at high pH and by both OH and H radicals in more acid solutions. However, G(decolorization) in very acid solutions exceeds the value of $G(\mathrm{OH}) + G(\mathrm{H})$ which amounts to about 6.0. This must be explained by some additional decomposition reactions which probably are caused by reactive radiolysis products of trinitromethane. It has been observed that the color of all irradiated solutions slowly decreased after irradiation while unirradiated trinitromethane solutions remained unchanged.

Some data on the radiolysis of dinitromethane in aqueous solution are included in Fig. 1. Here a marked dependence of the yield on the pH of the solution also exists. Dinitroformaldoxime is also formed as one of the radiolysis products in neutral and acid solutions. This must be due entirely to the thermal reaction 5, the nitrous acid reacting here having been formed by some decomposition reaction which involves breakage of a C–N bond.

---

[5] The formula of methazonic acid[3] has erroneously been assigned to this compound.

COMMUNICATIONS TO THE EDITOR

THE CONFIGURATION OF TETRAKIS-(4-METHYLIMIDAZOLE)-COPPER(II) ION

Sir:

Recently Nozaki, *et al.*,[1] in discussing their results on the association of 4-methylimidazole with copper(II) ions, have raised the question of the possible arrangement of four imidazole molecules about the central metal ion. They suggest that, because of marked steric hindrance, the tetrakis-(4-methylimidazole)-copper(II) ion cannot be completely planar and that "presumably some or all of the imidazole rings must be rotated out of the plane . . ., around the Cu–N bonds, so as to make mutual accommodation easier. Probably there is also some distortion of the orientation of the Cu–N bonds, so that they do not all lie in a single plane."

We have begun the determination of the crystal structure of tetrakis-(4-methylimidazole)-copper(II) nitrate. The observation that there are two copper atoms in a unit cell belonging to the space group $P2_1/a$ indicates that the copper atoms must lie at symmetry centers. The only possible centrosymmetric arrangement of four N atoms about the central Cu atom is a planar arrangement. Therefore there can be no out-of-plane distortion of the Cu–N bonds, and the steric hindrance is relieved by rotation of the imidazole rings about the Cu–N bonds, in accordance with the primary suggestion of Nozaki, *et al.*

4-Methylimidazole was prepared by the method of Weidenhagen and Hermann[2] as a waxy solid, m.p. 52–53°. Tetrakis-(4-methylimidazole)-copper(II) nitrate was prepared by adding the stoichiometric amount of 4-methylimidazole to an aqueous solution of copper(II) nitrate, slightly acidified with nitric acid. Upon standing, the desired product separated as a dark blue solid. The material was recrystallized from water–ethanol mixtures and crystals were grown by slow evaporation from water–ethanol. *Anal.* Cu, 11.67; C, 37.56; H,

---

[1] Y. Nozaki, F. R. N. Gurd, R. F. Chen and J. T. Edsall, THIS JOURNAL, **79**, 2123 (1957).

[2] R. Weidenhagen and R. Hermann, *Ber.*, **68**, 1953 (1935).

4.83; N, 27.20. Calcd. for $Cu(C_4H_6N_2)_4(NO_3)_2$: Cu, 12.31; C, 37.24; H, 4.69; N, 27.15.

Rotation and Weissenberg photographs taken with Cu Kα radiation (λ = 1.5418 Å.), internally calibrated with NaCl (a_0 = 5.6387 Å.), give: a_0 = 11.227, b_0 = 14.484, c_0 = 7.499, all ±0.01 Å., β = 97° 55′ ± 6′; density observed: 1.41 g./ml., calculated for 2 molecules per cell: 1.417 g./ml. Systematic absence of (h 0 l) for h odd and of (0 k 0) for k odd indicate the space group to be $P2_1/a$.

This work was performed under a grant from the National Institutes of Health.

DEPARTMENT OF CHEMISTRY H. MONTGOMERY
UNIVERSITY OF WASHINGTON
SEATTLE 5, WASHINGTON E. C. LINGAFELTER

RECEIVED APRIL 7, 1960

GAS-SOLID CHROMATOGRAPHY OF H_2, HD, AND D_2. ISOTOPIC SEPARATION AND HEATS OF ADSORPTION ON ALUMINA[1]

Sir:

The communication of Smith and Hunt[2] concerning the separation of hydrogen isotopes by gas–solid chromatography prompts a report of our continued study of such separations. As shown previously,[3] alumina columns at low temperatures with helium as the carrier gas lead to the separation of the nuclear spin isomers of hydrogen and deuterium (separation of the deuterium isomers is virtually complete at 65°K.). Since the HD/o-H_2 separation factor is nearly unity from 64–77.5°K., these species are not separated. However, the presence on the surface of the alumina of a catalyst which makes ortho–para interconversion rapid relative to motion along the column causes ortho and para isomers to appear as a single peak with a retention time intermediate (a weighted average) between the retention times expected for the individual isomers in the absence of equilibration. Since HD is unaffected, separation of H_2, HD, and D_2 into three peaks results.

Good isotopic separation results with helium as the carrier gas on columns of alumina "coated" with ferric oxide (Fig. 1). Peak tailing was virtually eliminated and essentially symmetrical peaks were obtained by adsorbing a small amount of carbon dioxide on the alumina. Large molecular species are *less* efficient in reducing peak tailing, presumably due to their inability to penetrate fine pores (*i.e.*, a molecular sieve effect). Employing the signal response factors for H_2, HD, and D_2 appropriate to the detector,[3] numerous standard hydrogen–deuterium mixtures (prepared volumetrically) were analyzed before and after exchange equilibration over a heated wire. The percentage of (total) deuterium of samples containing from 1 to 99 at. % deuterium was determined from peak areas with high accuracy: mean deviations for individual samples, 0.0–0.5%; over-all (all samples), 0.2%. The limit of detection of HD in H_2 or D_2 was less than 0.01%; hence, deuterium (as HD) can be detected in natural hydrogen.

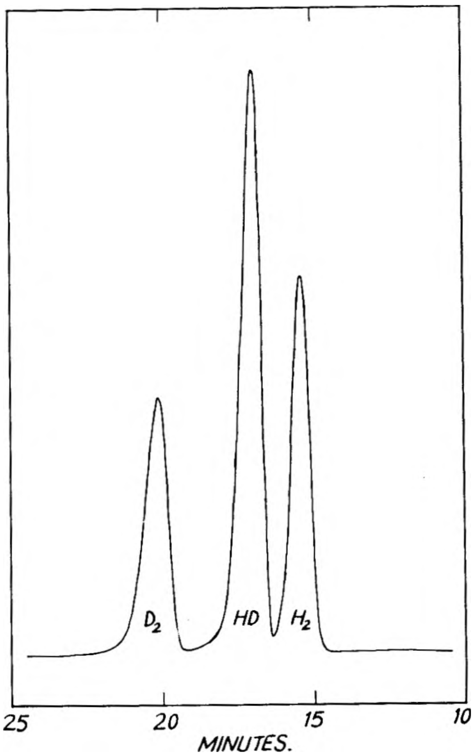

Fig. 1.—Chromatogram of 1.00 cc. sample of H_2–HD–D_2 on 365 × 0.5 cm. column (150–200 mesh alumina treated successively with 1.8 *M* ferric chloride, 3 *M* ammonium hydroxide, water, and then heated at 120° for 24 hours; partially deactivated with carbon dioxide; 77.4°K.; helium flow 112 cc./min. at room temperature and pressure).

Oxygen adsorbed on alumina is also quite effective in producing rapid ortho–para equilibration, chromatograms similar to that of Fig. 1 being obtained. Columns of strongly activated (480°, 8 hours) reagent-grade alumina (apparently iron-free) also lead to ortho–para equilibration. Partial deactivation with carbon dioxide *restores* ortho–para separation, removing the carbon dioxide causes equilibration again.

From linear plots of log (V_N/T) *versus* $1/T$ (65–77.4°K.), limiting isosteric heats of adsorption on alumina of varying activity have been determined.[4] Typical values in kcal./mole are p-H_2, 1.40; o-H_2, 1.55; HD, 1.51; o-D_2, 1.58; and p-D_2, 1.65 ($\alpha^{77.4}_{\text{o-H}_2,\text{p-H}_2}$, 1.34).[4] The *differences* in heats of adsorption of nuclear spin isomers (obtained directly from plots of log α *versus* $1/T$) are of considerable interest with regard to the theory[5] of ortho–para separations. These values increase with column activity: $\alpha^{77.4}_{\text{o-H}_2,\text{p-H}_2}$, 1.19 → 1.48; $\Delta H_{\text{o-H}_2} - \Delta H_{\text{p-H}_2}$, 90 → 170 cal./mole; $\Delta H_{\text{p-D}_2} - \Delta H_{\text{o-D}_2}$, 50 → 80 cal./mole.

DEPARTMENT OF CHEMISTRY WILLIAM R. MOORE
MASSACHUSETTS INSTITUTE OF TECHNOLOGY
CAMBRIDGE 39, MASSACHUSETTS HAROLD R. WARD

RECEIVED APRIL 28, 1960

---

[1] This research was supported by a grant from the Petroleum Research Fund administered by the American Chemical Society. Grateful acknowledgment is hereby made to the donors of this fund.

[2] H. A. Smith and P. P. Hunt, THIS JOURNAL, **64**, 383 (1960).

[3] W. R. Moore and H. R. Ward, *J. Am. Chem. Soc.*, **80**, 2909 (1958).

[4] V_N = net retention volume, α^T = separation factor (relative retention) at T °K.

[5] (a) Y. L. Sandler, THIS JOURNAL, **58**, 58 (1954); *J. Chem. Phys.*, **29**, 97 (1958); (b) A. A. Evett, *ibid.*, **31**, 565 (1959); (c) D. White and E. N. Lassettre, *ibid.*, **32**, 72 (1960).

Announcing . . . 1959 EDITION

American Chemical Society

DIRECTORY of
GRADUATE RESEARCH

INCLUDES: Faculties, Publications, and Doctoral Theses in Departments of Chemistry, Biochemistry, and Chemical Engineering at United States Universities.

- **All institutions which offer Ph.D. in chemistry, biochemistry, or chemical engineering**
- **Instructional staff of each institution**
- **Research reported at each institution for past two years**
- **Alphabetical index of approximately 3,000 faculty members and their affiliation; alphabetical index of 258 schools.**

The ACS Directory of Graduate Research, prepared by the ACS Committee on Professional Training, is the only U.S. Directory of its kind. The 4th edition includes all schools and departments, known to the Committee, which are concerned primarily with chemistry, biochemistry, or chemical engineering, and which offer the Ph.D. degree.

The Directory is an excellent indication not only of research reported during the last two years by the staff members at these institutions but also of research done prior to that time. Each faculty member reports publications for 1958-59; where these have not totaled 10 papers, some articles prior to 1958 are reported. This volume fully describes the breadth of research interest of each member of the instructional staff.

Because of the indexing system, access to information is straightforward and easy—the work of a moment to find the listing you need. Invaluable to anyone interested in academic or industrial scientific research and to those responsible for counseling students about graduate research.

Compared to the 1957 edition, this new volume will contain 118 more pages, list approximately 200 additional faculty members, and include 22 additional schools.

Special Offer: Save $2.50. Copies of the 1957 edition of the Directory, formerly $3.50 each, may be purchased in combination with the current edition for a total price of $5.00 for the two volumes. Possession of both copies provides continuity of reference information. Orders for 1957 editions only will be billed at the regular $3.50 rate.

Paper bound . . . . 752 pages $4.00

ORDER FROM: Special Issues Sales

American Chemical Society
1155 - 16th Street, N.W. • Washington 6, D.C.

NO. 19 EPR AT WORK SERIES

HIGH SENSITIVITY EPR AS A TOOL IN FREE RADICAL RESEARCH

(ELECTRON PARAMAGNETIC RESONANCE)

The V-4500 100 kc EPR Spectrometer offers to the scientist the following important features:

Sensitivity $2 \times 10^{11} \Delta H$ unpaired electron spins at a response time of one second. (ΔH is the signal line width in gauss.)

Sample temperature variable from $-196^\circ C$ to $+300^\circ C$.

Sample irradiation by U-V or visible light.

EXAMPLE

Identification of Intermediate Substrate Free-Radicals formed during Peroxidatic Oxidations

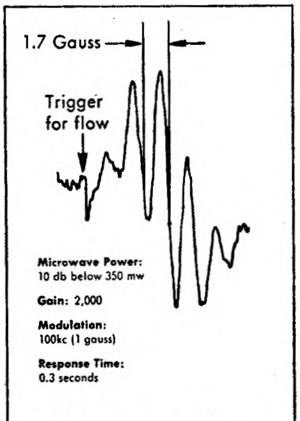

Fig. A. Semiquinone

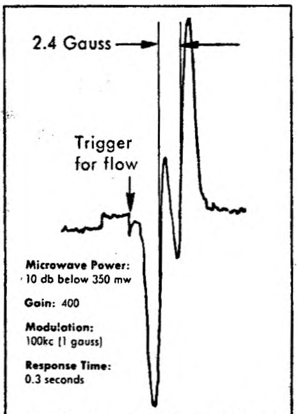

Fig. B. Ascorbate Intermediate

A considerable amount of work utilizing the technique of electron paramagnetic resonance (EPR) to detect free-radical production in typical enzyme-substrate oxidation-reduction reactions has been reported. For the most part the EPR signals that have been observed in the system have been associated with the enzyme itself, or with a change in valance state (i. e., to a paramagnetic state) of the metal in the metalloflavoproteins. In no case has evidence been presented to associate the free radical signal with the substrate undergoing oxidation or reduction. The EPR technique is valuable not only for detecting free radicals but can also be used to identify the type of free radicals in a system and provides a direct measure of their concentration, since the total intensity of the spectral lines is directly proportional to the concentration of free radical intermediates present. With the improved sensitivity and larger sample volumes obtainable, it is now possible to re-investigate free radical production in these biological systems.
In the research described (see illustrations), EPR has been used to detect, identify, and follow the kinetics of free radical formation and decay in the oxidation of ascorbic acid by an enzyme in H_2O_2 solution. These observations were made with a Varian 100 kc EPR Spectrometer, utilizing a flat sample cuvette attached to a flow system for kinetic measurements. The enzyme was recrystallized Japanese turnip peroxidase.*

Figure A illustrates the free-radical spectrum obtained from a mixture of enzyme ($8 \times 10^{-8}M$) and a solution of hydroquinone ($10^{-2}M$), H_2O_2 ($10^{-2}M$) and acetate buffer (pH 4.8). The measured concentration of free radicals from this enzyme reaction was $1.3 \times 10^{-6}M$ in the steady state.

Figure B shows the intermediate formed during the peroxidatic oxidation of ascorbic acid in a steady state reaction. The concentration of free radicals resulting from the reaction of ascorbic acid ($10^{-2}M$), H_2O_2 ($10^{-2}M$), and peroxidase ($1.6 \times 10^{-7}M$) at $pH = 4.8$, was $7.2 \times 10^{-6}M$.

There is no doubt that the free radicals generated during the peroxidatic oxidations of hydroquinone and ascorbic acid are derived from the substrates.** The enzymic generation of free radicals from substrates, which have been observed in this investigation by electron paramagnetic resonance spectroscopy, suggests that aerobic life may have an inherent genetic instability due to mutations which such free radicals could produce. This interesting possibility seems to merit further investigation.

* *Samples courtesy of I. Yamazaki and H. S. Mason, Department of Biochemistry, University of Oregon Medical School, Portland, Oregon, U. S. A.*

** *See: Yamazaki, Mason and Piette; Biochem. and Biophys. Comm; Vol. 1, No. 6, pp. 336-337.*

For literature which fully explains the 100 kc EPR Spectrometer and its application to basic and applied research in physics, chemistry, biology and medical research, write the Instrument Division

VARIAN associates
PALO ALTO 52, CALIFORNIA

NMR & EPR SPECTROMETERS, MAGNETS, FLUXMETERS, GRAPHIC RECORDERS, MAGNETOMETERS, MICROWAVE TUBES, MICROWAVE SYSTEM COMPONENTS, HIGH VACUUM EQUIPMENT, LINEAR ACCELERATORS, RESEARCH AND DEVELOPMENT SERVICES